LONG TERM MONITORING OF SEASONAL AND WEATHER STATIONS AND ANALYSIS OF DATA FROM SHRP PAVEMENTS

ODOT 8880

State Job No. 14693(0)

FINAL REPORT

Submitted to

The Ohio Department of Transportation

Case Western Reserve University

Department of Civil Engineering

March, 2004

Prepared in Cooperation with the Ohio Department of Transportation and the U.S. Department of Transportation, Federal Highway Administration

1. Report No.	2. Government Accession No.	3. Recipient's Catalog No.
FHWA/OH-2004/004		

4. Title and subtitle.	5. Report Date
Long Term Monitoring of Seasonal Weather Stations and Analysis of Data from SHRP Pavements	March 2004
	6. Performing Organization Code
7. Author(s) J. Ludwig Figeroa	8. Performing Organization Report No.
	10. Work Unit No. (TRAIS)
9. Performing Organization Name and Address Case Western Reserve University Department of Civil Engineering 10900 Euclid Avenue Cleveland, OH 44106	11. Contract or Grant No. State Job No. 14693(0)
	13. Type of Report and Period Covered Final Report
12. Sponsoring Agency Name and Address Ohio Department of Transportation 1980 W Broad Street Columbus, OH 43223	14. Sponsoring Agency Code

15. Supplementary Notes

16. Abstract

External agents such as traffic and climate directly affect the life of flexible and rigid pavements. To understand the influence of these factors, a test road located on U.S. 23, just North of Delaware in Ohio, was constructed as part of the Federal Highway Administration's SHRP Program. Material properties and the effect of environmental factors on pavements were studied. Knowing the dynamic response of pavement materials and environmental factors to which they are exposed, back calculation procedures to estimate the resilient modulus and the modulus of subgrade reaction of the subgrade soil from non-destructive testing deflections were developed using ILLIPAVE and ILLISLAB for flexible and rigid pavements, respectively. Relationships between the resilient modulus at the break point and the degree of saturation were developed for the subgrade soil, while relationships between resilient modulus and temperature were developed for asphaltic materials. All test data, including moisture content, pavement and soil temperature and resistivity, as well as weather-related parameters collected at all instrumented sections at the test road were processed. Seasonal findings include solar radiation versus temperature relations, asphalt concrete temperature versus air temperature equations, temperature differentials on PCC slabs, moisture content estimations for the subgrade soil and depth of frost penetration determination. A comparison of the degree of saturation vs. depth among sections with and without drains did not show any significant difference in reducing the degree of saturation in sections with drains. A comparison between precipitation and degree of saturation showed a lag of 80 to 85 days in higher degree of saturation after substantial precipitation occurs. Displacement time histories obtained by the FWD were evaluated, along with two dynamic pavement analysis programs: Plaxis and FWD-DYN. Comparisons of time history of displacement plots of both actual and simulated data showed that Plaxis and FWD-DYN over estimated deflections at and near the point of loading. This could be the result of the difference in loading rates for laboratory testing of pavement materials compared to the FWD test loading rate.

17. Key Words	18. Distribution Statement
Pavement Design, Flexible and Rigid Pavement Evaluation, Non-Destructive Testing, Backcalculation Dynamic Analysis of Pavements	No Restrictions. This document is available to the public through the National Technical Information Service, Springfield, Virginia 22161

19. Security Classif. (of this report)	20. Security Classif. (of this page)	21. No. of Pages	22. Price
Unclassified	Unclassified		

Form DOT F 1700.7 (8-72) Reproduction of completed page authorized

LONG TERM MONITORING OF SEASONAL AND WEATHER STATIONS AND ANALYSIS OF DATA FROM SHRP PAVEMENTS

ODOT 8880

State Job No. 14693(0)

FINAL REPORT

March, 2004

Submitted to

The Ohio Department of Transportation

by

J. Ludwig Figueroa

Department of Civil Engineering

CASE WESTERN RESERVE UNIVERSITY

Cleveland, Ohio 44106

Prepared in Cooperation with the Ohio Department of Transportation and the U.S. Department of Transportation, Federal Highway Administration

Table of Contents

THIS PAGE LEFT INTENTIONALLY BLANK

List of Tables

List of Figures

LONG TERM MONITORING OF SEASONAL AND WEATHER STATIONS AND ANALYSIS OF DATA FROM SHRP PAVEMENTS

Abstract

External agents such as traffic and climate directly affect the life of flexible and rigid pavements. To understand the influence of these factors, a test road located on U.S. 23, just North of Delaware in Ohio, was constructed as part of the Federal Highway Administration's (FHWA) Strategic Highway Research Program (SHRP).

In order to eventually develop a mechanistic design procedure, two parallel topics: material characterization and the effect of environmental factors on pavements were studied. Knowing the dynamic response of pavement materials and environmental factors to which they are exposed, back calculation procedures to estimate the resilient modulus and the modulus of subgrade reaction of the subgrade soil from non-destructive testing deflections were developed.

Materials characterized in this study were the embankment (BE15) soil, the Asphalt Treated Base (ATB) and the Permeable Asphalt Treated Base (PATB). Relationships between the resilient modulus at the break point and the degree of saturation were developed for the subgrade soil. Similarly, relationships between resilient modulus and temperature were developed for asphaltic materials.

Problems with Topp's universal equation, as the calibration curve used to determine the volumetric moisture content of a soil were encountered. Laboratory tests were conducted, and calibration curves were developed for the subgrade soil found at the test site.

All test data, including moisture content, pavement and soil temperature and resistivity, as well as weather-related parameters collected at all instrumented sections at the test road were processed and subjected to quality control, to be uploaded to databases.

Seasonal findings include solar radiation versus temperature relations, asphalt concrete temperature versus air temperature equations, temperature differentials on Portland Cement Concrete slabs, moisture content estimations for the subgrade soil and depth of frost penetration determination.

A comparison of the degree of saturation vs. depth among sections with and without drains did not show any significant difference in reducing the degree of saturation in sections with drains. A related comparison between increased precipitation and degree of saturation indicated a lag of 80 to 85 days in increased degree of saturation after substantial precipitation occurs.

Using the results from the material characterization section and the developed environmental relations, finite element analyses were conducted using ILLIPAVE and ILLISLAB for flexible and rigid pavements. Back calculation nomographs for flexible pavements were developed for the different layer configurations found at the Ohio Test Road. For rigid pavements, a back calculation program was developed and a backcalculation nomograph applicable

to slabs built at the test road is proposed to estimate the modulus of subgrade reaction.

Displacement time histories obtained by the FWD were evaluated, along with two dynamic pavement analysis programs: Plaxis and FWD-DYN. Comparisons of time history of displacement plots of both actual and simulated data showed that Plaxis and FWD-DYN over estimated deflections at and near the point of loading. This could be the result of the difference in loading rates for laboratory testing of pavement materials compared to the FWD test loading rate.

THIS PAGE LEFT INTENTIONALLY BLANK

Chapter 1

INTRODUCTION

Over the past decade, significant funding has been provided, at both the state and federal levels, to study the factors effecting the performance of multi-layered asphalt concrete (AC) and Portland Cement Concrete (PCC) pavements and the response of these pavements to those factors for use in the development of mechanistic pavement design procedures. These initiatives have resulted in the establishment of working “field laboratories” to conduct long-term controlled testing towards this goal. In effect, the behavior of actual multi-lane highways in the state of Ohio has been observed through three interlinking research topics. These topics include environmental factors, material characterization, and load testing.

As part of these efforts, the Ohio Test Road was constructed along U.S. 23, about 16km (10 miles) north of Delaware, OH, through the Federal Highway Administration’s (FHWA) Strategic Highway Research Program (SHRP). This road was planned and constructed with seasonal and structural response instrumentation for the purpose of collecting parameters affecting the mechanical and weather-related response of pavements.

The three-mile long test site exhibits a fairly consistent subgrade soil, thus facilitating the comparison of the performance of studied pavement sections. The test road includes four different SPS (Specific Pavement Studies) sections including:

SPS-1: Strategic Study of Structural Factors for Flexible Pavements.

SPS-2: Strategic Study of Structural Factors for Rigid Pavements.

SPS-8: Study of Environmental Effects in the Absence of Heavy Traffic.

SPS-9: Asphalt Program Field Verification Studies.

Each SPS section is divided into test sections. In total there are 38 sections, 18 instrumented to monitor seasonal, 15 to monitor structural response and 5 with no instrumentation at all.

Five of the instrumented test sections and the weather station were assigned to Case Western Reserve University for data collection and study. These included: SPS-1 J2 or 390102, SPS-2 J3 or 390203, SPS-2 J5 or 390205, SPS-2 J12 or 390212 and SPS-9 ODOT or 390901.

This report is organized in five major sections with the aim of meeting the objectives of the research project.

In the first section, included in Chapter 2 and following previous studies by Figueroa and DeButy (1998), the temperature dependency of the Asphalt Treated Base [ATB] and the Permeable Asphalt Treated Base [PATB] is investigated in the laboratory. Also, predictions of the resilient modulus at the break point vs. the degree of saturation were established for the subgrade soil. Calibration curves for the FHWA probes installed at the test road were developed to determine the volumetric moisture content and ultimately the degree of saturation of subgrade soils

Chapter 3 discusses the methodology used and software developed to process seasonal and weather data collected at all seasonal test sites and the weather station. An accompanying data disk contains all processed files meeting SHRP's guidelines to be uploaded into SHRP's database.

Seasonal findings are discussed in detail in Chapter 4. These include: stiffness-temperature relationships for bituminous materials and temperature distributions in PCC

slabs, moisture content-degree of saturation and stiffness property determinations for the subgrade soil, and depth of frost penetration estimations.

Knowing the stiffness properties of the pavement materials, back calculation procedures for both flexible and rigid pavements were developed and are presented in Chapter 5. Finite elements computer codes such as ILLIPAVE and ILLISLAB were used in the development of the suggested methodologies to determine the resilient modulus at the break point, in flexible pavements, and the modulus of subgrade reaction, in rigid pavements. The back calculation procedure is based on measurements obtained from non-destructive testing methods such as the Falling Weight Deflectometer (FWD).

Chapter 6 examines two computer codes currently available for the dynamic analysis of flexible pavements with the aim of back calculating subgrade stiffness properties from the time series of loading and deflection, obtained during FWD testing. Comparisons of results between static and dynamic methods and actual test data are also included in this chapter.

Finally, Chapter 7 summarizes significant findings and conclusions resulting from this investigation.

THIS PAGE LEFT INTENTIONALLY BLANK

Chapter 2

MATERIAL CHARACTERIZATION AND EQUIPMENT CALIBRATION

2.1. Introduction

In order to study the load response behavior of flexible and rigid pavements, the stiffness properties of materials used in their construction must be determined. The materials sampled and tested in the laboratory included the embankment (subgrade) soil (labeled: BE15), the Asphalt Treated Base (ATB) and the Permeable Asphalt Treated Base (PATB).

This chapter focuses on the determination of the resilient modulus as the fundamental stiffness property of each material. In addition to this, calibration curves were developed to determine the moisture content of the subgrade soil from readings obtained by Time Domain Reflectometry (TDR) probes installed at the Ohio Test Road site.

2.2. Resilient Modulus of Asphalt Treated Base (ATB) and Permeable Asphalt Treated Base (PATB)

The Indirect Tension for Resilient Modulus for Bituminous Mixtures test method (ASTM D 4123-82) was used to test 101.6 mm (4") diameter Asphalt Treated and Permeable Asphalt treated Base cores, obtained at the Ohio Test Road. The test is conducted using a repeated indirect tensile test set-up under controlled temperature and controlled loading conditions, with a typical load application time of 0.1 seconds and a rest period of 1.9 seconds, with an applied load nearing 444.8 N (100 lbs). The load is applied to the 101.6 mm (4”) disks

along the diameter through a narrow curved loading strip, while the load, the vertical and horizontal deformations are recorded to calculate the Poisson's ratio and the resilient modulus by the following equations.

$$\mu = \frac{3.59\Delta H}{\Delta V} \tag{2.1}$$

$$E_r = \frac{P(\mu + 0.27)}{t\,\Delta H} \tag{2.2}$$

Where:

E_r = Resilient modulus of elasticity (psi)
P = Applied repeated load (lb)
υ = Resilient Poisson's ratio
t = Specimen thickness (in)
ΔH = Total recoverable horizontal deformation (in)
ΔV = Recoverable vertical deformation (in)

The constants included in these equations are valid in the English system, however all results have been converted to SI units.

Tables 2.1 and 2.2 show the resilient modulus for the ATB and the PATB at temperatures ranging between 0 and 38^{o}C (32 and 101^{o}F). Resilient modulus test data was fitted with second order polynomial curves as shown in Figure 2.1 along with their corresponding polynomial equations and coefficient of determination (R^2) of 85 and 73 percent respectively.

As expected, the resilient modulus values of ATB were generally higher than those of PATB. However, the resilient modulus of both materials at high temperatures are very close to each other, and a drastic reduction in material stiffness is noticed as temperature increases.

Table 2.1. Resilient Modulus Determination for ATB

Sample	T (^{o}C)	T (^{o}F)	Resilient Modulus (MPa)	Resilient Modulus (psi)
1	3	37	4027	584202
1	3	37	3647	529008
2	0	32	6460	937028
2	0	32	6663	966421
3	0	32	6164	894063
3	0	32	6336	919113
2	3	38	3836	556454
2	3	38	3915	567936
3	4	40	2905	421353
3	4	40	2871	416449
1	16	60	1753	254310
1	16	60	2183	316648
2	16	60	2309	334892
2	16	60	2286	331620
3	13	55	2941	426650
3	13	55	2718	394234
1	20	68	1951	283014
1	20	68	2402	348405
2	19	67	1718	249141
2	19	67	1871	271452
3	19	67	2389	346541
3	19	67	2869	416206
1	34	93	331	48010
1	34	93	310	44934
2	34	93	659	95622
2	34	93	447	64884
3	34	93	586	85024
3	34	93	633	91851

The above results were compared with those obtained by Figueroa and DeButy (1998), as shown in Figure 2.2, where asphalt concrete (AC) cores were tested. As expected the resilient modulus of the AC is greater than the resilient modulus of both ATB and PATB. All three materials seem to converge to similar values at high temperatures indicating that the remaining stiffness of all materials

is primarily due to aggregate frictional resistance, while the cohesion provided by the asphalt cement has considerably decreased.

Table 2.2. Resilient Modulus Determination for PATB

Sample	T (^{o}C)	T (^{o}F)	Resilient Modulus (MPa)	Resilient Modulus (psi)
1	0	32	4474	648937
1	0	32	3947	572567
3	0	32	2842	412182
3	0	32	3437	498607
2	2	36	2656	385308
2	2	36	2134	309478
3	2	36	2134	309562
3	2	36	2098	304298
1	16	60	1581	229317
1	16	60	1325	192250
3	16	60	1473	213631
3	16	60	1564	226813
1	20	68	1842	267259
1	20	68	2105	305316
3	20	68	1553	225240
3	20	68	1802	261323
1	38	101	817	118560
1	38	101	909	131861
3	38	101	654	94884
3	38	101	748	108439

Again a polynomial equation yields the best fit for the test data for typical Ohio mixtures. Equation 2.3 defines the curves of best fit with the coefficients listed in Table 2.3 (in both SI and English units) for each type of asphalt concrete (ODOT items 446 types 1 and 2), in conjunction with the curve-fit coefficient of determination, R^2. Figure 2.2 also includes a graphical representation of the regression equation trend lines for both types of mixes.

$$E_r = a_0 + a_1 P + a_2 P^2 \qquad (2.3)$$

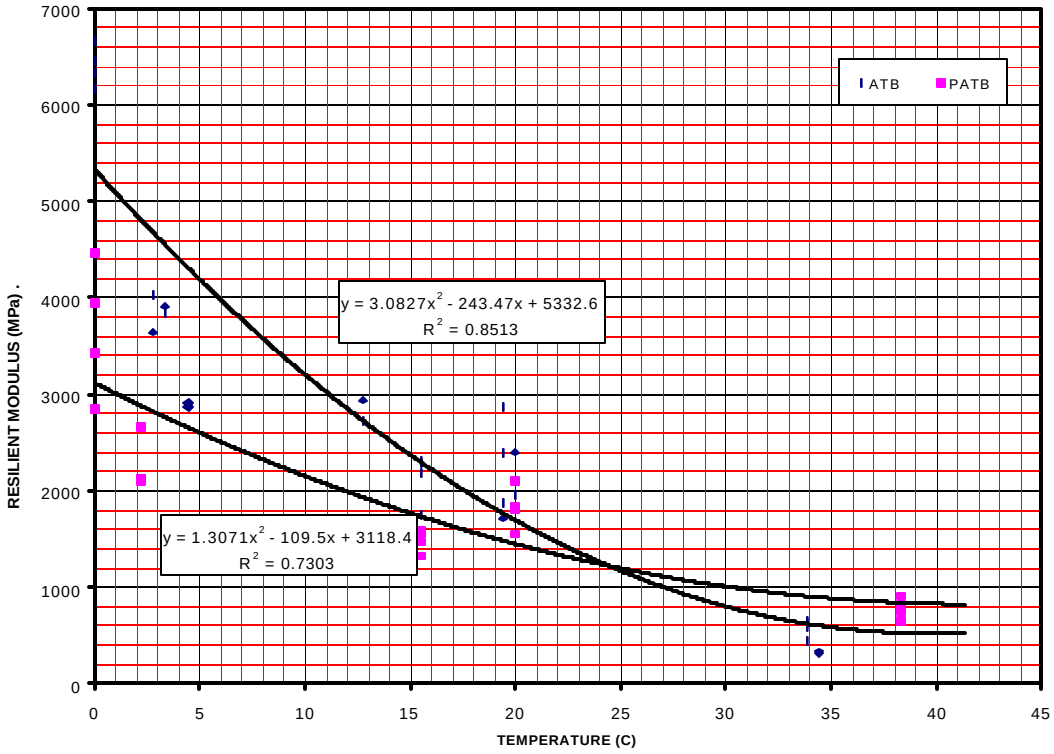

Figure 2.1. Resilient Modulus vs. Temperature [ATB and PATB]

where:

E_r = Resilient modulus MPa in SI units or (psi x 10^6 in English units)

a_0, a_1, a_2 = Regression constants listed in Table 2.3:

Columns 2 & 3 for SI units
Columns 4 & 5 for English units

P = Asphalt concrete temperature: Deg. C in SI units or (Deg F in English units)

Table 2.3. Equation 2.1 Regression Coefficients

Coefficient	SI Units AC (item 446)		English Units AC (item 446)	
	Type 1	Type 2	Type 1	Type 2
a_0	12659	12118	3.5405	3.1164
a_1	-562.10	-473.59	-0.0611	-0.0487
a_2	5.8344	3.9292	2.57×10^{-4}	1.73×10^{-4}
R^2	0.8548	0.6403	0.8547	0.6403

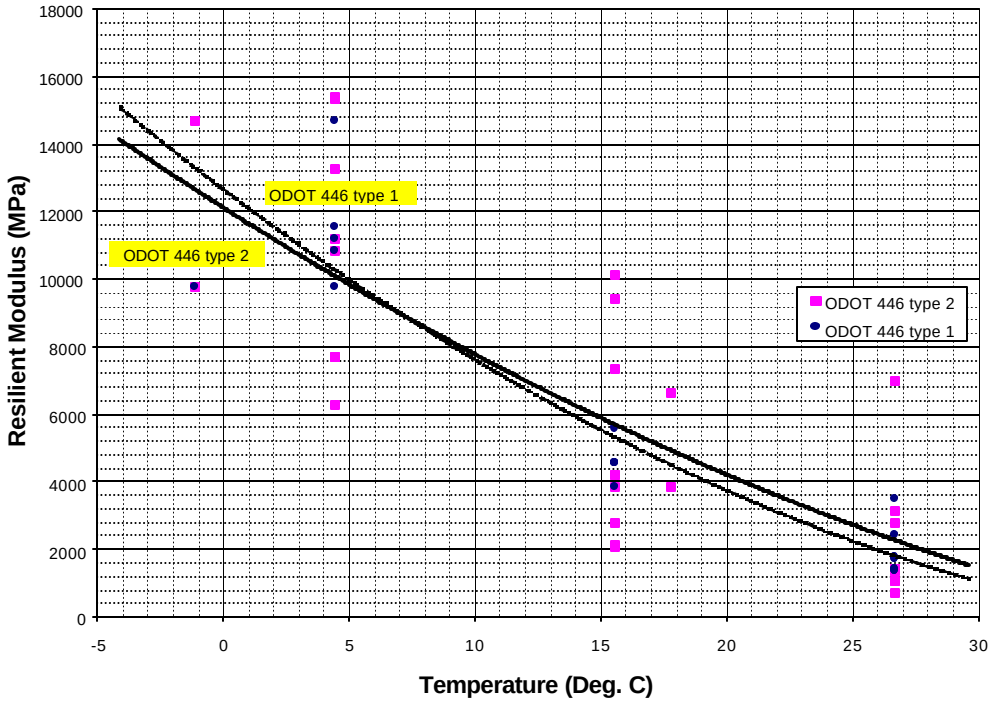

Figure 2.2. AC Modulus vs. Temperature

2.3. Index Properties and Resilient Modulus of Fine-Grained Soils

Prior to conducting resilient modulus testing on the embankment (BE15) soil, it was necessary to determine its index properties and compaction characteristics, on samples obtained at the borrow pit, adjacent to the test site. Results of these tests are presented next.

2.3.1. Specific Gravity

Table 2.4 shows the results of four specific gravity (G_S) tests and their average . These tests were conducted according to ASTM D 854 and AASHTO T 100 specifications. It should be noted that the determined G_S value falls within the expected range for a silty clay.

Table 2.4. Specific Gravity of Embankment Soil

Soil	Test 1	Test 2	Test 3	Test 4	Av. G_S
BE15	2.726	2.721	2.712	2.684	2.71

2.3.2. Atterberg Limits

The liquid and plastic limits were determined following ASTM D 4318 and AASHTO T 89 and T 90 specifications. Table 2.5 presents the test results.

Table 2.5. Atterberg Limits

Soil	Liquid Limit	Plastic Limit
BE15	34.3%	21.1%

Based on these limits, and knowing that it is mostly fine-grained, the embankment soil classifies as an A6 soil by the AASHTO Soil Classification System or CL by the Unified Soil Classification System.

2.3.3. Moisture-Density Relationships

To determine the compaction characteristics of the embankment soil, both standard and modified Proctor compaction tests were conducted in accordance with ASTM D 698-78 and AASHTO T99-90 and T180-90 specifications,

respectively. Figure 2.3 shows both the standard and modified Proctor compaction curves along with the zero air-voids curve, determined for a specific gravity of 2.71. Table 2.6 lists the optimum moisture contents and maximum dry unit weights corresponding to each test.

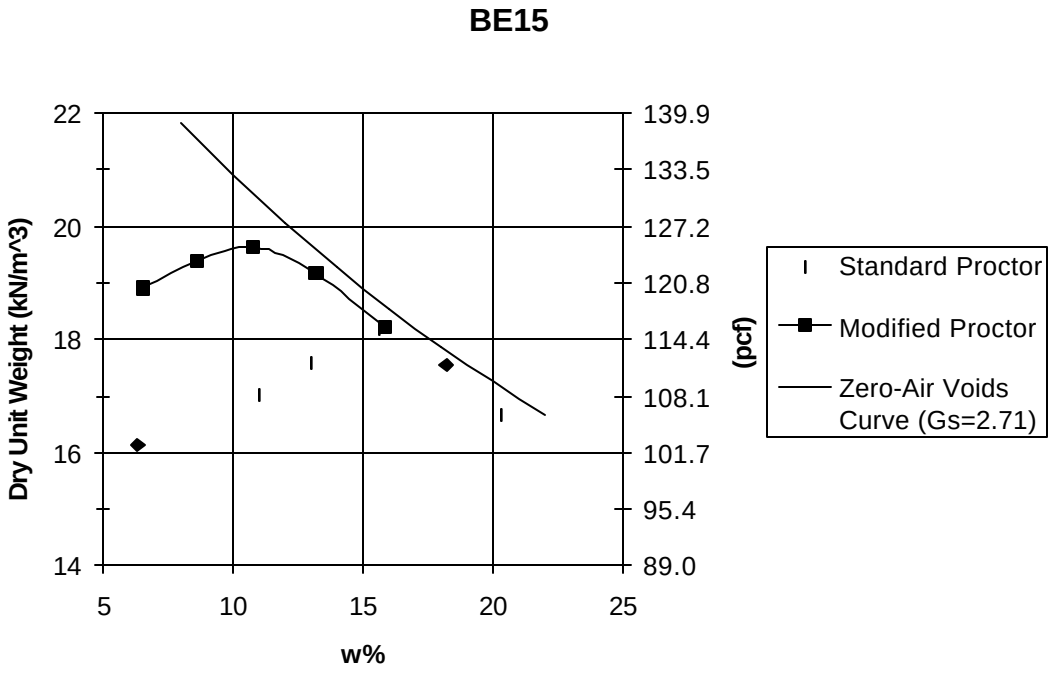

Figure 2.3. Moisture-Density relations for BE15 embankment soil.

Table 2.6. Optimum Moisture Content and Maximum Dry Unit Weight

	Standard Proctor			Modified Proctor		
	W_{opt} (%)	$\gamma_{d\ max}$ (pcf)	$\gamma_{d\ max}$ (KN/m^3)	W_{opt} (%)	$\gamma_{d\ max}$ (pcf)	$\gamma_{d\ max}$ (KN/m^3)
BE15	16.0	115.7	18.2	10.25	124.7	19.6

2.3.4. Resilient Modulus of the Embankment (Subgrade) Soil

The resilient modulus of the subgrade soil is one important factor that determines the design parameters of a pavement. A pavement is subjected to

static and dynamic loads that reach the subgrade soil. The resilient modulus measures the soil's ability to withstand dynamic loads. This modulus is affected by the degree of saturation by a decrease in its magnitude with an increase in the moisture content.

Extensive resilient modulus testing of the embankment (BE15) soil was conducted, primarily focused on developing relationships between the resilient modulus and the degree of saturation. One of the most accepted and used models to characterize the resilient modulus of a fine-grained soil is the Thompson and Robnett's Bilinear Model (Thompson and Robnett, 1976). This model, presented in Figure 2.4, indicates that as the normal (deviator) stress increases on the test specimen, the resilient modulus decreases linearly at a slope K_1 up to a value of the deviator stress (designated as σ_{di}). Beyond this value, the decrease in the resilient modulus is more gradual but still linear at a slope designated as K_2. These two lines are traced following the results of linear regression analyses of two groups of data points, after dividing them at an obvious deviator stress where a change in the slope occurs. The resilient modulus at the break point is designated as E_{ri}.

Figueroa et al. (1994), in a study for the Ohio Department of Transportation determined the resilient modulus characteristics of typical Ohio subgrade soils and their variation with the degree of saturation (S_r). His experiments including A-4, A-6, and A-7 soils indicated that the resilient modulus at the break point E_{ri}, correlated very well with the degree of saturation. Similar

relationships will be developed for the BE15 embankment soil found at the Ohio Test Road.

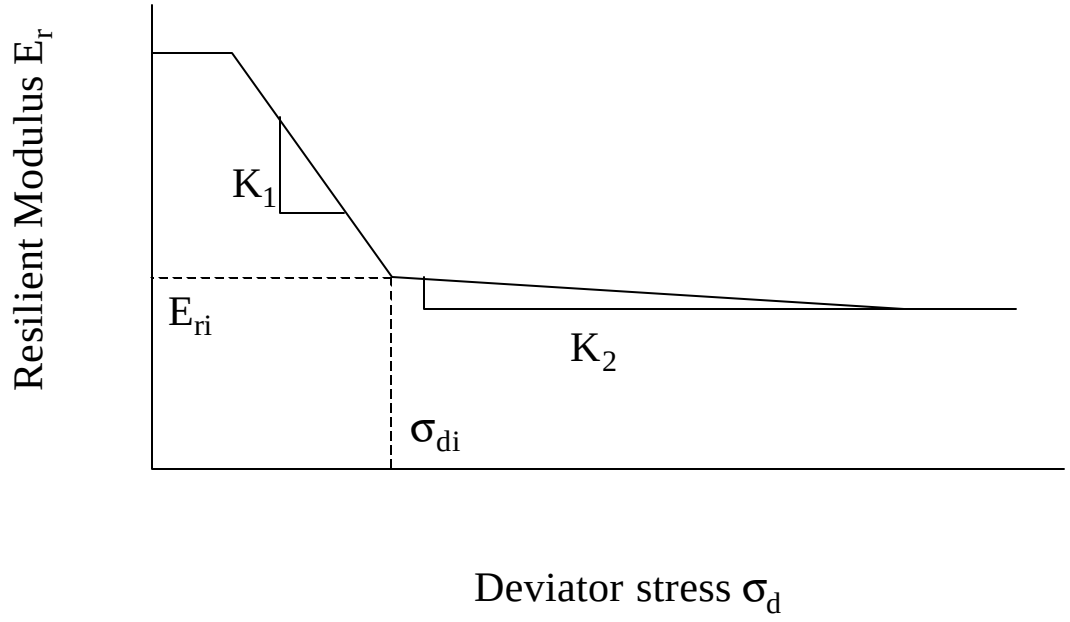

Figure 2.4. Thompson-Robnett Bilinear Model (Thompson and Robnett 1976)

Resilient modulus samples were prepared at a target unit weight but variable moisture content, leading to degrees of saturation ranging between 60 and 100%. Each moisture level included the testing of three replicates with all test results presented in Table 2.7.

As seen in Table 2.7, neither the dry unit weight nor the degree of saturation of the soil varied significantly from one sample to another from the same target group. Accordingly, a straight average evaluation was performed and the results are shown immediately after each set of 3 tested samples.

Table 2.7. Resilient Modulus Test Results for BE15 Soil

Sample	γ_d (kN/m^3)	w (%)	Sat (%)	E_{ri} (kPa)	σ_{di} (kPa)	K_1 (kPa/kPa)	K_2 (kPa/kPa)
1	17.5	11.5	61.0	119809	22.2	-3152.1	-35.187
2	17.4	11.9	61.7	126755	15.8	-5741.5	-123.41
3	17.2	12.5	62.5	116225	29.4	-4121.7	-258.11
Average	**17.4**	**12.0**	**61.7**	**120930**	**22.5**	**-4338.4**	**-138.9**
1	17.4	13.7	70.6	104801	17.9	-3614.1	-255.5
2	17.3	13.2	66.5	117780	22.2	-7323.7	-568.34
3	17.1	14.1	69.6	110967	23.4	-7364.8	-330.91
Average	**17.3**	**13.6**	**68.9**	**111183**	**21.2**	**-6100.9**	**-384.9**
1	17.4	15.9	82.5	56768	29.0	-5036.5	-368.97
2	17.2	16.5	83.1	71549	24.9	-4645.5	-498.25
3	17.1	16.7	82.2	82582	20.1	-11029	-710.86
Average	**17.2**	**16.4**	**82.6**	**70300**	**24.7**	**-6903.7**	**-526.0**
1	17.4	17.8	92.1	26058	18.7	-13777	-368.87
2	17.3	18.3	92.8	38326	17.5	-5786.7	-496.26
3	17.5	17.6	92.2	25224	19.9	-7059.2	-283.89
Average	**17.4**	**17.9**	**92.3**	**29869**	**18.7**	**-8874.3**	**-383.0**
1	17.1	19.7	97.0	11667	12.5	-2986.8	-68.686
2	17.2	19.7	98.6	11488	13.7	-4031	-33.317
3	17.3	19.4	97.6	11170	16.8	-2261.8	-5.1013
Average	**17.2**	**19.6**	**97.8**	**11442**	**14.3**	**-3093.2**	**-35.7**
1	16.8	21.2	99.2	9063	13.1	-2078.4	-22.941
2	16.9	21.2	100.7	9543	11.6	-1449.7	-8.5693
3	17.0	20.8	100.7	10714	11.8	-1895.4	-46.702
Average	**16.9**	**21.1**	**100.2**	**9773**	**12.2**	**-1807.8**	**-26.1**

A plot with all the average curves is shown in Figure 2.5. Although some slight inconsistencies, such as intersecting lines, are reflected in the plot, an effort was made to adjust these results as accurately as possible in a three-dimensional chart form. Linear equations for both groups (to the left and the right of the break point) of slopes of the type

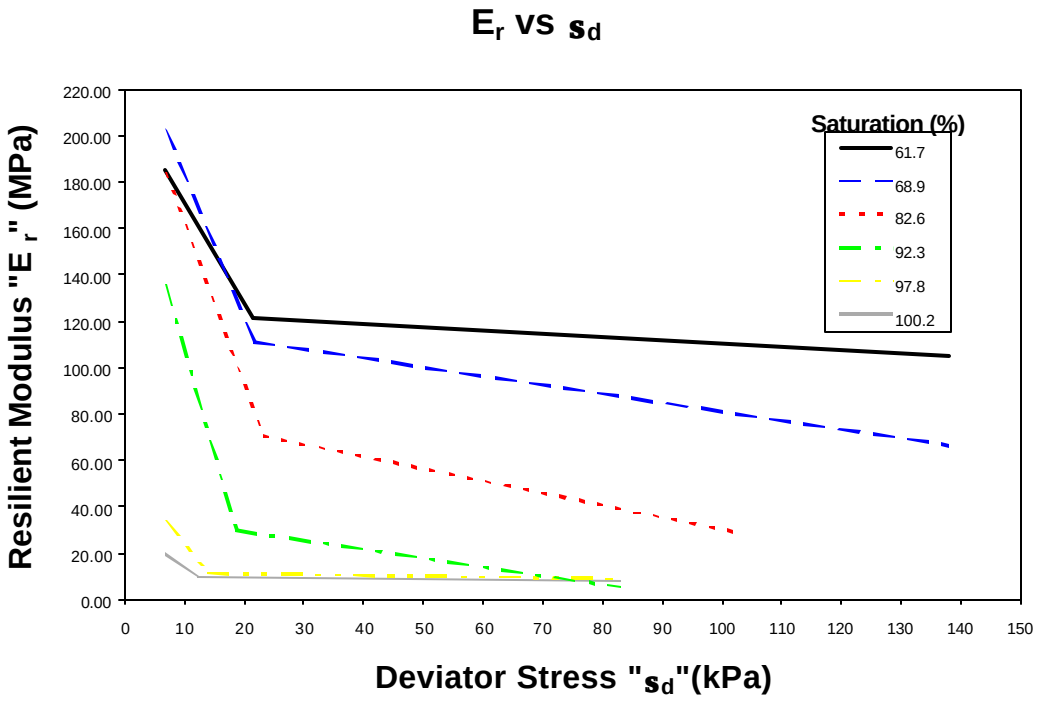

Figure 2.5. Results: Resilient Modulus vs. Deviator Stress at Different Degrees of Saturation

$$E_r = a + bS_r + c\sigma_d, \qquad (2.4)$$

(with E_r and σ_d in kPa and Sr as %)

were found with a coefficient of determination (R^2) for K_1 slopes of 85.3 percent, and for K_2 slopes of 95.7percent. The constants for the first group of slopes were:

$$a = 532461.8$$
$$b = -4406.1$$
$$c = -5418.3$$

And for the second group:

$$a = 318500$$
$$b = -3033.5$$
$$c = -258.8$$

This generalized chart is presented in Figure 2.6.

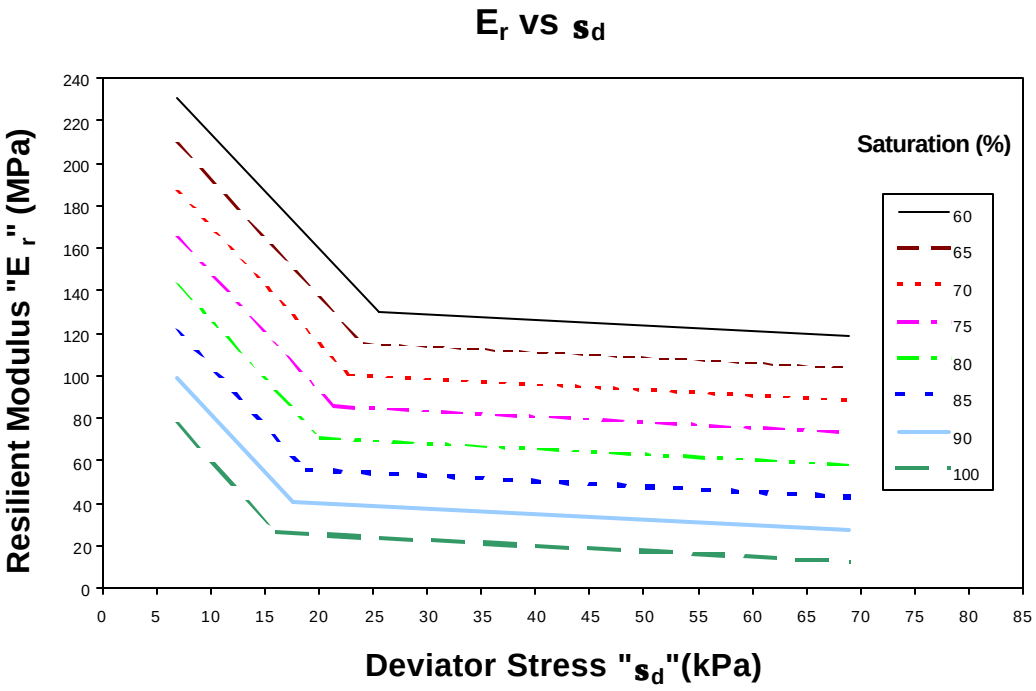

Figure 2.6. Resilient Modulus vs. Deviator Stress at Different Degrees of Saturation

A plot of Resilient Modulus at the break point vs. Saturation was configured using all eighteen test results and a linear relationship with a coefficient of determination (R^2) of 97.6 percent was developed, as shown in Figure 2.7, in which:

$$E_{ri} = 319.59 - 3.106 S_r \,, \qquad (2.5)$$

with:

E_{ri} = Resilient Modulus at the break point in MPa

S_r = Degree of Saturation in %

It should be indicated that this relationship agrees reasonably well with the relationship previously developed by Figueroa et al. (1994) for A-6 soils.

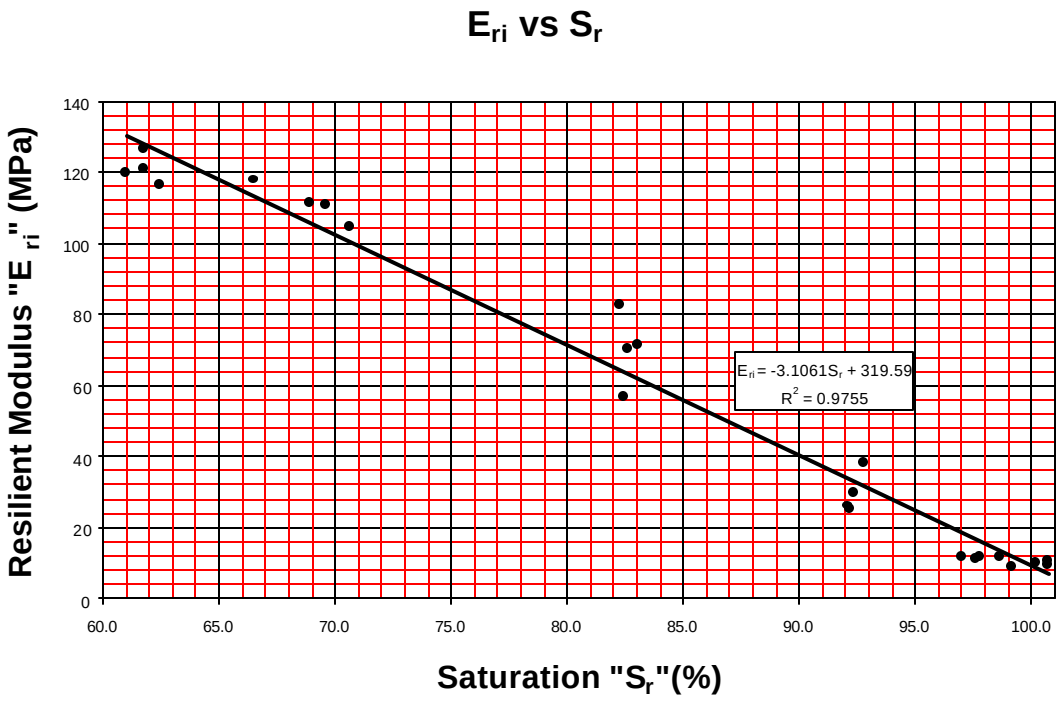

Figure 2.7. Resilient Modulus at the Break Point vs. Saturation

Charts of deviator stress at the break point and K_1 and K_2 vs. degree of saturation were prepared from the data contained in Table 2.7 as shown in Figures 2.8 and 2.9, along with their respective regression equations. It is to be noted that both K_1 and K_2 are barely affected by the degree of saturation and can taken as constants for all practical purposes

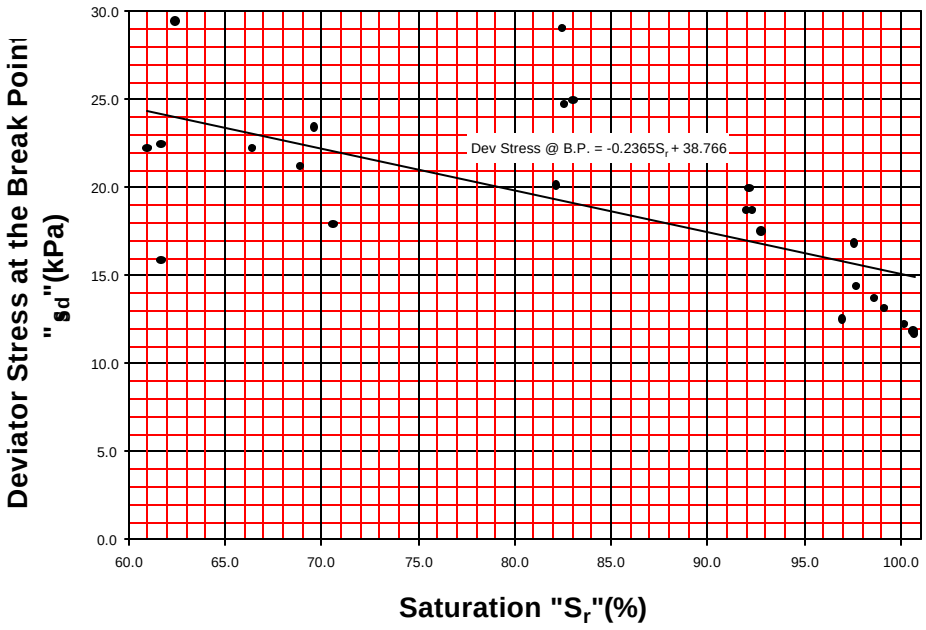

Figure 2.8. σ_{di}, vs. Degree of Saturation

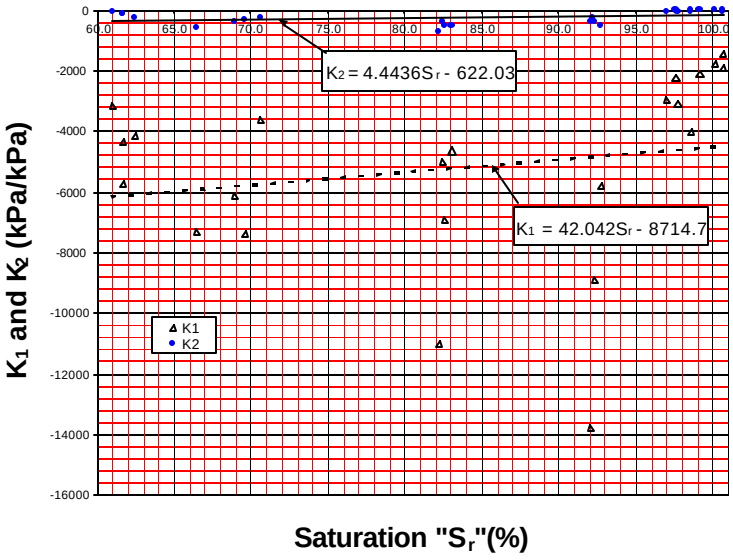

Figure 2.9. K_1 and K_2 vs. Degree of Saturation

2.4. Time Domain Reflectometry (TDR) Probe Calibrations

2.4.1. Overview

Time Domain Reflectometry (TDR) is an electromagnetic technique that has multiple uses such as spatial location and volumetric water content determination. Its first use is most commonly known as RADAR and dates from the 1930's. An electromagnetic signal is sent and any change in the medium is reflected and received by the source. Knowing the spatial characteristics and the reflected waveform, measurements such as distance, as a radar use, or moisture content can be determined.

Some of the areas of study where the TDR technique plays an important role include: soil moisture content determination, soil and rock deformation, structural deformation, and pore water pressure estimation.

Advantages of the TDR technique for moisture determination include a fast and simple analysis, a relationship between the dielectric constant K_a and θ=volumetric moisture content (VMC) that is non hysteretic and insensitive to drift (Suwansawat and Benson, 1999), a reasonable cost and availability for the used equipment, the option of being remote controlled, and the fact that is nondestructive once the probes are embedded at the desired location.

TIME DOMAIN REFLECTOMETRY SIGNAL

To calculate θ, the obtained dielectric constant K_a has to be evaluated. For this, an apparent length L_a determination has to be previously completed. After eliminating the non-significant losses generated in the signal propagation (Roth

et al., 1990) the dielectric constant can be estimated by means of the following equation:

$$K_a = \left[\frac{L_a}{(L)(V_p)}\right]^2 \tag{2.6}$$

where:

K_a= dielectric constant.

L_a= apparent length.

L= length of probe (m); (0.203m for FHWA probes).

V_p= ratio of actual propagation velocity to the speed of light; usually 0.99 (Klemunes, 1998).

Five methods are commonly used for the evaluation of L_a and these are: Method of Tangents (Raab et al., 1994, Klemunes, 1998); Method of Peaks (Raab et al., 1994, Klemunes, 1998); Method of Diverging Lines (Raab et al., 1994, Klemunes, 1998); Alternate Method of Tangents (Raab et al., 1994, Klemunes, 1998); and the Campbell Scientific Method (Bliskie, 1995, Klemunes, 1998).

For laboratory evaluation, Topp et al. (1985) recommended that the area of influence of the probe is 1.4 times the spacing between the rods. Other authors such as Knight et. al. (1994) suggested that the signal is practically unaffected at a one-rod spacing distance from the center of the probe, and Suwansawat (1997) and Suwansawat and Benson (1999) suggested that for probes with rod spacing dimensions of less than 60 mm, a length of 100 mm would include the majority of the field energy.

PREVIOUS MOISTURE CONTENT CALIBRATIONS

The best known calibration equation relating K_a and θ, was formulated by Topp et al. (1980) after conducting a total of 18 experiments that included 4 different types of soils. “Topp’s Universal Equation” is a third-degree polynomial and is shown below:

$$\boldsymbol{q} = -0.053 + 0.0292K_a - 0.00055K_a^2 + 4.3\times10^{-6}K_a^3 \qquad (2.7)$$

Topp suggested that his relationship was practically unique, but recent studies by Helkelrath et al.(1991), Roth et al. (1990) and Suwansawat (1997), disagree with this fact.

Klemunes (1998) studied a total of 28 different types of soils developing a best fit equation model and a hierarchical methodology that combines a regression equation with the mixing model theory.

The best fit equation is presented below and was obtained by evaluating K_a by the method of tangents.

$$V_w = \left(1.8612e^{(-0.0263K_a)}\right)K_a^{\,1.1081} \text{ if } \left(K_a \le 35\right) \qquad (2.8)$$

$$V_w = \left[38.046 + 0.2022\left(K_a - 35\right)\right] \text{ if } \left(K_a \ge 35\right) \qquad (2.9)$$

Where V_w is the same volumetric moisture content (θ).

His second methodology includes four different levels of volumetric moisture content evaluation depending on the known characteristics of the material in study. Level 4 is a general model for all soils; level 3 predicts the moisture content if information on whether the soil is coarse or fine-grained is given; level 2 can be used if the AASHTO classification is known, and level 1

could be used if the specific soil is calibrated in the laboratory. The most accurate and recommended level is the first one (level 1). Level 2 lacked information in certain areas such as the soil types A-6, A-7-5 and A-7-6.

His hierarchical model is represented by the following equation:

$$V_w(\%) = \frac{(5La - 1) - B_0 \frac{g_d}{G_s g_w}}{B_1} \qquad (2.10)$$

Where B_o and B_1 are the best fit coefficients and are given by the approaching level (1 to 4).

2.4.2. Laboratory Calibration Procedure

EQUIPMENT

The equipment used primarily consisted of a Tektronix 1502C Cable reader, FHWA TDR probes, a multiplexer, and a portable computer as the data acquisition system.

The Tektronix 1502C consists of a pulse generator that produces a voltage, a sampler which transforms the signal from high to low frequency, and an oscilloscope that records the reflected signal. The Tektronix 1502C sends an electrical pulse to the cable and measures the reflected signal. Since the unit is sensitive to impedance changes, a curve with peaks is recorded detecting any discontinuity.

The TDR (FHWA) probe, has three rods each about 0.203 m long. The rods have a separation of 38.1 mm between each other, and are connected to a circuit board which in turn is connected to a coaxial cable. The coaxial cable may

be connected to the multiplexer (for multiple sensors) or directly to the Textronix 1502C (for a single sensor).

The multiplexer has the function of controlling the different transmission channels. The 10 probes installed in each section of the Ohio Test Road are connected to the multiplexer, which is in turn connected to the Textronix 1502C. The multiplexer “jumps” from one probe to the next to collect the curve trace similar to that shown in Figure 2.10. In the calibration experiments conducted in the laboratory the multiplexer was used to connect 5 different probes.

PROCEDURE

Three constant dry unit weight groups of 5 samples each were subjected to the measurement of their TDR response at different moisture content levels. Each group of samples was prepared at a target compaction level (dry unit weight).

Plywood boxes with approximate dimensions of 266.7 mm (10.5 in) in length, 165.1 mm (6.5 in) in width and 120.6 mm (4.75 in) in height, served as containers of the soil samples. These dimensions were selected to fit the TDR probe and to assure a minimal effect on the signal as a result of the proximity of end restraints.

Soil was weighed to achieve a desired dry unit weight and different amounts of water were added to obtain various levels of the gravimetric moisture content. The influence of the probe is approximately a cylinder with a diameter of 1.4 times the spacing between the rods (Topp et al., 1985) so the first compacted

layer reached an approximate thickness of 1.5 inches. The probe was placed and another layer of soil was compacted until all weighed soil was used. If the obtained height after compaction was larger than desired, the sample was statically compacted on a universal material testing machine to achieve the required volume and consequently the target dry unit weight.

Three groups of 5 homogenous samples, each of the 5 at a different moisture content were tested. Measurements of TDR signals and gravimetric moisture content (ASSHTO T265-91, ASTM D2261-90) were taken after approximately one day of sample preparation to assure moisture uniformity in the soil specimen.

The volumetric moisture contents obtained in the laboratory were compared with the TDR traces to develop a suitable probe calibration, applicable to the embankment soils existing at the Ohio Test Road Site.

2.4.3. Results

Klemunes (1998), in his research for the FHWA, determined that the best way to obtain the apparent length L_a to calculate the volumetric moisture content of the soil was to use the Method of Tangents.

This method, shown in Figure 2.10, determines the first inflection point of the signal (Point A) at the intersection of the maximum horizontal tangent, and the inner tangent of the signal. The second point (Point B) is given by the intersection of the minimum horizontal tangent and the outer tangent. The apparent length L_a is given by the distance between both points.

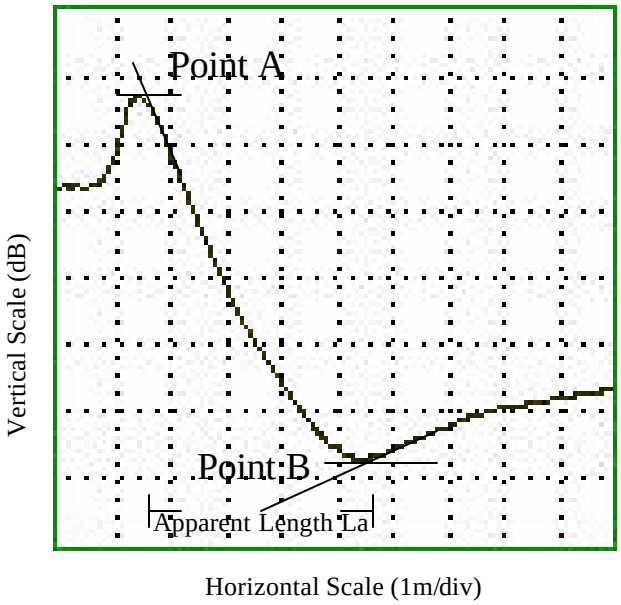

Figure 2.10. Method of Tangents (Klemunes, 1998)

Based on Klemunes' statistical analysis, who obtained a coefficient of determination of 81 percent, this method was chosen for the current study.

Two ways to calculate the volumetric moisture content were established by Klemunes (1998). The first one accounts for the best fit of experimental data, and the second one has a mathematical mixing model approach refined by his experimental results. The best fit equation is a composite model given by the following equations:

$$V_w = \left(1.8612e^{(-0.0263K_a)}\right)K_a{}^{1.1081} \text{ if } \left(K_a \le 35\right) \quad (2.11)$$

$$V_w = \left[38.046 + 0.2022\left(K_a - 35\right)\right] \text{ if } \left(K_a \ge 35\right) \quad (2.12)$$

The mathematical approach estimates the volumetric moisture content by means of the equation:

$$V_w(\%) = \frac{(5La - 1) - B_0 \frac{g_d}{G_s g_w}}{B_1} \quad (2.13)$$

Where, B_0 and B_1 are coefficients that depend directly of the type of soil and have been estimated from his experimental results.

In Klemunes' study, values of 1.5 for B_0 and 7.56 for B_1 are recommended for fine grained soils (level 3) unless a previous calibration determines more accurate coefficients. For this particular study values of 0.9 for B_0 and 9.8 for B_1 were estimated as the best fit coefficients for the most accurate calculation of the volumetric moisture content in the field.

Knowing these two approaches, relationships were developed from the analysis of experimental data, obtained after testing the subgrade soil, to optimize the volumetric moisture content in the field by TDR procedures. Figure 2.11, shows the relationship between the laboratory results, the equation of best fit and the mathematical model.

From these results, line of equity plots were developed for both methods to select the equation to be used to obtain the volumetric moisture content of the soil under consideration. Figures 2.12, 2.13 and 2.14 show this line of equity relationship and their coefficient of determination (R^2).

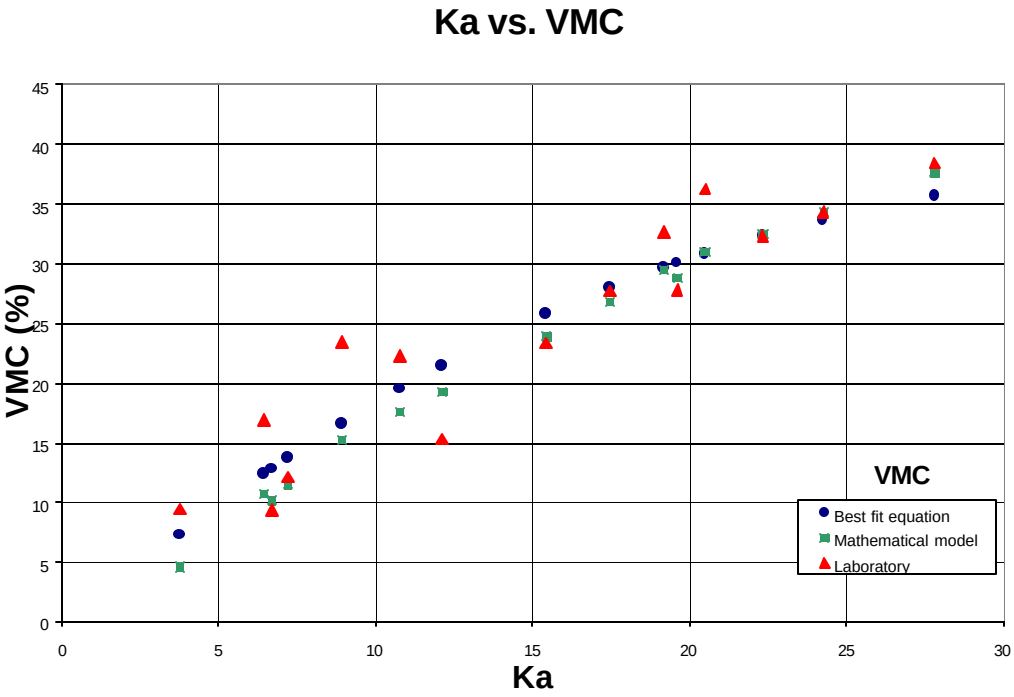

Figure 2.11. Volumetric Moisture Content vs. K_a for All Methods of TDR Estimation

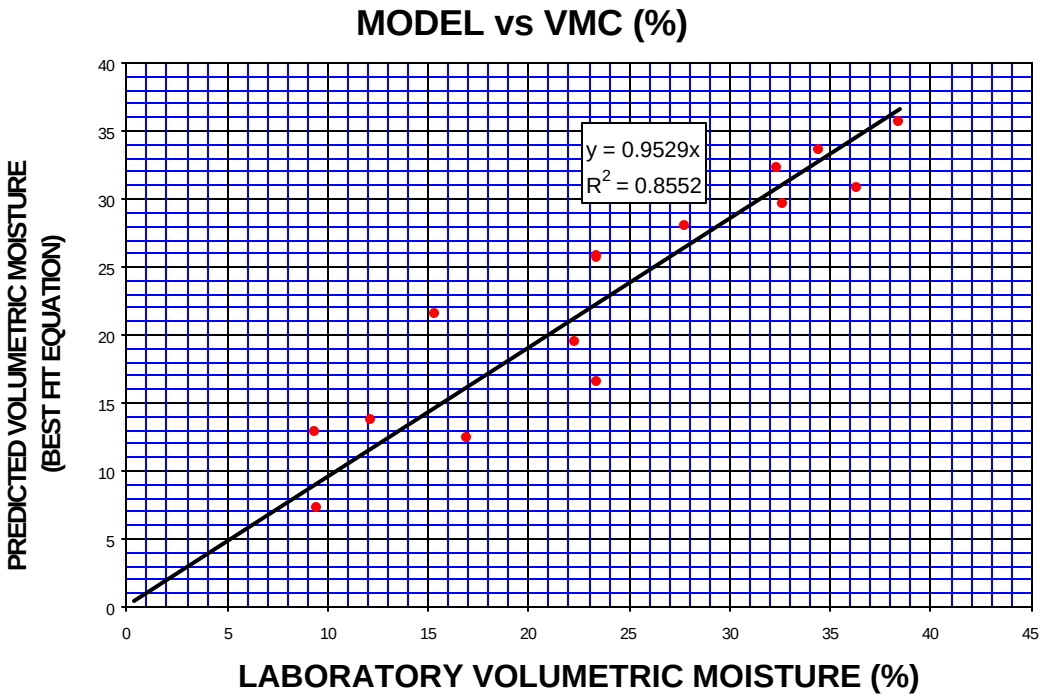

Figure 2.12. Best Fit Equation: Predicted Volumetric Moisture Content vs. Laboratory Moisture Content

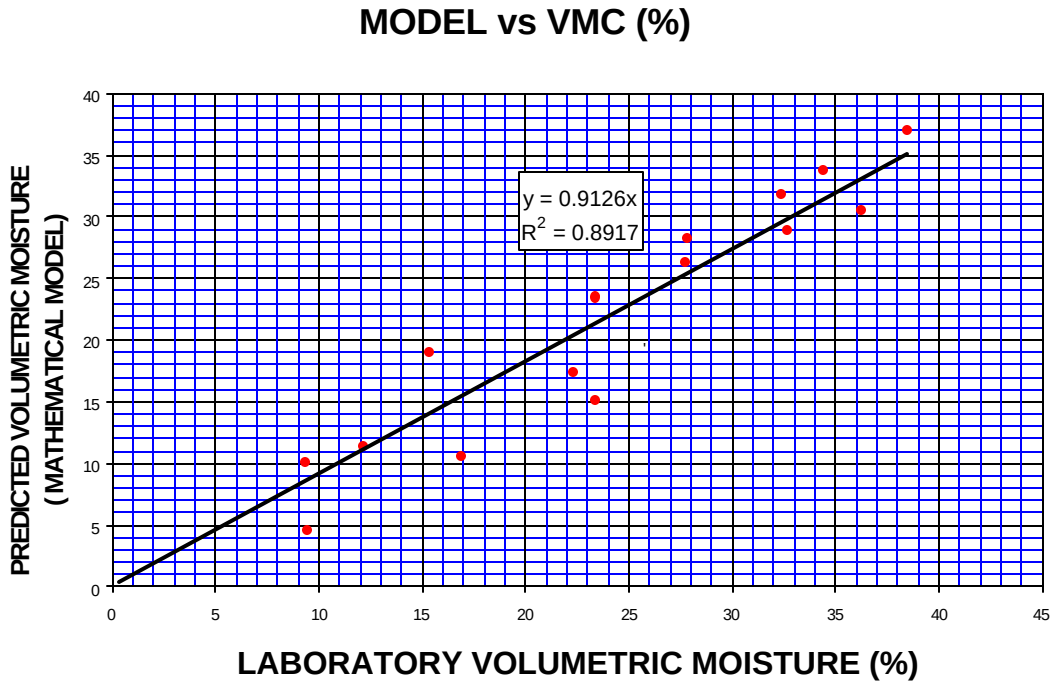

Figure 2.13. Mathematical Model Prediction: Predicted Volumetric Moisture Content vs. Laboratory Moisture Content

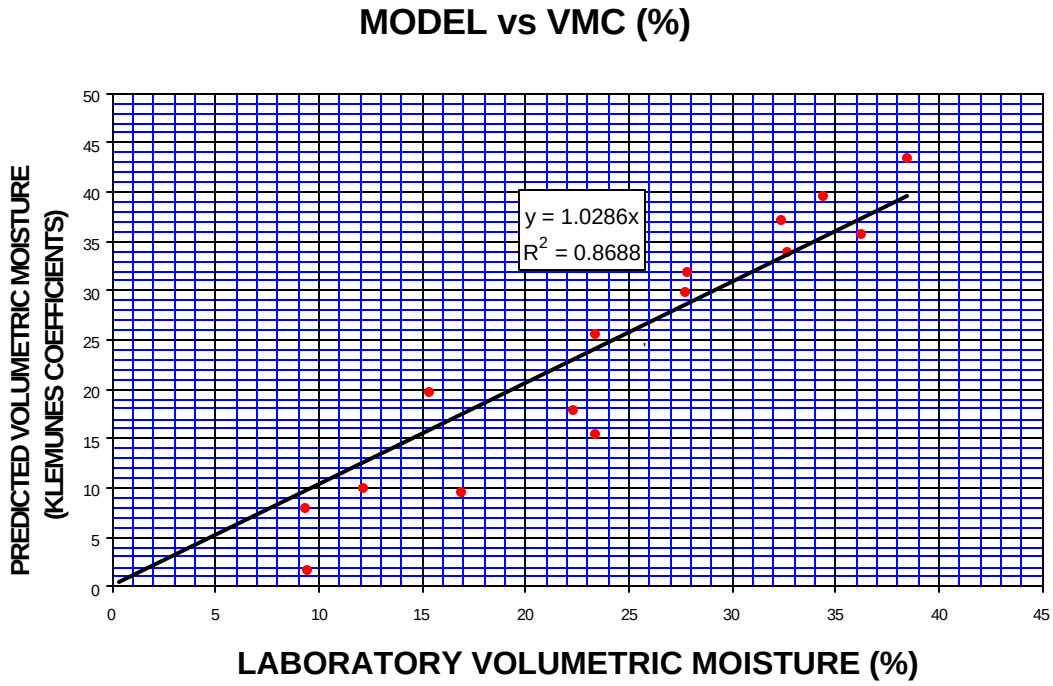

Figure 2.14. Mathematical Model Prediction: Predicted Volumetric Moisture Content vs. Laboratory Moisture Content (Klemunes coefficients for fine soils)

With values of 85.5 and 89.2 percent for the best fit approach and the mixing model respectively, the accuracy in the estimation of the volumetric moisture content is reflected.

An additional best fit procedure was attempted on the laboratory results. A plot of the three experiments shows a variation in the volumetric moisture content obtained by the TDR method considering different dry unit weights. Values of 14.93, 17.29 and 18.86 kN/m^3 (95, 110 and 120 lb/ft^3), were nominally selected for the calibration. However; depending on the obtained final volume and gravimetric moisture content these values slightly varied from their target figure. A plot of these experiments showing a trend line for each group of unit weights is depicted in Figure 2.15.

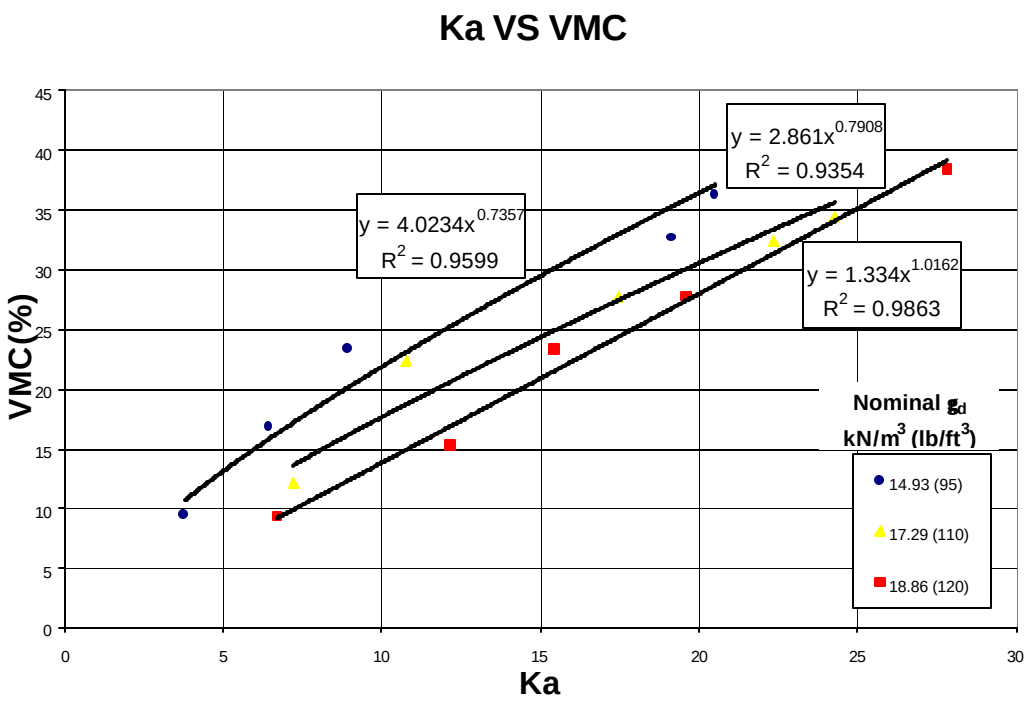

Figure 2.15. Laboratory Volumetric Moisture Content vs. Ka for Different Dry Unit Weights

A multi variable regression analysis was conducted with the dry unit weight and the dielectric constant as the independent variables and the volumetric moisture content as the dependent one. A polynomial equation was developed, resulting in R^2 values above 97.8 percent indicating the close correlation existing between the variables. This equation is presented below with its respective coefficients.

$$\boldsymbol{q} = a + bK_a + cKa^2 + d/g_d \qquad (2.14)$$

Where θ is the volumetric moisture content, K_a the dielectric constant and γ_d the dry unit weight.

With coefficients equal to:

$$a = -25.807$$
$$b = 1.947$$
$$c = -0.0198$$
$$d = 2761.867$$

This representation is shown in figures 2.16 and 2.17 showing along with the two other models for volumetric moisture content prediction by the TDR technique.

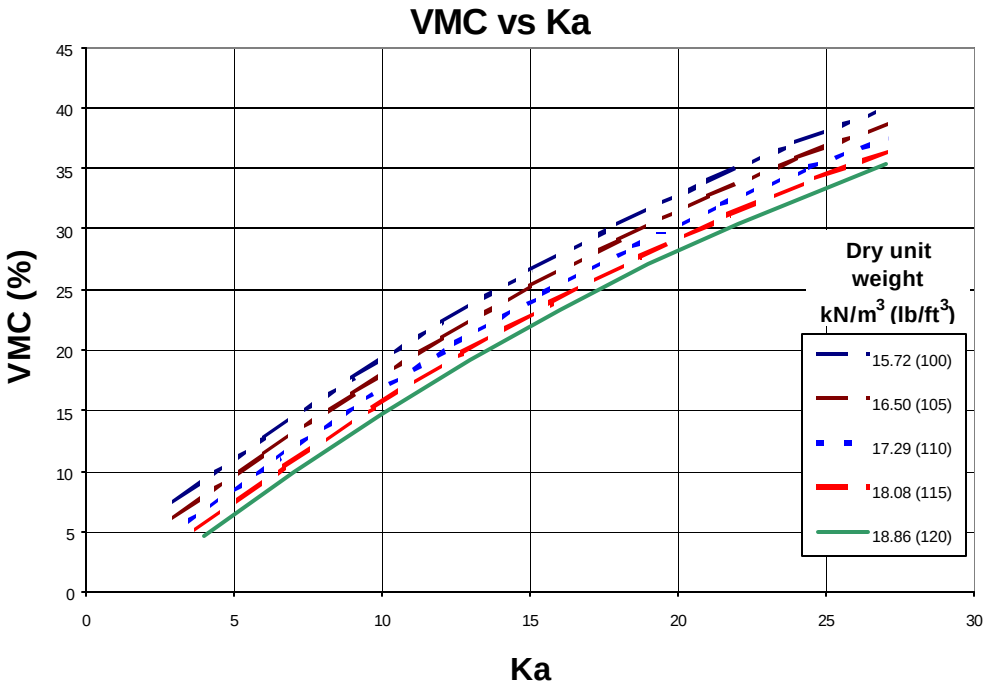

Figure 2.16. Variation of the Volumetric Moisture Content vs. Ka and γ_d

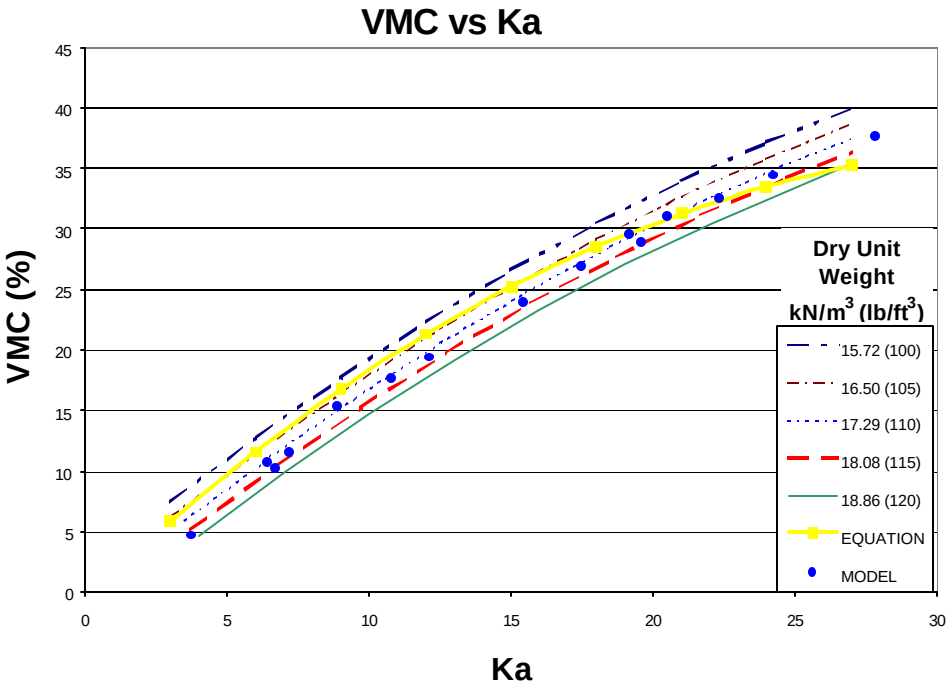

Figure 2.17. Variation of the Volumetric Moisture Content vs. Ka and γ_d (including equation and model)

Chapter 3

SEASONAL AND WEATHER DATA PROCESSING

3.1. OVERVIEW

This chapter describes the type of seasonal and weather data files collected at the Ohio test road site to be used in subsequent chapters. Some of these data files needed to be modified to meet SHRP uploading guidelines.

Each seasonal instrumentation station is capable of collecting pavement and soil temperature on an hourly basis using the continuously operating Onsite unit, while a second setup consisting of the Mobile unit is scheduled to obtain volumetric moisture contents with depth along with resistivity measurements. Resistivity readings are intended to detect the depth of frost penetration. Both moisture content and resistivity readings are obtained normally once a month. The frequency is increased to twice a month during March and April.

The weather station operates continuously and it is programmed to store data summaries on an hourly and daily basis. Description of quantities being monitored will be presented letter in this chapter.

3.2. DATA RETRIEVAL

3.2.1. Onsite Unit

As mentioned above, the Onsite unit for monitoring temperatures operates continuously; however data must be downloaded to a personal computer once a month by connecting a serial cable and an interface (for PC protection) to the CR10 Onsite logger unit and executing the program CR10x, provided by SHRP. Using a station file (*.stn) residing in the working directory corresponding to the designated test section, the CR10 is instructed of the date and time of data collection. The station file is then updated automatically for its use during the following month's data collection schedule.

After downloading is complete, the user is offered the option of checking if the data has been downloaded properly, through the intrinsic execution of the ONSFIELD program. This program allows the user to graphically view the temperature data.

3.2.2. Mobile Unit

To begin data acquisition with the Mobile unit, the resistivity and TDR probe cables existing at each test section pull box must be connected first to the numbered ports of a multiplexer. Next, a TDR cable tester is connected to the multiplexer board and a CR10 logger unit, which in turn is linked with a serial cable and interface to a portable computer. The CR10x program is executed to

upload the source code and time to the CR10 to activate the cable tester and resistivity monitoring unit. Once the data collection is completed and uploaded to the computer, the quality of resistivity and TDR data can be checked in the field by the intrinsic execution of the MOBFIELD program. All ten TDR traces corresponding to each moisture sensor are displayed as well as a graph of the resistivity values throughout the subgrade. Should problems be immediately visible in the graphs, the user can repeat the monitoring process.

3.2.3. Weather Station

Weather station data can be collected with a frequency of up to six months, in view of the storage capabilities of the CR10 unit, managing the weather station components. As per SHRP's guidelines all stored files are uploaded to a portable computer using a comma-delineated format. This is achieved through the program SMCOM and physically connecting the portable computer to the weather station CR10 through the serial interface. As in the previous two cases file quality can be checked through the program AWSCHECK

3.3. DATA PROCESSING AND UPLOADING

Once data has been downloaded from the CR10's at both the seasonal sites and the weather station, it has to be checked and edited for quality. If the data meets quality assurance checks, it can be uploaded to the LTPP database. From this point, the data can be accessed by any organization wishing to examine and analyze the results.

To facilitate the process of data analysis, two computer programs are provided by SHRP to analyze and edit the data in a consistent format. A separate program was supplied for both seasonal road data and weather station data. The former is known as SMPCheck (Seasonal Monitoring Program Check), while the latter is known as AWSCheck (Automated Weather Station Check). Both provide a menu-driven front-end that allows for easy use on a DOS platform.

A typical SHRP Onsite station contains air temperature and rainfall gages. However, because of the compactness of the Ohio Test Road and the significant number of Onsite tests sections (18), it was deemed appropriate to use the air temperature and rainfall data collected at the weather station for all Onsite sections. Obviously, the files collected at each of these stations do not contain the air temperature and rainfall information required for the successful uploading of these files. It was then necessary to write a computer program (RW.BAS) to process each .ONS files where both air temperature and rainfall

data (extracted from the weather station files) are inserted in the proper fields to meet SHRP processing and uploading guidelines. A description of this program is presented next.

3.3.1. RW.BAS Program

As previously indicated, this program was written to facilitate the extraction of air temperature and rainfall data from weather station files to be inserted in the proper fields in files collected at the Onsite station. The RW.BAS program is written in GWBASIC with a text copy included in Appendix A.

Before using this program, it was necessary to append and divide the collected weather station files into separate files containing weather station data for a complete year spanning from January 1st to December 31st. These files were prepared using a text editor and were named Y1996, Y1997,….Y2002. These files need to be placed in the DOS working directory along with the files to be modified to include air temperature and rainfall data, before execution of the RW.BAS program can begin.

Following SHRP's naming protocol, a typical Ohio Test Road Onsite file would be named 39SC02ED.ONS indicating that this seasonal (S) file was collected in Ohio (39) at section C (corresponding to section 390212) and being the fifth (letter E in the alphabet) file collected in the year 2002 (02) in April (letter D). The .ONS file extension indicates that it corresponds to the Onsite logging

unit. Files collected by the Mobile unit to obtain the soil moisture content follow identical naming guidelines, except that the file extension changes to .MOB.

When the RW.BAS program is executed, it queries the user for the filename to be modified (such as 39SC02ED.ONS) as well as the name of the modified file (such as 39MC02ED.ONS). Note that M has replaced S indicating that this is a modified file from the original, with the inserted air temperature data at the corresponding times of the day and days at the proper data fields to allow processing for quality assurance through the SMPCHECK program.

3.3.2. SMPCheck Program

The SMPCheck Program requires the user to specify a site and to enter relevant installation data such as sensor depth and soil properties specific to that site. The user can then monitor the onsite and mobile data using graphs prepared by the program. In order to meet SHRP specifications, the data must pass a Level D check before it can be uploaded. This check is performed by the program alerting the user to the current status. If the data passed all checks, an upload file can be created whereas data that failed must be edited for content. All can be done within the program.

3.3.2.1. Procedure

Once the SMPCheck program is installed and executed, the user is immediately prompted for a specific site identification number that includes state code, site letter designation, and the SHRP number. For Ohio, the SPS2-J12 section, for example, would be entered as 39 P 0102. Once the Escape key is pressed, the program creates a subdirectory within the SMPCHECK directory, in this case 39P, which in itself contains five subdirectories: CHKFILE, IMSDATA, ONSDATA, MOBDATA, and PROINFO. The user must then copy the individual onsite and mobile data files downloaded and modified (in the case of .ONS files) from the CR10s into the ONSDATA and MOBDATA directories, respectively. It is important that these files be previously renamed according to SHRP guidelines, as previously indicated.

With each site directory created, the DATA PROCESS menu is selected that allows the user to enter project data, or to process onsite and mobile data. If the “Project Data” option is selected, the user has the option to enter one of five types of site data. This includes information that was collected during sensor installation at each site and was recorded on the corresponding data sheets provided by SHRP. The identification number of each data sheet corresponds to the number following the available options on the menu, and include:

1) Instrument Location and TDR Depth (IO2),
2) Thermistor Probe Depth (CO2),

3) Resistivity Probe Depth (CO3),
4) Field Gravimetric Moisture Content (IO5), and
5) Field Measured Dry Density (IO7).

Once all available data is entered, the computer automatically stores the information in the PROINFO subdirectory where it must now be checked for quality. This is done by choosing the OFFICE QC option on the main menu, and then selecting the "C and D Level" option. The program will then check the data for allowable content based on SHRP's guidelines, and a file named SC#*.qc (where SC is the two-digit state code, # is the site ID, and * is either 'MANUL, ONSIT, MOBLE, or PRJCT' depending on the type of data being processed) will be created in the CHKFILE subdirectory. Using any editor, the user can view this file to determine if the data has passed Level D status. If it hasn't, the user must find and correct any mistakes made on the data entry screens and execute the quality check again.

With project data entered, the user can proceed to process the onsite, mobile, or manual data that has been collected. Manual data consists of any preliminary readings collected with equipment other than the onsite and mobile dataloggers. If required, all sensors can be monitored including air temperature probes and rain gauge devices now contained in the modified files. Equipment for manual data collection is described in the Seasonal Monitoring Program Guidelines and will not be discussed here.

At this time, the user can process onsite or mobile data. If the “Onsite Data” option is selected, the program displays all data files available in the site directory for processing. One or all of the files may be selected, whereupon a screen is displayed listing all chosen files and their start and end dates for data collection. Typically, these files will have overlapping dates which the computer will adjust automatically. If two or more files start on the same day, it is only necessary to select the one file that has the latest end date. If necessary, the user may make time corrections for Daylight Saving Time by adding or subtracting up to two hours from specific days. Data file groups for a given year (say the year 2002) were processed including a maximum of 14 .ONS or .MOB files, since data collections are normally conducted on a monthly basis, except for March and April when moisture data is collected twice. The number of files that can be processed at once is limited by the available memory in DOS

With this complete, the program checks the data files, adjusts for overlap and time corrections, and then prepares six graphs that include the following:

1) daily average, min, max air temperature and rainfall data,
2) daily average air, rainfall, and first 5 MRC sensors temperature data,
3) daily all 18 MRC sensors average temperatures,
4) daily all 18 MRC sensors maximum temperatures,
5) daily all 18 MRC sensors minimum temperatures, and
6) hourly air temperature, rainfall, and first 5 MRC sensors temperature data.

With the graphs displayed, the user must scan for possible data points that are clearly inaccurate and that may reveal equipment malfunction. If any are

found, the editing keys listed on the screen are used to remove the points. At this point the program generates two files: an edited file such as 39CONSIT.EDT for section C and a file named Rt56limt.RNG containing plot scaling limits which are stored in the ONSDATA subdirectory. With this complete, as with the project data, the onsite data must pass a level D quality check. To do this, the OFFICE QC option is again selected on the main menu, followed by the "C and D Level" option. Once "Onsite Data" is chosen, the computer performs a quality check similar to that performed by the user. The results of this check are written to two files, 39Consit.msg and 39Consit.qcr (for the processed section C), that are placed in the CHKFILE subdirectory. When viewed, the *.qcr file lists the status of each type of data field checked by the program. For Onsite and Mobile data, the description of every field is listed in Appendix B of the Seasonal Monitoring Program Guidelines. If a field did not pass level D status, as required by SHRP, a description or list of the bad data points is provided so that the user can return to the graphs and remove the faulty data in the edited file. Appendix A of the SMPCheck Manual (USDOT-FHWA, 1996) provides sample graphs of acceptable and unacceptable data to help the user identify bad data points. The quality check must be performed each time the data is edited until every field passes Level D. Should the user attempt to create an upload file, any data not passing Level D will not be included.

As in the Onsite data, the mobile data analysis is conducted in a similar manner. Once selected, plots of the TDR traces and resistivity values are displayed. For mobile data, however, it is only necessary to choose those plots which are valid by typing the corresponding number under the graph, while inaccurate points in the resistivity plot can be individually edited out. Appendix B of the SMPCheck manual provides samples of acceptable and unacceptable data. The computer will include these plots for processing and quality control when the OFFICE QC option is selected. Again, a 39Cmoble.msg and a 39Cmoble.qc file (for section C) are created displaying selected data and quality control status, respectively. These files are stored in the CHKFILE subdirectory. If a file does not pass Level D, the mobile data must be re-evaluated to find the problem. Similarly an edited filed such as 39CMOBLE.EDT (for section C) containing edited TDR and resistivity traces is generated and stored in the MOBDATA subdirectory.

To preserve edited and quality control data, it was deemed appropriate to change the extension of all files generated indicating the year of data. For example for Onsite and Mobile data corresponding to 2002 the file extensions were changed from:

.MSG	to	.M02
.QC or QCR	to	.Q02
.EDT	to	.E02
.RNG	to	.R02

This step was necessary after preparing the upload files, since the processing of a new group of files corresponding to a different year overrides existing files with extensions MSG, QC, QCR, EDT and RNG.

With all of the project, manual, onsite, and mobile data passing quality level D, it is then necessary to create the upload file to be sent to the data storage facility. This is performed by selecting the IMS OUTPUT option on the main menu followed by the "Create Upload File" option. A screen appears displaying all of the data available for upload (which has passed Level D), and the user is prompted to select which data to include in the upload file. Any or all of the data can be selected whereupon the computer creates a file in the IMSDATA subdirectory following the format below:

ssmMddyy.UPL

where ss is the LTPP two digit state code in which the test section is located
39 for Ohio,
m is the SMP multiple site agency code; A= 1st SMP section in state,
B=2nd, C=3rd such as 390212….
M is the letter designation for month that upload file is created; A-Jan,
B-Feb……,
dd is the day the upload file was created,
yy are the last two digits of the year the upload file was created, and
UPL is the file name extension used for all upload files (SMPCheck '96, D-1).

A second file with the same name but extension .LOG is also generated and placed in the IMSDATA subdirectory containing the range of dates spanning the data processed and the type of project data included in the .UPL file. With the

creation of the upload file, the analysis is complete, and the user can begin the process on any remaining instrumentation sites.

Summaries of processed files for each monitored section are included in Appendix B1 for Onsite (.ONS) data files and in Appendix B2 for Mobile (.MOB) data files. Some of the original files collected needed to be renamed in order to follow SHRP naming guidelines. Both old and new names are included in the summaries. The summaries also contain the start and end date and time for ONS files following the Julian calendar and the data collection date for MOB files

3.3.2.2. Problems

In all, the SMPCheck program is straightforward and easy to use. However, a few problems were encountered that did not allow the program to complete execution and prepare the data correctly.

The first of these problems involved time overlaps within the same Onsite file. Although the program was developed to eliminate the overlaps between separate data files, it cannot remove an overlap within one file. Therefore, it was necessary to manually edit the file and delete the repeated data. In addition, many data files began with fields that had been cut in part during data collection because of the ring memory type of storage in the CR10, and as a result did not specify a field number. Again, these lines were manually deleted.

Once the program was able to execute properly, several problems were found in the Onsite data for every site. These were noticeable while viewing the daily maximum and daily minimum soil temperature graphs. At several days throughout the year, large, unexplained upward or downward spikes appeared in all of the sensor readings. While this may not be uncommon for sensors near the pavement surface, sensors in the deeper subgrade soil typically maintain constant temperatures with little or slow variation on a day to day basis. It was noticed, however, that these spikes only occurred on days that data was downloaded from the onsite units. It is believed that these spikes were the result of the datalogger preparing the daily report for this date, with only a partial record of hourly data available to determine daily highs, lows, and averages. All these spikes were subsequently eliminated from the edited ONS files

3.3.3. AWSCheck Program

The AWSCheck Program (USDOT-FHWA, 1996) used to monitor weather station data follows the same format and procedure for the SMPCheck Program previously described. Again, the data is displayed graphically whereupon the user removes unreasonable data points, and an upload file is created providing the data passes the level D check.

3.3.3.1. Procedure

Like the SMPCheck Program, the user is immediately prompted for the site identification for the weather station that includes the state code, site code, and SHRP section ID. For Ohio, the state code is 39 and the site code is 'A'. Site code is determined from the number of weather station sites in the state using 'A' for the first, 'B' for the second, and so on. As for the SHRP section ID, it was assumed that this would be the number for the site closest to the weather station since it was not actually installed at a particular test site. For the Ohio Test Road, the closest section was SPS2-J3, or 0203. Once this has been entered, the computer creates subdirectories much like those described above. The user must then copy the collected data files to the newly created AWSDATA subdirectory, and then proceed to process the project data and weather station data. Project data consists of information relating to weather station positioning

at the site such as elevation, latitude, and longitude, and is only entered once for the only weather station installed at the Ohio Test Road.

After selecting the “AWS Data” option under the “Data Processing” menu, the user must select which data files to be processed. Data files that begin on the same date, but end with different end dates will be combined by the program unless the user specifies which file to use. Again, a correction for Daylight Saving Time is available that allows up to two hours to be added or subtracted from within desired time spans.

With this complete, the “View selected data” option is chosen, and the program displays several options for viewing, including:

1) daily average, min, max air temperature and precipitation data,
2) daily relative humidity, solar radiation, and precipitation data,
3) daily wind information
4) hourly temperature and precipitation data,
5) hourly relative humidity and precipitation data,
6) hourly solar radiation and precipitation data, and
7) hourly wind information.

As with the Onsite data, the weather station data must be checked for quality and consistency. Options 1 through 3 above only permit viewing of the data, while options 4 through 7 permit the user to edit the data manually. Obvious faulty data, such as extremely high or low temperatures for a season, is removed by selecting a start date and end date, and then deleting the points in between. After all of the data has been checked and edited if necessary, the “Office QC” option is selected from the main menu, followed by the “C&D Level” option. The

computer then checks the data for allowable ranges and writes the status level to a file in the “CHKFILE” directory. If the status has passed Level D, an upload file may be created as done with the onsite data. If necessary, the user must re-edit the data until the status passes Level D.

Summaries of processed weather station files are included in Appendix B3, depicting start and end date and time, following the Julian calendar.

3.3.3.2. Problems

Unlike the SMPCheck program, processing ran smoothly for the weather station data, and an upload file was created with very little editing required. The only problem involved the weather station itself in which during the first activation of the station, the selected option in the uploaded program to the CR10 indicated that the unit would stop collecting data after all memory had been used, rather than selecting the ring memory option where the oldest data is deleted to provide space for new data. As a result, several weeks of data are missing and appear as a blank area on the graphs. Fortunately, however, this does not affect the data that was obtained. Subsequent operation of the weather station has been performed with the ring memory option that allows for up to approximately six months of data storage without any losses between collection periods.

THIS PAGE LEFT INTENTIONALLY BLANK

Chapter 4

SEASONAL FINDINGS

4.1. Introduction and Data Analysis

Pavement life depends on its loading history and on the climatic effects to which it is subjected. To understand these weather phenomena, the Ohio Test Road was fully equipped with sensors that are capable of measuring temperature in the pavement and the soil moisture at different depths. It is also equipped with a weather station, thus relationships between the climate and the pavement conditions maybe established.

Data has been collected in a nearly continuous basis from the time the test road was open to traffic in mid-1996 until the time of writing of this report. Some of the test sections have already failed and have been replaced. Thus, the original instrumentation of these sections either ceased to work or was removed during section replacement. Results including solar radiation vs. temperature relations, temperature differentials in PCC slabs, asphalt concrete temperature relations, moisture content estimations and depth of frost penetration predictions are discussed.

DATA ANALYSIS

The analyzed data was checked and edited for quality by means of: the Seasonal Monitoring Program Check (SMPCheck Users Guide, 1996) and the Automated Weather Station Check (AWSCheck Users Guide, 1996) program, as it was described in the previous chapter. Both programs provide a menu-driven

front-end that allows for easy use on a DOS platform, permitting the user to edit out faulty data.

The “Onsite” information is continuously collected, and every month is downloaded to a computer. The program groups the different collected files, adjusts for overlaps and time corrections, and prepares the following plots:

1. Daily average, min, max air temperature and rainfall data.
2. Daily average air, rainfall, and first 5 MRC sensors temperature data.
3. Daily all 18 MRC sensors average temperatures,
4. Daily all 18 MRC sensors maximum temperatures,
5. Daily all 18 MRC sensors minimum temperatures,
6. Hourly air temperature, rainfall, and first 5 MRC sensors temperature data.

Figure 4.1 shows examples of typical plots for section 390203 obtained by the SMPCHECK program using data collected in 2002 at the ONSITE logging unit.

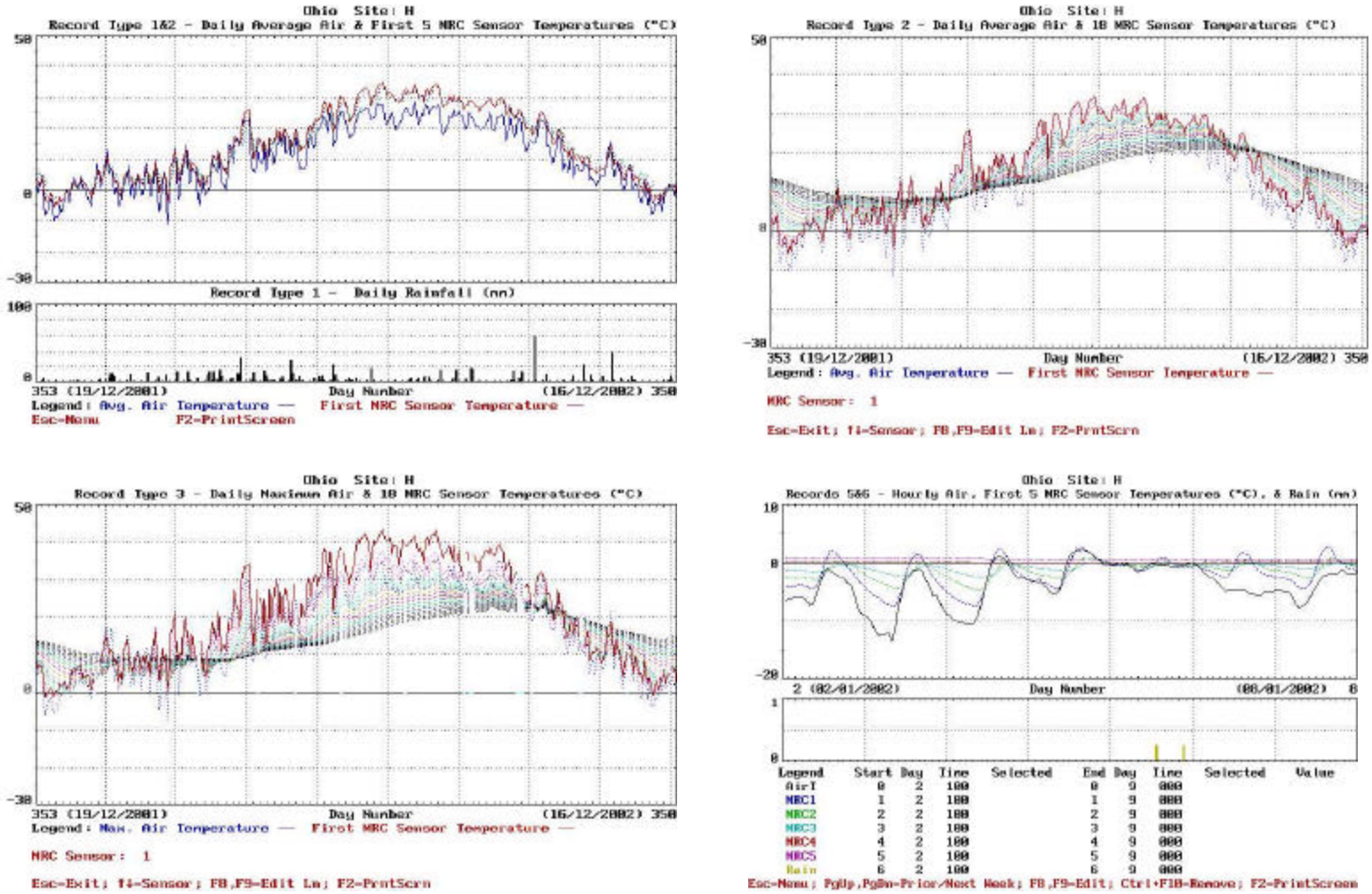

Figure 4.1. Typical SMPCHECK Displays for Onsite Data

The MOBILE data sets include the TDR traces for moisture content determination at discrete points with depth and a plot of resistivity values, also with depth, obtained from probes installed at each monitoring station. This data was collected once or twice a month depending on the time of the year. In early spring (March and April), when the moisture content is expected to vary more widely the mobile information was acquired twice a month, while in the remaining months the collection was performed only once. Figure 4.2 shows typical

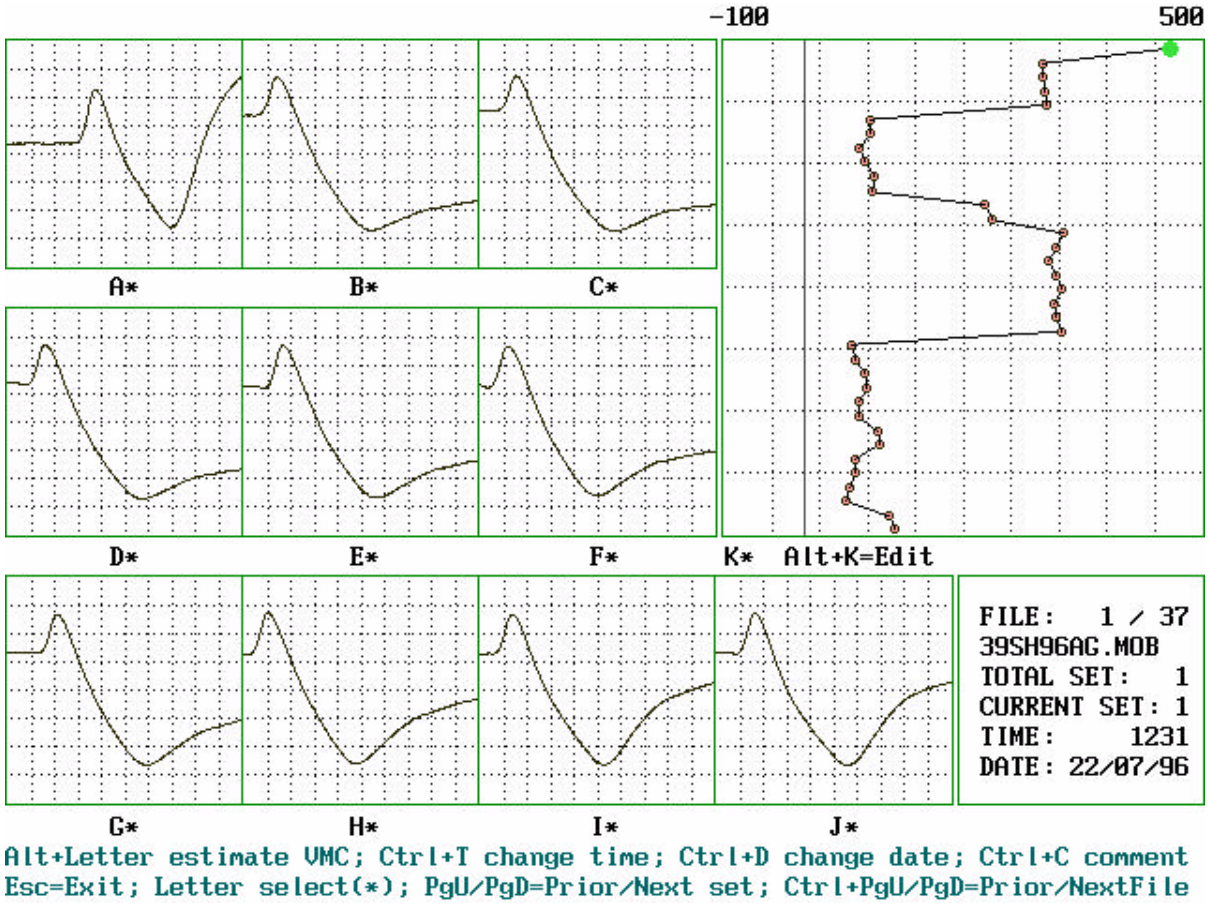

Figure 4.2. Typical SMPCheck Display for Mobile Data

summary graphs generated by SMPCHECK for section 390203 in July of 1996. The program offers the option of eliminating faulty TDR traces or unreasonable resistivity values.

AWSCHECK

The AWSCheck program is used to monitor the weather station installed at the Ohio Test Road. The procedure for data processing is available in the AWSCHECK users guide published in 1996 and follows a similar format as the SMPCHECK program, as described in Chapter 3. The program appends the collected files, eliminating any overlaps and generates a continuous edited file. Plots containing the following parameters are generated, in order to evaluate the influence of climatic effects on pavement performance:

1. Daily average, min, max air temperature and precipitation data.
2. Daily relative humidity, solar radiation, and precipitation data.
3. Daily wind information.
4. Hourly temperature and precipitation data.
5. Hourly relative humidity and precipitation data.
6. Hourly solar radiation and precipitation data.
7. Hourly wind information.

Graphs showing the information obtained from the AWSCHECK program are shown in Figure 4.3.

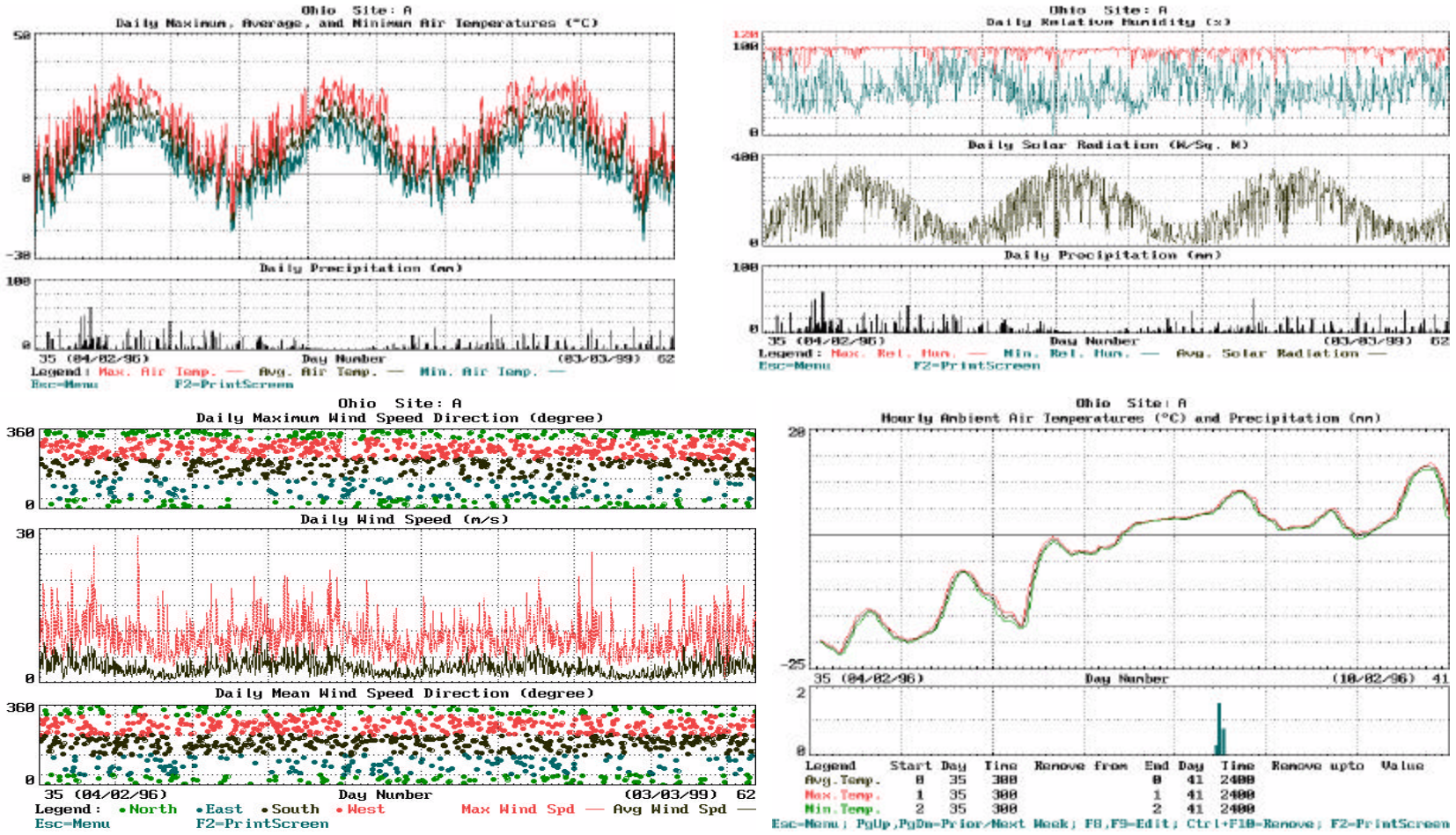

Figure 4.3. Typical AWSCHECK Display

4.2. Solar Radiation vs. Temperature

Solar radiation was plotted vs. average air temperature and curves of best fit were developed as shown in Figure 4.4. The coefficient of determination was approximately 43 percent for a total of one thousand and one hundred points. This value shows a significant relationship between both variables.

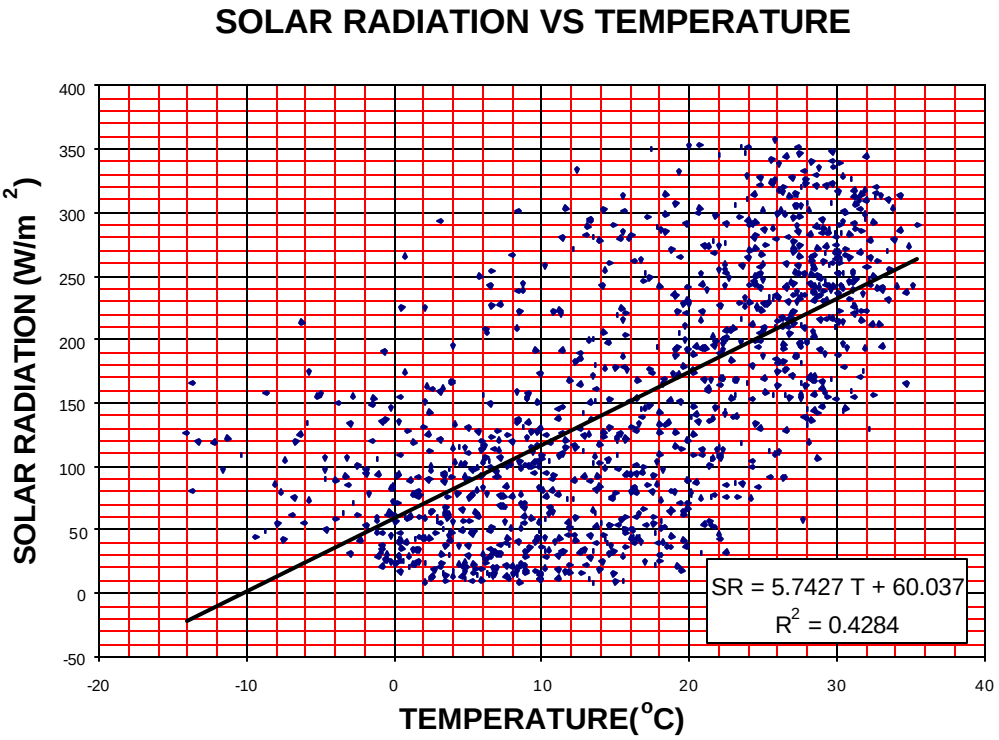

Figure 4.4. Solar Radiation vs. Temperature

Temperature and solar radiation were plotted over time to establish a general tendency. As seen in Figure 4.5, sinusoidal curves of the type:

$$y = A\sin\left(\frac{2px}{365} - O\right) + C \qquad (4.1)$$

describe the seasonal variation of temperature and solar radiation, where *y* is the temperature or the solar radiation, *x* is the day of the year using the Julian calendar, A is the amplitude, O is the date offset and C is the shift in the *y* axis. The sine is calculated with the angle in radians. The resulting equations are:

For Solar Radiation:

$$y = 101.9 \sin\left(\frac{2\pi x}{365} - 90\right) + 154.20 \qquad (4.2)$$

with R2 = 0.57

For Average Air Temperature

$$y = 12.91 \sin\left(\frac{2\pi x}{365} - 100\right) + 16.35 \qquad (4.3)$$

with R2 = 0.71

The “cumulative” Julian scale shown in Figure 4.5 starts January 1 of 1996, and is continuous until the beginning of the spring of 1999, to facilitate the plotting of three years of data. Obviously a new year starts every 365 or 366 days (on a leap year). Equations 4.2 and 4.3 are applicable using either a standard or cumulative Julian calendar since a complete cycle for the sine function has been normalized to 365 days. The Offset in Equations 4.2 and 4.3 indicates that the average temperature lags the solar radiation by about 10 days, that is the peaks or valleys in the solar radiation are reached earlier in the year than in the average air temperature.

The correlation developed between solar radiation and air temperature would allow the installation of only one of the two instruments to obtain both parameters, thus reducing instrumentation costs (McCuen, 1998).

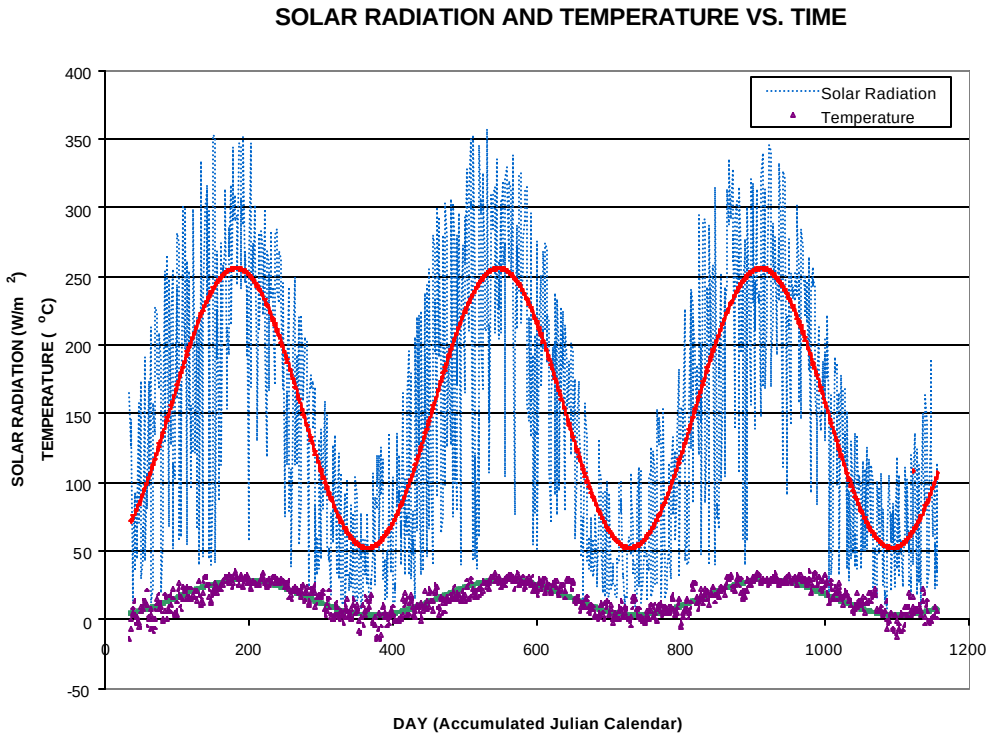

Figure 4.5. Solar Radiation and Temperature vs. Time

The importance of solar radiation in pavement studies is in that it may affect the rate of aging of pavement materials, in particular asphalt concrete by the effects of ultraviolet light. It may also accentuate slab deformations in Portland Cement Concrete.

4.3. Asphalt Concrete-Air Temperature Relations

Figueroa (2001), in a previous study for the Ohio Department of Transportation, developed regression equations relating the average asphalt

concrete pavement temperature to the air temperature, expressed by the equation:

$$P = C1 + C2\ A + C3\ A^2 \qquad (4.4)$$

where

C1, C2, and C3 = Regression constants.

P = Average AC or asphaltic material temp. (Deg C).

A = Air temperature (Deg C).

for eight counties throughout Ohio. The monitoring stations installed at each of the eight counties were selected among other considerations, to determine the change in asphalt concrete temperature corresponding to a change in latitude for a given air temperature.

Statistical regression analyses were conducted on the combined daytime and nighttime values to develop regression equations between the average AC temperature and the air temperature. Such equations would be useful in inferring the average AC or asphaltic material modulus based on air temperature readings, as it will be shown later.

The monitoring station locations in order of increasing latitude were located in Adams, Athens, Licking, Knox, Crawford and Wood (8.1), Lucas and Wood(2.85) county. Examination of the obtained regression equation coefficients for each of the eight monitoring stations indicates that the state of Ohio may be subdivided into three general temperature zones: North, (from the North Shore to Mansfield – Mount Vernon) Central (from Mansfield – Mount Vernon to Lancaster) and South (from Lancaster to the southern state line). This division is

useful in assessing the average AC modulus on a seasonal or monthly basis for any future implementation of mechanistic pavement design procedures.

Individual regression equations for each climatic zone as well as for all of Ohio were determined by grouping data from stations located within the specific climatic zone and all of them together as shown in Table 4.1. It is worth noting that the overall equation approaches the equation determined for the central zone of the state. The coefficient of determination R^2 for each regression equation is also shown in this table (R^2>0.84 in all cases), indicating the highly significant relationship between the two temperatures in every combination.

Table 4.1 also includes the results of a similar regression analysis of data obtained at the Ohio Test Road including air temperature measurements from the weather station and average asphalt concrete temperature obtained in section 390901. The coefficients obtained at the Ohio Test Road relating air temperature to average asphaltic material temperature agree reasonably well with those obtained for the central climatic zone.

It is instructive to note that the coefficient C1 (intercept at zero air temperature) for the most part, tends to decrease with increasing latitude. This indicates that asphalt concrete temperature will be higher in the southern part than in the northern part of the state.

Table 4.1 Average AC Temp. vs. Air Temp. Coefficients

Location	No. of Points	C1	C2	C3	R^2
NORTH	75414	4.1409	0.9423	0.0027	0.8640
CENTRAL	118290	4.8118	0.8860	0.0052	0.8418
SOUTH	61152	5.2834	0.9113	0.0055	0.8431
ALL SITES	254856	4.7055	0.9107	0.0045	0.8475
Ohio Test Road	24133	5.0952	0.8889	0.0114	0.9117

ALL SITES: Adams, Athens, Crawford, Knox, Licking, Lucas, Wood(2.85) and Wood(8.1)
NORTH: Lucas, Wood(2.85) and Wood(8.1)
CENTRAL: Crawford, Knox, Licking
SOUTH: Adams, Athens

Equation 4.4 can be combined with appropriate forms of Equation 2.3 to develop direct relationships between the resilient modulus of the asphalt concrete, the asphalt treated base, or the permeable asphalt treated base and the air temperature. Examples of these are shown in Figures 4.6, 4.7 and 4.8, using data obtained in section 390901 of the Ohio Test Road.

4.4. Temperature Variations within the Asphalt Concrete-Layer

A statistical analysis of temperature data from three sensors embedded in the asphaltic layers of section 390901 was performed to obtain the time of the day when the asphalt concrete reaches an approximately constant temperature throughout its thickness. This would be the ideal time to conduct Falling Weight Deflectometer (FWD) tests. The plot of constant temperature vs. time in "cumulative" Julian days between January 1, 1996 and the end of 1997 shown in

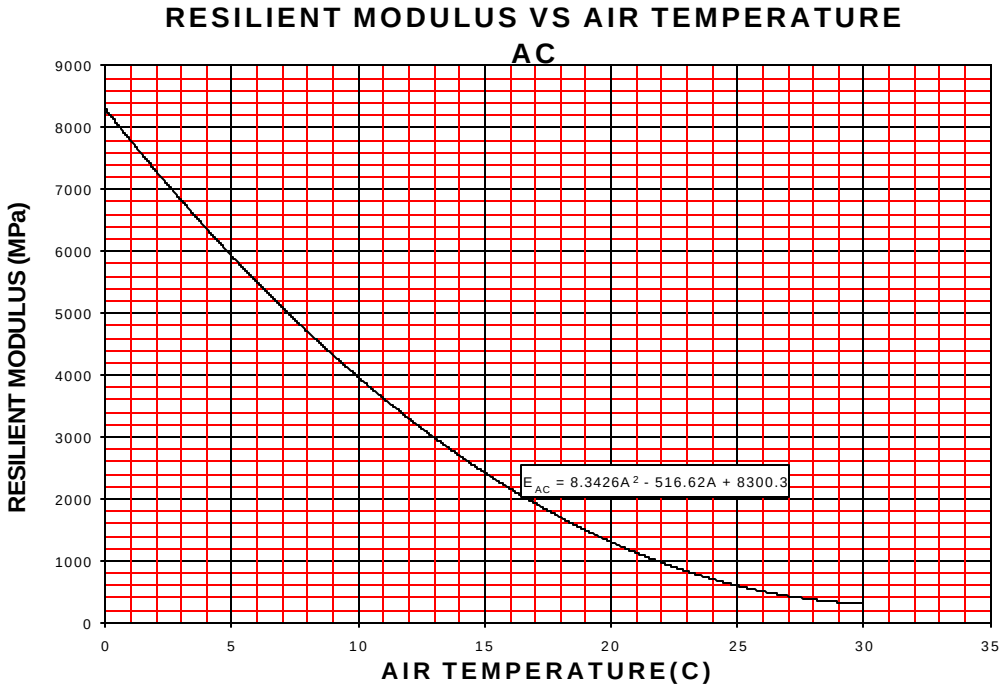

Figure 4.6. Resilient Modulus vs. Air Temperature for Asphalt Concrete

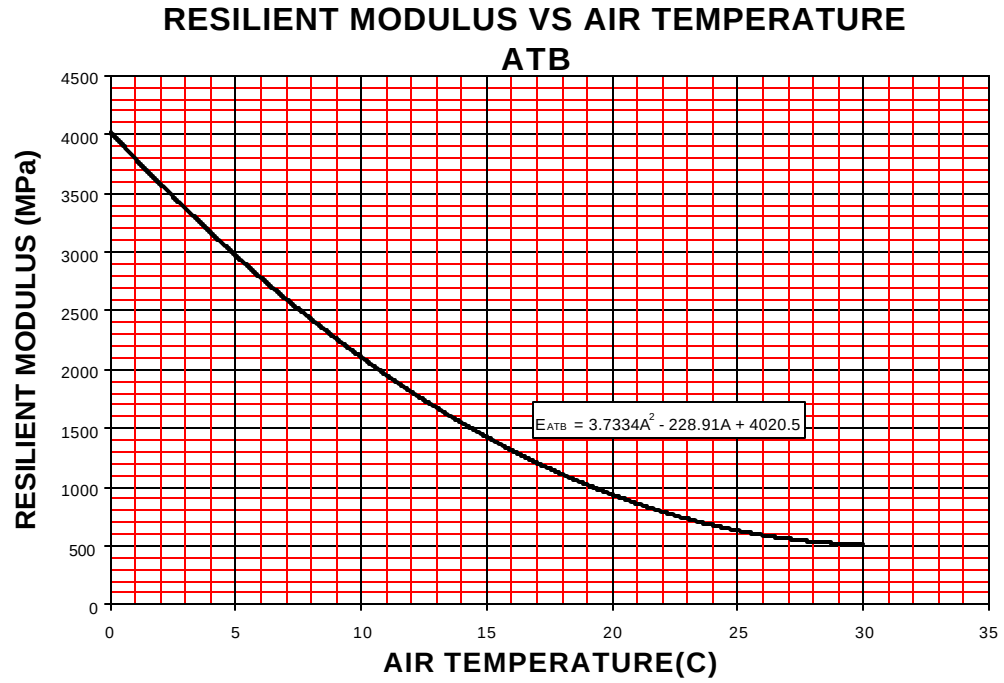

Figure 4.7. Resilient Modulus of ATB vs. Air Temperature

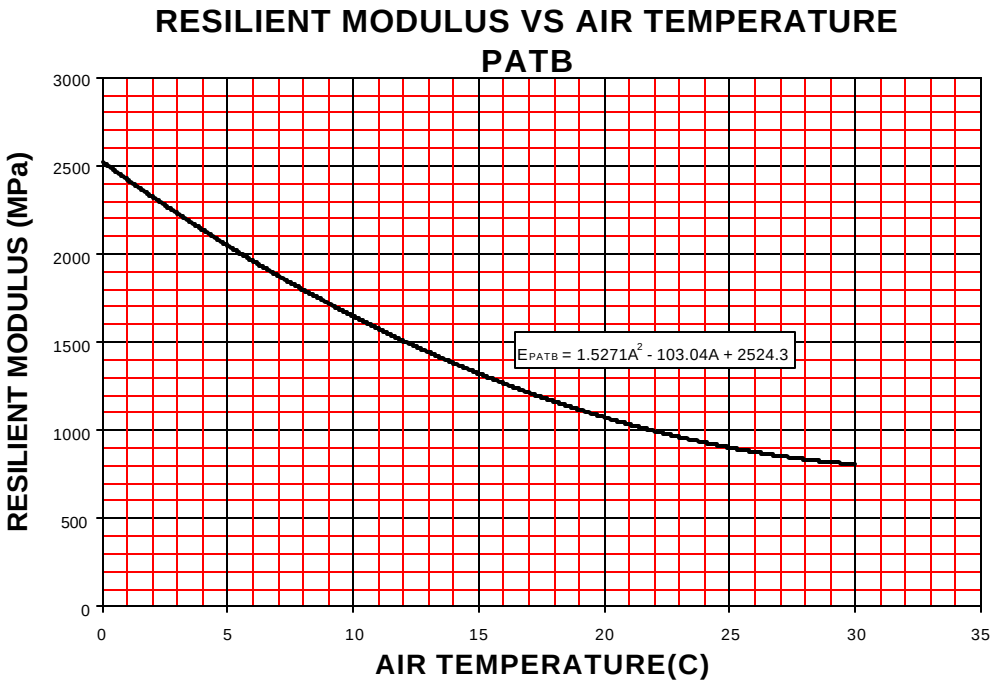

Figure 4.8 Resilient Modulus of PATB vs. Air Temperature

Figure 4.9 displays a seasonal dependency. Knowing that high temperatures lead to lower resilient modulus, summer was selected for study.

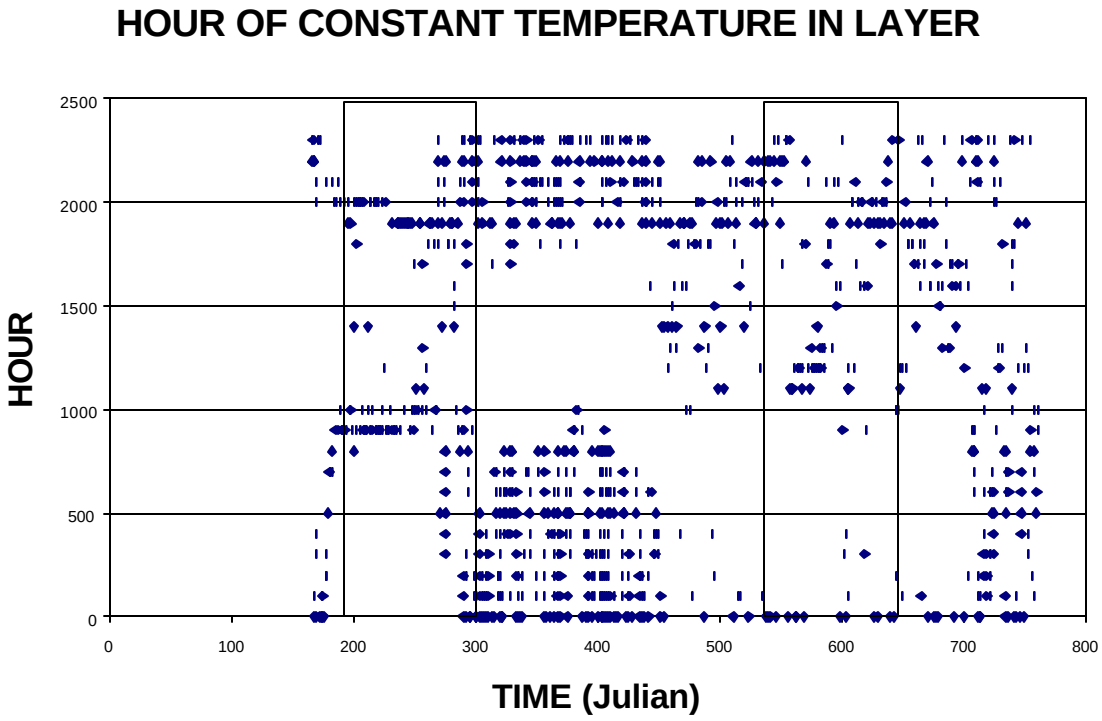

Figure 4.9. Hour of Constant Temperature in Layer

Figure 4.10 shows the frequency distribution of data points with respect to the time of the day in which a near zero temperature gradient is detected. The distribution includes data points for the 1996 and 1997 summer, from which it is determined that the most probable times of the day of little or no thermal gradient in the asphalt concrete layer were between 9:00 a.m. and 8:00 p.m. (represented by the peaks).

A similar set of data points was plotted to elucidate the times of the day when the maximum temperature gradient occurs within the asphalt concrete, yielding the hours of 6:00 a.m. and 3:00 p.m. These times also correspond to the valleys in Figure 4.10.

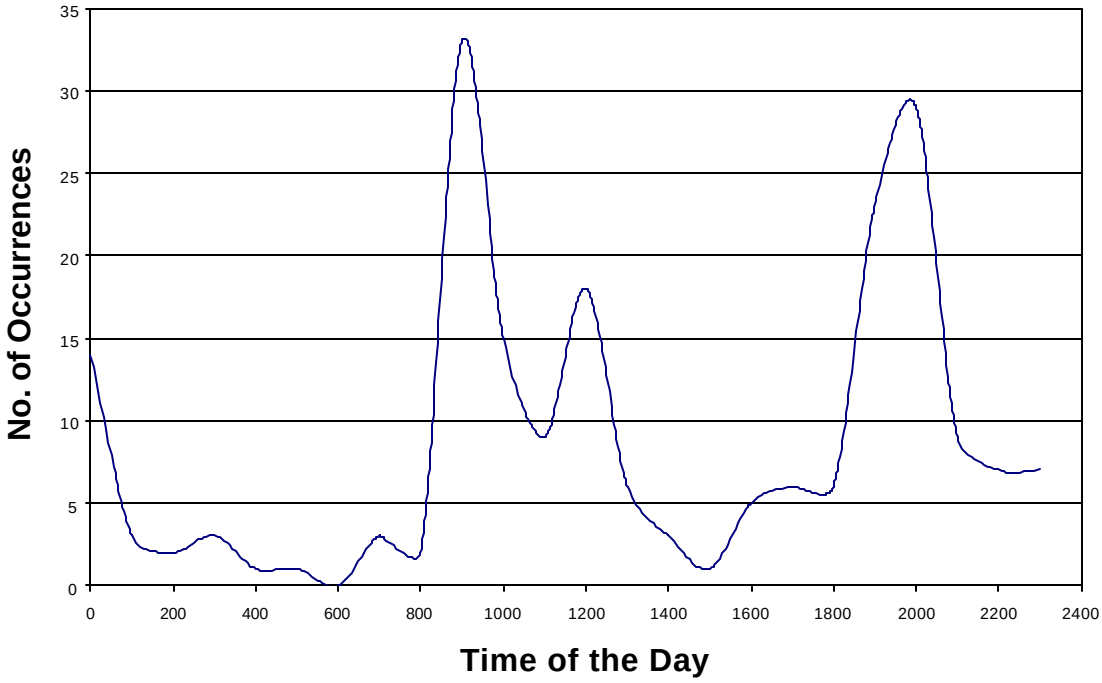

Figure 4.10. Frequency Distribution for Zero Temperature Gradient in the AC

The monthly and seasonal variation of asphalt concrete stiffness is of importance in future mechanistic pavement design procedures. Due to the direct dependency of AC stiffness on temperature, monthly and seasonal AC temperature averages were calculated from data obtained at station 390901 between June of 1996 and March of 1999 AC temperature averages were calculated for both daytime and nighttime hours as shown in Figure 4.11 (on a daily basis) and Tables 4.2 (monthly averages) and 4.4 (seasonal averages). Average monthly or seasonal temperatures include periods of complete data. Other periods were not included because of equipment malfunction. or temperature sensor breakdown,

Knowing the average monthly and seasonal AC temperatures, which are presented at the bottom of Tables 4.2 and 4.4, it is expedient to calculate the

average AC resilient modulus using Equation 2.3 in combination with the average pavement temperature. The resulting average AC resilient moduli are included in Tables 4.3 (monthly averages) and 4.5 (seasonal averages).

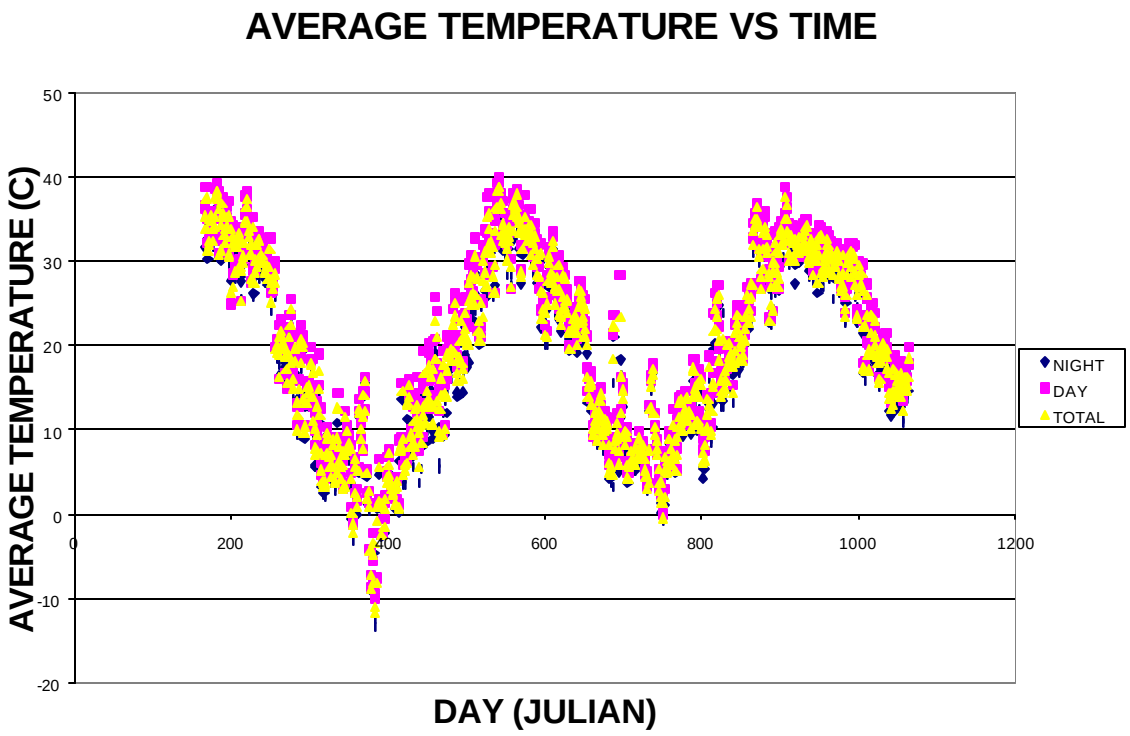

Figure 4.11. Average Temperature vs. Time. (Section 390901)

Table 4.2. Monthly Average Asphalt Concrete Temperature (Section 390901) (deg C)

YEAR		JAN	FEB	MAR	APR	MAY	JUN	JUL	AUG	SEP	OCT	NOV	DEC
	Day	-	-	-	-	-	-	33.33	32.35	23.94	17.27	8.43	6.84
1996	Night	-	-	-	-	-	-	31.84	30.19	22.26	15.52	6.55	5.71
	Total	-	-	-	-	-	-	32.59	31.27	23.1	16.39	7.49	6.28
	Day	0.99	6.49	13.23	18.67	24.36	33.53	34.28	29.77	25.50	18.33	11.68	7.13
1997	Night	0.07	5.06	9.82	14.99	20.70	30.23	32.23	27.93	23.88	16.53	9.65	6.34
	Total	0.53	5.78	11.52	16.83	22.54	31.88	33.25	28.85	24.69	17.43	10.67	6.73
	Day	-	-	15.47	19.23	-	31.64	32.13	31.54	28.77	-	-	-
1998	Night	-	-	12.98	17.78	-	29.62	31.61	29.17	27.07	-	-	-
	Total	-	-	14.23	18.5	-	30.63	31.61	30.35	27.92	-	-	-
	Day	0.99	6.49	14.35	18.95	24.36	32.59	33.25	31.22	26.07	17.80	10.06	6.99
AV.	Night	0.07	5.06	11.40	16.39	20.70	29.93	31.89	29.10	24.40	16.03	8.10	6.03
	Total	0.53	5.78	12.88	17.67	22.54	31.26	32.48	30.16	25.24	16.91	9.08	6.51

- MISSING DATA

Table 4.3. Monthly Average Asphalt Concrete Resilient Modulus (Section 390901) (MPa)

	JAN	FEB	MAR	APR	MAY	JUN	JUL	AUG	SEP	OCT	NOV	DEC
Day	12108	9257	5794	4102	2428	538	420	797	1970	4502	7597	9017
Night	12620	9964	7009	5015	3524	1063	666	1243	2416	5150	8489	9484
Total	12363	9605	6389	4550	2953	790	556	1014	2189	4822	8036	9249

Table 4.4. Seasonal Average Asphalt Concrete Temperature (Section 390901) (deg C)

YEAR		SPRING	SUMMER	FALL	WINTER
1996	Day		31.64	12.49	5.57
	Night		29.88	10.84	4.02
	Total		30.76	11.67	4.80
1997	Day	23.12	31.56	14.21	-
	Night	19.36	29.60	12.60	-
	Total	21.24	30.58	13.40	-
1998	Day	-	31.76	-	
	Night	-	29.66	-	
	Total	-	30.71	-	
AVERAGE	Day	23.12	31.65	13.35	5.57
	Night	19.36	29.71	11.72	4.02
	Total	21.24	30.68	12.54	4.80

- INCOMPLETE OR MISSING DATA

Table 4.5. Seasonal Average Asphalt Concrete Resilient Modulus (Section 390901) (MPa)

	SPRING	SUMMER	FALL	WINTER
DAY	2782	712	6195	9709
NIGHT	3964	1108	6873	10494
TOTAL	3352	905	6530	10095

4.5. Temperature Differentials in Portland Cement Concrete Slabs

Changes in temperature within Portland Cement Concrete slabs lead to longitudinal expansion and contraction as well as warping. Two important cases need to be studied. The first one is when the surface of the slab has a higher temperature than its bottom. This change in temperature (Δt) generates tensile stresses at the bottom of the slab which combined with an applied load at the

center of the slab can lead to cracking thus reducing the life of the pavement. The second case is when the bottom of the slab is warmer than its top, thus tensile stresses are generated at the surface of the slab which in combination with edge traffic loads may also lead to slab cracking.

Estimations of the maximum change in slab temperature (positive slab temperature gradient) throughout the year were developed for stations 390203, 390205 and 390212. A clear relationship between these parameters is seen in Figures 4.12a, 4.12b and 4.12c. Readings were smoothed out by Fast Fourier Transform and a sinusoidal function was fitted to obtain the desired correlation. This function is of the type

$$y = A\sin\left(\frac{2\pi x}{365}\right) + C \qquad (4.5)$$

where *y* is the actual air temperature or the positive air temperature gradient, *x* is the day of the year in the "cumulative" Julian scale (between January 1, 1996 and the beginning of the spring, 1999), A is the amplitude and C is the shift in the *y* axis. Values of A and C are indicated in each graph for both air temperature (upper graph) and slab temperature (lower graph). The angle is calculated in radians.

As seen in the plots, the best fit curves for the three studied sections are almost identical. The positive gradient varies between sections by approximately 2 degrees Celsius. Relationships between average air temperature and the positive gradient were developed and are shown in Figures 4.13a, 4.13b and 4.13c with their respective equations.

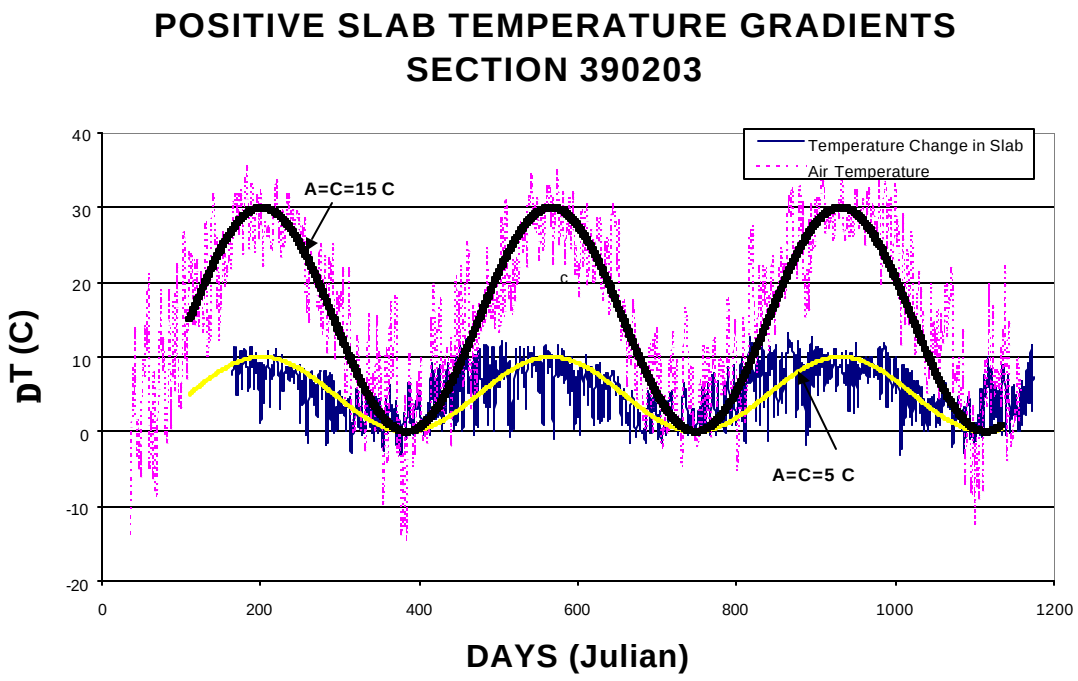

Figure 4.12a. Positive Slab Temperature Gradient vs. Time [Section 390203]

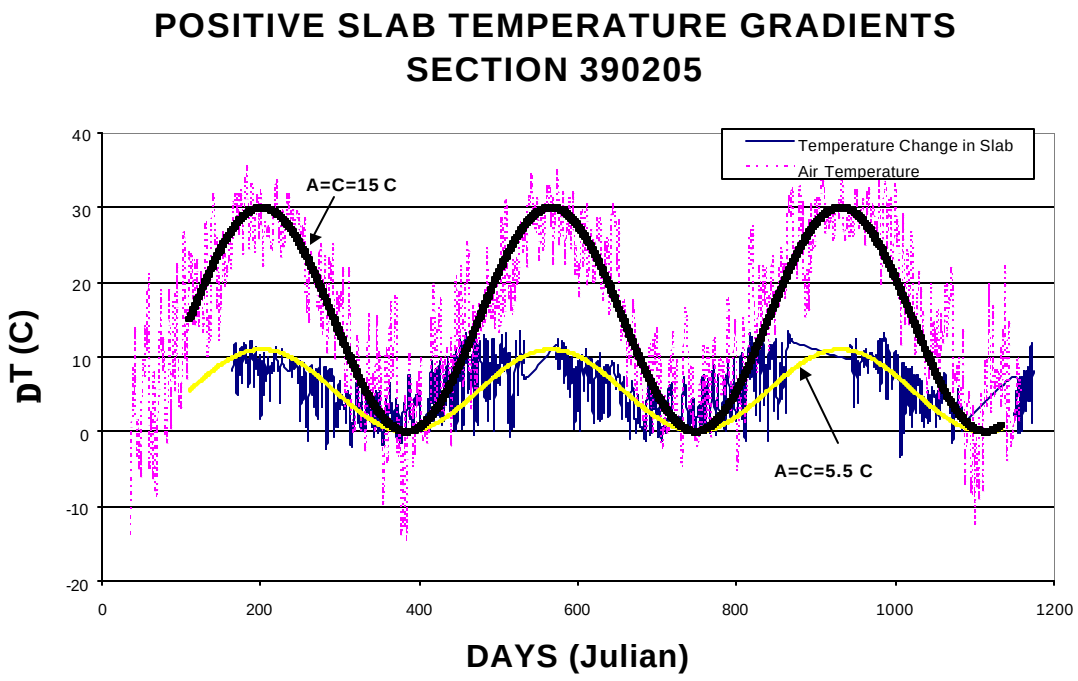

Figure 4.12b. Positive Slab Temperature Gradient vs. Time [Section 390205]

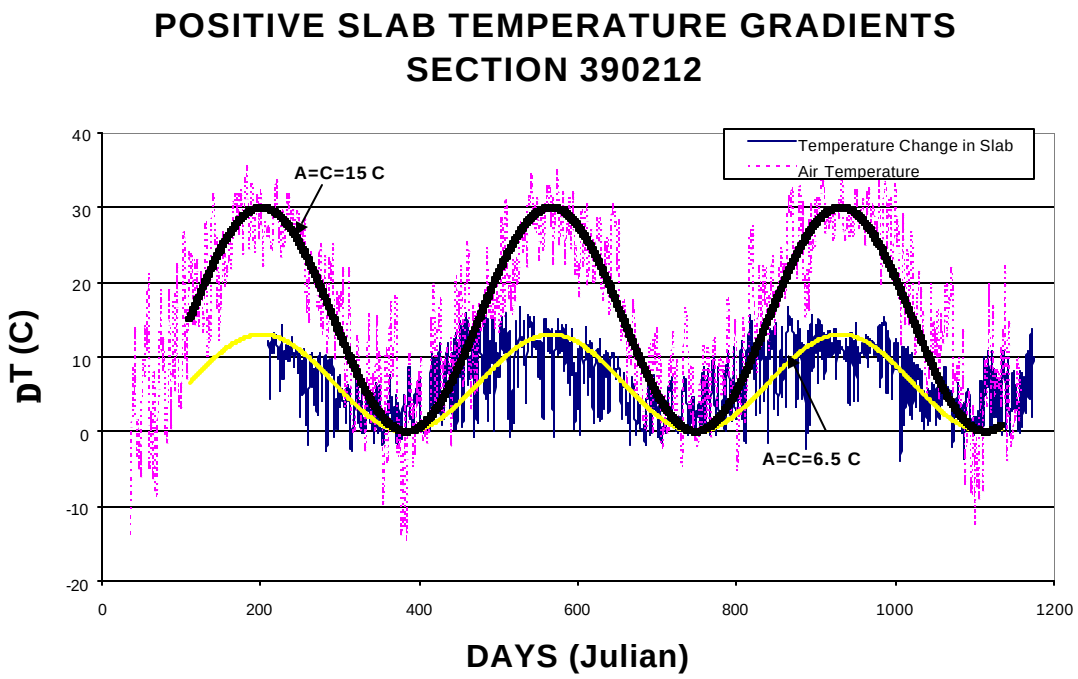

Figure 4.12c. Positive Slab Temperature Gradient vs. Time [Section 390212]

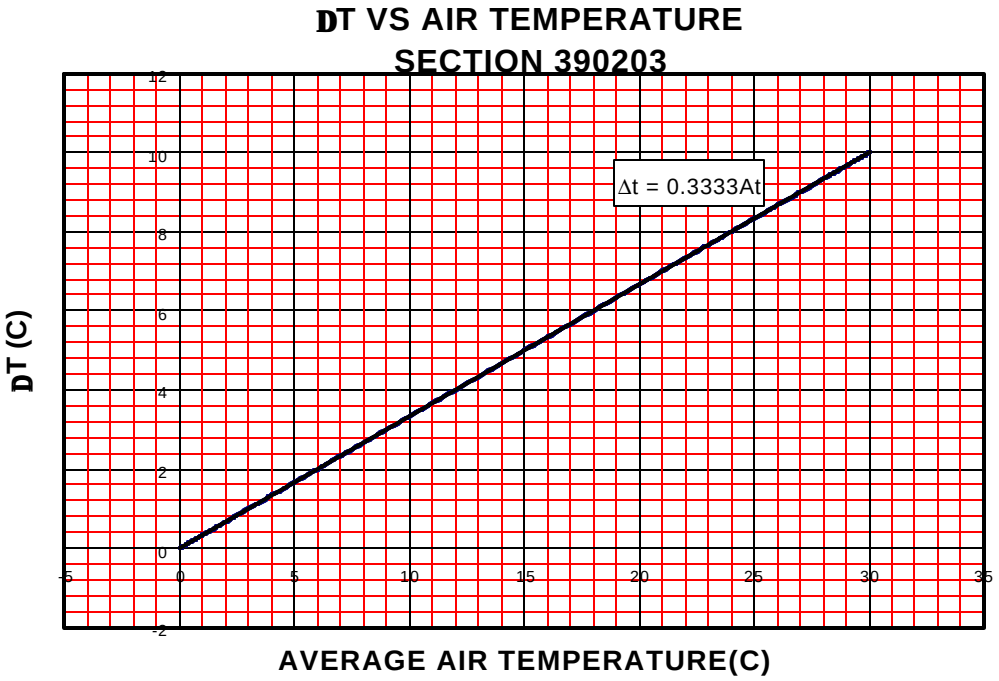

Figure 4.13a. Positive Slab Temperature Gradient vs. Average Air Temperature {Section 390203]

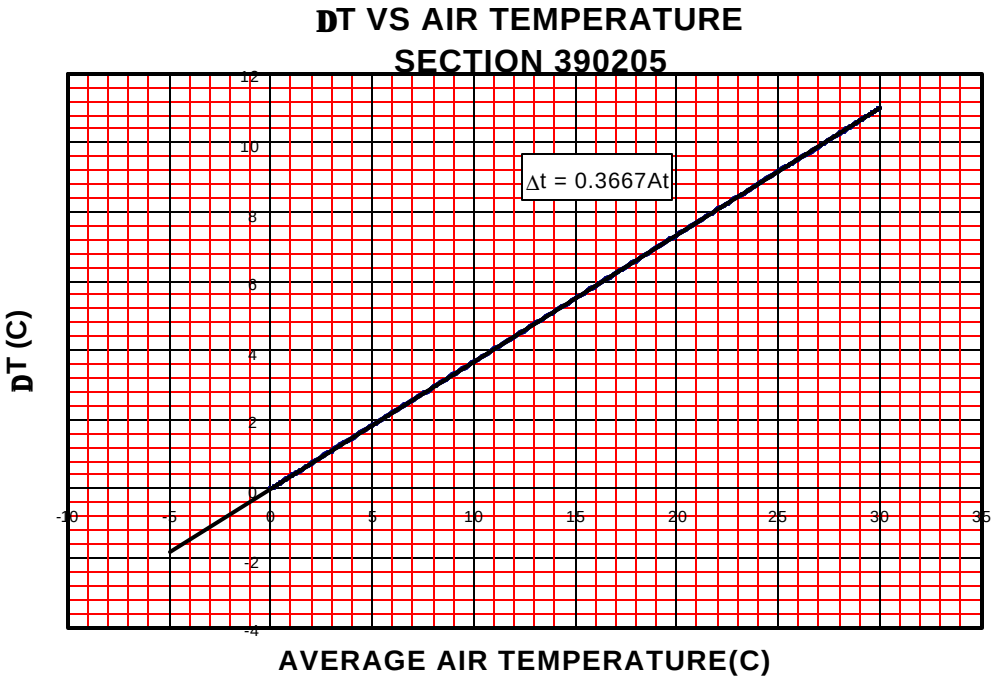

Figure 4.13b. Positive Slab Temperature Gradient vs. Average Air Temperature {Section 390205]

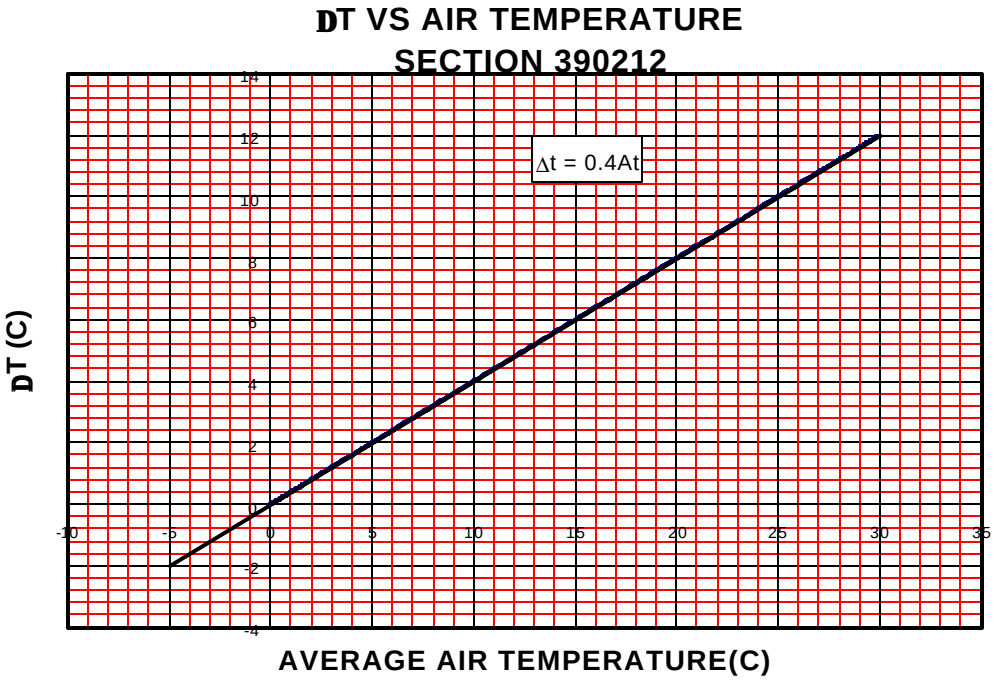

Figure 4.13c. Positive Slab Temperature Gradient vs. Average Air Temperature [Section 390212]

Knowing the difference in height between the top and bottom sensors, values of positive slab temperature differentials per cm. of thickness were established as shown in Table4.6.

Table 4.6. Positive Slab Temperature Gradient per cm. of Thickness

SECTION	DT per cm. (^{o}C/cm)
390203	0.437
390205	0.665
390212	0.524
Average	**0.543**

Estimations of the minimum change in slab temperature (lower temperature at the surface and higher temperature at the bottom or negative gradient) were also developed following the same procedure. General equations of the type

$$y = -\left|\left[A\sin\left(\frac{2px}{365}\right) + C \right]\right| \qquad (4.6)$$

were obtained.

Figures 4.14a, b and c show the actual data and fitted sinusoidal functions of the negative slab temperature gradient and average air temperature vs. time for the three stations, while Figures 4.15a, b and c depict the relationship between the two temperatures.

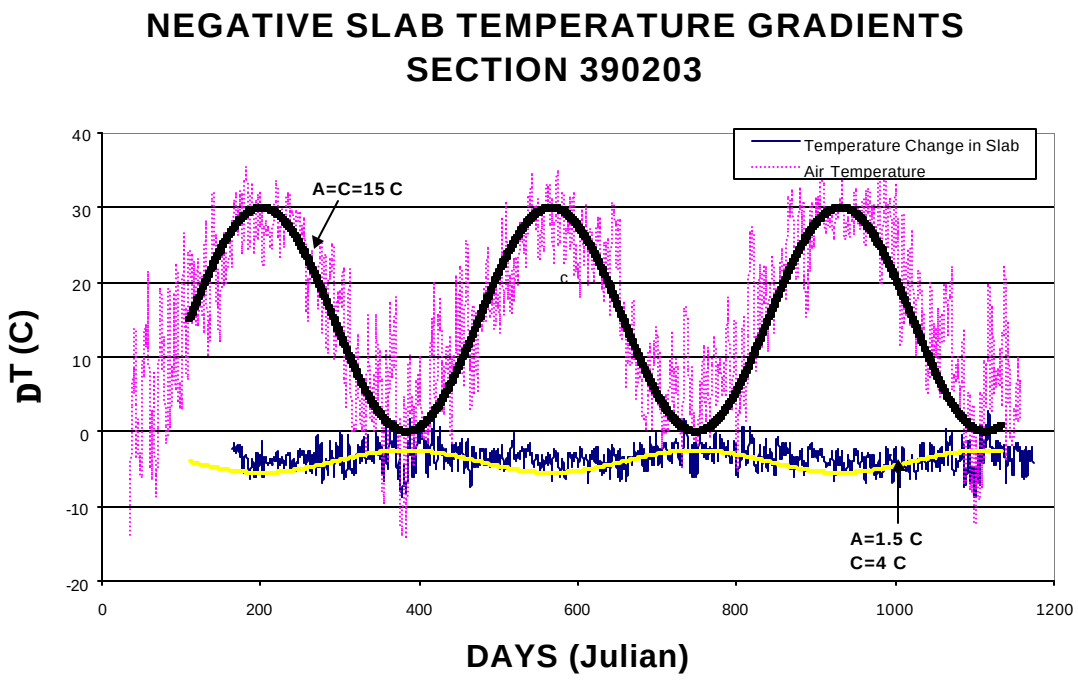

Figure 4.14a. Negative Slab Temperature Gradient vs.Time [Section 390203]

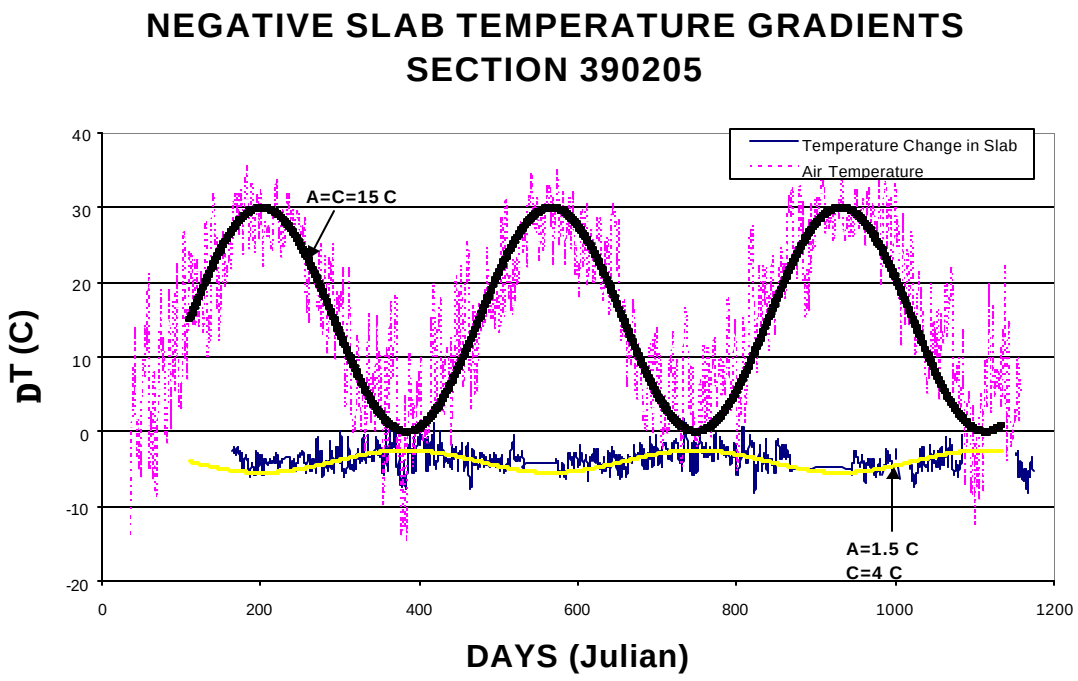

Figure 4.14b. Negative Slab Temperature Gradient vs.Time [Section 390205]

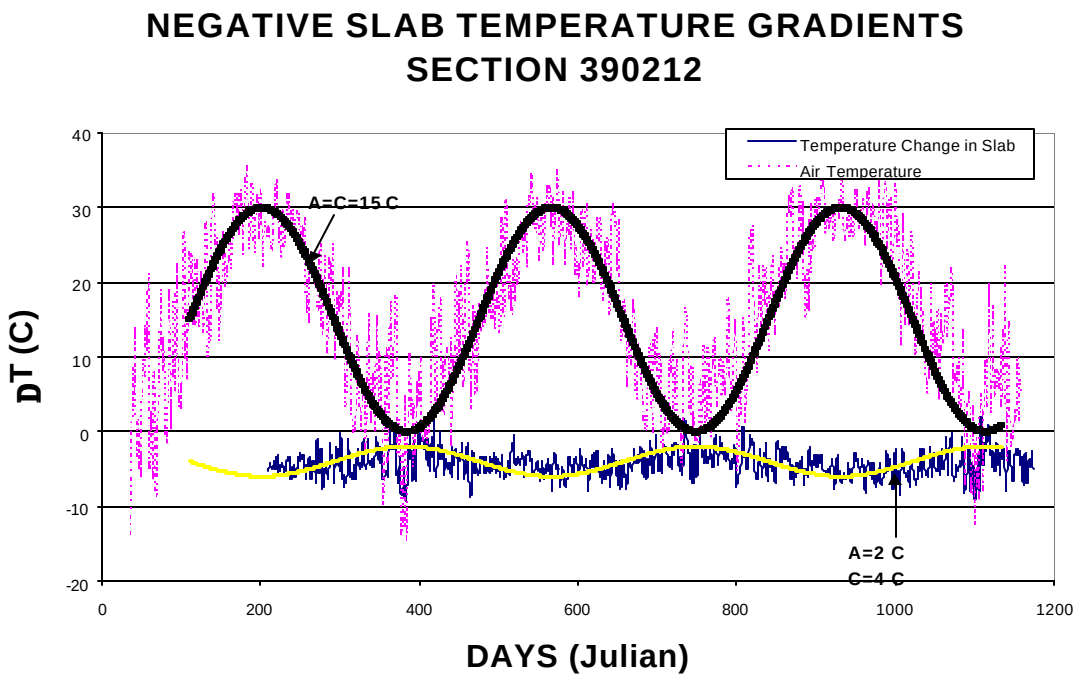

Figure 4.14c. Negative Slab Temperature Gradient vs. Time [Section 390212]

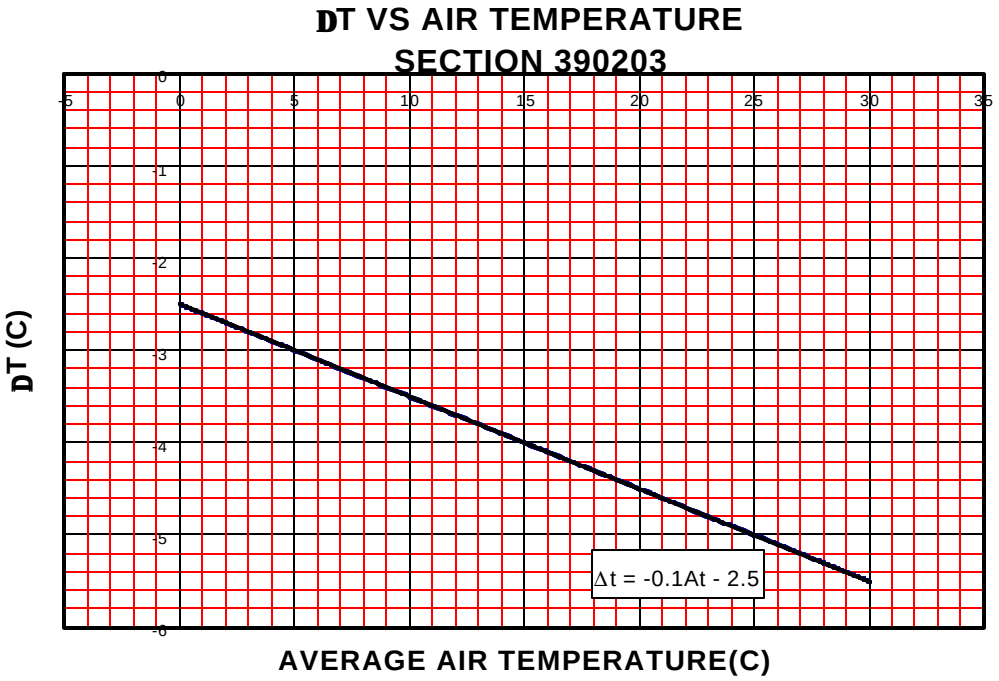

Figure 4.15a. Negative Slab Temperature Gradient vs. Average Air Temperature [Section 390203)

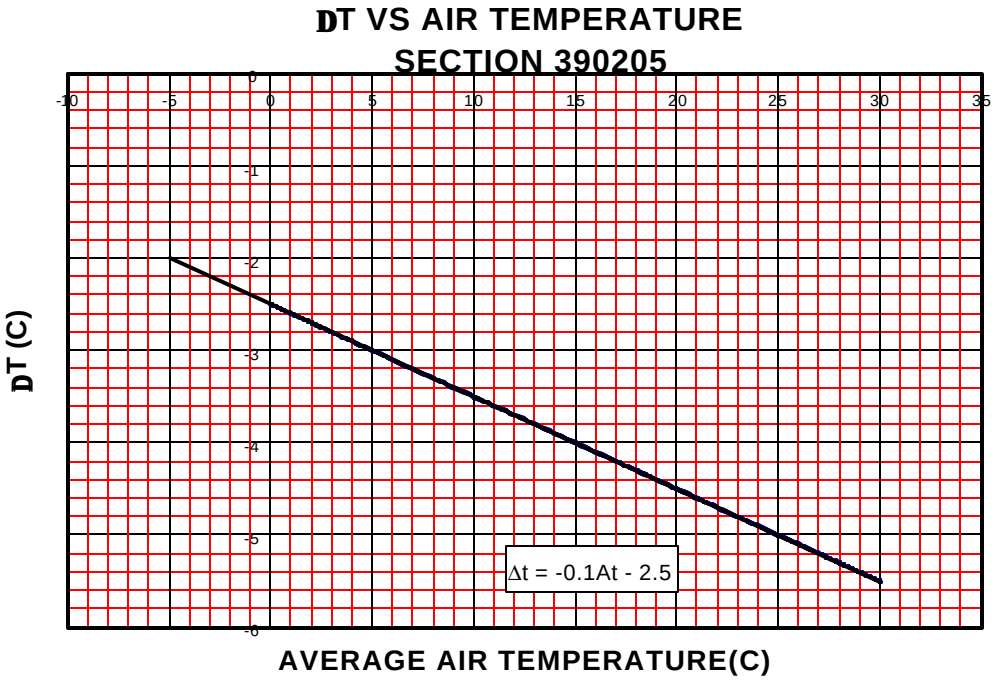

Figure 4.15b. Negative Slab Temperature Gradient vs. Average Air Temperature [Section 390205)

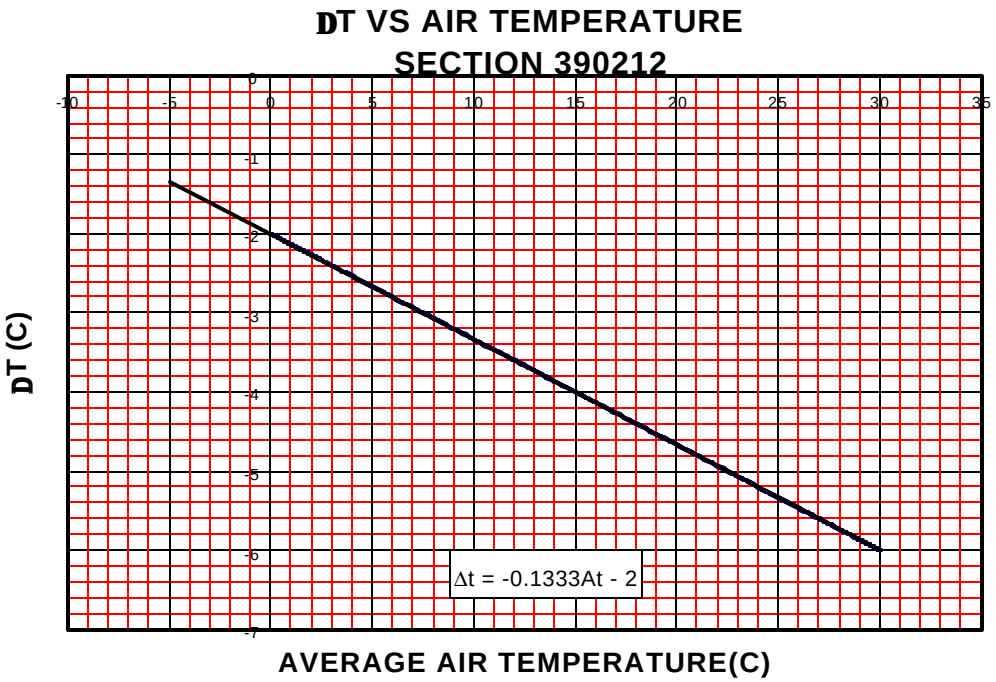

Figure 4.15c. Negative Slab Temperature Gradient vs. Average Air Temperature [Section 390212)

Similarly, the negative slab temperature differential per cm. of thickness was estimated for the different pavement sections and an average value was calculated as shown in table 4.7.

Table 4.7. Negative Slab Temperature Gradient per cm. of Thickness

SECTION	ΔT per cm. (°C/cm)
390203	-0.24
390205	-0.334
390212	-0.263
Average	**-0.279**

A statistical analysis was conducted to obtain typical hours when the higher positive gradient, the higher negative gradient and no temperature gradient occur within the slab, as shown in Figure 4.16.

As seen in Figure 4.16, an evident trend throughout the year is noticed for the positive and negative temperature gradients. For the least temperature difference (no change in temperature) a seasonal variation is noted. Winter gives a very uniform distribution, while summer shows two defined hours. Figure 4.17 depicts the hours with least temperature change during the summer.

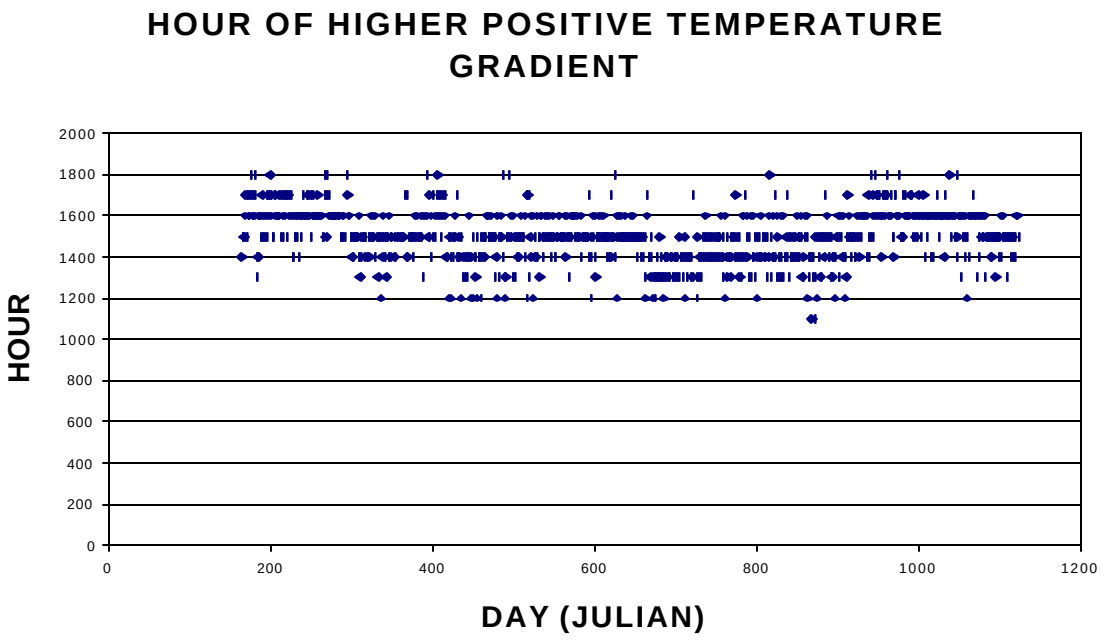

Figure 4.16. Positive, Negative and No Temperature Gradient vs. Time

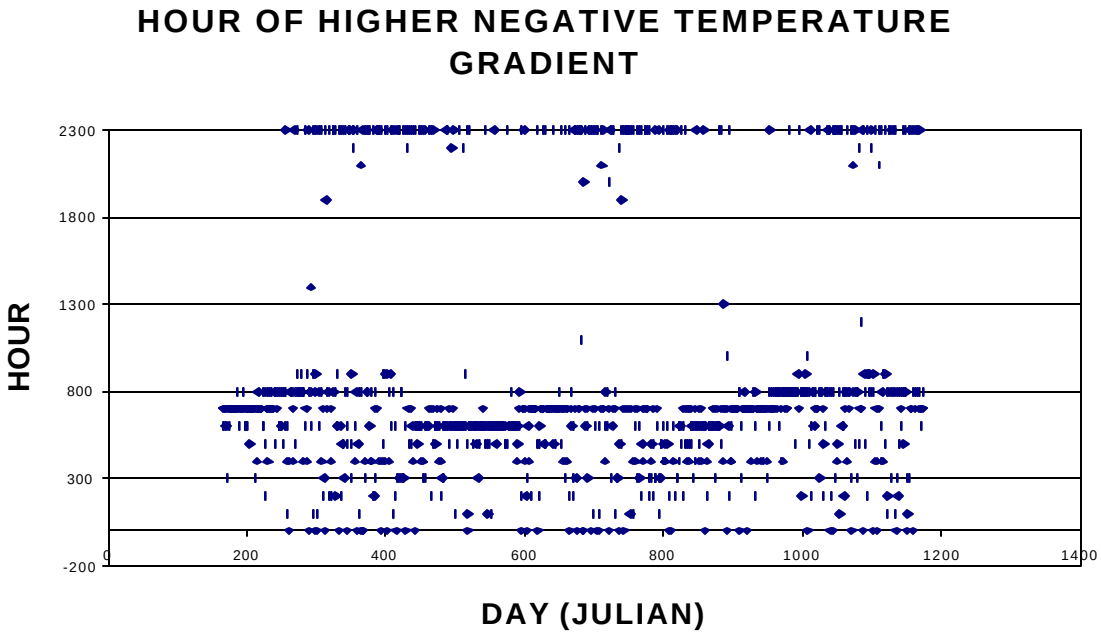

Figure 4.16. Positive, Negative and No Temperature Gradient vs. Time (cont.)

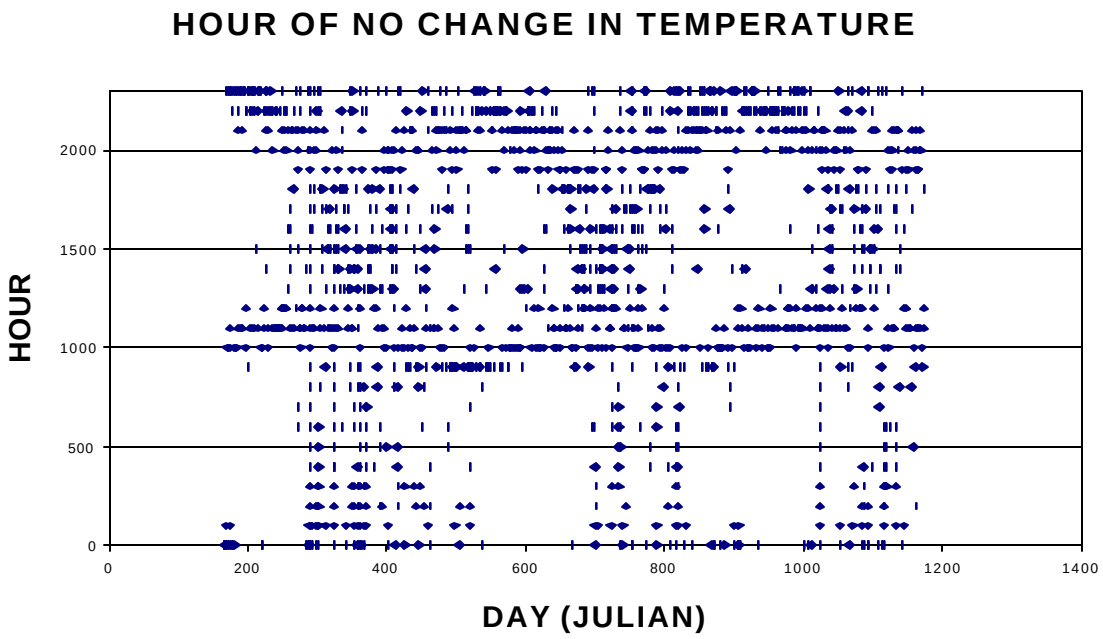

Figure 4.16. Positive, Negative and No Temperature Gradient vs. Time (cont.)

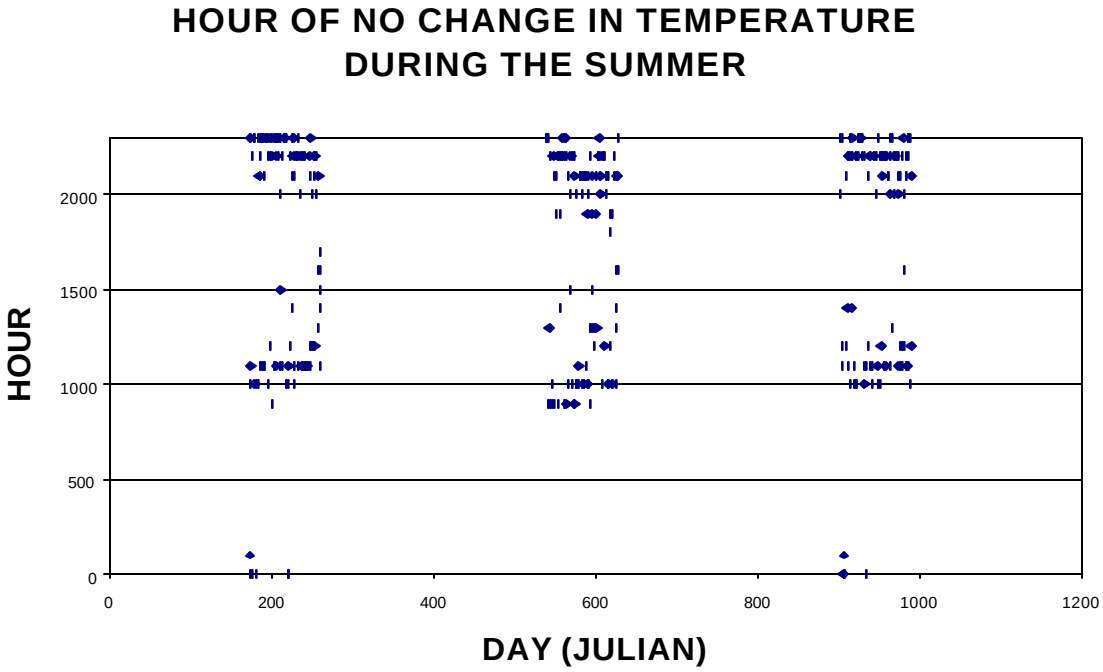

Figure 4.17. Least Temperature Change vs. Time during the Summer

Plots of number of occurrences per hour were generated as given in Figure 4.18 clearly depicting the most common hour for each of the three cases.

The typical hour(s) for each gradient is (are):

- 3 p.m. for positive gradient,
- 7 a.m. and 12 a.m. for negative gradient, and
- 11 a.m. and 10 p.m. for no gradient during the summer.

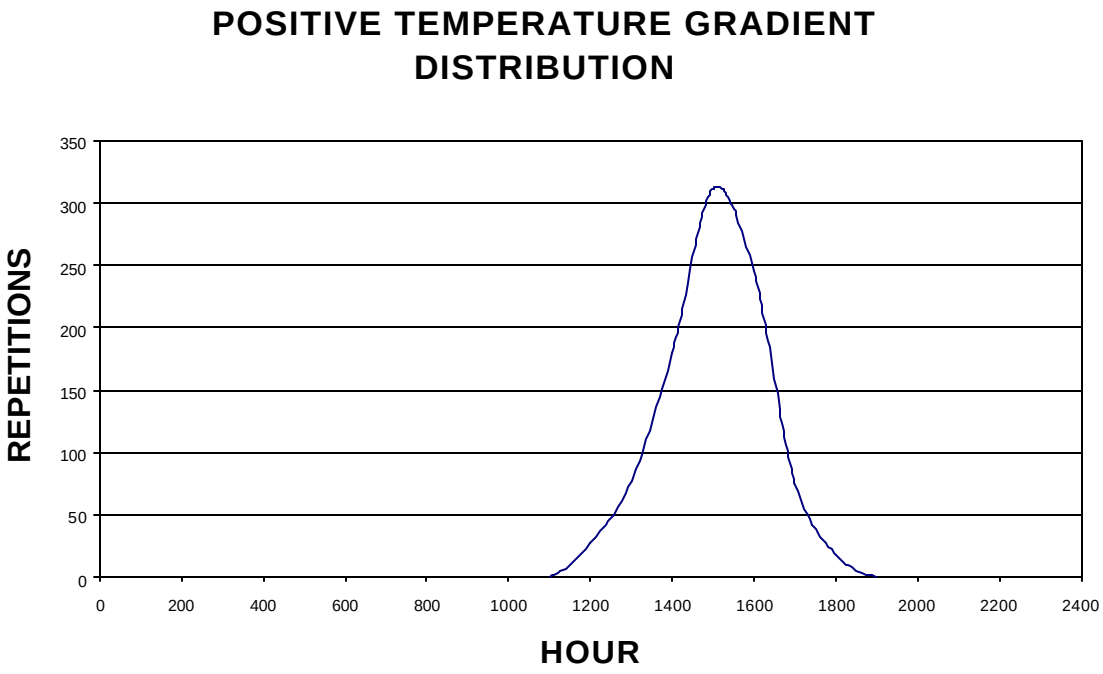

Figure 4.18. Hourly Temperature Distributions

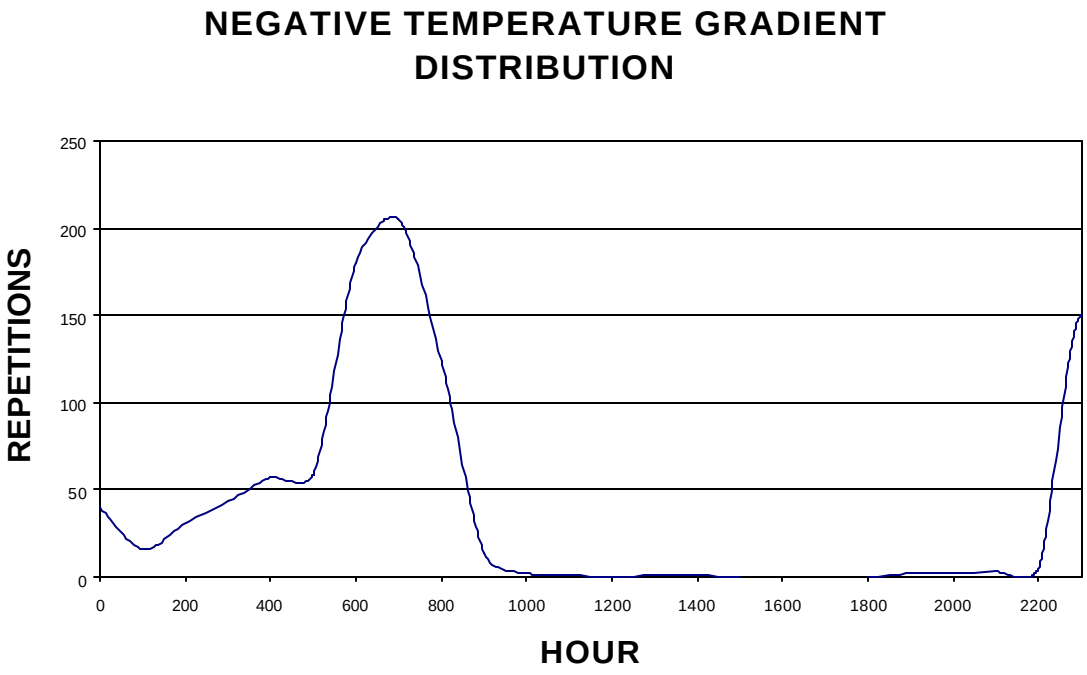

Figure 4.18. Hourly Temperature Distributions (cont.)

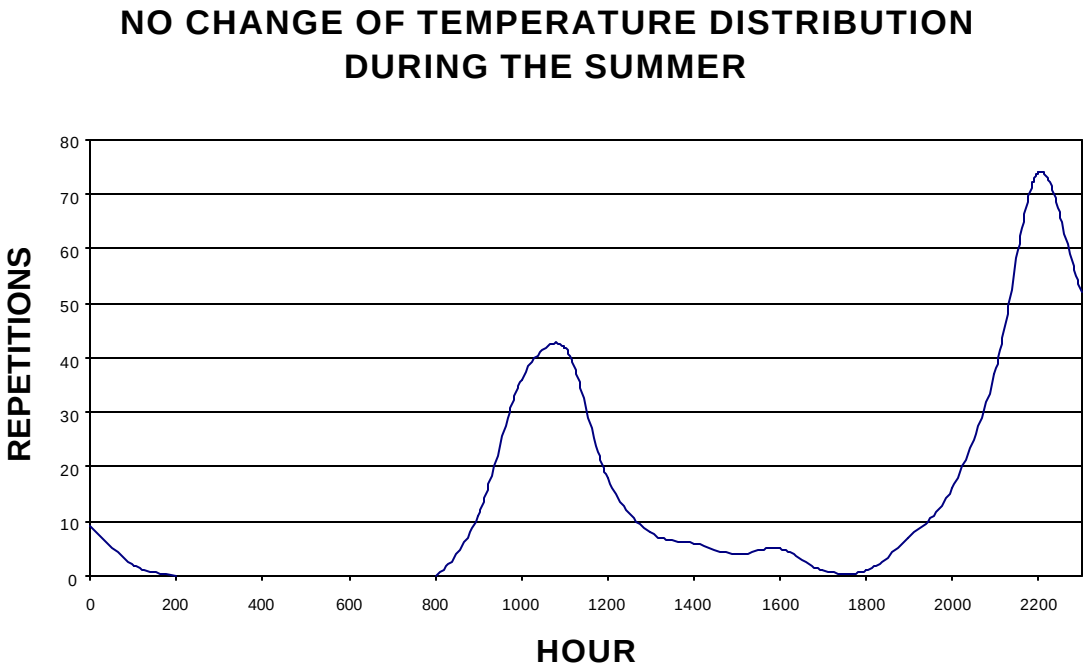

Figure 4.18. Hourly Temperature Distributions (cont.)

4.6. Depth of Frost Penetration Estimates

One important factor that generates damage in a road system is the heaving caused by frost penetration. A variety of methodologies that consider the thermodynamic principles of heat transfer have been established to predict this value. These methods generally use Fourier's diffusion equation:

$$\frac{\partial T}{\partial \boldsymbol{q}} = \boldsymbol{a}\frac{\partial^2 T}{\partial X^2} \tag{4.7}$$

T is the temperature at a certain depth, θ is the time, and α is the thermal diffusivity related to the thermal conductivity k and volumetric heat C.

Stefan's equation is considered to be the simplest of the analytical methods of frost penetration predictions (Aldrich, 1956, Dempsey, 1976). This equation generally predicts large values of frost penetration. In freezing climates the accuracy of this equation can reach 90 percent, but as the latitude decreases its accuracy may drop to values near 50 percent (Aldrich, 1956). Stefan's formula is presented below:

$$DFP = \sqrt{\frac{48 \cdot k_f \cdot SFI}{L}} \tag{4.8}$$

DFP is the depth of frost penetration; k_f is the frozen thermal conductivity given in Btu/hr.ft.deg F; SFI is the surface freezing index; and L is the latent heat of fusion given in Btu /ft^3. The latent heat of fusion depends on the dry unit weight γ_d of the soil and is given by means of the next equation were w is the gravimetric moisture content.

$$L = 1.434 \cdot w \cdot g_d \tag{4.9}$$

Aldrich and Paynther (1956) developed the modified Berggren equation which in general gives more accurate results than Stefan's formula. The expression for this equation is given as follows.

$$DFP = \lambda\sqrt{\frac{48 \cdot k \cdot SFI}{L}} \tag{4.10}$$

λ is the correction parameter that includes volumetric heat effects; these are neglected by Stefan's formula (Aldrich, 1956), and k is the thermal conductivity which is normally taken as the average between the unfrozen and the frozen thermal conductivity. In this model, the input temperature is assumed to be a sinusoidal function as shown in Figure 4.19, which agrees with the curves presented in the previous section.

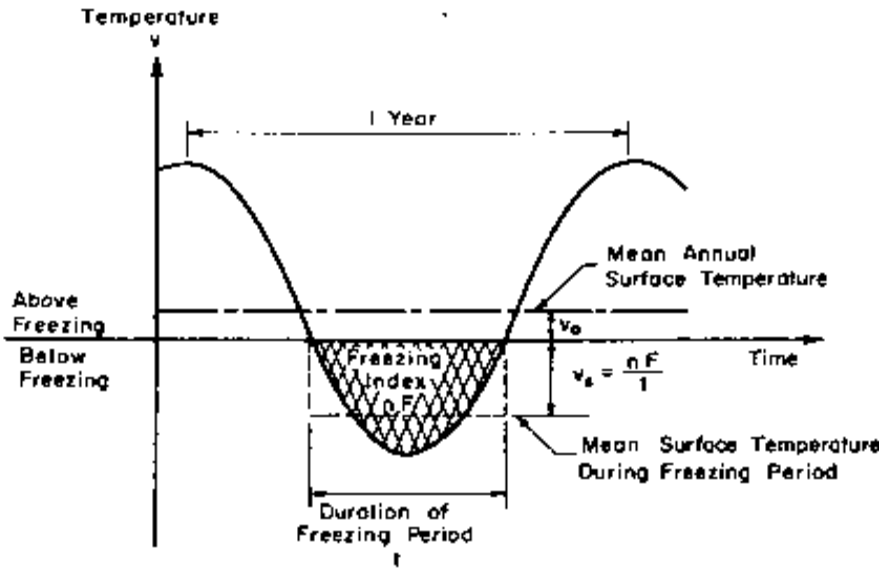

Figure 4.19. Sine Curve for Assumed Annual Variation in Surface Temp. (Aldrich, 1956)

To calculate λ, parameters α and μ must be determined. These parameters are described by the following formulae:

Thermal ratio, $a = \frac{v_o}{v_s}$ (4.11)

Fusion parameter, $m = \frac{C}{L} v_s$ (4.12)

where C is the volumetric heat given in Btu/ft^3.deg F. Common values for this parameter for PCC and soils are close to 30 Btu/ft^3. Figure 4.20 shows the chart to obtain the correction parameter for the modified Berggren equation.

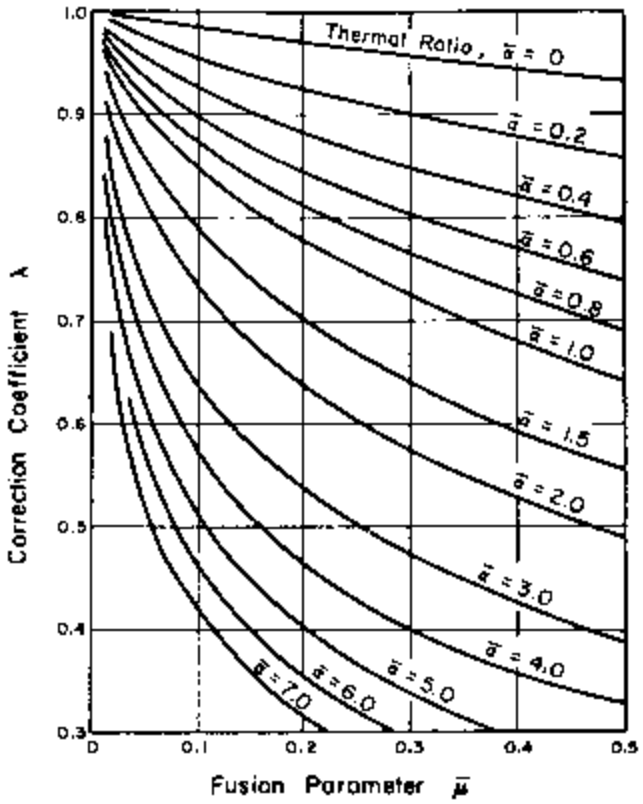

Figure 4.20. Correction Parameter for the Modified Berggren Equation (Aldrich, 1956)

Thermistor data from stations 390901, 390203, 390205 and 390212 was used to determine the different values of frost penetration for three consecutive

winters starting from 1996. A typical MRC thermistor probe assembly installed at the Ohio Test Road is shown in Figure 4,21. Values below zero degrees Celsius were considered to be freezing points for depth of frost penetration estimation.

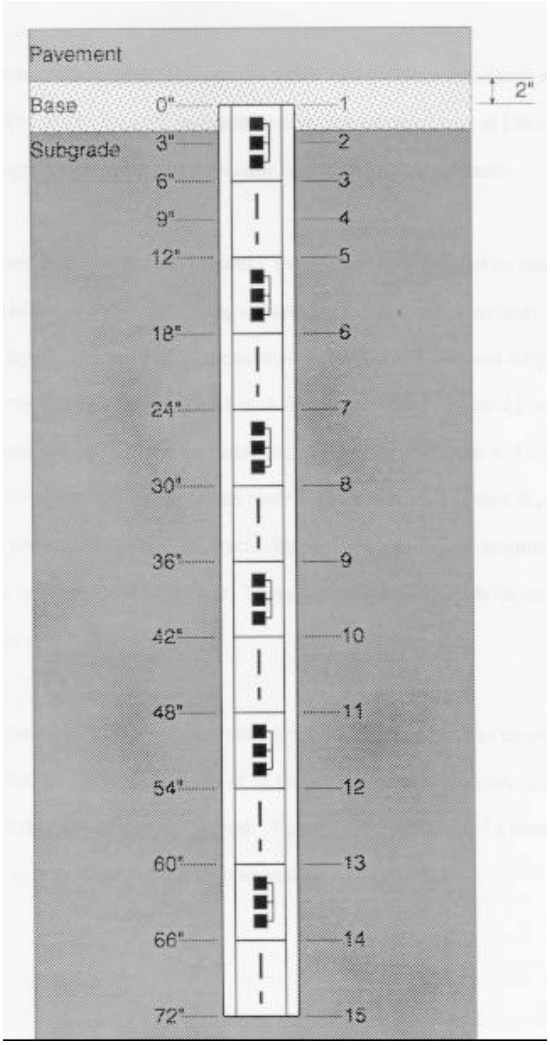

Figure 4.21. Typical Thermistor Probe Assembly (Sargand, 1994)

Plots of frost penetration vs. time were obtained from the analysis. Figure 4.22 shows this variation for the 1996-1997 winter. It should be indicated that

Julian day 367 corresponds to January 1, 1997 and so on to facilitate the frost penetration vs. day using this cumulative scale. Charts for the following years are included in appendix C.

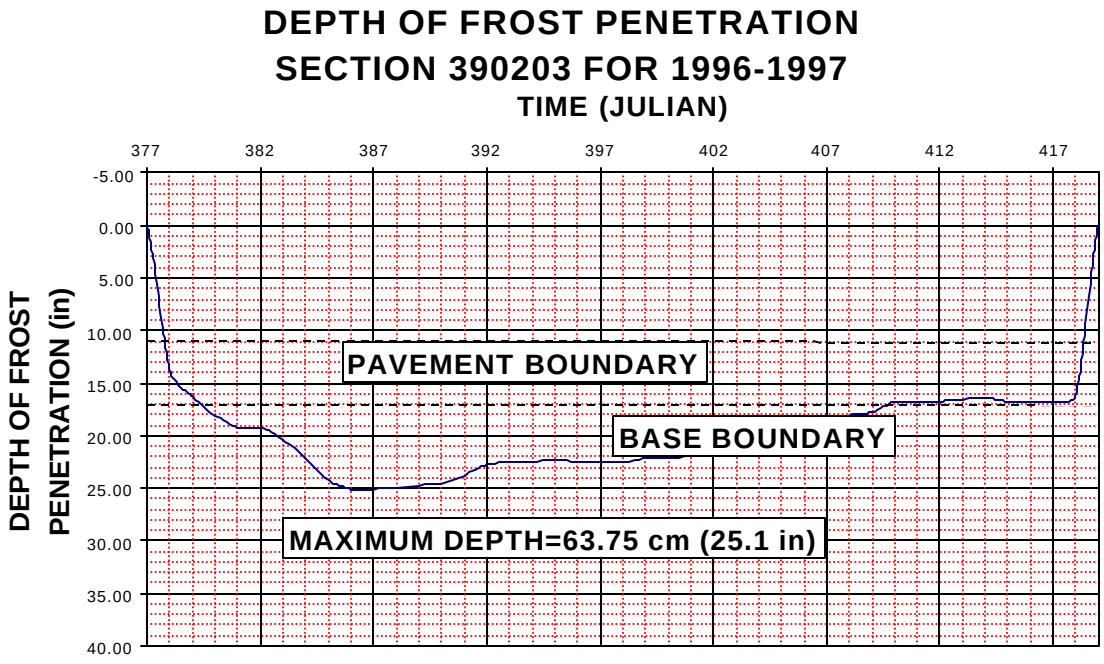

Figure 4.22. Depth of Frost Penetration vs. Time (All sections)

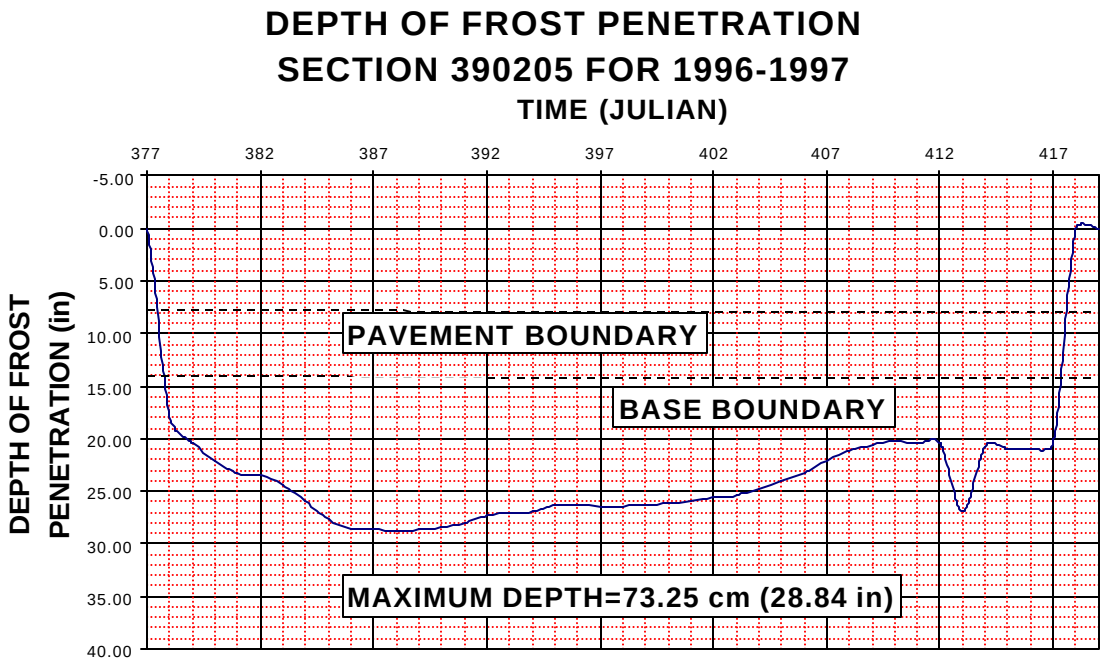

Figure 4.22. Depth of Frost Penetration vs. Time (All sections) (cont.)

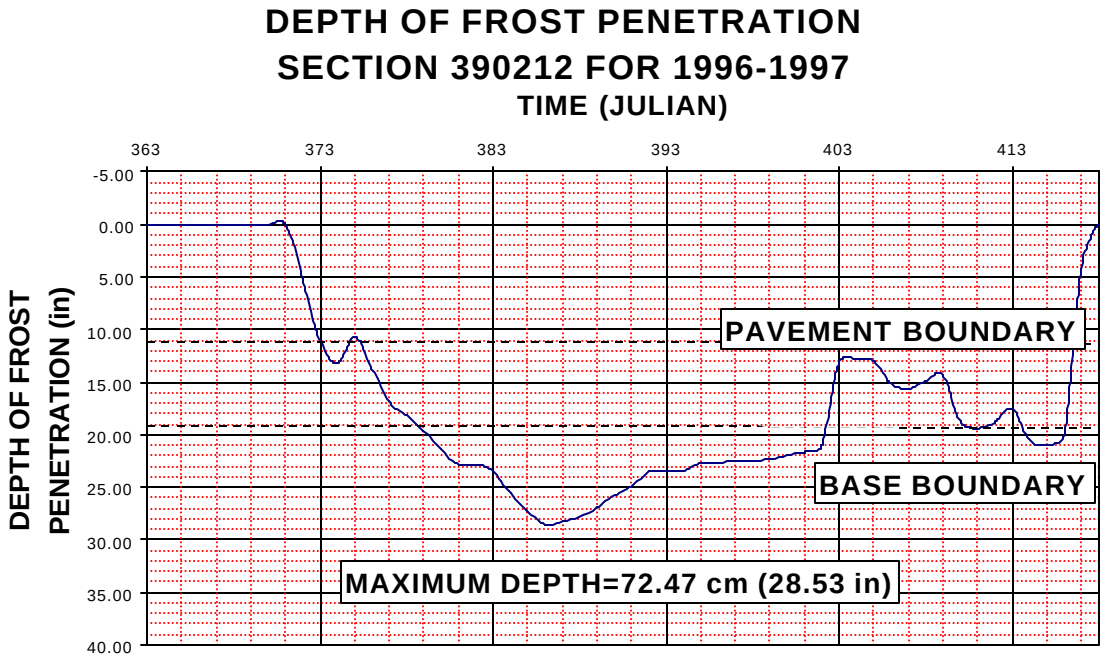

Figure 4.22. Depth of Frost Penetration vs. Time (All sections) (cont.)

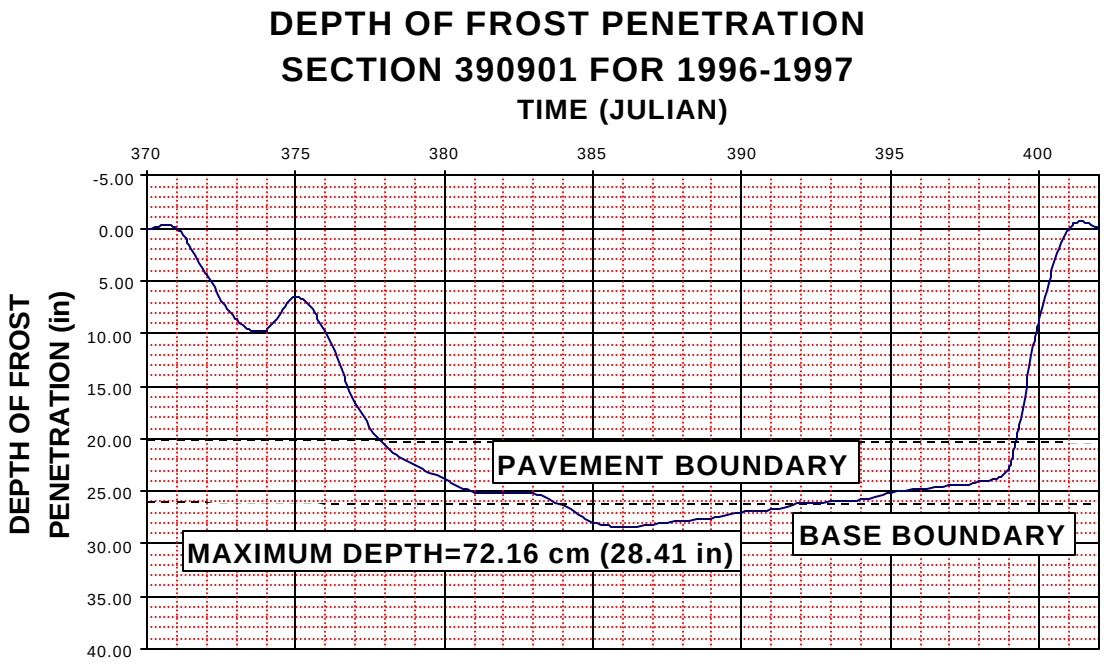

Figure 4.22. Depth of Frost Penetration vs. Time (All sections) (cont.)

As mentioned before, depth of frost penetration predictions may be established using Stefan's formula or the modified Berggren equation for homogenous systems. A multilayer model based on this latter procedure was proposed for a final depth of frost penetration estimation.

The estimation procedure has three different levels of accuracy. For level 1 different properties of the pavement have to be known such as the strata, the specific unit weight and water content of each material, and the surface temperature during the freezing period. For level 2 the strata and the average air temperature during the freezing period is required, and for level 3 only the average air temperature is needed.

The calculation of the surface freezing index (SFI) is the first step needed to estimate the depth of frost penetration. For level 1 in the PCC pavements, this index is the area under the curve, when temperatures are below freezing, of the time series function established by the surface temperature. Plots of these functions for station 390203 are depicted in Figure 4.23, where a cumulative Julian day was also used to facilitate plotting. Plots for other stations, when it was possible to obtain them, are included in Appendix C. These estimates were made using the trapezoidal method.

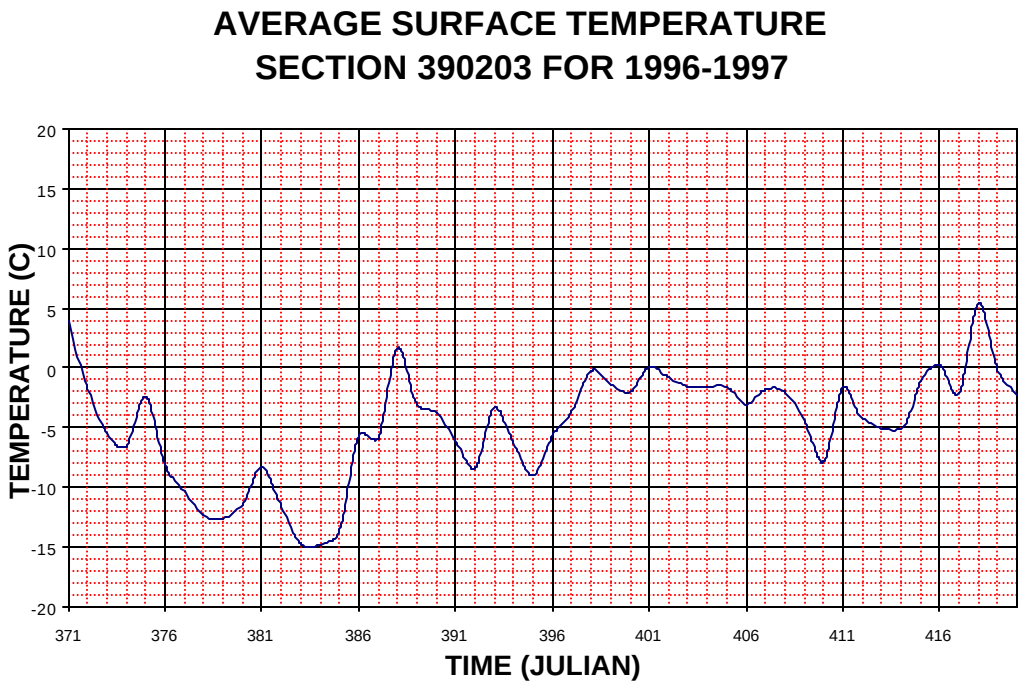

Figure 4.23. Surface Temperature vs. Time (Section 390203: 96-97, 97-98 and 98-99)

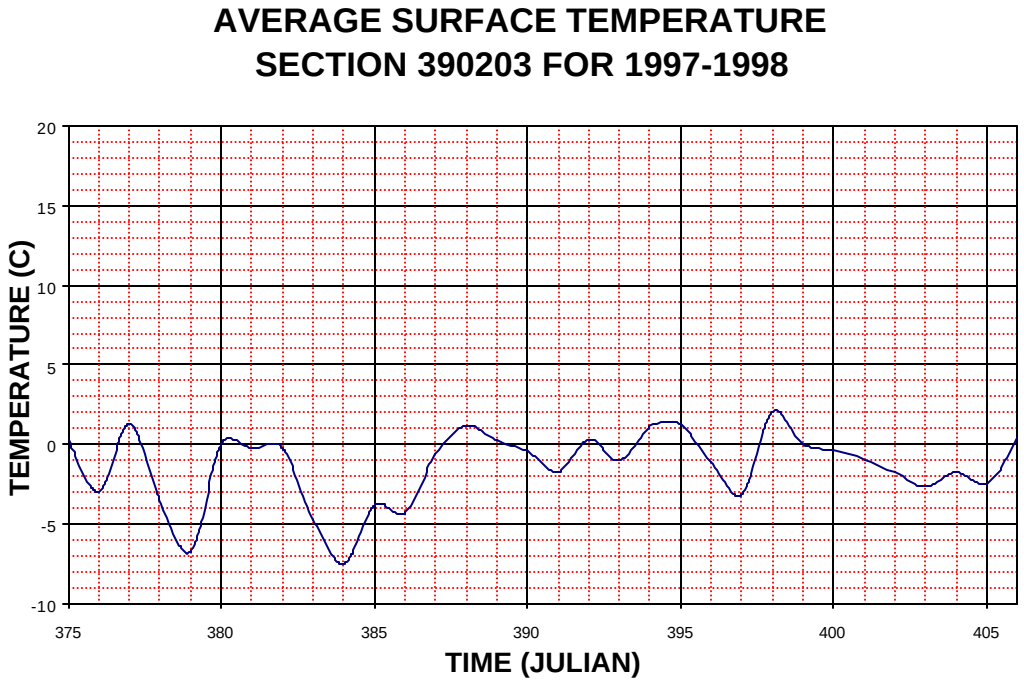

Figure 4.23. Surface Temperature vs. Time (Section 390203: 96-97, 97-98 and 98-99) (cont.)

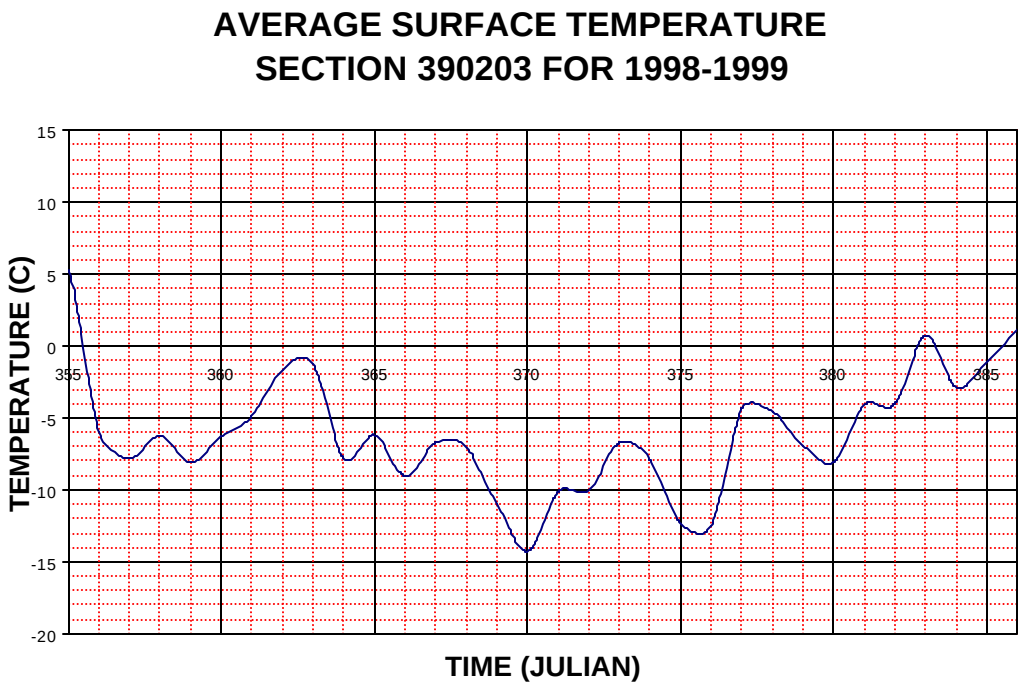

Figure 4.23. Surface Temperature vs. Time (Section 390203: 96-97, 97-98 and 98-99) (cont.)

The limits for the freezing period were chosen observing the time series. Days with average temperatures below zero followed by days with positive temperatures that would generate more positive than negative areas where not included. This procedure differs from the sinusoidal curve proposed by Aldrich in 1956, but in a general scheme the obtained values in both procedures are similar. Due to malfunctions of the upper thermistor in the AC pavement (station 390901), the calculated air freezing index was used as the surface freezing index. This last assumption agrees with Aldrich's approach, and doesn't generate major errors in the depth of frost penetration estimation.

Knowing the surface freezing index, the material properties and geometry of the road, calculations for the frost penetration were perfected following the next procedure:

1. Using the modified Berggren equation (Aldrich, 1956) without including the correction factor λ, a calculation for the frost penetration assuming a homogeneous first material layer (in this case PCC) was performed given the calculated surface freezing index.

$$DFP = \sqrt{\frac{48 \cdot k \cdot SFI}{L}} \qquad (4.13)$$

2. If the depth is lower than the first layer the calculated value is the non-corrected depth of frost penetration. If it is higher the SFI used to freeze the total thickness is calculated by means of the same equation reverted.

$$\frac{Layer_1^{\,2} \cdot L}{48 \cdot k} = SFI_1 \qquad (4.14)$$

3. Knowing the SFI_1 and the properties of the second layer the equation for the frost penetration is given by the next equation (SFI_2 is the subtraction of SFI_1 from the total surface freezing index).

$$DFP = \sqrt{\frac{48 \cdot k_1 \cdot SFI_1}{L_1} + \frac{48 \cdot k_2 \cdot SFI_2}{L_2}} \qquad (4.15)$$

4. As in step 2, if the depth is lower than the sum of the two layers the non-corrected depth of frost penetration is the obtained value if not, the SFI_2 is calculated solving the equation above for the SFI_2.

$$\frac{\left(layer_1 + layer_2\right)^2 - \frac{48 \cdot k_1 \cdot SFI_1}{L_1}}{48 \cdot k_2} \cdot L_2 = SFI_2 \qquad (4.16)$$

5. The same procedure continues for “n” number of layers until the non-corrected depth of frost penetration is obtained.

Average values of k of 0.64 and 0.8 for PCC and AC respectively, 1.5 for coarse and 1.1 for fine soils were used to determine the depth of frost penetration (Aldrich, 1956).

To find the corrected depth of frost penetration the correction factor λ (25) must be determined. Following Aldrich’s procedure to establish an average value for the correction factor, values of the volumetric heat (C) and the latent heat (L) have to be calculated.

C is estimated as the average of the unfrozen (C_u) and frozen (C_f) volumetric heat. These parameters are given by the following equations:

$$C_u = \gamma_d \left(0.17 + \frac{\omega}{100} \right)$$
$$C_f = \gamma_d \left(0.17 + \frac{0.5 \cdot \omega}{100} \right) \qquad (4.17) \text{ \& } (4.18)$$

where γ_d is the dry unit weight in pcf and ω is the gravimetric moisture content in percentage. Knowing C and L for each material, average values C_{wt} and L_{wt} have to be establish for the total depth. This values are calculated by means of the following equations:

$$C_{wt} = \frac{C_1 \cdot d_1 + C_2 \cdot d_2 + ...C_n \cdot d_n}{X}$$
$$C_{wt} = \frac{L_1 \cdot d_1 + L_2 \cdot d_2 + ...L_n \cdot d_n}{X} \qquad (4.19) \text{ \& } (4.20)$$

where X is the non-corrected depth of frost penetration, and d is the thickness of a layer within the depth ($X=d_1+d_2+.....d_n$).

Knowing C_{wt} and L_{wt} values for V_o, V_s, α and μ were calculated. Table 4.8 shows the results for λ for all the PCC sites.

Table 4.8. Estimated values of λ

STATION	PERIOD	l
390203	96-97	0.7
390203	97-98	0.61
390203	98-99	0.72
390205	96-97	0.72
390205	97-98	0.64
390205	98-99	
390212	96-97	0.69
390212	97-98	0.62
390212	98-99	0.7
Average	Total	**0.68**

Knowing the average correction factors, the depth of frost penetration was estimated achieving level 1.

A general average of λ was calculated to be approximately 0.68 for the PCC sections under study. Also average values of 4.3, 10, and 17 percent for the gravimetric moisture content and the 22.64, 19.65 and 17.29 kN/m^3 (144, 125 and 110 lb/ft^3) for specific unit weight of the three layer system (PCC, base and subgrade respectively) were estimated from sensors in the field and from laboratory tests. These average values were estimated to achieve a second level of accuracy for the depth of frost penetration.

A surface temperature vs. air temperature plot for the PCC sites was developed using data from the weather station, as shown in Figure 4.24 with its respective equation. A value of 57 percent for the coefficient of determination was estimated using only the range of freezing days. Observing the surface freezing period and the air freezing period a difference in time was established. The surface freezing period for PCC structures is greater than the air freezing period. An average difference among the three sites was calculated as 4.7 days. Knowing the relationship between surface temperature and air temperature, and the average difference between air and surface freezing periods, an SFI given the air temperature series may be established, achieving level 2. This level is more general due to the approximations generated when average values are included in the analysis. Table 4.9 shows the SFI estimation following the procedure mentioned above.

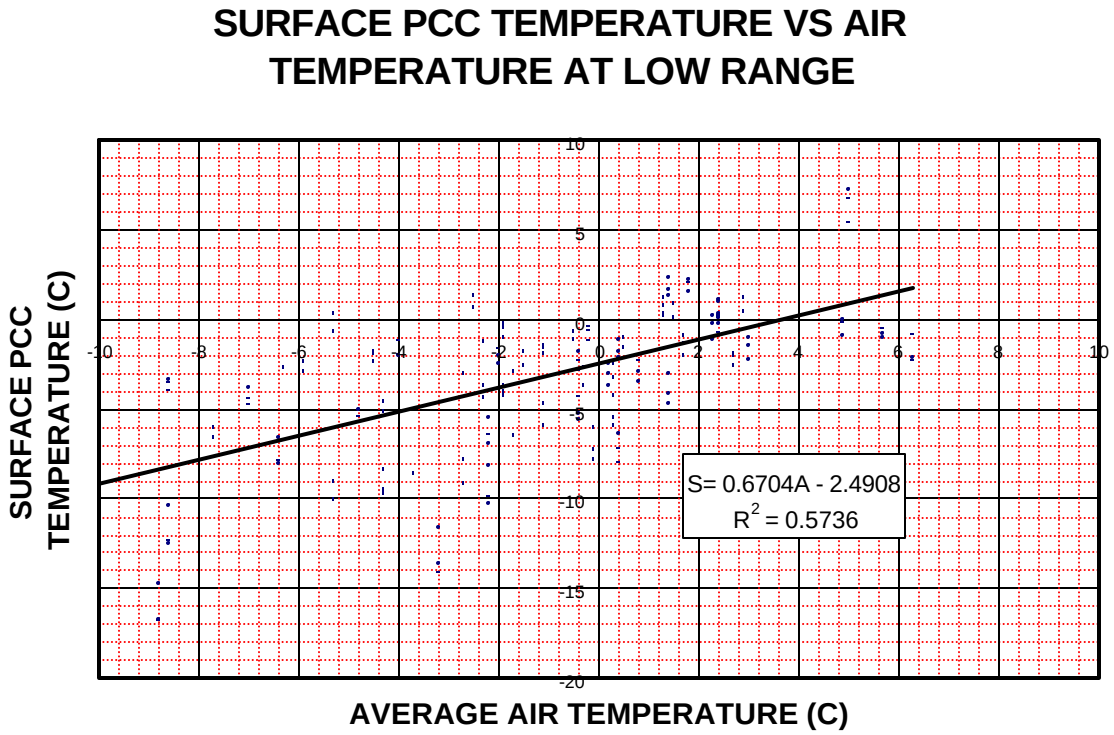

Figure 4.24. Surface PCC Temperature vs. Average Air Temperature

Table 4.9. Surface freezing index estimation (Level 2)

Average Air Temperature (C)	Estimated Surface Temperature (C)	Estimated Surface Temperature (F)	Air Freezing Period (days)	Surface Freezing Period Field (days)	Corrected Freezing Period (days)	Surface Freezing Index (Deg. F days)
-4.34	-5.40	22.28	43	50	47.7	463
-0.36	-2.73	27.08	27	30	31.7	156
-7.17	-7.30	18.87	26	30	30.7	403

Average thickness for the pavement layers of 25.13 cm. (9.5 in.) for the PCC layer and 17.78 cm. (7 in.) for the base layer were estimated for the Ohio Test Road. These general values, combined with the approximations included in level 2 led to a plot of Frost Penetration vs. SFI. This chart is the resulting level 3 in the hierarchical procedure. This plot with its general equation are shown in Figure 4.25.

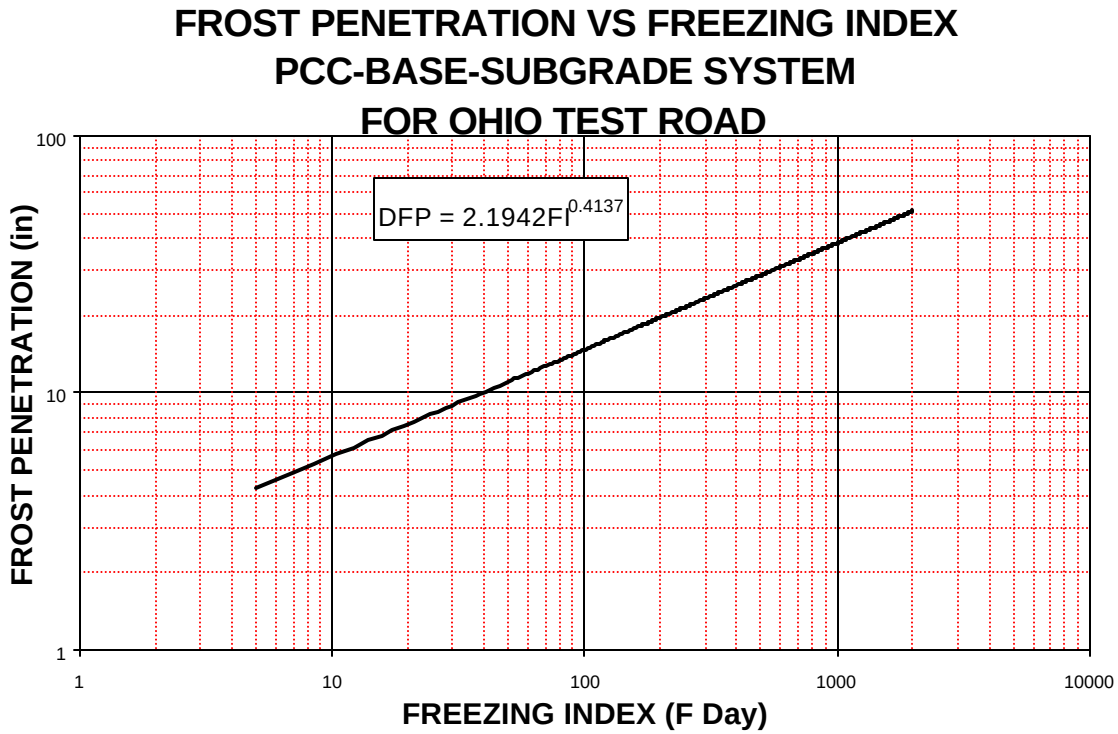

Figure 4.25. Frost Penetration vs. Freezing Index for PCC-Base-Subgrade System

Estimated values at the three different levels for PCC-Base-Subgrade structures for the Ohio Test Road are presented in Table 4.10.

Table 4.10. Depth of Frost Penetration Estimation (PCC-Base- Subgrade system)

Site	FI Level 1	FI level 2	DFP field cm (in)	DFP level 1 cm (in)	DFP level 2 cm (in)	DFP level 3 cm (in)
390203	461	463	63.75 (25.1)	65.79 (25.9)	68.07 (26.8)	70.61 (27.8)
390203	112	156	38.35 (15.1)	34.34 (13.52)	43.18 (17.0)	44.96 (17.7)
390203	380	403	58.17 (22.9)	60.99 (24.01)	63.75 (25.1)	66.55 (26.2)
390205	576	463	73.15 (28.8)	79.65 (31.36)	69.85 (27.5)	70.61 (27.8)
390205	164	156	38.61 (15.2)	40.31 (15.87)	40.64 (16.0)	44.96 (17.7)
390205		403	72.39 (28.5)		62.99 (24.8)	66.55 (26.2)
390212	520	463	72.39 (28.5)	76.10 (29.96)	68.83 (27.1)	70.61 (27.8)
390212	115	156	40.64 (16.0)	39.04 (15.37)	44.70 (17.6)	44.96 (17.7)
390212	432	403	62.48 (24.6)	67.11 (26.42)	64.77 (25.5)	66.55 (26.2)

Regression lines were established showing the relationship between the field frost penetration and the estimated ones at the three levels. R^2 values of 98, 89, and 91 percent where obtained for each respective level. Plots showing these relationships are shown in Figure 4.26.

Average values of 5.33, 11.43 and 8.38 cm (2.1, 4.5 and 3.3 in.) of difference between the measured and the estimated depth of frost penetration were calculated for each respective level. Finally, maximum deviation values of 2.29, 4.32 and 5.08 cm. (0.9, 1.7 and 2.0 in.) were determined.

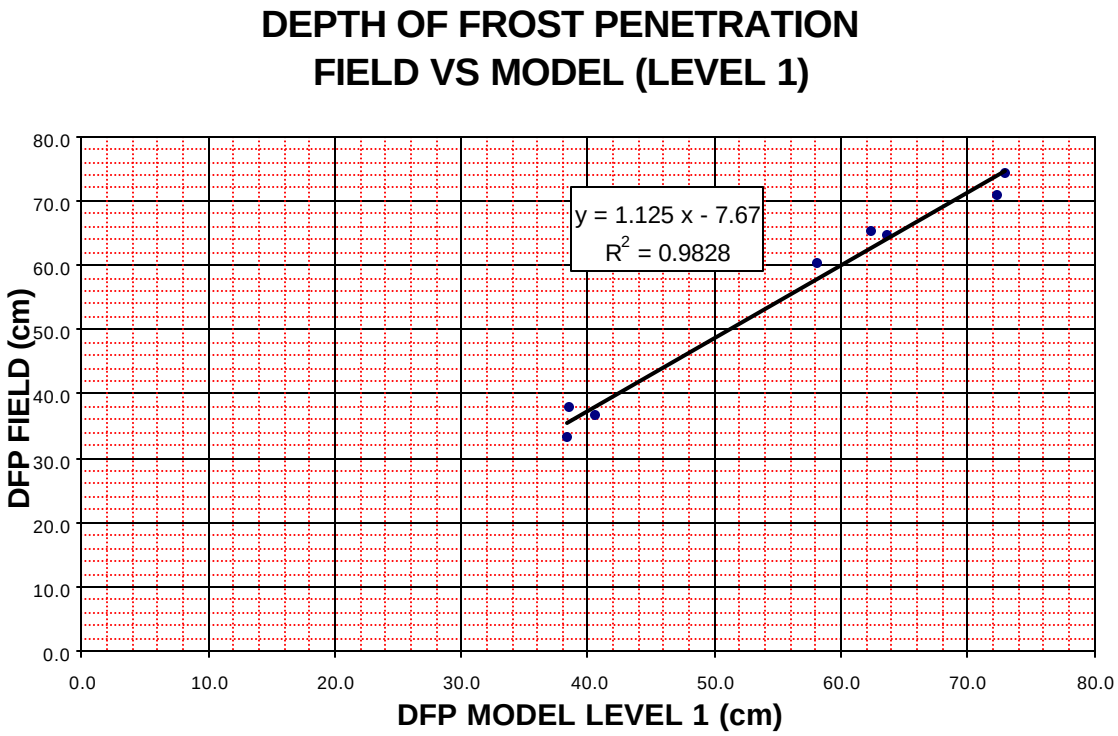

Figure 4.26. Relation between the Measured and the Estimated DFP (all levels)

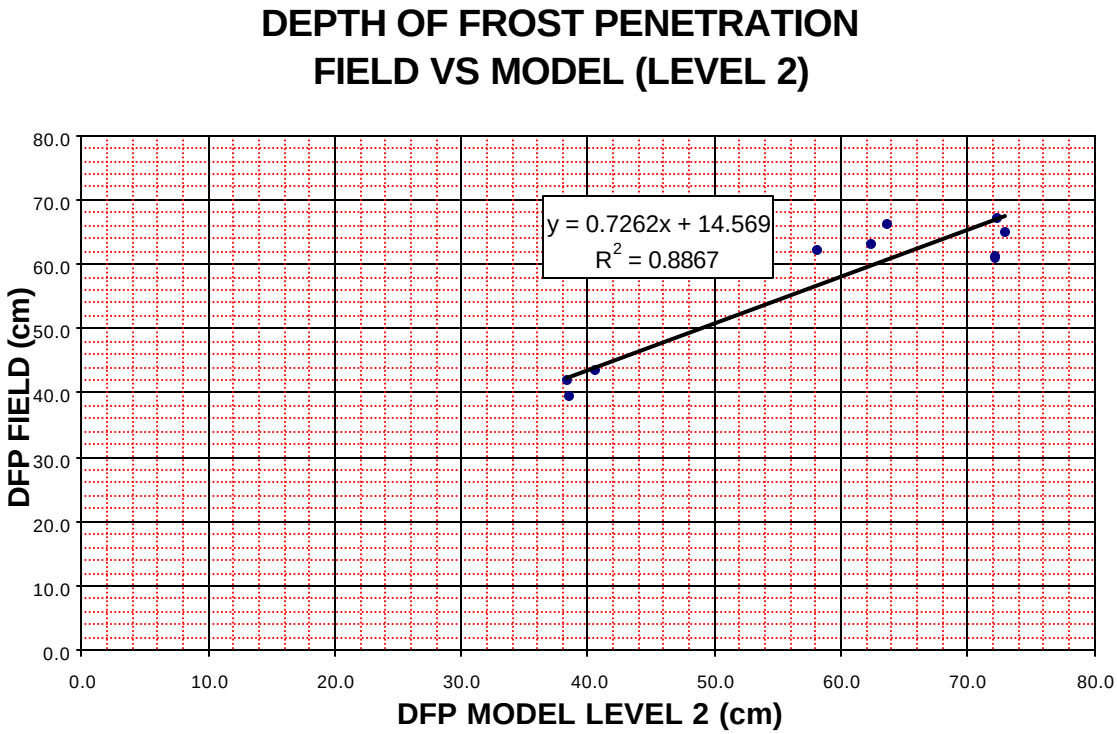

Figure 4.26. Relation between the Measured and the Estimated DFP (all levels) (cont.)

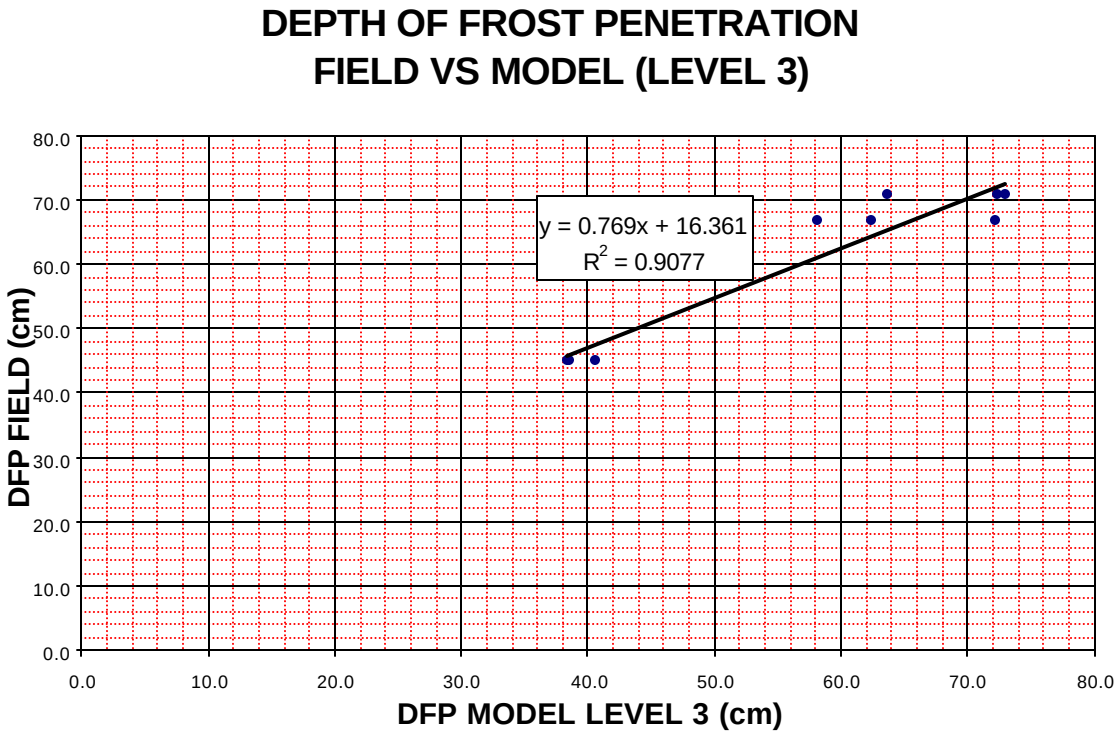

Figure 4.26. Relation between the Measured and the Estimated DFP (all levels) (cont.)

Due to problems of the surface thermistor installed in the field, level 1 wasn't achieved for the Asphalt Concrete sections, thus the surface freezing index for the site, was estimated as the air freezing index to obtain level 2.

The same averaging procedure for the pavement layers was established to achieve level 3. An average value of λ of 0.62 was estimated. The first layer was considered to be a compound between the asphalt concrete and the treated asphalt concrete base. The second was the granular base and the third was the subgrade. Average values of 45.72 and 15.24 cm. (18 and 6 in.) for the first two layers were estimated. A plot representing level 3 is shown in Figure 4.27.

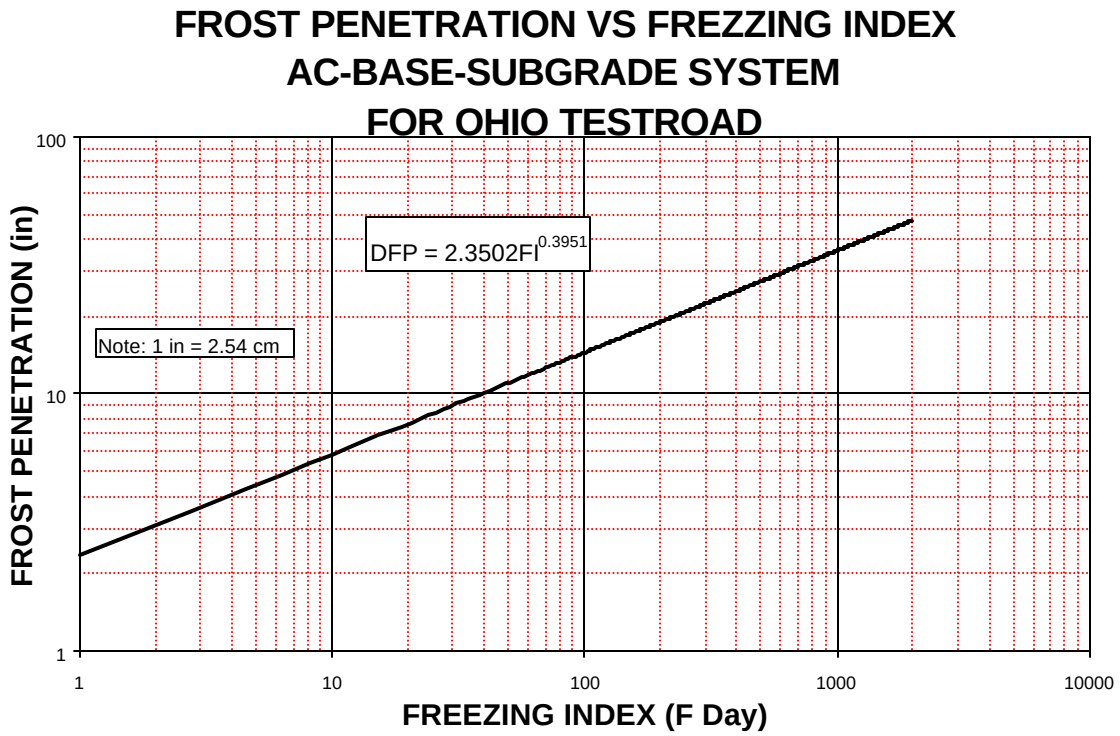

Figure 4.27. Frost Penetration vs. Freezing Index for AC-Base-Subgrade System

Estimated values at the three different levels for AC-Base-Subgrade structures for the Ohio Test Road are presented in Table 4.11.

Table 4.11. Depth of Frost Penetration Estimation (AC-Base Subgrade system)

Freezing Period	Site	SFI=AFI	DFP field cm (in)	DFP level 2 cm (in)	DFP level 3 cm (in)
96-97	390901	418	72.1 (28.4)	70.0 (27.5)	61.6 (24.3)
97-98	390901	133	34.5 (13.6)	35.5 (14.0)	42.4 (16.7)
98-99	390901	341	68.1 (26.8)	64.1 (25.2)	57.1 (22.5)

A maximum value of 4.06 cm. (1.6 in.) between the measured frost penetration and the estimated one (level 2) was found with an average deviation of 2.39 cm. (0.94 in.). Figure 4.28 shows the comparison between the estimated and actual depths of frost penetration at each of the two levels along with the regression equation and the R^2 coefficient.

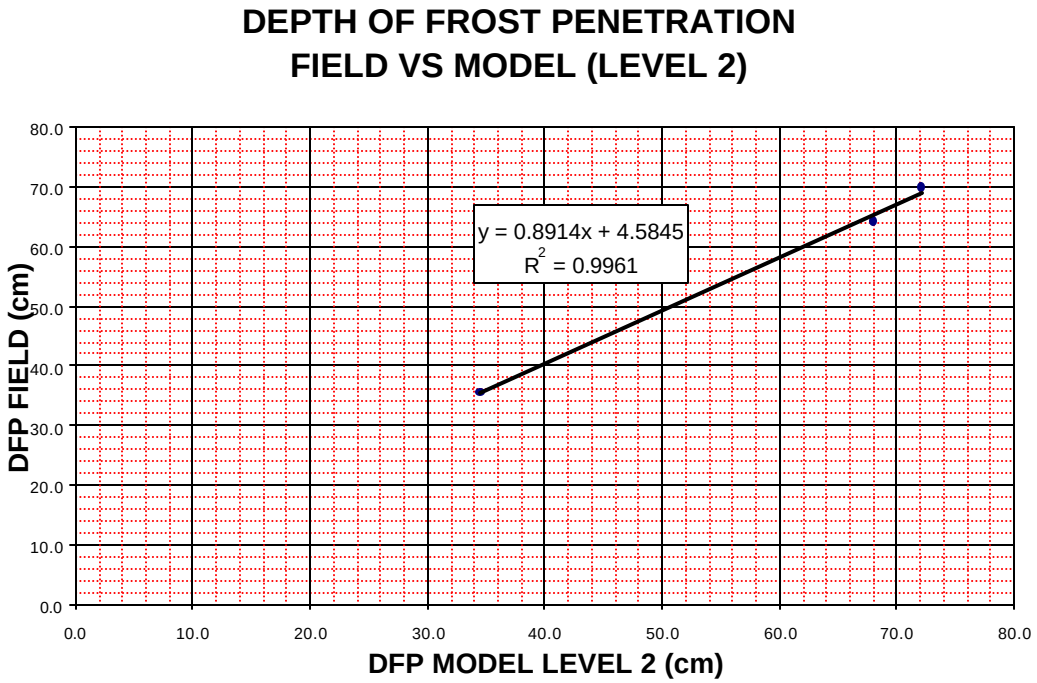

Figure 4.28.Relation between the Measured and the Estimated DFP (all levels)

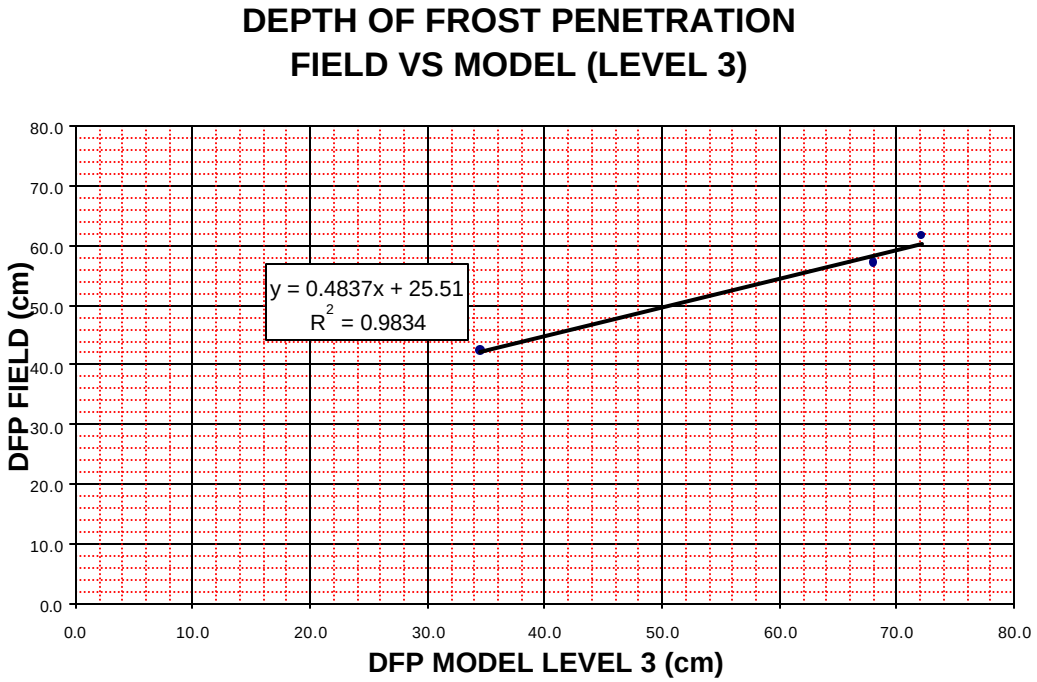

Figure 4.28.Relation between the Measured and the Estimated DFP (all levels) (cont.)

Values of frost penetration within the subgrade soil were calculated for the four stations considered, as given in Table 4.12.

Table 4.12. Subgrade Soil Frost Penetration

Section	1996-1997 cm (in)	1998-1999 cm (in)
390203	20.6 (8.1)	15.0 (5.91)
390205	37.7 (14.84)	36.8 (14.47)
390212	24.2 (9.53)	14.3 (5.62)
390901	6.1 (2.41)	4.5 (1.78)

In summary, a multilayer model based on the modified Berggren equation as summarized in the flow chart presented in Figure 4.29, was developed to

determine the depth of frost penetration. Three levels of accuracy for PCC pavements were tested with the first one being the most accurate. Values for the coefficient of determination of 99, 89 and 91 percent were calculated with average deviation values of 2.29, 4.32 and 5.08 cm. (0.9, 1.7 and 2.0 in.) respectively. Differences between the three levels of accuracy are relatively small thus level 3 is strongly recommended for a PCC-Base-Subgrade system given the fairly easy determination of the input parameters. Magnitude and average temperature of the freezing period are necessary to determine the surface freezing index which directly determines the frost penetration. The surface freezing index may be replaced by the air freezing index without incurring a high error in the frost penetration estimation.

This multilayer model is a direct procedure as opposed to Aldrich's (Aldrich, 1956) which involves an iterative analysis. Convergence errors are avoided with the direct method, and very accurate solutions are obtained.

Technical problems in the upper thermistor led to some differences in the AC-Base-Subgrade system approach. The air freezing index was assumed to be the surface freezing index. The same multilayer model was used approaching levels 2 and 3 and once again level 3 is recommended for AC-Base-Subgrade systems for the Ohio Test Road, because of its simplicity.

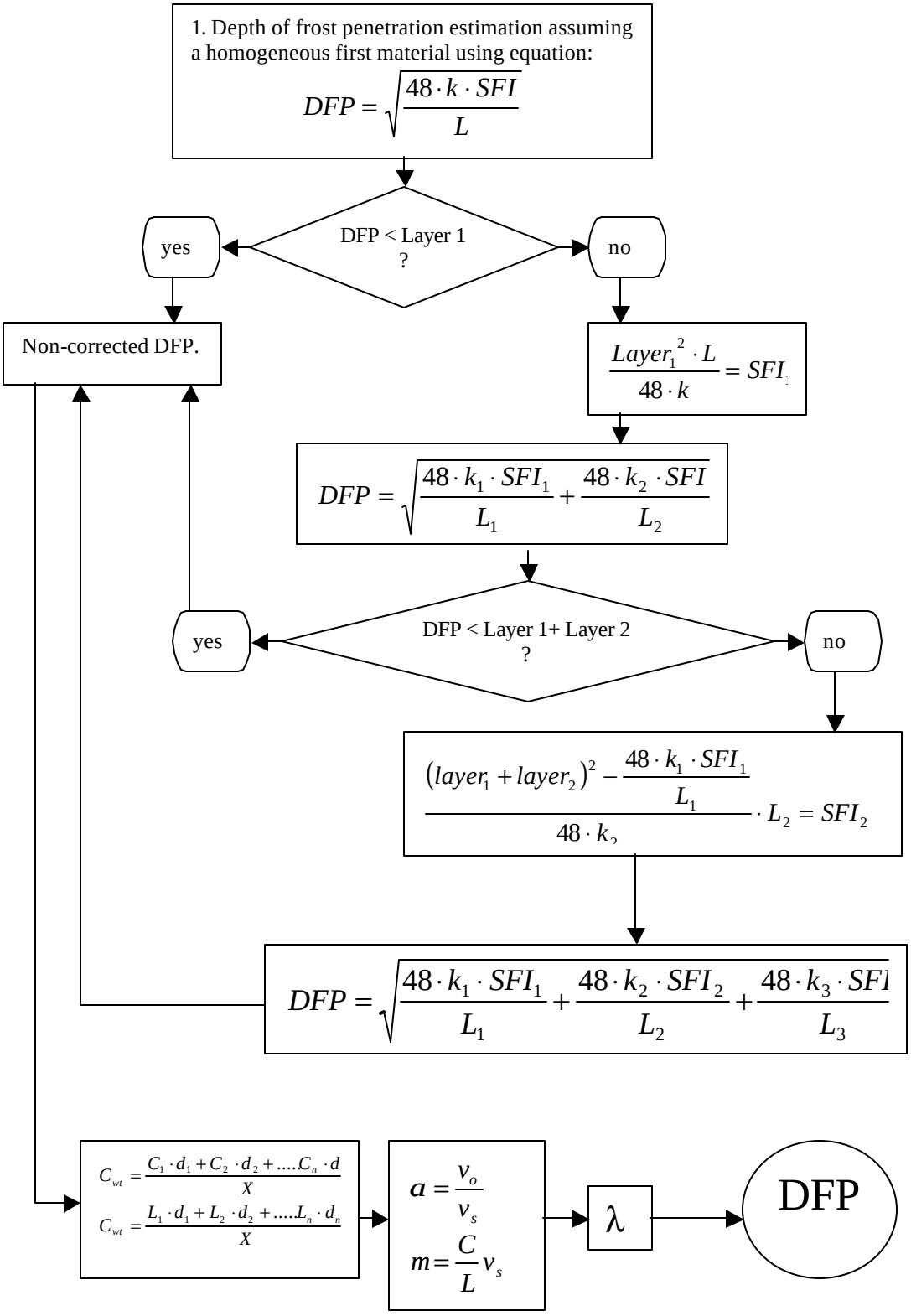

Figure 4.29. Proposed Model for DFP Estimation

Effective frost penetration depths in the subgrade were calculated. Values for the AC were lower than those of the PCC structures. Calculated frost penetration depths indicated a maximum of 6.35 and 38.1 cm (2.5 and 15 in) for the AC and PCC pavement sections analyzed at the Ohio Test Road. The substantial difference in the depth of penetration into the subgrade is more the result of a thicker flexible pavement than a rigid pavement. The absolute depth of frost penetration only differs by about 2.5 cm (1 in.) in both cases.

4.7. Moisture Content-Degree of Saturation Estimates

Monthly measurements were taken at each site (twice in March and April) to determine the variation of the moisture content in the subgrade soil. Apparent length readings were established for each embedded sensor. The calibration curve developed in the laboratory with Klemunes' hierarquical model at Level 1 was used to determine the volumetric moisture content. After calculating the volumetric moisture content the gravimetric moisture content was determined given the relationship between both parameters shown below, Figueroa et al. (1998):

$$w = q\left(\frac{r_w}{r_d}\right) \tag{4.21}$$

Where θ is the volumetric moisture content, w the gravimetric moisture content, ρ_w the density of water and ρ_d the dry density of the soil.

The gravimetric moisture content normally used in design was directly related to the degree of saturation by means of the following equation:

$$S_r = \frac{w \cdot G_s}{\frac{G_s \cdot g_w}{g_d} - 1} \qquad (4.22)$$

where S_r is the degree of saturation, γ_w is the unit weight of the water, γ_d is the dry unit weight of the soil and G_s its specific gravity.

The specific gravity has an average value of 2.7 (Figueroa et al., 1998) and the dry unit weight of the soil varies between 105 and 120 lb/ft^3. Knowing that the saturation has a maximum value of 100 percent, and assuming that the subgrade is going to reach saturation at certain periods during the year, the dry unit weight of the soil was back-calculated. Tables with values of the degree of saturation for the different days of the year when data was acquired were generated and are included in Appendix D.

Plots of saturation vs. time were developed to determine the seasonal variation of the degree of saturation. An example of these is shown in Figure 4.30 for Section 390203, starting on July 22, 1996 and ending on December 17, 2002. The plot is presented in a “cumulative” Julian scale (to facilitate a continuous plotting) where the first day of 1996 is day 1, while December 17, 2002 corresponds to the 2543th day. S2 through S10 represent sensor numbers from top to bottom in the subgrade at this station.

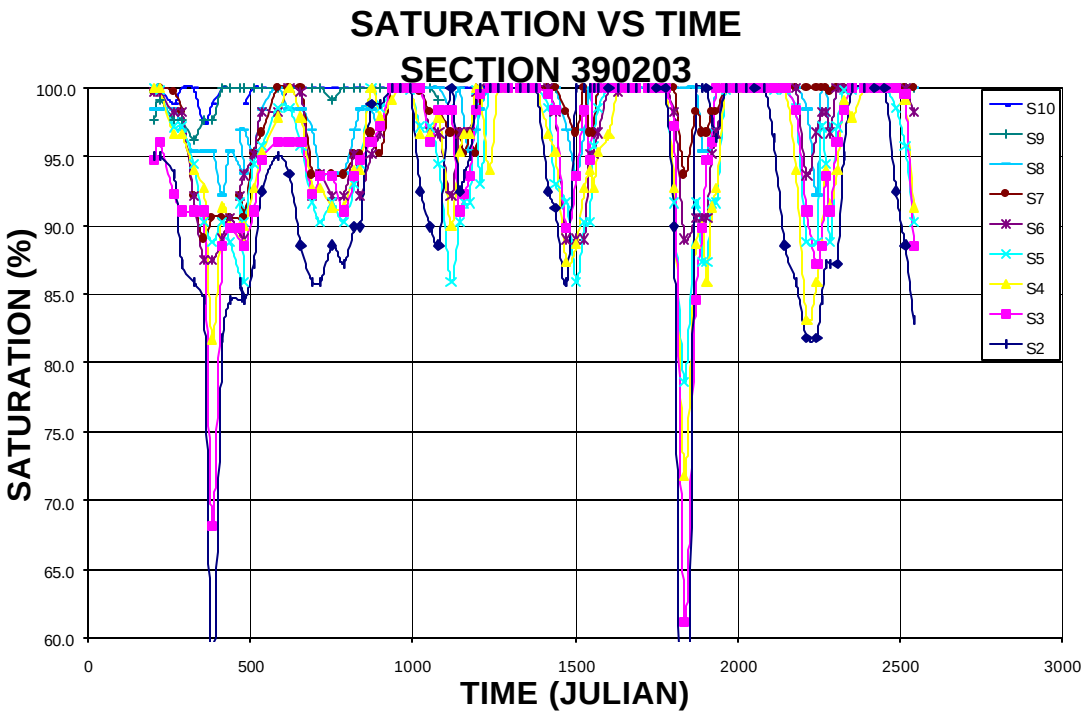

Figure 4.30. Degree of Saturation vs. Time

The low valleys observed in this figure typically corresponded to periods when the soil was frozen. Average seasonal values of the degree of saturation were determined for each year and are tabulated in Appendix D for Sections 390203, 390205, 390212 and 390901. Using these tables is then possible to determine an overall seasonal average considering seven years of moisture data. Tables 4.13 to 4.16 show these overall seasonal averages vs. embedded sensor depths measured from the top of the subgrade.

		DEPTH								
	cm	7.6	22.9	38.1	53.3	68.6	83.8	99.1	129.5	160.0
	in	3	9	15	21	27	33	39	51	63
Sat (%)	SPRING	95.2	96.4	95.2	95.6	96.9	97.4	98.4	100.0	99.9
	SUMMER	98.4	98.6	99.6	99.6	99.8	100.0	99.7	99.7	99.9
	FALL	90.4	96.7	96.5	95.9	97.7	98.2	98.9	99.5	99.9
	WINTER	88.0	90.0	90.2	90.1	91.9	95.8	96.0	96.5	99.7

Table 4.13. Average Seasonal Degree of Saturation vs. Subgrade Depth [Section 390203]

		DEPTH									
	cm	15.2	30.5	45.7	60.9	76.2	91.4	106.7	121.9	152.4	182.9
	in	6	12	18	24	30	36	42	48	60	72
Sat (%)	SPRING	95.9	96.2	98.1	98.6	97.6		97.7	98.5	99.8	99.4
	SUMMER	97.9	98.2	98.9	99.3	100.0		100.0	100.0	100.0	99.7
	FALL	91.8	93.9	97.6	98.3	98.6		99.2	99.1	99.8	99.1
	WINTER	87.0	90.2	95.0	95.5	94.0		95.7	97.1	99.7	98.8

Table 4.14. Average Seasonal Degree of Saturation vs. Subgrade Depth [Section 390205]

		DEPTH								
	cm	10.2	25.4	40.6	55.9	71.1	86.4	101.6	132.1	162.6
	in	4	10	16	22	28	34	40	52	64
Sat (%)	SPRING	93.7	94.6	93.4	94.7	92.9	97.9	99.8	98.7	100.0
	SUMMER	97.0	99.5	99.3	99.4	99.2	99.9	100.0	100.0	100.0
	FALL	91.1	96.2	93.7	96.0	95.5	98.4	100.0	99.2	100.0
	WINTER	83.8	90.6	88.3	90.4	88.7	95.7	98.2	97.1	99.8

Table 4.15. Average Seasonal Degree of Saturation vs. Subgrade Depth [Section 390212]

		DEPTH							
	cm	**7.6**	**22.9**	**38.1**	**53.3**	**68.6**	**83.8**	**99.1**	**129.5**
	in	**3**	**9**	**15**	**21**	**27**	**33**	**39**	**51**
Sat (%)	**SPRING**	95.9	95.8	96.4	97.0	95.3	98.1	98.7	97.3
	SUMMER	94.8	99.8	100.0	99.8	98.9	99.9	100.0	98.9
	FALL	92.0	94.6	97.2	96.6	94.1	98.6	98.9	96.3
	WINTER	92.2	90.1	91.5	91.5	92.1	96.3	97.7	98.6

Table 4.16. Average Seasonal Degree of Saturation vs. Subgrade Depth [Section 390901]

Plots for the average seasonal degree of saturation vs. subgrade depth are presented in Figures 4.31 to 4.34 for the four studied sections. These figures consistently show that the subgrade soil has a higher degree of saturation during the summer and a lower degree of saturation during the winter. The fall and spring degrees of saturation are intermediate. These observations imply that there exists a time lag between the higher rainfall in the spring and the higher degree of saturation in the summer, as it will be examined below in detail.

Sections 390212 and 390901 were built with lateral drains, while sections 390203 and 390205 were built without drainage. The examination of Figures 4.31 to 4.34 does not show any significant influence in reducing the degree of saturation in sections with drains.

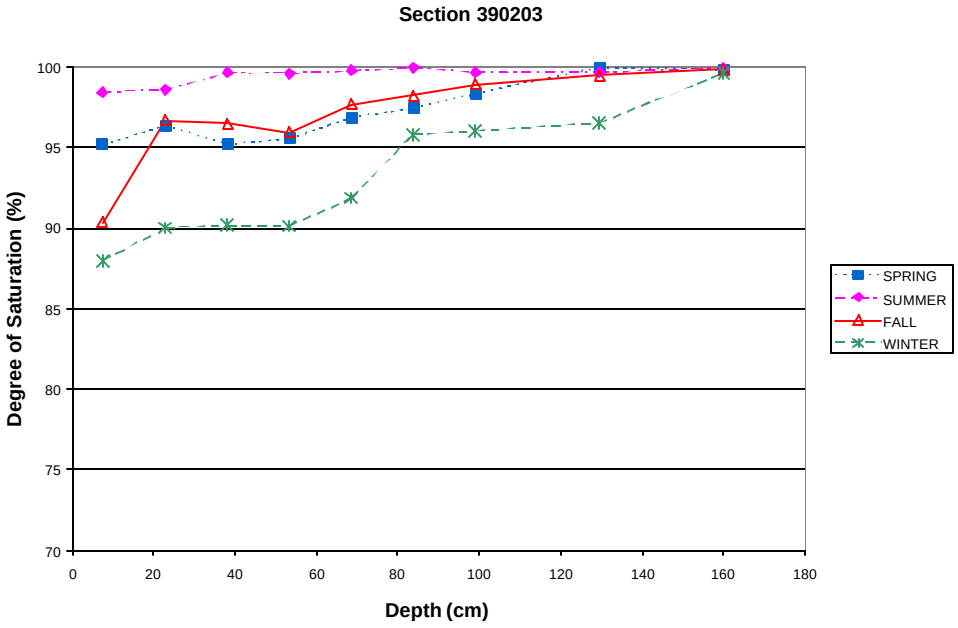

Figure 4.31. Average Seasonal Degree of Saturation vs. Subgrade Depth [Section 390203]

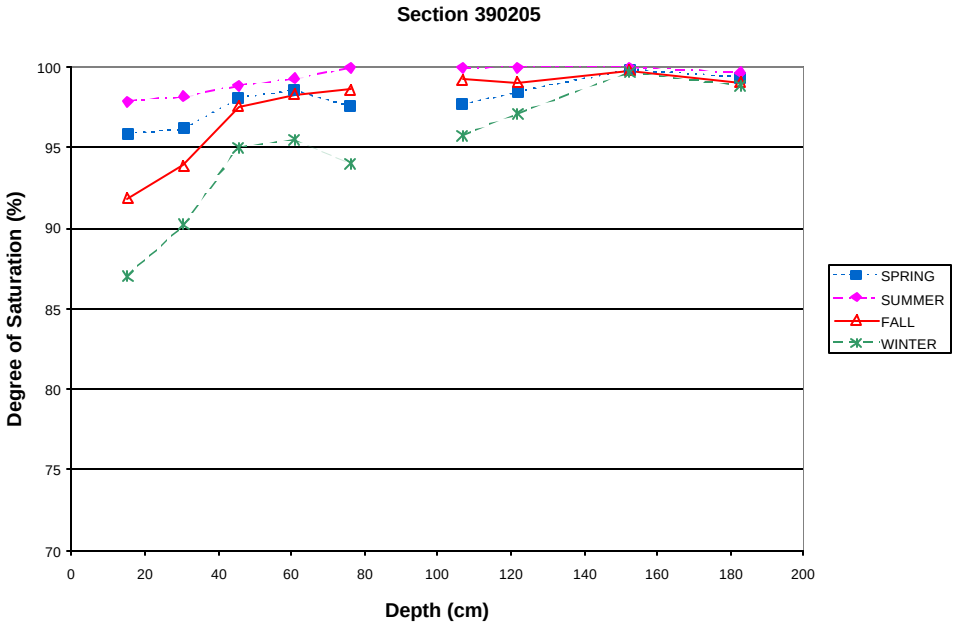

Figure 4.32. Average Seasonal Degree of Saturation vs. Subgrade Depth [Section 390205]

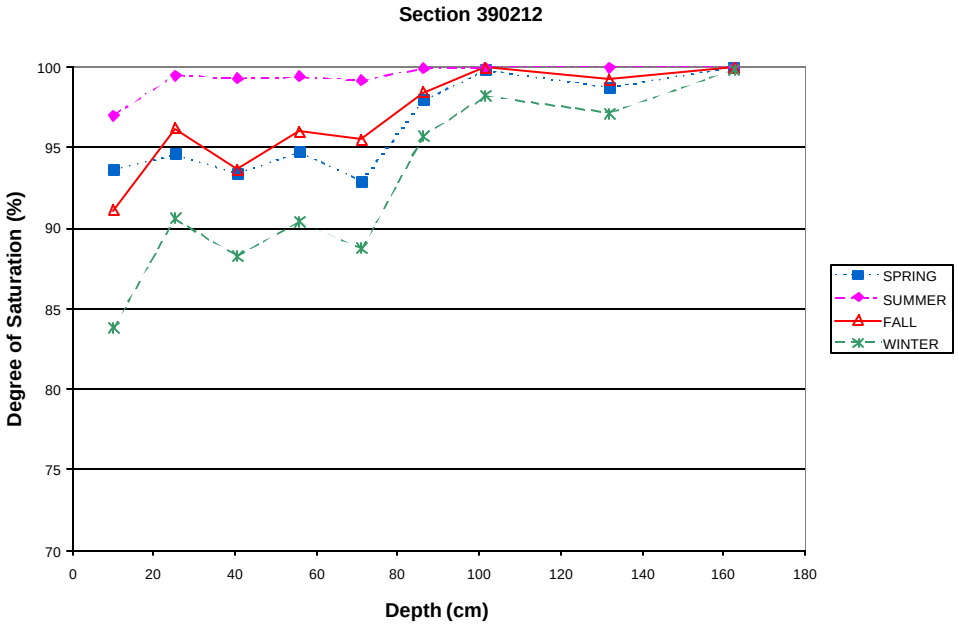

Figure 4.33. Average Seasonal Degree of Saturation vs. Subgrade Depth [Section 390212]

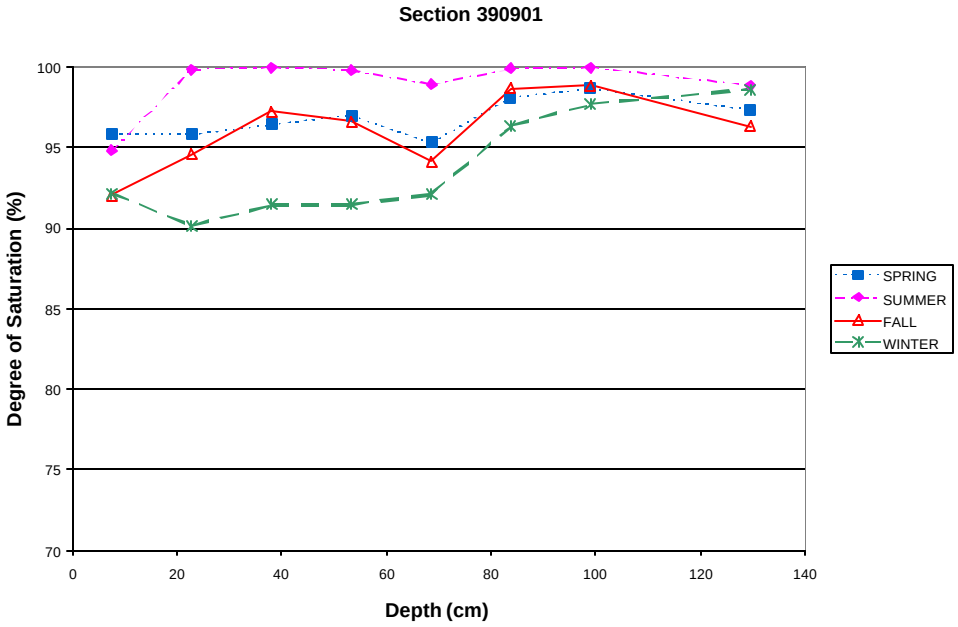

Figure 4.34. Average Seasonal Degree of Saturation vs. Subgrade Depth [Section 390901]

Rainfall information was plotted jointly with the degree of saturation measured by sensor S2 in Section 390901, to determine whether or not precipitation may be related to the degree of saturation of subgrade soils. Monthly precipitation data obtained from the weather station (included in Appendix D) between August of 1996 and December of 2000 was used to develop Figure 4.35, along with the monthly degree of saturation calculated for sensor S2 (also tabulated in Appendix D). The chart uses a cumulative Julian date in the horizontal axis to facilitate plotting starting with January 1st, 1996 as day 1.

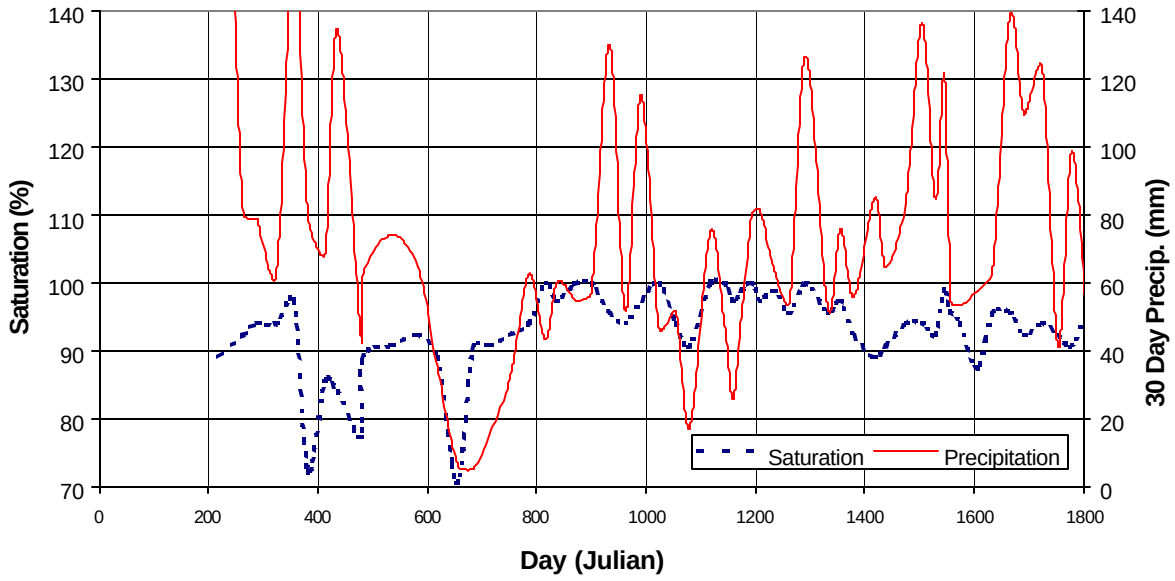

Figure 4.35. Degree of soil saturation (Sensor S2) and thirty day rainfall shifted forward 80 days (Section 390901)

This figure indicates that there is a relationship between the thirty-day accumulated precipitation 80 days before a saturation reading is taken. Note that the horizontal axis of the graph shows the accumulated Julian day the saturation

values were measured and that precipitation readings are 30 day accumulations shifted 80 days forward. As demonstrated in the graph, significant drops in precipitaiton result in significant drops in degree of soil saturation and viceversa.

Similarly, finer scale one-week accumulated rainfall values were calculated and related with the top subgrade sensor (S2) degree of saturation in section 390203. Although no direct relationship was found between the two parameters an 85-day shift was observed between them, as shown in Figure 4.36. The vertical scale has been deleted since the degree of saturation has been shifted down in order to allow a closer visual comparison between the two parameters.

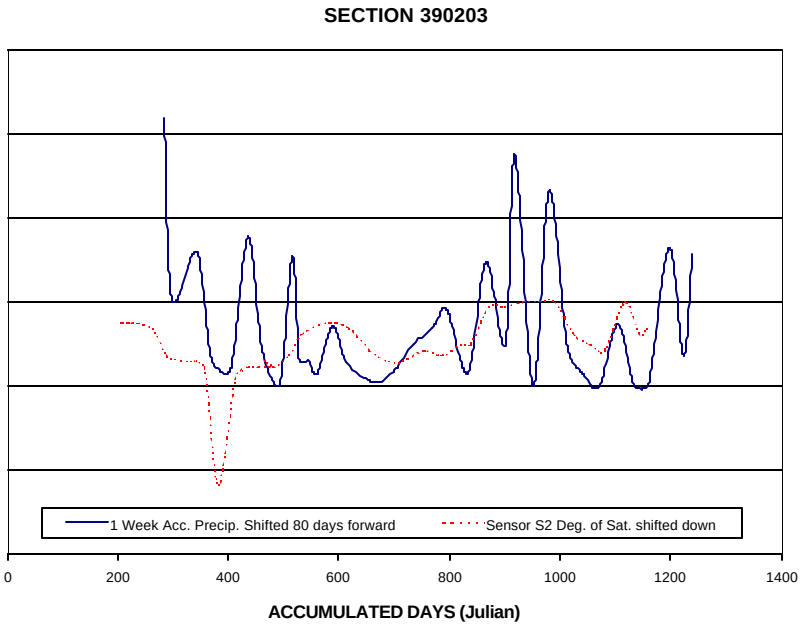

Figure 4.36. Degree of soil saturation (Sensor S2) and one-week rainfall shifted forward 85 days (Section 390203)

In conclusion, the lag between the increase in degree of saturation within the subgrade soil with respect to increased precipitation varies between 80 and 85 days at the Ohio Test Road site.

4.8. Seasonal Resilient Modulus of the Subgrade Soil Estimates

Calculated degrees of saturation for each section and season, as summarized in Tables 4.13 to 4.16, can be used in combination with Equation 2.5 (or Figure 2.7) to infer the resilient modulus of subgrade soils at the break point. Figures 4.37 to 4.40 show the variation of the seasonal resilient modulus at the break point vs. depth for each of the four sections considered. As expected, the resilient modulus is higher when the degree of saturation is lower and vice versa.

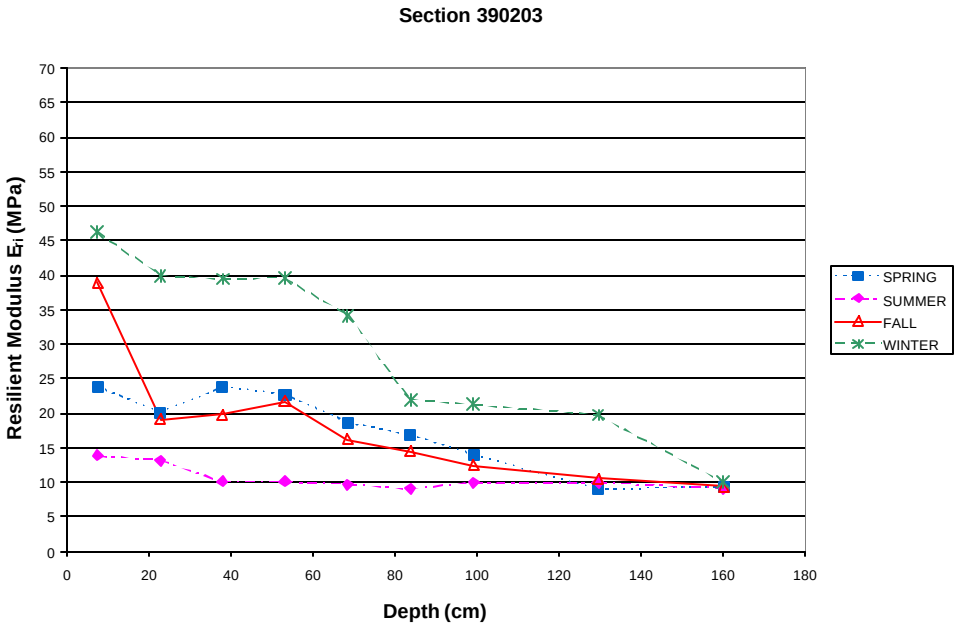

Figure 4.37. Seasonal Resilient Modulus vs. Depth (Section 390203)

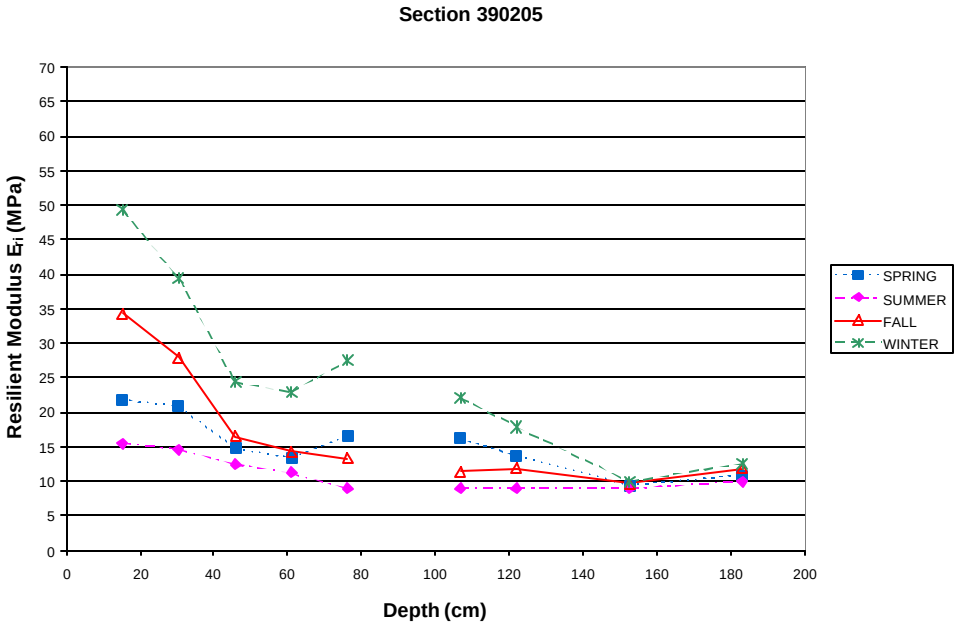

Figure 4.38. Seasonal Resilient Modulus vs. Depth (Section 390205)

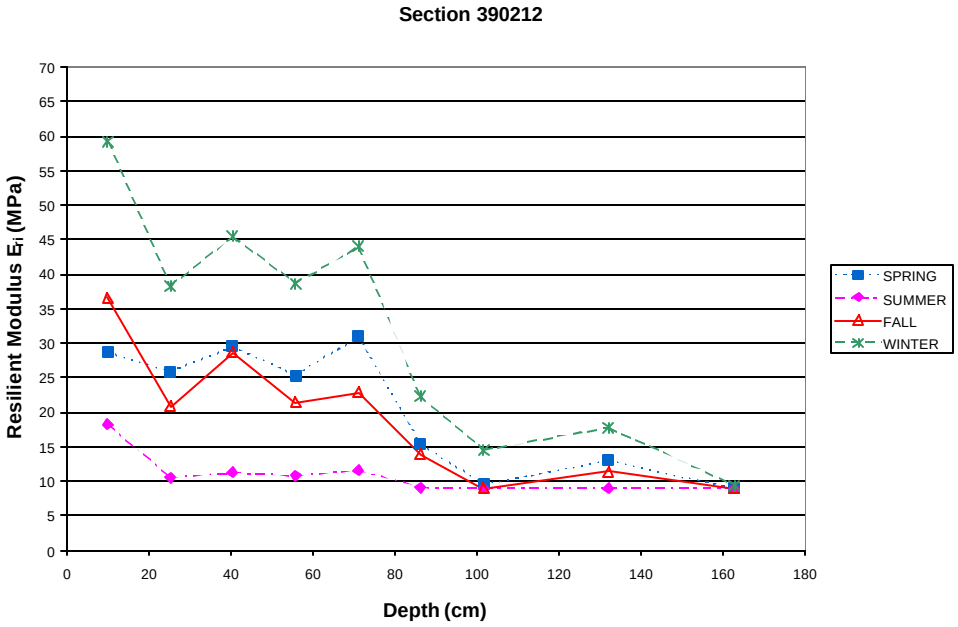

Figure 4.39. Seasonal Resilient Modulus vs. Depth (Section 390212)

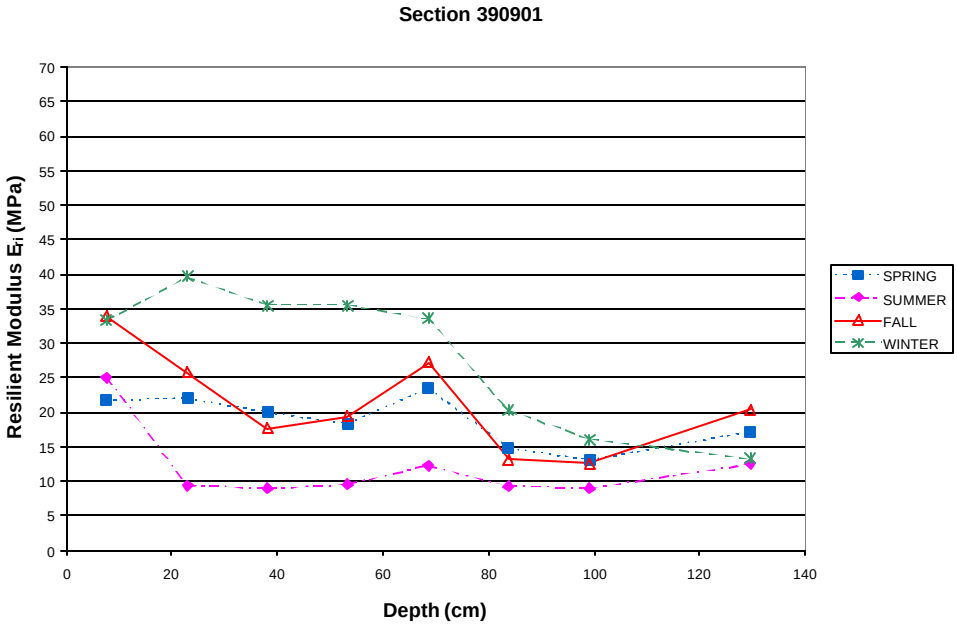

Figure 4.40. Seasonal Resilient Modulus vs. Depth (Section 390901)

Chapter 5

BACK CALCULATION OF STIFFNESS PROPERTIES OF SUBGRADE SOILS BASED ON MEASURED FWD DEFLECTIONS

5.1. Introduction

The main objective of this chapter is to develop nomographs to back calculate the resilient modulus of a subgrade for flexible pavements, and the modulus of subgrade reaction for rigid pavements, based on Falling Weight Deflectometer (FWD) measurements.

Two finite element programs, developed at the University of Illinois, were the primary pavement analysis tools: ILLIPAVE was used to perform the flexible pavement studies, while a modified version of ILLISLAB was used for rigid pavement analyses. This chapter includes the generation of nomographs for both types of pavements, and the development of a back calculation program to estimate the modulus of subgrade reaction based on ILLISLAB.

5.2. Backcalculation of the Resilient Modulus of Subgrade Soils Based on Measured FWD Deflections at the Ohio Test Road Site

5.2.1. Overview

Figueroa et al. (1994) evaluated ILLIPAVE (U. of Illinois, 1979) as a suitable flexible pavement analysis program after comparing surface deflections generated by a Falling Weight Deflectometer (FWD) with the calculated deflections with this finite elements program for different types of subgrade soils. Based on this

conclusion this program was used as the principal tool to develop back calculation nomographs for the Ohio Test Road.

The resilient modulus characteristics of the A-6 subgrade soil found at the Ohio Test Road site were discussed in detail in Section 2.3.4. Figure 2.6 shows the relationship between Deviator Stress and Resilient Modulus for different degrees of saturation following the Thompson and Robnett (Thompson et al., 1976) model.

Section 4.3 describes the relationship between the asphalt concrete temperature and air temperature in the field [Equation 4.4]. These results, combined with the laboratory testing were used to develop plots relating the air temperature and the resilient modulus for the asphalt concrete and for the asphalt treated bases (ATB-PATB), as shown in Figures 4.6 to 4.8, respectively.

The following section describes the method used to develop resilient modulus of the subgrade soil (AASHTO A-6) back calculation nomographs for typical sections found at the Ohio Test Road. These nomographs imply the use of the Thompson- Robnett resilient modulus model for subgrade soil stiffness and supporting relationships between air temperature and stiffness properties of asphaltic materials.

5.2.2. Nomograph Development

Knowing the asphaltic material properties, the geometry of the pavements used in the Ohio Test Road and the average seasonal response, back calculation nomographs to obtain the resilient modulus of the subgrade soil (E_{ri}) were

developed from the FWD deflections. Factors affecting these deflections are the applied load, the asphalt concrete thickness, the base material thickness, the asphalt concrete resilient modulus, the base resilient modulus and the resilient modulus of the subgrade soil.

The pavement is exposed to average temperature values that vary between –1.1 and 26.7^{o}C (30 and 80^{o}F). This variation results in a resilient modulus variation for the asphalt concrete between 689 and 10341 MPa (100 and 1500 ksi). Thus values of 689, 5515 and 10341MPa (100, 800, and 1500 ksi) were adopted to represent the seasonal variation.

Typical variation of the degree of saturation was measured between 85 and 100 percent by moisture sensors installed at the Test Road. Thus values of 80, 90 and 100% were selected to infer the resilient modulus models necessary in ILLIPAVE.

Base types used at the Test Road included Dense Aggregate Base (DGAB), Asphalt Treated Base (ATB), Permeable Asphalt Treated Base (PATB), Permeable Cement Treated Base (PCTB) and Lean Concrete Base (LCB). DGAB, ATB and PATB were the most common base types used in the asphalt concrete studies, leading to a total of six typical pavement profiles, present at the Ohio Test Road:

AC-DGAB

AC-ATB

AC-ATB-PATB (PATB fixed at 4 inches)

AC-ATB-DGAB (DGAB fixed at 4 inches)

AC-PATB-DGAB (PATB fixed at 4 inches)

AC-ATB-PATB-DGAB (All fixed thickness')

The combination of these factors led to a total of 567 cases. The properties of the materials were obtained in the laboratory as mentioned in previous sections, except for the DGAB that is modeled by the following the equation:

$$E_r = 32811\theta^{0.33} \quad (5.1)$$

Where θ is the sum of the three principal stresses in kPa and E_r is the DGAB resilient modulus also in kPa. This model was previously evaluated by Figueroa et al. (1994) for the same application with a high degree of accuracy.

In the case of asphalt treated bases, the temperature was assumed to be constant from the surface to the bottom of the base. For high temperatures this assumption approaches actual field conditions. During the winter the temperature variation from the surface to the bottom of the asphalt layer is higher, but the fact that the slope of the resilient modulus vs. air temperature curve for ATB and PATB is much lower than the one for the AC, thus introducing a low error that is acceptable for nomograph development. For the estimated resilient modulus values, average air temperatures were estimated as 0.6, 8.7 and 23.9^{o}C (33, 47.7 and 75^{o}F). At these temperatures the resilient modulus for the asphalt concrete bases are 1275, 3440 and 5198Mpa (185, 499 and 754 ksi) for ATB and 1248, 2261 and 3061 MPa (181, 328 and 444 ksi for the PATB). Unit weights for the materials used in the analysis are presented in Table 5.1.

Table 5.1. Material Unit Weights

MATERIAL	Unit Weight (kN/m^3)	Unit Weight (pcf)
AC	22.00	140
ATB	22.00	140
PATB	22.00	140
DGAB	21.22	135
A-6(subgrade)	17.61	112

General relationships were obtained by conducting a statistical analysis. The equations obtained are expressed by:

$$\log(d) = a_0 + a_1 \cdot t_{ac} + a_2 \cdot t_{base} + a_3 \cdot E_{ac} + a_4 \cdot E_{ri} + a_5 \cdot P \qquad (5.2)$$

where:

δ = Deflection at the center of load application (mm) or (in).

t_{ac}=Thickness of the asphalt concrete (mm) or (in).

t_{base}=Thickness of the base (mm) or (in).

E_{ac}=Resilient Modulus of the asphalt concrete (MPa) or (ksi).

E_{ri}= Resilient modulus at the break point of the subgrade soil (MPa) or (ksi).

P= Applied load (kN) or (lb).

a_0,a_1,a_2,a_3,a_4,a_5= Regression constants.

Tables 5.2 and 5.3 summarize the coefficients applied to Equation 5.2 for the studied pavement profiles with their corresponding Coefficient of Determination (R^2). Values for the Coefficient of determination R^2 between 80 and 98 percent were obtained in the regression equations. This variation is attributed to the nonlinear response of pavement layers. For a flexible pavement, the maximum deflection is not linearly proportional to the applied load given the non-linearity of

the materials in use. The granular base modulus varies with the sum of the principal stresses, and the moduli of AC layers vary with the temperature. A higher variation is found in the AC materials, thus structures with more than one asphaltic material layer reflect higher dispersion represented by lower R^2 values.

Table 5.2. Summary of the Coefficients for the Backcalculation Nomographs (SI Units)

BASE	a_0	a_1	a_2	a_3	a_4	a_5	R^2
ATB	-0.41635	-6.4469E-04	-7.2179E-04	-4.1368E-05	-3.9513E-03	8.4744E-03	0.92285
DGAB	0.16665	-3.0776E-03	-2.9283E-06	-5.5110E-05	-3.3445E-03	8.8766E-03	0.93845
ATB-DGAB	-0.34387	-1.1994E-03	-1.2163E-03	-4.3308E-05	-1.8920E-03	8.3794E-03	0.92359
ATB-PATB	-0.43973	-1.1948E-03	-1.1932E-03	-4.6502E-05	-2.1085E-03	8.4059E-03	0.79780
PATB-DGAB	-0.43034	-9.8602E-04	-2.9887E-05	-8.8194E-06	-3.0178E-03	9.2575E-03	0.98487

Table 5.3. Summary of the Coefficients for the Backcalculation Nomographs (English Units)

BASE	a_0	a_1	a_2	a_3	a_4	a_5	R^2
ATB	-1.82118	-0.01638	-1.83300E-02	-2.85191E-04	-2.72400 E-02	3.77009E-05	0.92285
DGAB	-1.23819	-0.07817	-7.43778E-05	-3.79930E-04	-2.30571E-02	3.99490E-05	0.93845
ATB-DGAB	-1.74870	-0.03046	-3.08900E-02	-2.98569E-04	-1.30436E-02	3.72781E-05	0.92359
ATB-PATB	-1.84457	-0.03035	-3.03100E-02	-3.20588E-04	-1.45362E-02	3.73961E-05	0.79780
PATB-DGAB	-1.83517	-0.02504	-7.59136E-04	-6.08007E-05	-2.08051E-02	4.11850E-05	0.98487

These equations can be graphically solved using the nomographs shown in Figures 5.1 to 5.10. Knowing the first sensor deflection given by the FWD, the air temperature when the test was conducted (from which to the resilient modulus of asphaltic materials can be calculated), and the layering of the pavement structure; E_{ri} can be estimated following the procedure indicated below:

- A line is plotted between the deflection read by the FWD and its applied load.
- A normal line to the axis from this intersection is drawn and the quantity C is determined.
- Starting at the left box, a line between the base and the AC thickness is traced and the normal to the vertical axis is plotted as shown in each nomograph, which also designates a point on this axis.
- Then, a line is traced from this point through quantity C, obtained above, which is continued to intersect the vertical axis on the right box.
- A horizontal line is traced from this vertical axis to intersect the AC modulus (which can be inferred from the air temperature-resilient modulus of the AC relationship shown in Figure 4.6, since the air temperature is measured by the FWD at the time of testing).
- A normal to the E_{ri} axis is traced from this point to the axis to read the resilient modulus at the break point on the horizontal axis.

For the fixed pavement profile composed of AC, ATB, PATB and DGAB, the procedure used was different. For this case, there are three unknown variables for each load, which leads to a more direct estimation procedure. Equations of the type

$$d = a + b \cdot E_{ac} + c \cdot E_{ac}^2 + f \cdot \ln(E_{ri}) \qquad (5.3)$$

were obtained, and three parameter charts for each load were developed for each load. Note that that the units in this equation are as follows: E_{ac} is in MPa or ksi, E_{ri} is in MPa or psi and d is in mm or in. The equation coefficients are

presented in Tables 5.4 and 5.5 and the corresponding graphs are shown in Figures 5.11 to 5.16. Each line in these figures corresponds to a value of E_{ri} in MPa or psi as indicated on the adjoining line type table. It is to be noted that R^2 values close to 100 percent were found showing a great level of accuracy for the back calculation of the resilient modulus of the subgrade soil.

Table 5.4. Summary of coefficients for the Backcalculation Nomographs for AC-ATB-PATB-DGAB profile (SI Units).

BASE	P(kN)	a	b	c	f	R^2
ATB-PATB-DGAB	40	0.44913	-3.6996E-05	2.08319E-09	-0.04868	0.99656
	53.38	0.58374	-4.8018E-05	2.70305E-09	-0.06350	0.99590
	66.72	0.75063	-6.2410E-05	3.52106E-09	-0.08105	0.99632

Table 5.5. Summary of coefficients for the Backcalculation Nomographs for AC-ATB-PATB-DGAB profile (English Units).

BASE	P(lb)	a	b	c	f	R^2
ATB-PATB-DGAB	9000	0.02722	-1.0041E-05	3.89796E-09	-1.9164E-03	0.99785
	12000	0.03542	-1.3033E-05	5.05782E-09	-2.49993E-03	0.99744
	15000	0.04543	-1.6939E-05	6.58844E-09	-3.1911E-03	0.99540

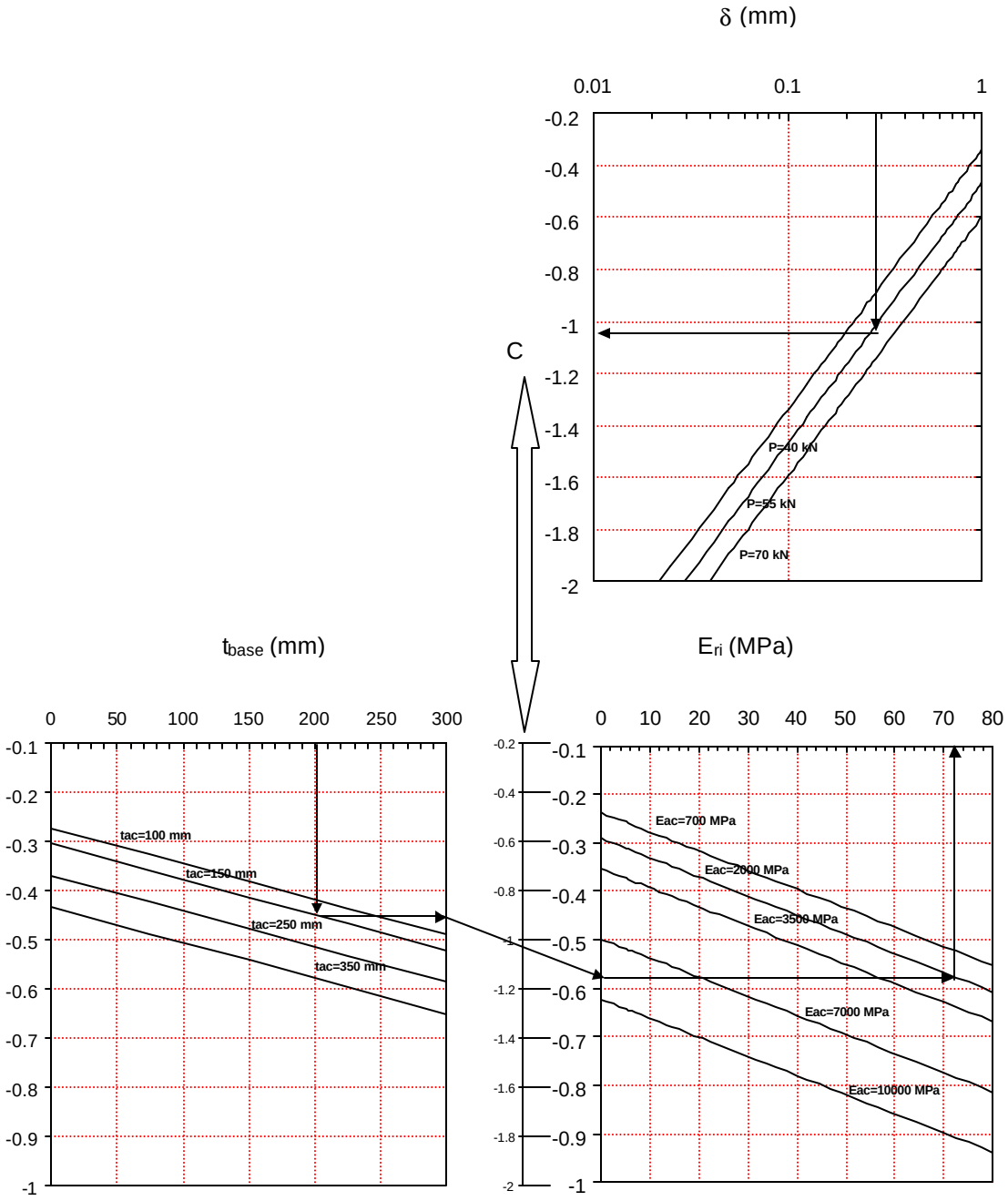

Figure 5.1. Backcalculation Nomograph for A-6 Soil [ATB] (SI Units)

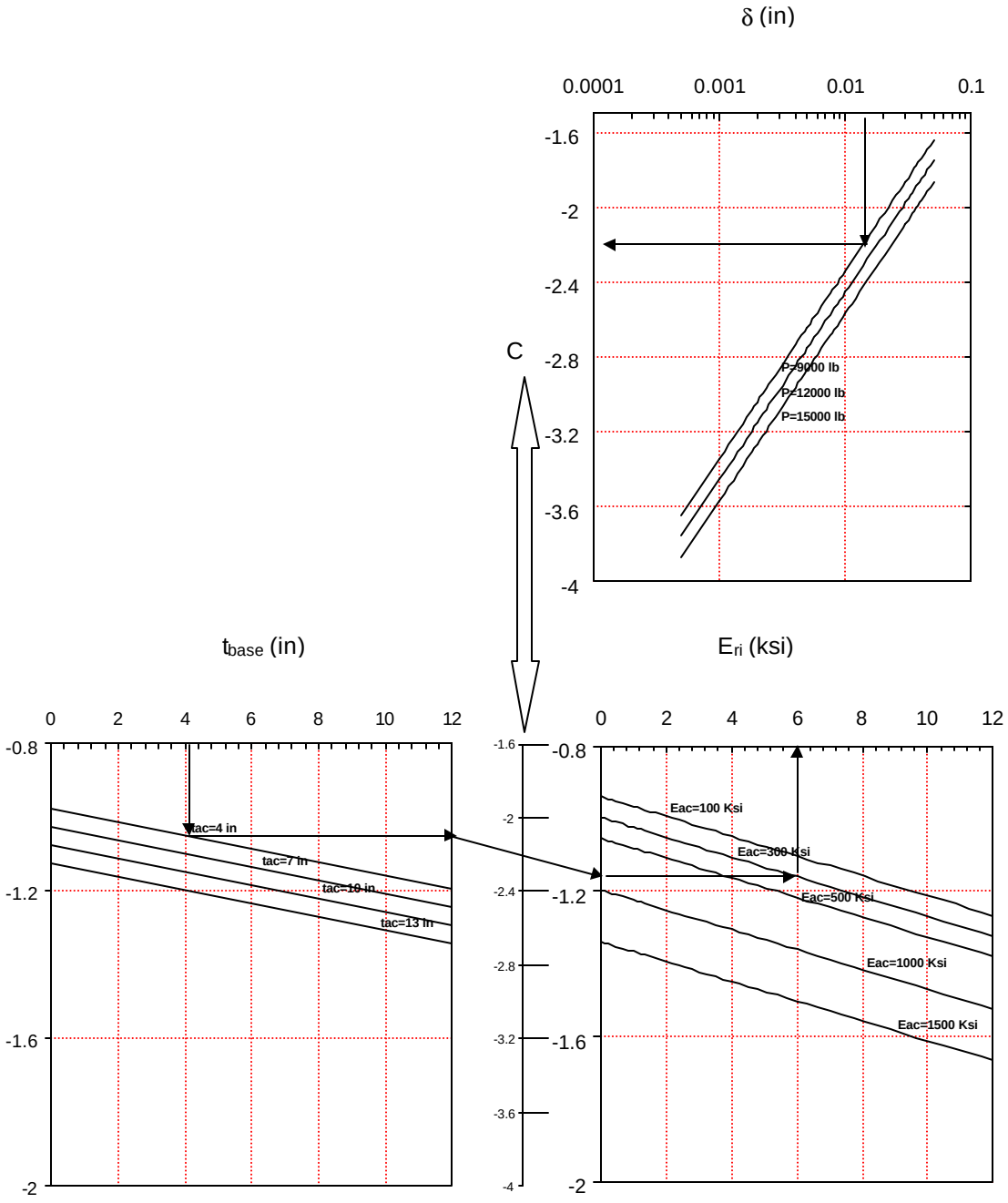

Figure 5.2. Backcalculation Nomograph for A-6 Soil [ATB] (English Units)

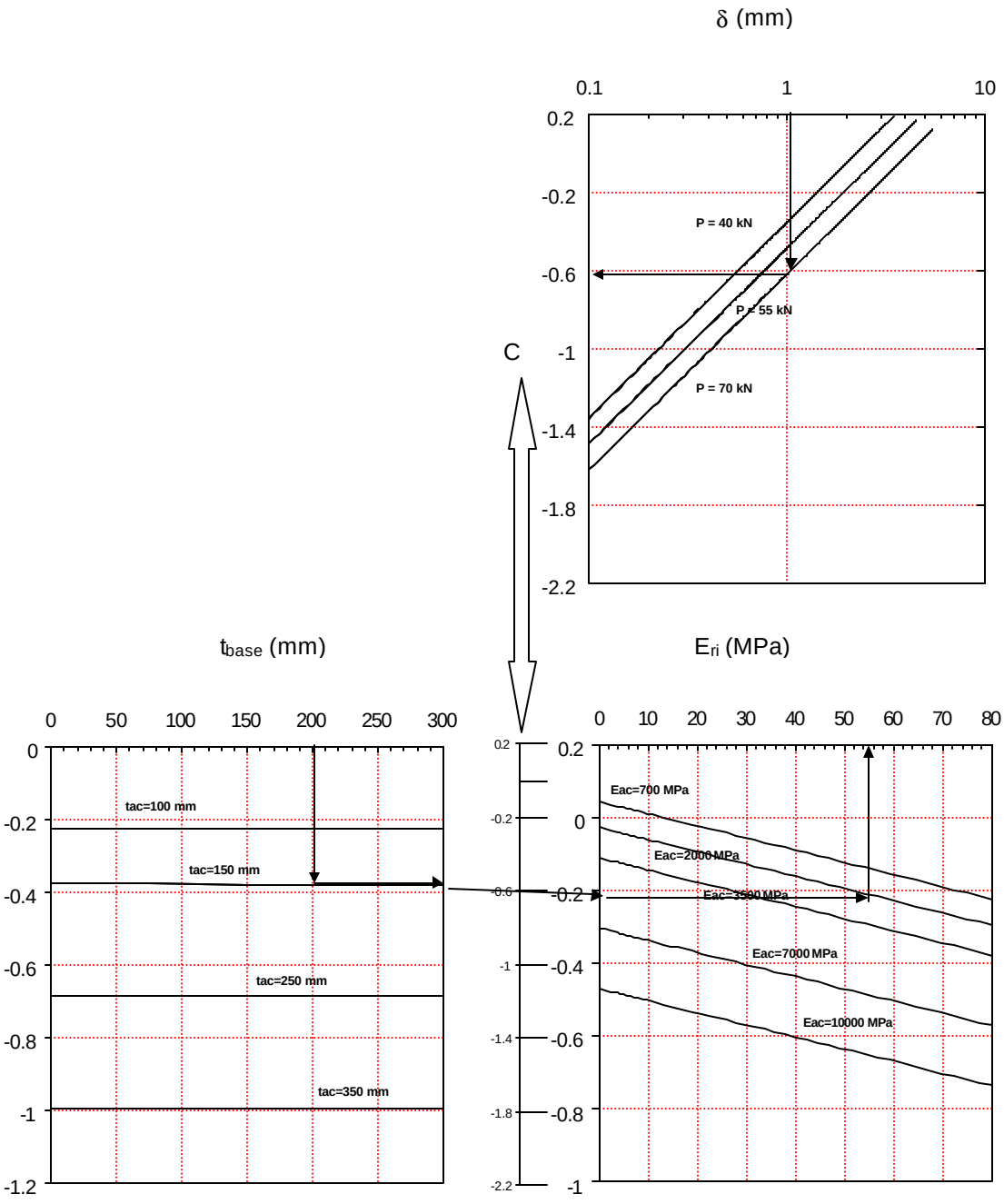

Figure 5.3. Backcalculation Nomograph for A-6 Soil [DGAB] (SI Units)

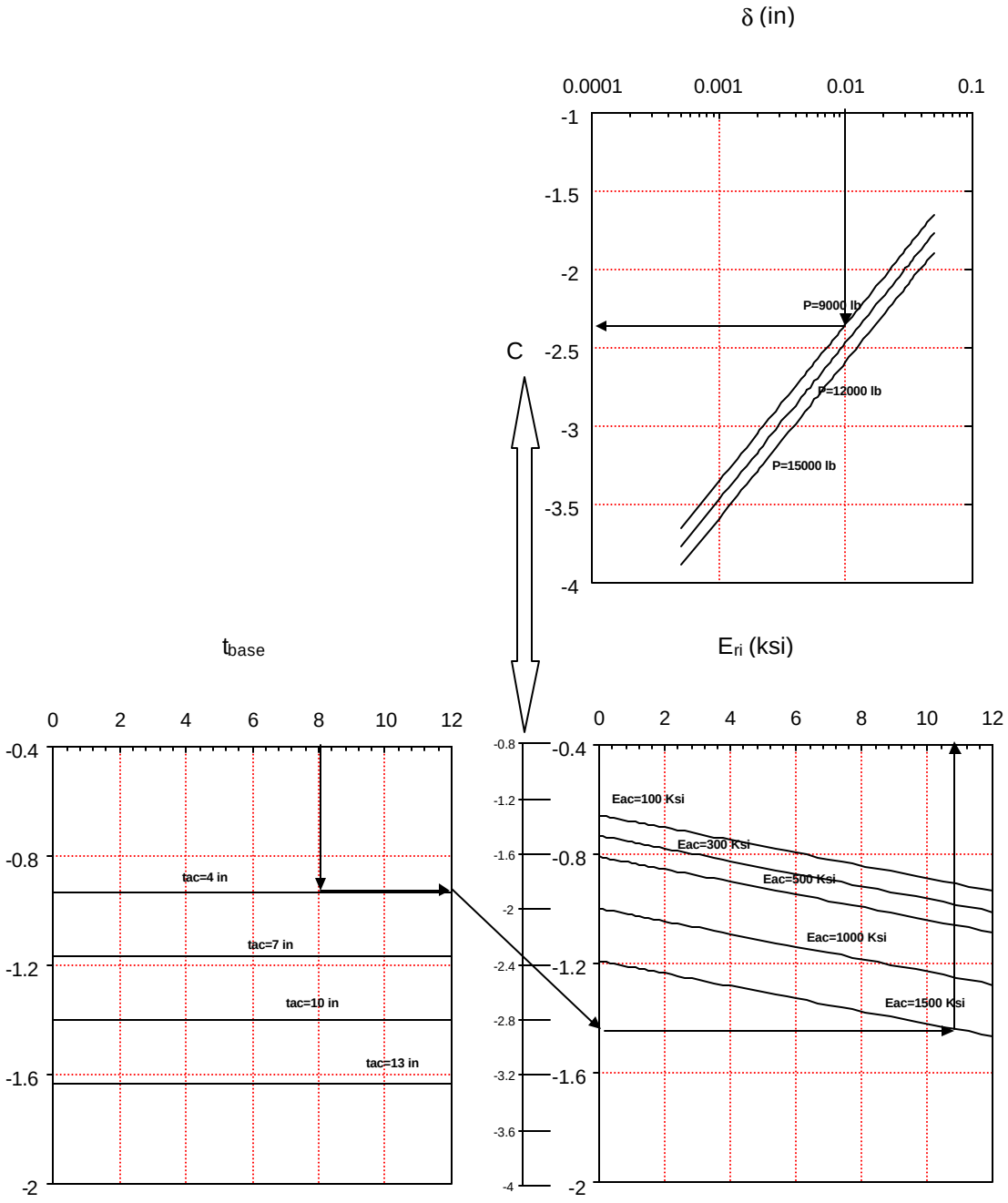

Figure 5.4. Backcalculation Nomograph for A-6 Soil [DGAB] (English Units)

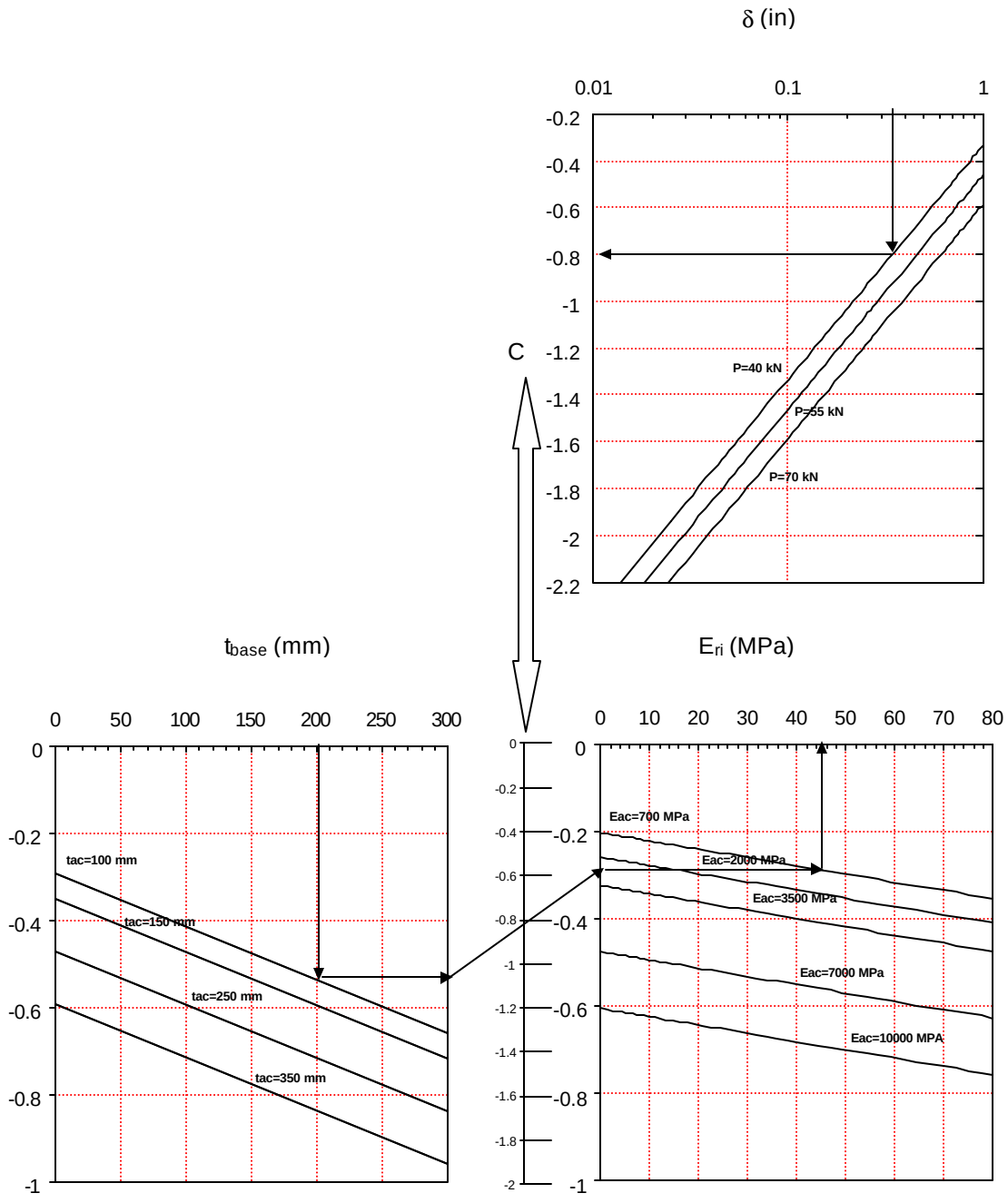

Figure 5.5. Backcalculation Nomograph for A-6 Soil [ATB-DGAB (102 mm or 4 in)] (SI Units)

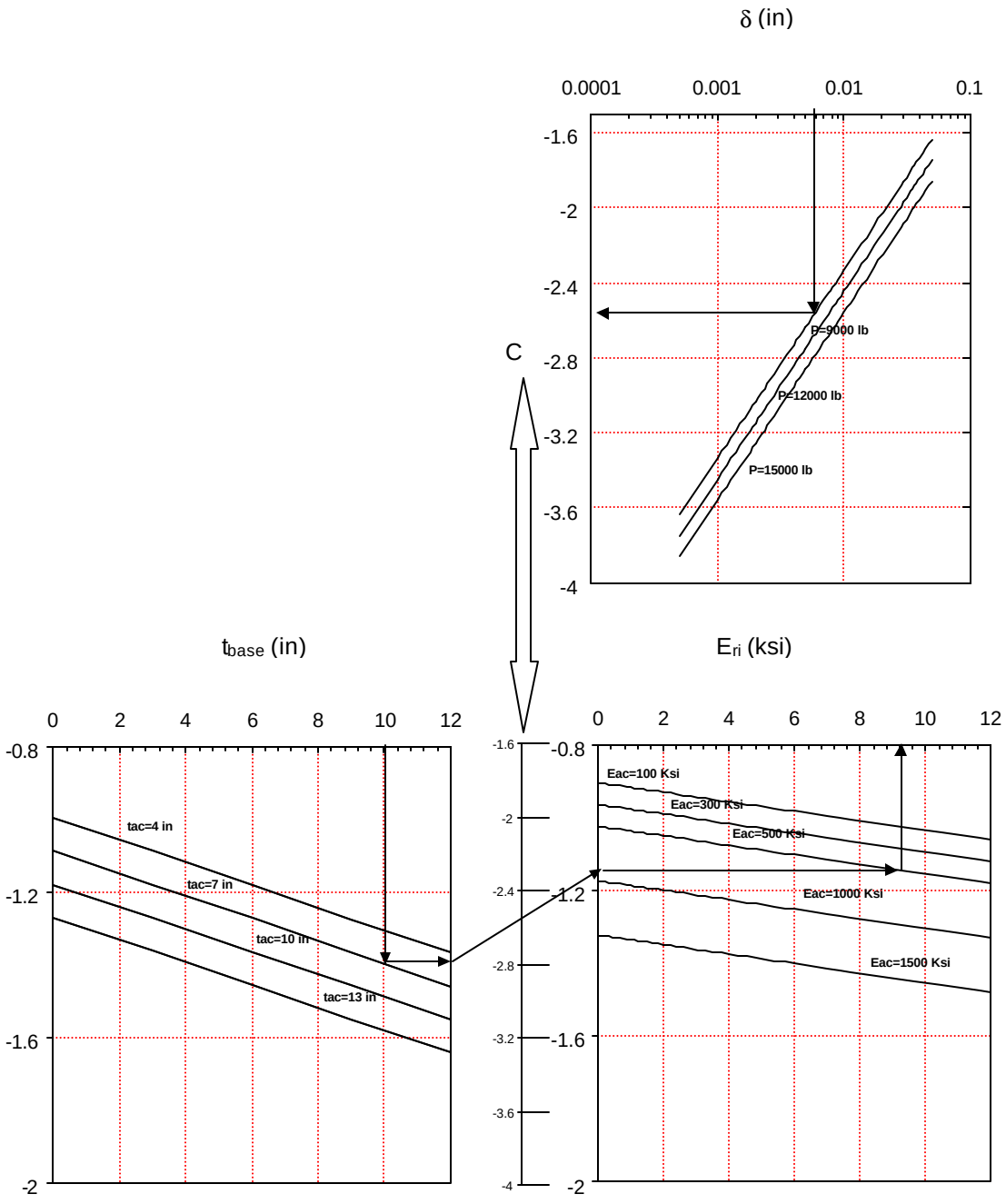

Figure 5.6. Backcalculation Nomograph for A-6 Soil [ATB-DGAB (4 in)] (English Units)

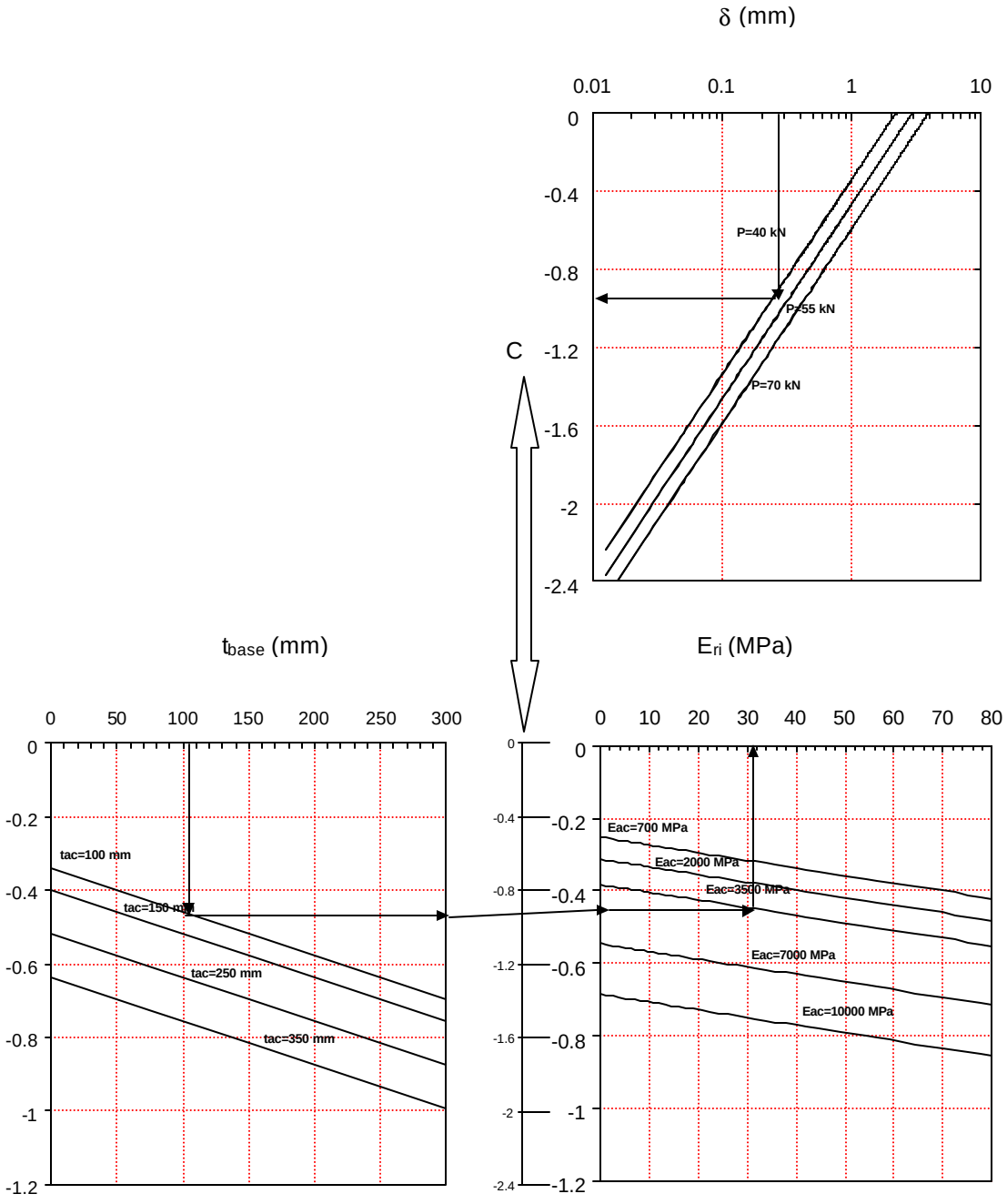

Figure 5.7. Backcalculation Nomograph for A-6 Soil [ATB-PATB (102 mm or 4 in)] (SI Units)

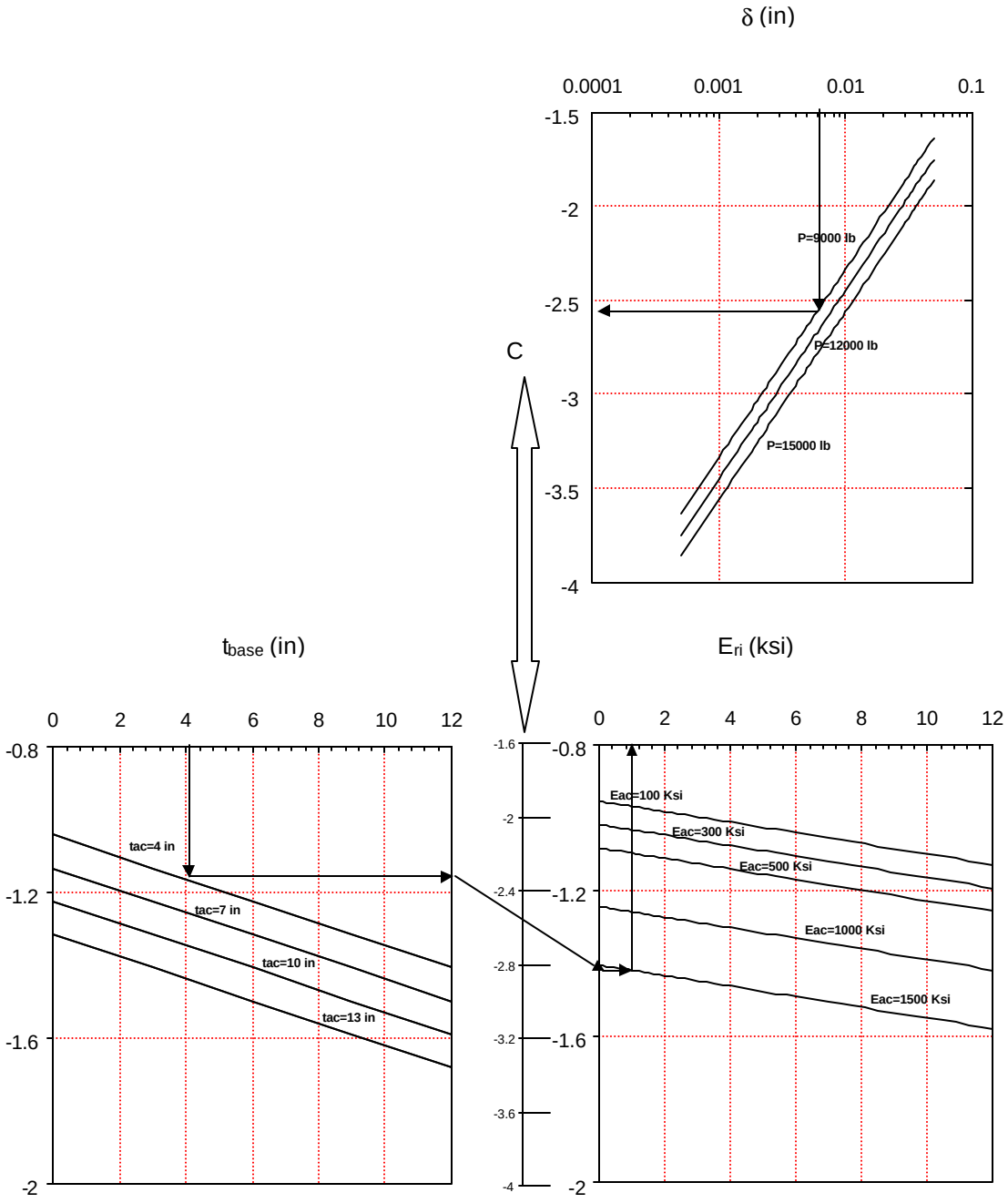

Figure 5.8. Backcalculation Nomograph for A-6 Soil [ATB-PATB (4 in)] (English Units)

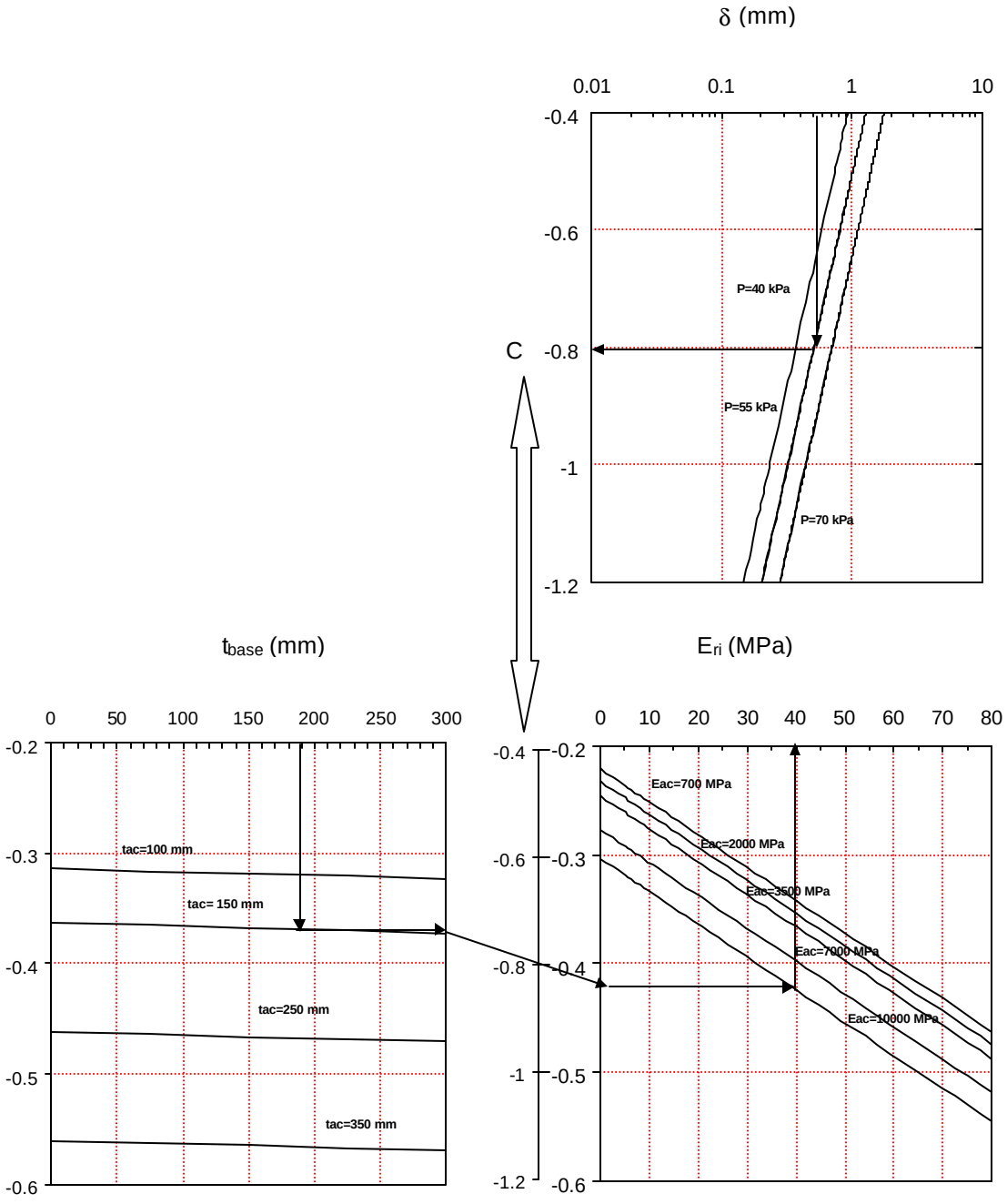

Figure 5.9. Backcalculation Nomograph for A-6 Soil [PATB (102 mm or 4 in) – DGAB] (SI Units)

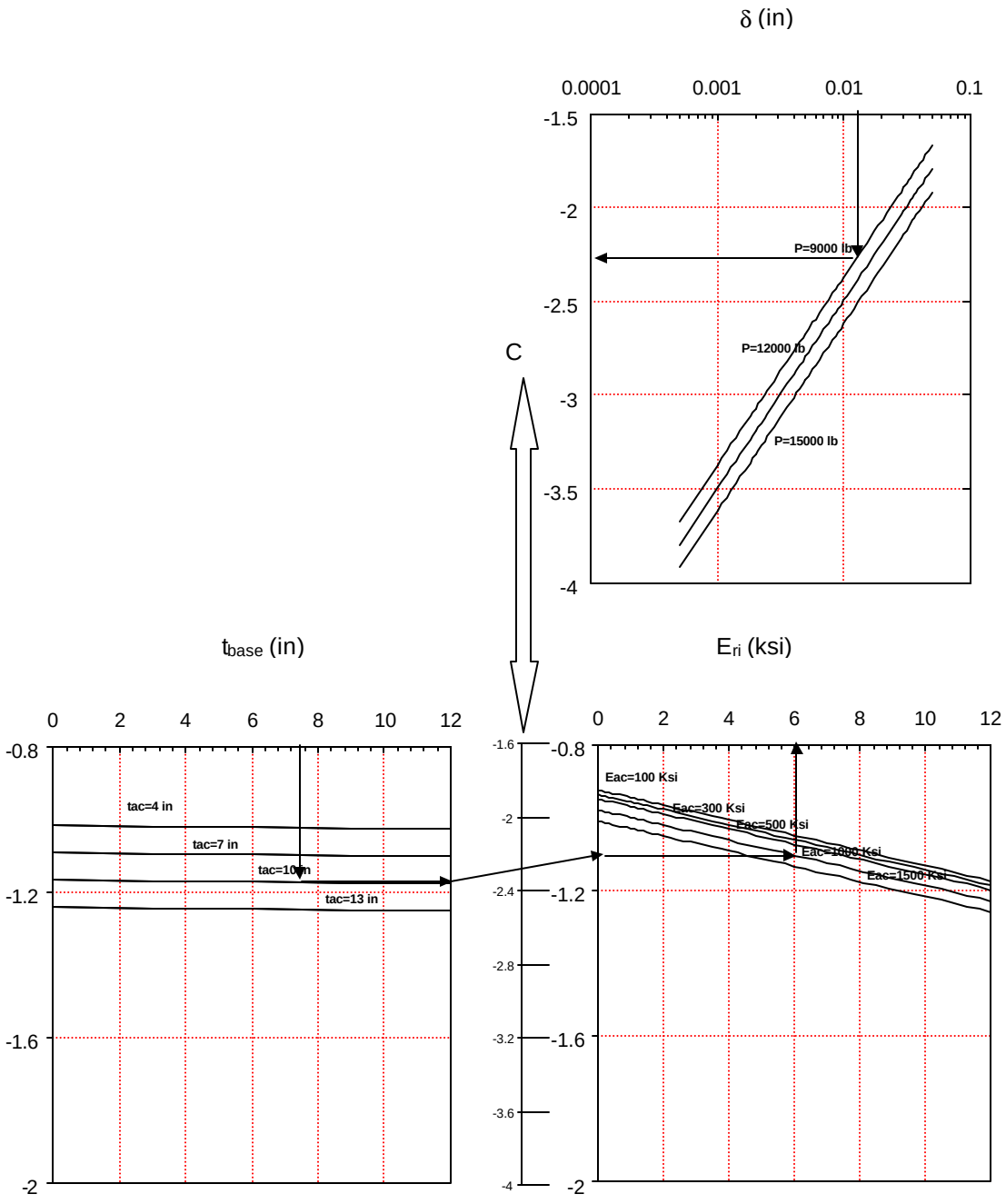

Figure 5.10. Backcalculation Nomograph for A-6 Soil [PATB (4 in) –DGAB] (English Units)

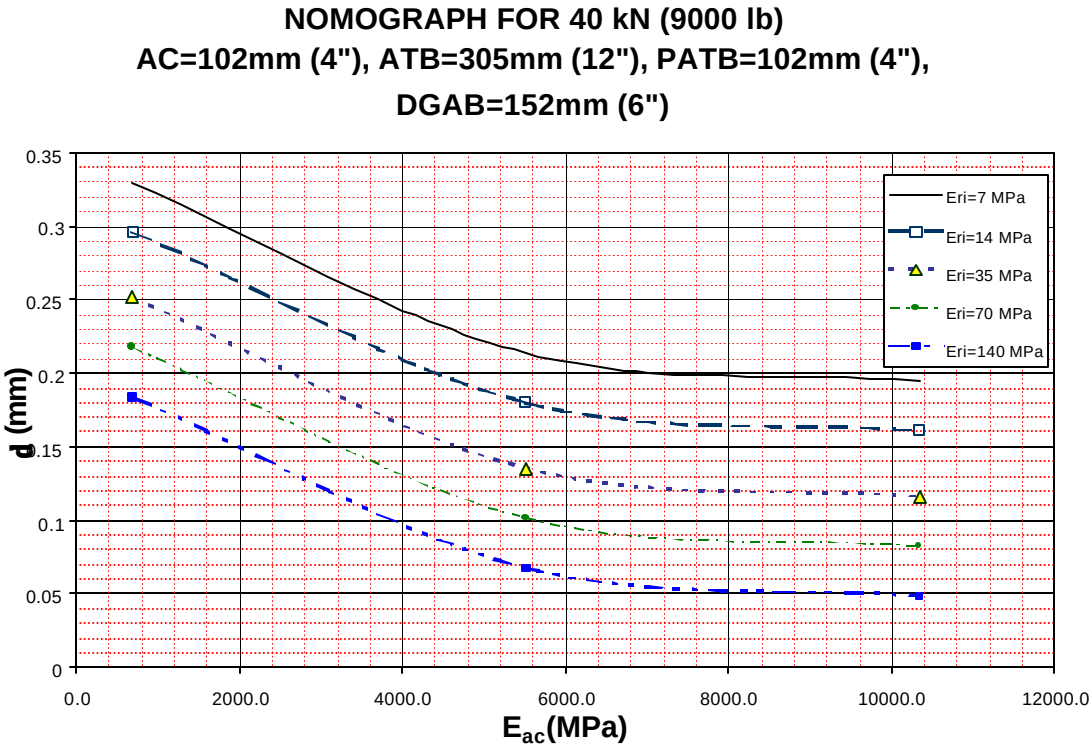

Figure 5.11. 40 kN Backcalculation Nomograph for AC-ATB-PATB-DGAB

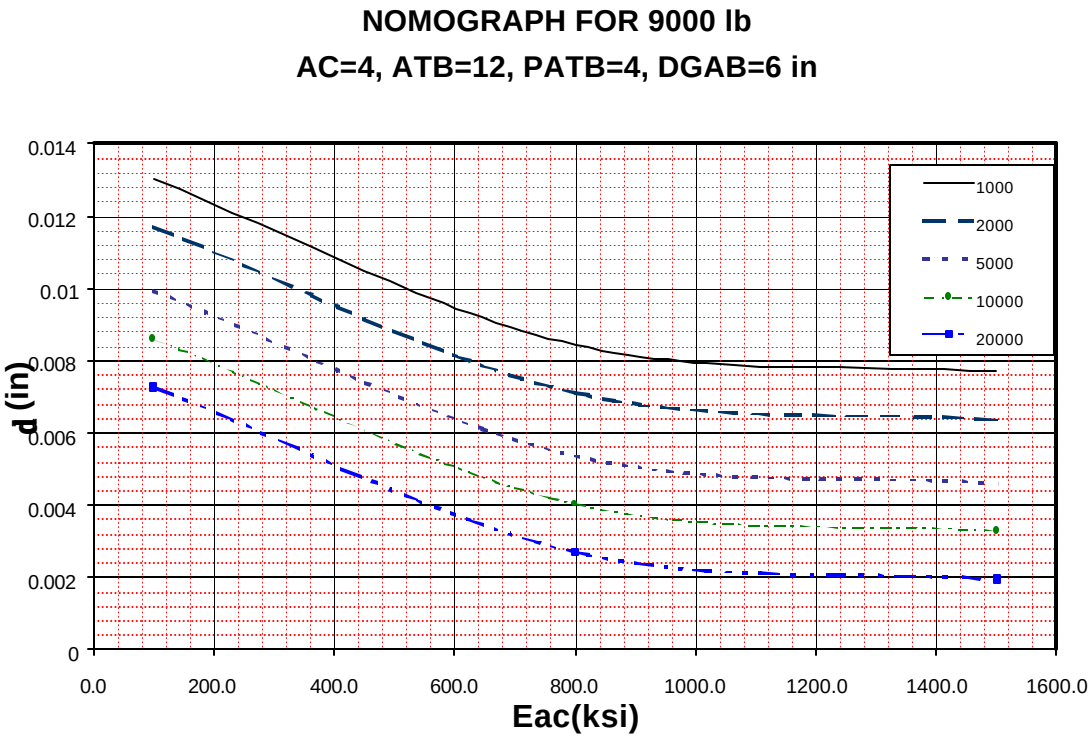

Figure 5.12. 9000lb Backcalculation Nomograph for AC-ATB-PATB-DGAB

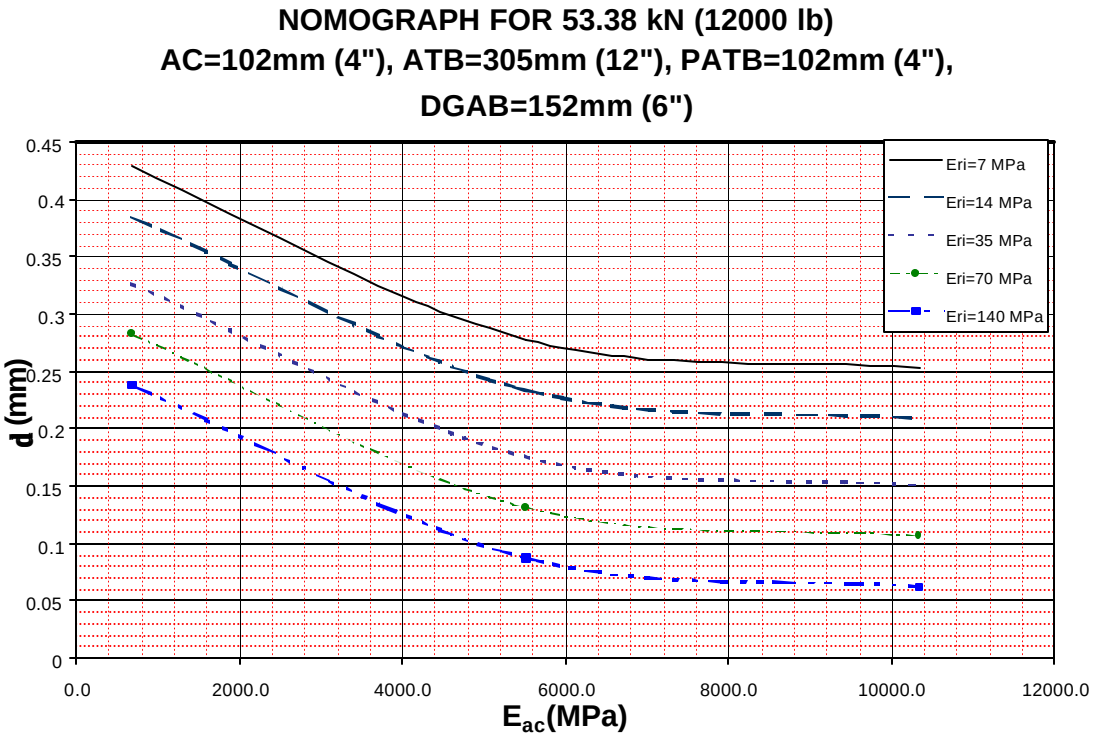

Figure 5.13. 53.38 kN Backcalculation Nomograph for AC-ATB-PATB-DGAB

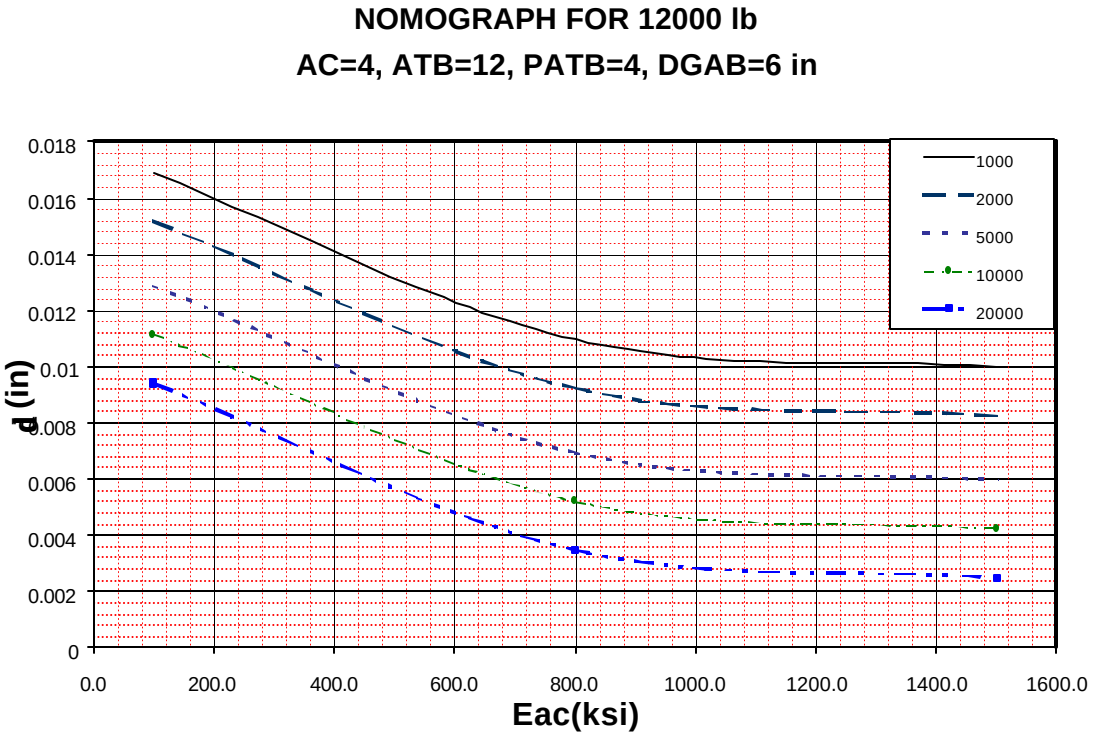

Figure 5.14. 12000 lb Backcalculation Nomograph for AC-ATB-PATB-DGAB

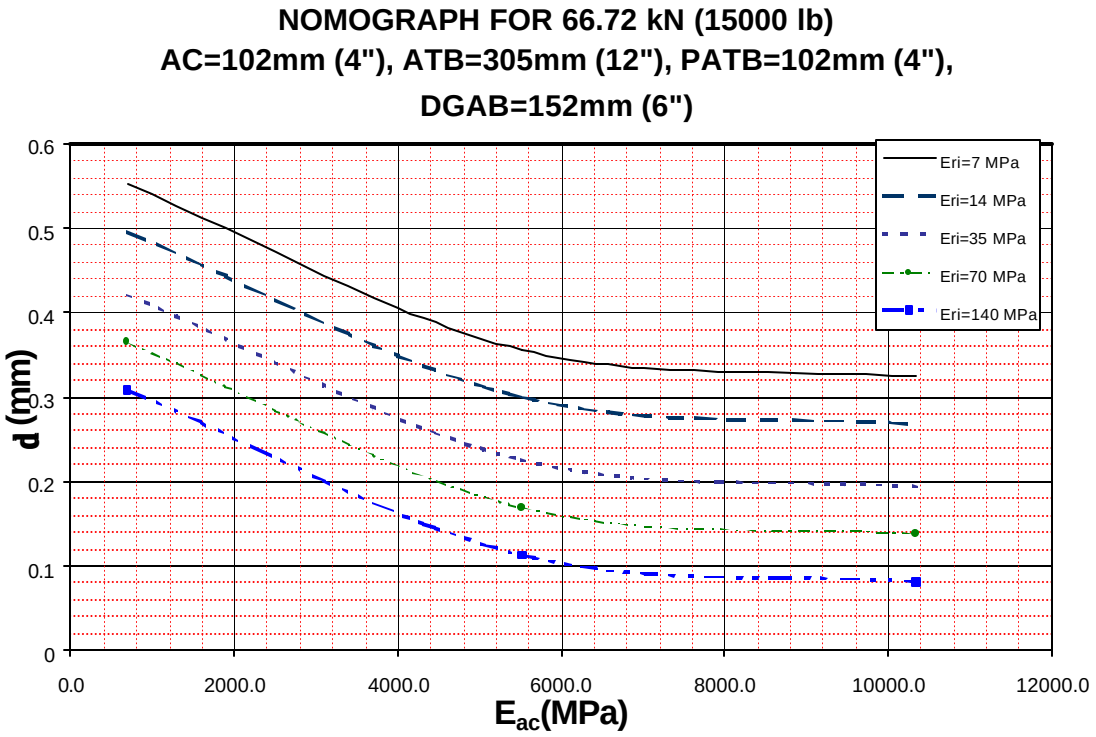

Figure 5.15. 66.72 kN Backcalculation Nomograph for AC-ATB-PATB-DGAB

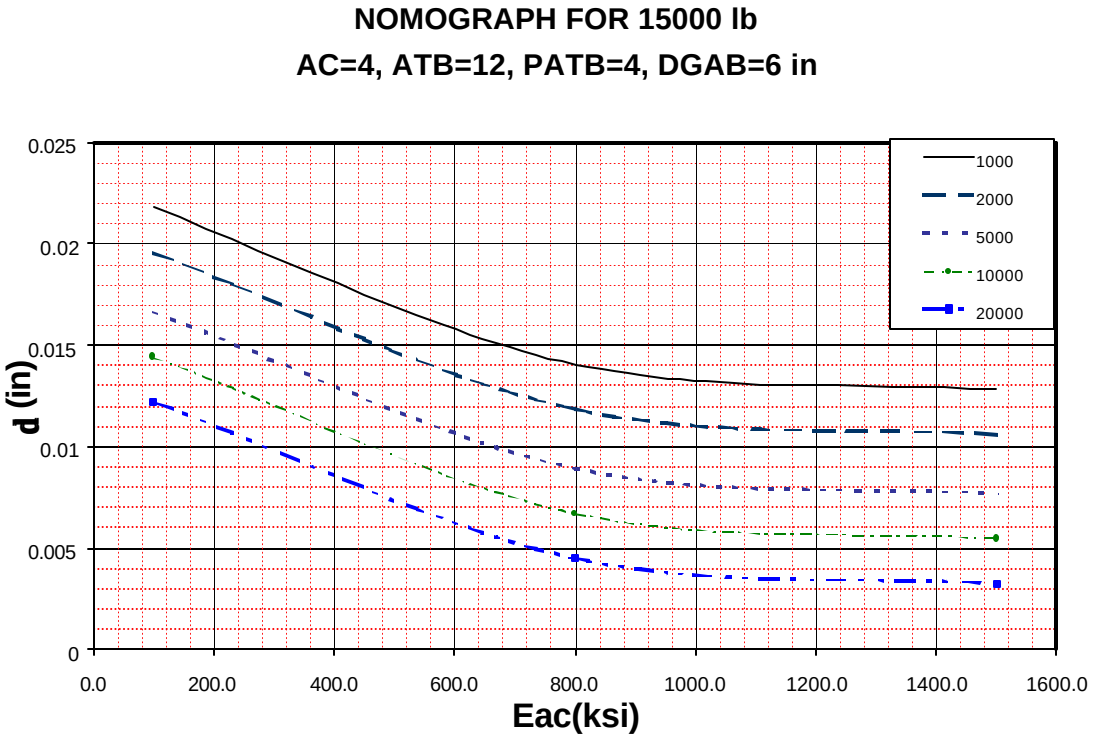

Figure 5.16. 15000 lb Backcalculation Nomograph for AC-ATB-PATB-DGAB

5.3 Backcalculation of the Modulus of Subgrade Reaction Based on Measured FWD Deflections at the Ohio Test Road Site

5.3.1. Overview

Given the low stresses to which a subgrade soil under a rigid pavement is subjected, the Thompson and Robnett model for resilient modulus is not applied. The subgrade is modeled as a bed of springs with constant k known as the Westergard modulus of subgrade reaction.

Westergard developed equations to obtain the maximum deflection given an applied load at the center, edge and corner of a PCC slab. With the introduction of the finite element method, computer programs were developed to analyze rigid pavements using the traditional modulus of subgrade reaction to characterize the stiffness of subgrade soils. ILLISLAB, a finite elements program developed at the University of Illinois (U. of Illinois, 1984), allows the calculation of deflections, stresses and strains at critical locations in rigid pavements.

5.3.2. Program Development

Using ILLISLAB as a starting base, a back calculation program to obtain the modulus of subgrade reaction (k) was developed. The program is based on an iterative procedure starting with an unknown (k) value entered manually along with the maximum surface deflection obtained from FWD tests. The modulus from the previous iteration is modified given a calculated error, until the final deflection differs by less than 0.00005 inches. As ILLISLAB, the program may consider load

transmission between different slabs, bonding or the absence of it, a base material and the load may be applied in different parts of the slab. Figure 5.17 shows the rapid convergence of the modulus of subgrade reaction achieved by the program.

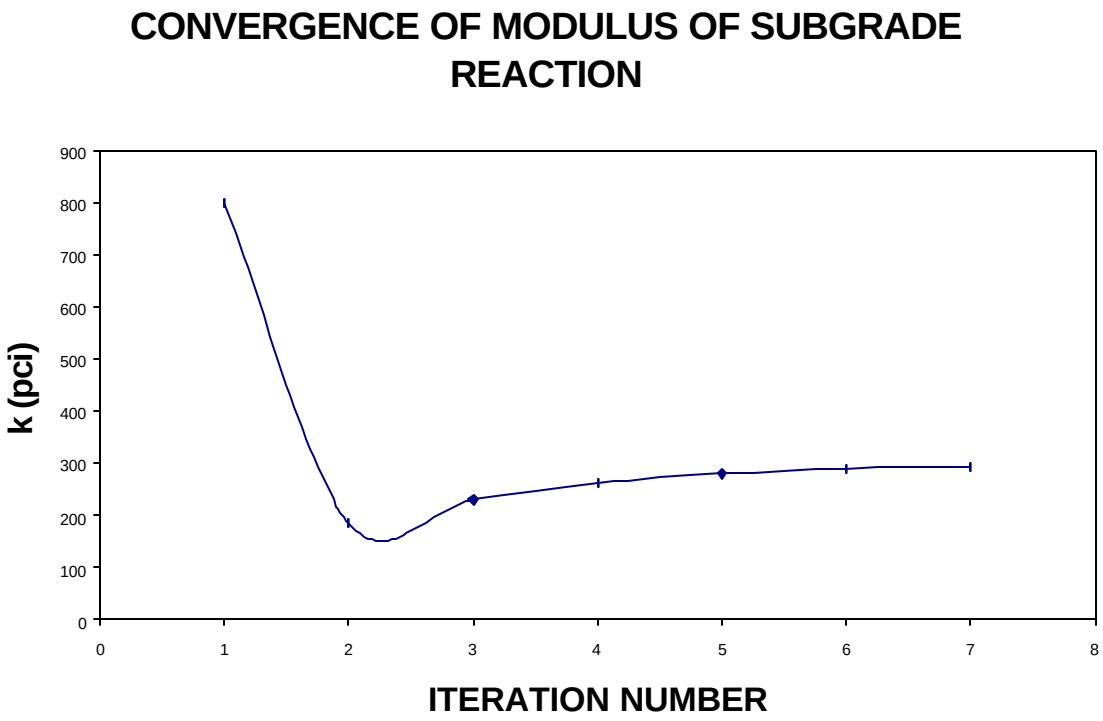

Figure 5.17. Convergence of Modulus of Subgrade Reaction.

Parameters needed to back calculate (k) include: the modulus of elasticity of the PCC slab and its thickness, the modulus of elasticity of the base and its thickness, the geometry of the slab, the applied load and the maximum deflection obtained from the FWD tests.

The sensitivity of the back-calculated modulus of subgrade reaction to a variation in the modulus of elasticity of a non-bonded base is very low when the base thickness is low. This indicates that if the modulus of the base is unknown, a

reasonable assumption of it is not going to lead to a high variation of (k). An unreasonable assumption of the modulus of elasticity may lead to more significant errors in the back calculated (k) with thicker bases. These two findings are clearly shown in Figures 5.18 and 5.19 in English units.

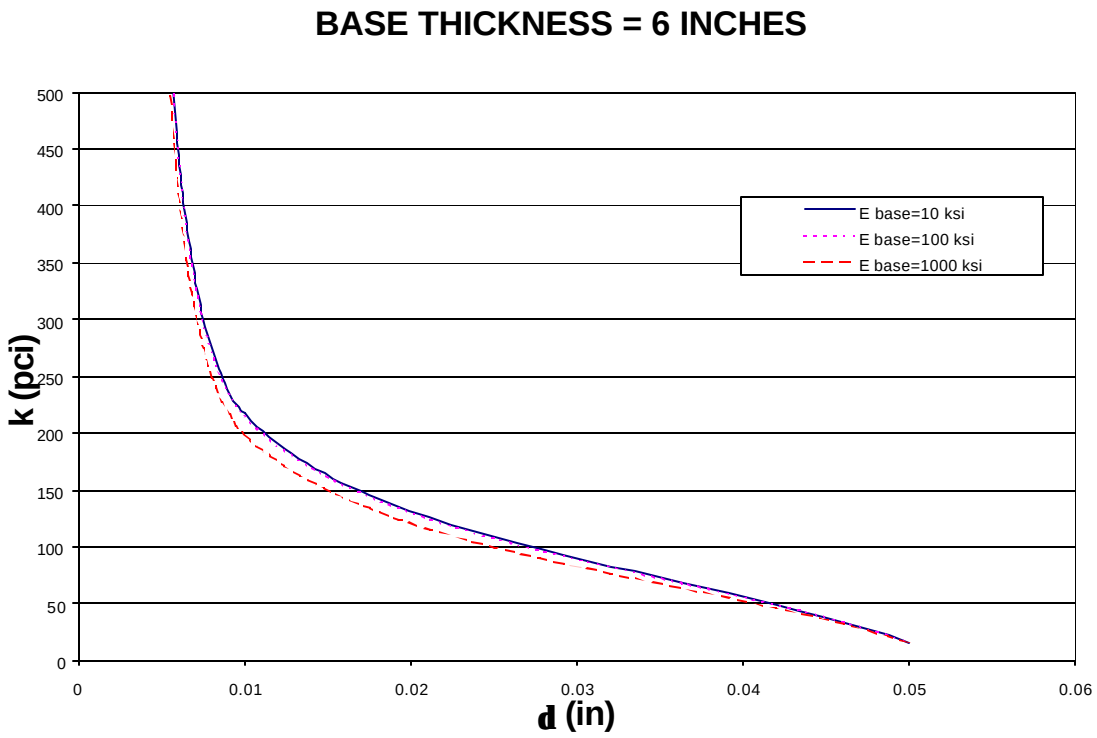

Figure 5.18. Modulus of Subgrade Reaction vs. Maximum Surface Deflection (Thin Base).

5.3.3. Nomograph Development

To develop a graphical procedure to back calculate (k) statistical analyses were performed on a total of 324 cases analyzed with the backcalculation program, including pavement sections with a constant PCC modulus of elasticity and a constant geometry of the slab. The modulus of elasticity of the PCC was assumed to be constant with a value of 27576 Mpa (4000 ksi). The PCC slabs used in the

Ohio Test Road are 3.65 or 4.27 m (12 or 14 ft) wide and 4.57 m (15 ft) long with varying thickness depending on the monitored section. The smaller slabs 3.65x4.57 m (12x15 ft), with thickness of 203.2, 279.4 and 355.6 mm (8, 11 and 14 inches). Three base moduli of 68.94, 3447 and 6894 MPa (10, 500 and 1000 ksi)

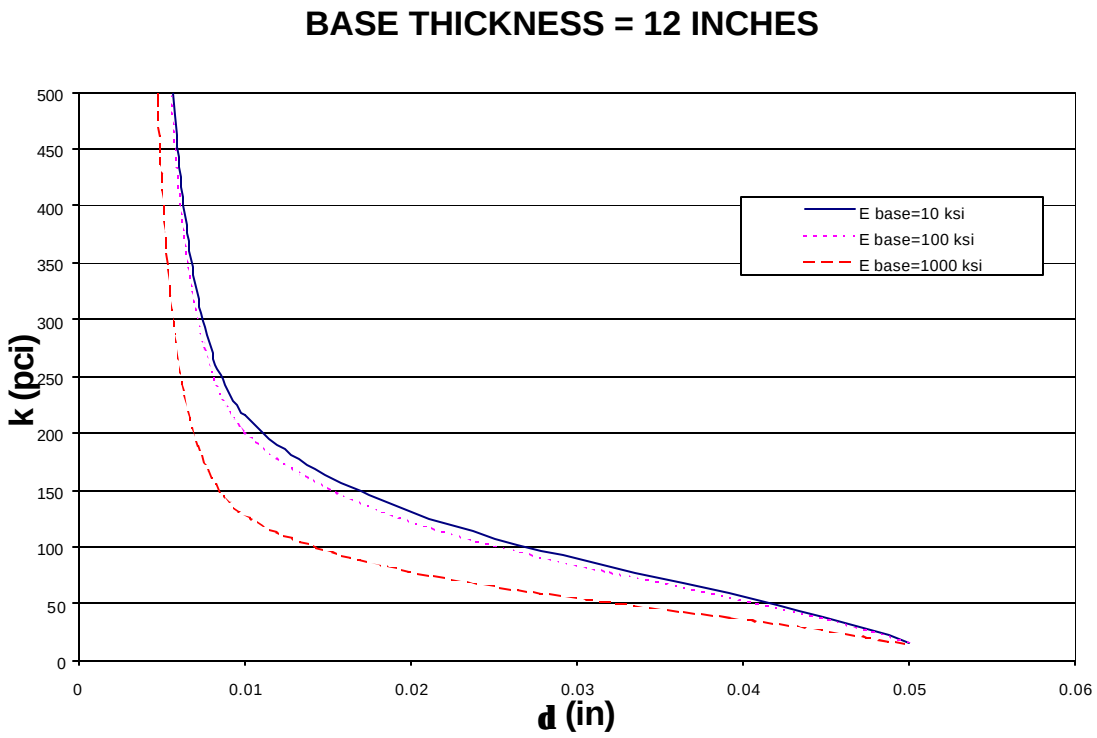

Figure 5.19. Modulus of Subgrade Reaction vs. Maximum Surface Deflection (Thick Base).

with base layer thickness of 152.4, 228.6 and 304.8 mm (6, 9 and 12 inches) were selected for analysis.

The FWD test is performed at three different levels of load and is conducted when the temperature variation through the slab is minimal to avoid the effects of curling. Three different load levels of 40.32, 53.76 and 67.2 kN (9000, 12000 and 15000 lb.) applied at the center of the slab (to minimize effects between slabs) were used in the nomograph development.

The regression equation showing the relationship between the surface deflection and other independent parameters of interest in rigid pavement design and obtained from the analyses previously described is presented below:

$$\log(\boldsymbol{d}) = a_0 + a_1 \cdot t_{pcc} + a_2 \cdot t_{base} + a_3 \cdot E_{base} + a_4 \cdot \log(k) + a_5 \cdot P \qquad (5.4)$$

where:

δ= Deflection at the center of load application (mm) or (in).

t_{pcc}=Thickness of the PCC slab (mm) or (in).

t_{base}=Thickness of the base (mm) or (in).

E_{base}=Elastic Modulus of the base (MPa) or (ksi).

k= Modulus of subgrade reaction (MN/m^3) or (pci)

P= Applied load (kN) or (lb).

a_0,a_1,a_2,a_3,a_4,a_5= Regression coefficients.

The regression coefficients along with the Coefficient of Determination R^2, are presented in Table 5.6. Modulus of subgrade reaction backcalculation nomographs for a non-bonded 3.65x4.57 m (12x15 ft) slab are shown in Figures 5.20 and 5.21. The SI Units nomograph has been adjusted to consider integer quantities in layer thickness and stiffness as well as loading.

Table 5.6. Regression Coefficients for the Backcalculation Nomographs.

	a_0	a_1	a_2	a_3	a_4	a_5	R^2
SI Units	0.38813	0.001348	-1.89996E-03	-6.2785E-06	-0.72280	8.55091E-03	0.97318
Eng. Units	-0.60685	-0.03425	-4.82589E-03	-4.3284E-05	-0.72280	3.80413E-05	0.97276

An identical procedure to that used in the flexible pavement nomographs to obtain the resilient modulus at the break the point E_{ri} is followed in Figures 5.20 and 5.21 to back calculate the modulus of subgrade reaction k.

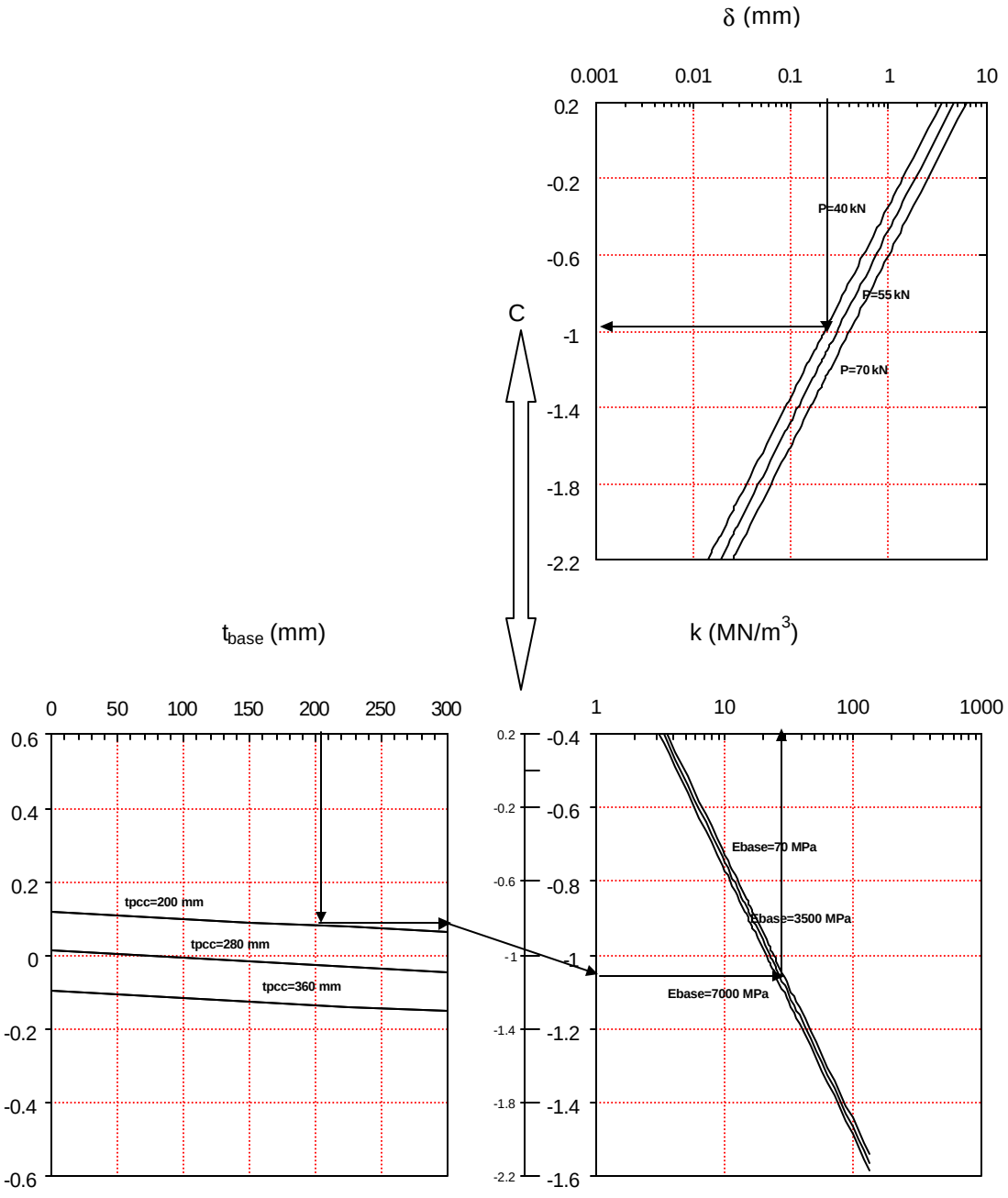

Figure 5.20. Backcalculation Nomograph for a Non-Bonded 3.65x4.57 m (12x15 ft.) PCC Slab (SI Units).

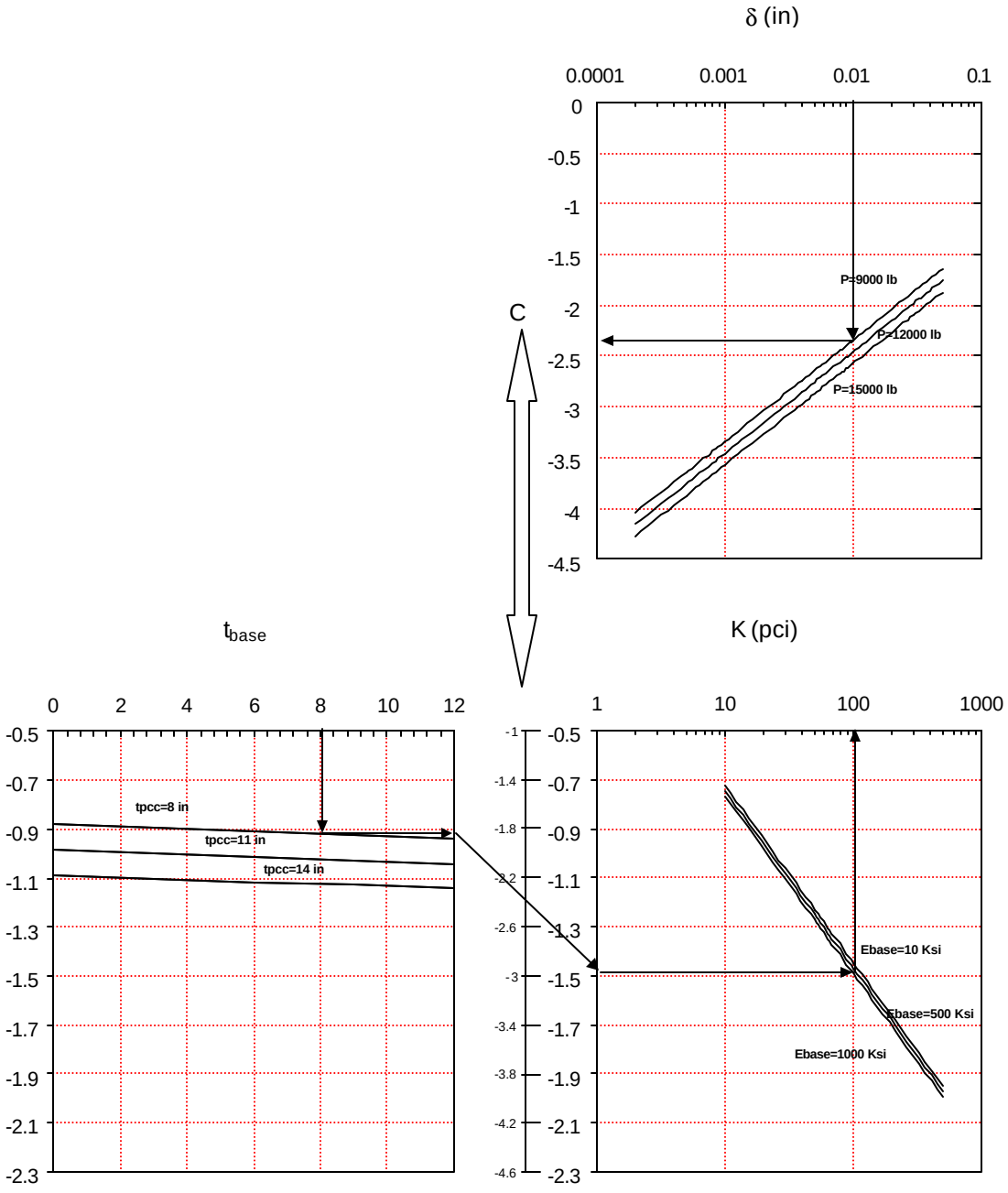

Figure 5.21. Backcalculation Nomograph for a Non-Bonded 12x15 ft. PCC Slab (English Units).

Chapter 6

DYNAMIC ANALYSIS OF FLEXIBLE PAVEMENTS

6.1 Background

The design of a multi layered pavement system involves the limitation of three parameters:

1. Surface deflections
2. Tensile strain at the bottom of the asphaltic concrete layer
3. Compressive stress or strain applied to the subgrade.

Excessive surface deflections result in high tensile strains at the bottom of the asphalt layer and high stress application to the subgrade. Tensile strains in the asphalt result in failure of the pavement surface due to fatigue cracking manifested as alligator map cracking. High stress on the soft subgrade soil results in permanent deformation of the subgrade and all layers above it resulting in failure of the pavement due to the appearance of ruts on the pavement surface.

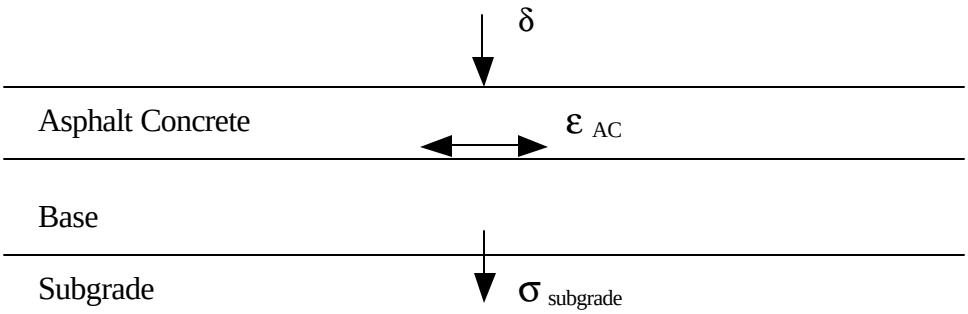

Figure 6.1. Pavement Design Limiting Parameters

Current pavement design procedures, such as the AASHTO design method are based on empirical methods that have been developed through experience and observation of pavement performance with time. These methods do not allow for the exact prediction of stresses, strains, and displacements of a pavement system. In order to develop a more reliable pavement design procedure that would include pavement material properties, mechanistic design procedures that include analysis of stresses and strains in the pavement system should be considered.

Finite element software packages, such as ILLIPAVE, have been evaluated for the purposes of predicting structural behavior of pavement systems. This research has resulted in the development of design nomographs that can relate pavement structure and properties with deflections, due to particular traffic loadings. Such models were verified using the results of Falling Weight Deflectometer (FWD) testing on highway research projects including the Ohio Test Road and the nine Ohio moisture-temperature monitoring stations (Figueroa et. al, 1994) where precise structural properties are known for the time of testing based on moisture and temperature monitoring instrumentation. Although this analysis found a strong correlation between the experimental and theoretical results, the theoretical analysis did not include the dynamic nature of the experimental data, which is necessary for the complete and accurate analysis of dynamic test data that more closely simulates traffic loads. This chapter will detail the FWD testing method, static finite element analysis, and the use of dynamic finite element models.

Falling Weight Deflectometry

Falling Weight Deflectometry is a non-destructive load test that is performed on pavement systems for the purposes of evaluating pavement properties. A falling weight deflectometer (FWD) consists of a load plate, weights, and a series of geophones (velocity transducers) mounted on a trailer that can be towed by a truck. The load plate consists of a twelve-inch diameter disk with a thin rubber pad that is placed on the asphalt surface. The weights are mounted on a shaft above the load plate and are raised hydraulically to a predetermined height. The height and magnitude of the weight can be varied to produce the desired impulse. To perform a test, the load plate and the series of geophones are lowered to the pavement surface. The weight is then lifted and dropped onto the load plate, producing and impulse load on the pavement surface. The load pulse is measured by a load cell which records load pressure with time. A typical load impulse from FWD testing is shown in Figure 6.2. The double peak is characteristic of the Dynatest brand falling weight deflectometer, which is used by ODOT as well as many other highway departments throughout the United States.

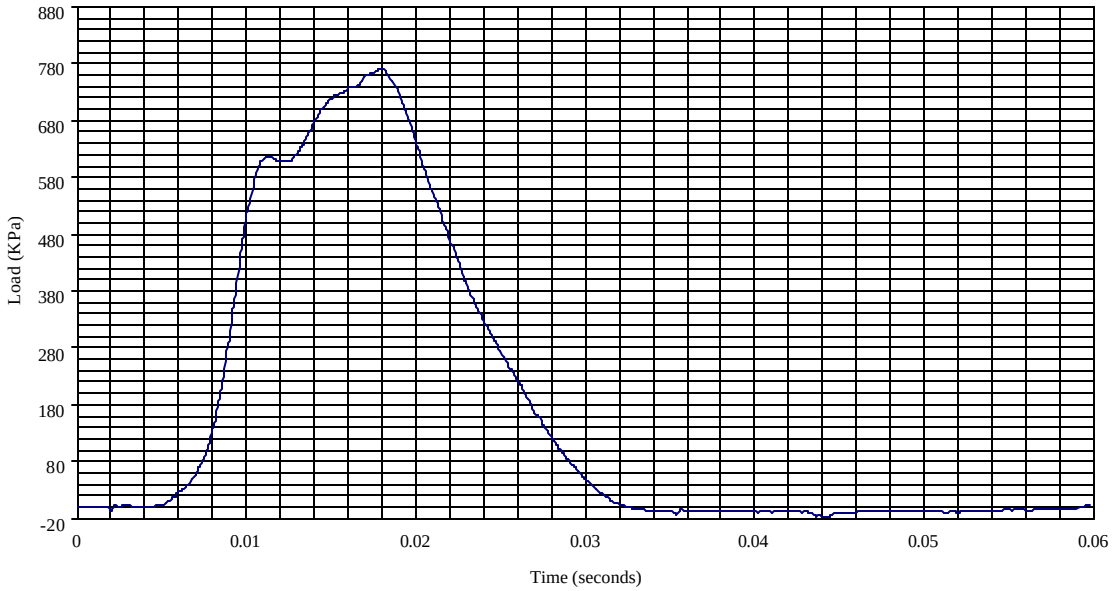

Figure 6.2. Dynatest FWD Load Pulse

The resulting surface deflections are recorded with time by geophones placed on the pavement surface. Geophones are typically placed at the following distances from the pulse:

Table 6.1. Geophone Configuration

Sensor	Distance from Impulse Source (in)	Distance from Impulse Source (m)
1	0	0
2	8	0.2
3	12	0.3
4	18	0.457
5	24	0.609
6	36	0.914
7	60	1.524

The first geophone measures the deflections directly under the center of the load plate through a small circular opening through the load plate. A typical time history of deflections is shown in Figure 6.3. Each curve corresponds to a geophone, and as expected, the displacements decrease in magnitude with distance from the load source. Also of interest is the time delay in the peak displacement recorded by each geophone, corresponding to the difference in time for the wave generated by the impulse load to reach the different sensors.

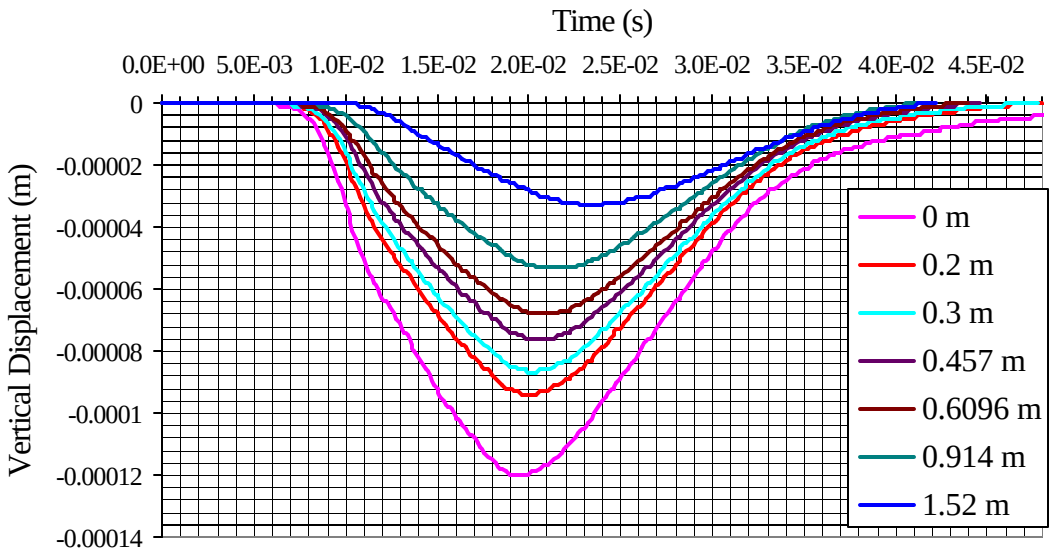

Figure 6.3. Deflection vs. Time record from a FWD test

Static Analysis of FWD Data

Traditional analysis methods of FWD data assume that the load applied during an FWD test is static resulting in calculated deflections. The maximum deflection measured by each geophone along the pavement surface is selected to configure a typical deflection bowl as shown in Figure 6.4. Each curve in this

figure represents the displaced shape of the pavement at a specific time of load application, as recorded by all the geophones. The dark curve is an envelope that demarcates the maximum of each time profile and is referred to as a deflection bowl. The resulting deflection bowl therefore removes the dimension of time from the test and allows the pavement system to be analyzed using a "statically" applied load.

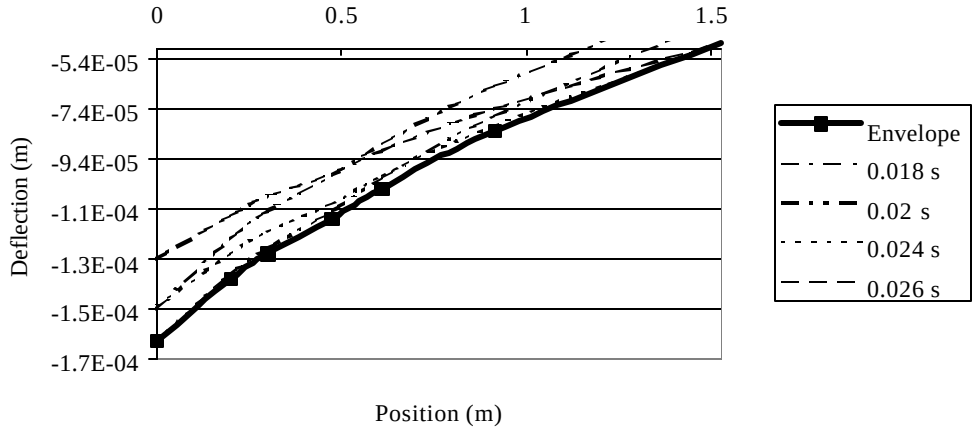

Figure 6.4. Deflection Bowl

Many back calculation programs have been developed to estimate the resilient modulus of the multi-layered pavement system components based on the results of FWD testing. Back calculation involves varying the modulus of the pavement layers and calculating deflections using the elastic layer theory until a suitable match for FWD field test deflections are found. These programs, however, have not been able to consistently produce accurate estimates of the stiffness properties of pavement system components.

Researchers have obtained better results through the use of forward calculation programs, such as finite elements and the spectral element method. These programs are reasonably accurate in predicting the deflections generated by an FWD test from forward calculations where the properties and structure of the multi-layered flexible pavement system and the applied loadings are known.

Figueroa et al., 1994 successfully developed a back calculation procedure for estimating the resilient modulus of subgrade soils based on compiled results of forward finite element analysis of multi-layered pavement systems of known properties, structure, and load. The results of these analyses are presented as equations and nomographs (a combination of interdependent graphs).

Figueroa et al., 1994, and later Alvarez, 2000, evaluated the program, ILLIPAVE, a finite element program specifically designed for the analysis of multi-layered pavement systems as a successful package for this task by comparing actual and predicted deflections from FWD testing. Data from numerous computer program runs was combined and a general relationship (and nomographs)) relating deflection, AC thickness, base thickness, modulus of AC, modulus of the subgrade soil, and applied load was developed, as it was discussed in Chapter 5.

6.2. Dynamic Analysis of FWD Data

Despite the success achieved in previous research to model FWD testing by approaching the problem as a static event, certain aspects of static analysis render it prone to errors. Static analysis does not consider the impact and time-

varying nature of the loading. Such nature is very important since the response of the multi-layered pavement system will depend on such aspects of loading as the magnitude, duration, and shape of the load pulse. Also the individual materials involved have different dynamic properties if the loading is applied statically or as an impact. According to Al-Khoury et al.,2000, the use of different load pulses at a single location will result in totally different results due to subgrade characteristics.

In order to examine the feasibility of using dynamic methods for pavement analysis and to provide new insights into the response of pavement subjected to FWD tests, dynamic simulations of FWD load pulses were conducted in an attempt to replicate the results of actual field tests. Two important pieces of information necessary to carry out a dynamic simulation – time history of displacements and the load pulse, have only recently been included in FWD test output files. The load pulse is necessary for applying the proper load to the model and the time history of surface displacements are necessary to verify the output. Two software packages were used for FWD test simulation, Plaxis and FWD-DYN. Knowing pavement system properties and applied loading, subgrade modulus was varied until a suitable match with experimental data was found.

6.2.1 FWD Test Sites

Based on availability of FWD testing on sections with working temperature-moisture equipment at the Ohio Test Road, section 390112 was

selected for evaluation.. Table 6.2 summarizes the layer thickness and material types for this section.

Table 6.2. Layer Profiles – Materials and Thickness
Section 390112

Material	Thickness cm (in)
AC	10.16 (4)
ATB	30.48 (12)
PATB	10.16 (4)

Prior to 1999, only maximum displacements were recorded from FWD testing by ODOT at the Ohio Test Road. Therefore the only time history of displacement data available is from tests conducted in September of 1999 and September of 2000. Each section where an FWD test was conducted was divided into 11 stations, numbered 0 through 500 with increments of 50 feet. Two FWD tests were conducted at each station, one on the center of the left lane, and one under the right wheel path of the left lane.

6.2.2. Material Properties

Material Properties were chosen for each layer based on available environmental and laboratory data. Previous studies by DeButy, 1997 and Alvarez, 2000 characterized the temperature dependency of the resilient modulus of the asphalt concrete, permeable asphalt treated base, and asphalt treated base, as discussed in Chapter 2. Temperatures of each layer for use in

the material characterization models were obtained from data collected at the Ohio Test Road. Thermistor depths for section 390112 are as follows:

Table 6.3. Thermistor Depths (Section 390112)

Material	Thermistor Depth cm (Inches)
Asphalt Concrete	2.54 (1)
	5.08 (2)
	8.9 (3.5)
Base	25.4 (10)

Since the temperature of the AC layer can have wide variations from the top to the bottom, the average temperature based on the mid-depth value of a linear fit to the three thermistor temperatures was selected. In the event that thermistors had malfunctioned, average asphalt temperatures were estimated based on the previously discussed equations relating air temperature to asphalt temperature. Average temperatures of base layers were estimated by linear interpolation of thermistor readings. The resilient modulus of the subgrade is based on the moisture content of the soil. Saturation data from September of 1999 and September of 2000 indicate that the subgrade was near saturation. The resilient modulus was initially estimated to be around 25,000 KN/m^2.

The following chart summarizes the assumed material properties corresponding to actual FWD test dates and times. These values were entered into the finite element models.

Table 6.4. Assumed Pavement Layer Stiffness for Finite Elements Analysis (Section 390112)

Date	Time	AC kPa	ATB kPa	PATB kPa
9/15/99 (258)	8:00 a.m.	5,018,115	1,363,700	1,214,150
9/26/00 (270)	11:00 a.m.	3,742,337	2,591,634	1,649,666

6.3 Analysis with Plaxis

Plaxis is a finite element code for soil and rock analysis. Included in Plaxis is a dynamics module that allows for dynamic analysis of a soil-structure system. Time integration is achieved through an implicit Newmark Scheme (Brinkgreve, 1998).

6.3.1 Finite Elements Model

Due to the cylindrical nature of the FWD test, the pavement structure is suitable for analysis using an axisymmetric model. The layered pavement system geometry was recreated in the Plaxis input module. See Figures 6.5 a and b for details. A unit distributed load was placed at the axis of symmetry to represent the loading from the FWD load plate. A unit distributed load was used because during the dynamic simulation it is multiplied by the magnitude of the load pulse at each point in time. This will be described in more detail later.

Bedrock at the Ohio Test Road is located at around 16 meters in depth and therefore the depth of the model was fixed at 16 meters. Boundary conditions were applied as follows: the axis of symmetry was fixed in the horizontal direction due to symmetry conditions. The bottom was fixed in the vertical direction to simulate the presence of bedrock. The outer side of the

model was bounded with an absorbent boundary. Absorbent boundaries act like dampers on the boundary of the model so that any stress waves that reach them are absorbed. This absorptive property prevents any stress waves from reflecting back into the model and skewing results.

Nodes were placed on the surface of the model at the precise locations of the geophones on a FWD so that displacements at those points could be measured and compared with actual data. The model was meshed using 15 node wedge shaped elements, which is the only element offered by Plaxis for three dimensional analysis. Figure 6.6 shows an example of a meshed geometry model. Care must be taken when choosing an element for dynamic finite element analysis because high order elements which are very good for modeling shear and bending, are not good for modeling wave propagation generated from dynamic loads that are applied very quickly. In the case of dynamic loads from FWD tests, the rate of loading is slow enough relative to the element size that it is not an issue and 15-noded elements are suitable. For the dynamic simulation, the actual load pulse, as measured by the FWD load cell, was applied to the model. At each time interval, the value of the load pulse was multiplied by the aforementioned unit load placed on the model.

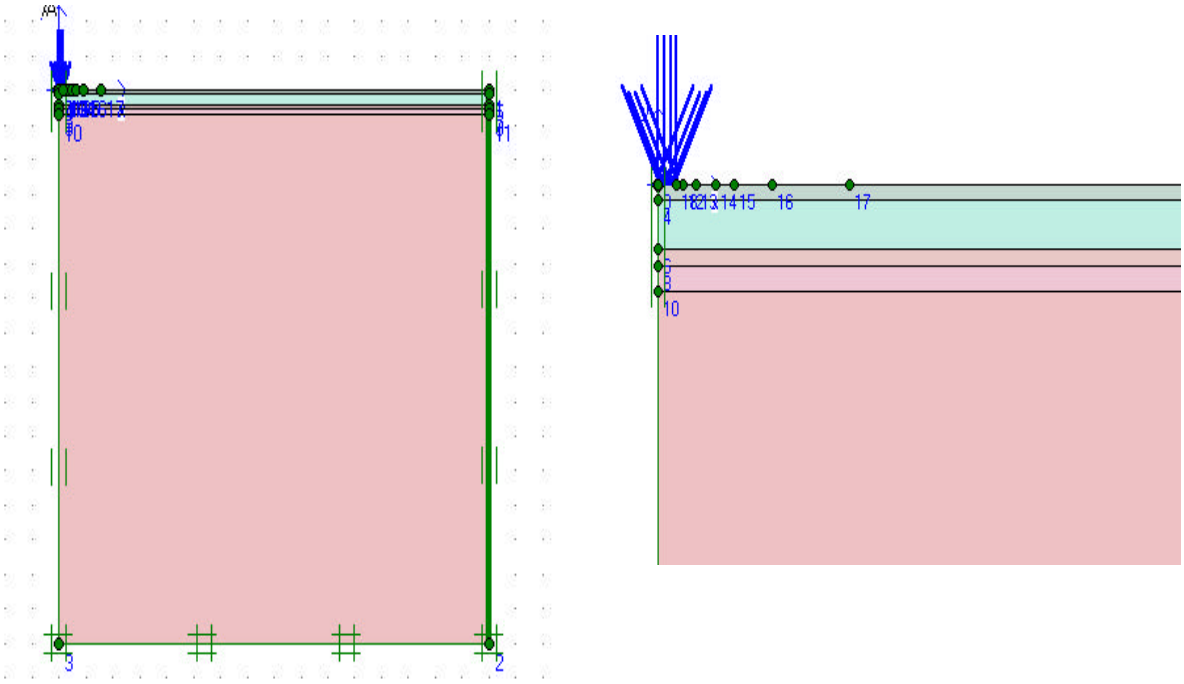

Figure 6.5. Example Plaxis Geometry Model:
(a) Model showing boundary conditions and
(b) close up showing pavement system layers

6.3.2 Displacement Response Results

At the end of a dynamic simulation, Plaxis plots a time history of displacement at predefined locations. These locations were chosen at the locations of the FWD geophones for comparison purposes. It was found that the break point modulus initially chosen for the subgrade resulted in gross overestimation of the surface deflections. It is known that the response of points far from the point of loading highly depend on the subgrade elastic modulus and are only weakly dependant on the elastic modulus of the AC and base layers (Majidzadeh, 1974). In order to achieve a better result, the modulus of the subgrade was increased until a better match for the deflections of the most distant geophone (152.4 cm. or 60 in.) was achieved. This increase in subgrade

modulus resulted in a closer match between Plaxis and actual data for all geophones. The process of matching the experimental and theoretical data is a tedious one due to the large amount of time that Plaxis takes to perform an analysis. Matches for section 390112 were determined for three stations: 0 (beginning), 250 (middle), and 500 (end) to show any material property changes along the length of the section.

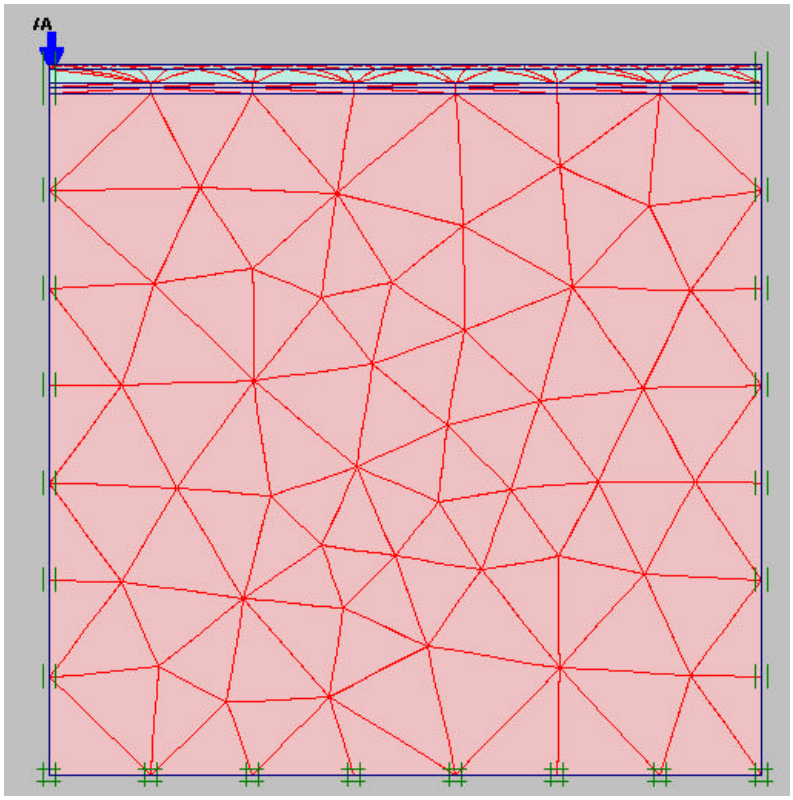

Figure 6.6. Meshed Plaxis Model

The following Figures 6.7 to 6.18 depict the calculated displacement responses for section 390112 along with actual data from field measurements for comparison purposes.

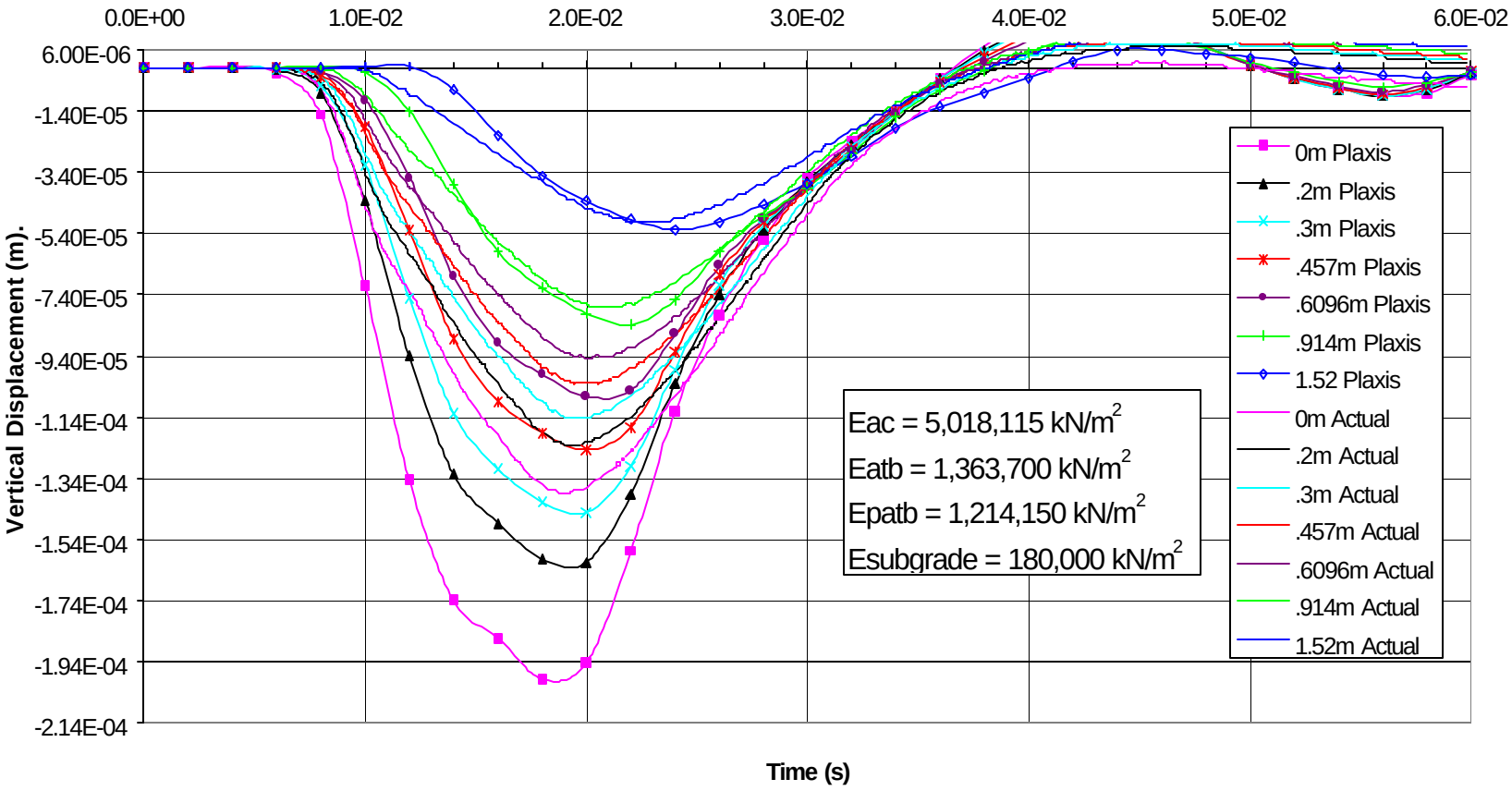

Figure 6.7.Plaxis Results For 390112 Station 0 Lane Center Line 9/15/99

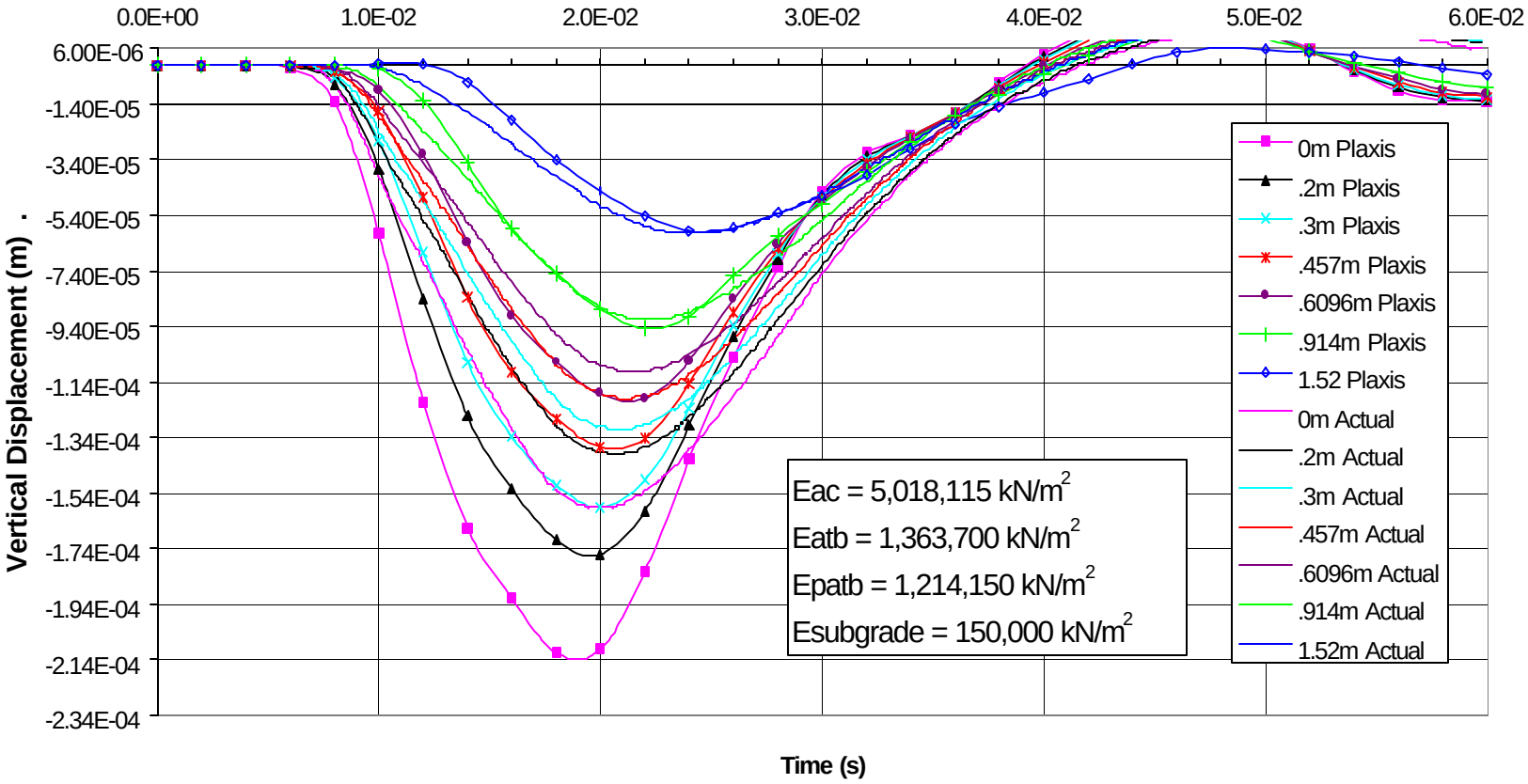

Figure 6.8. Plaxis Results For 390112 Station 250 Lane Center Line 9/15/99

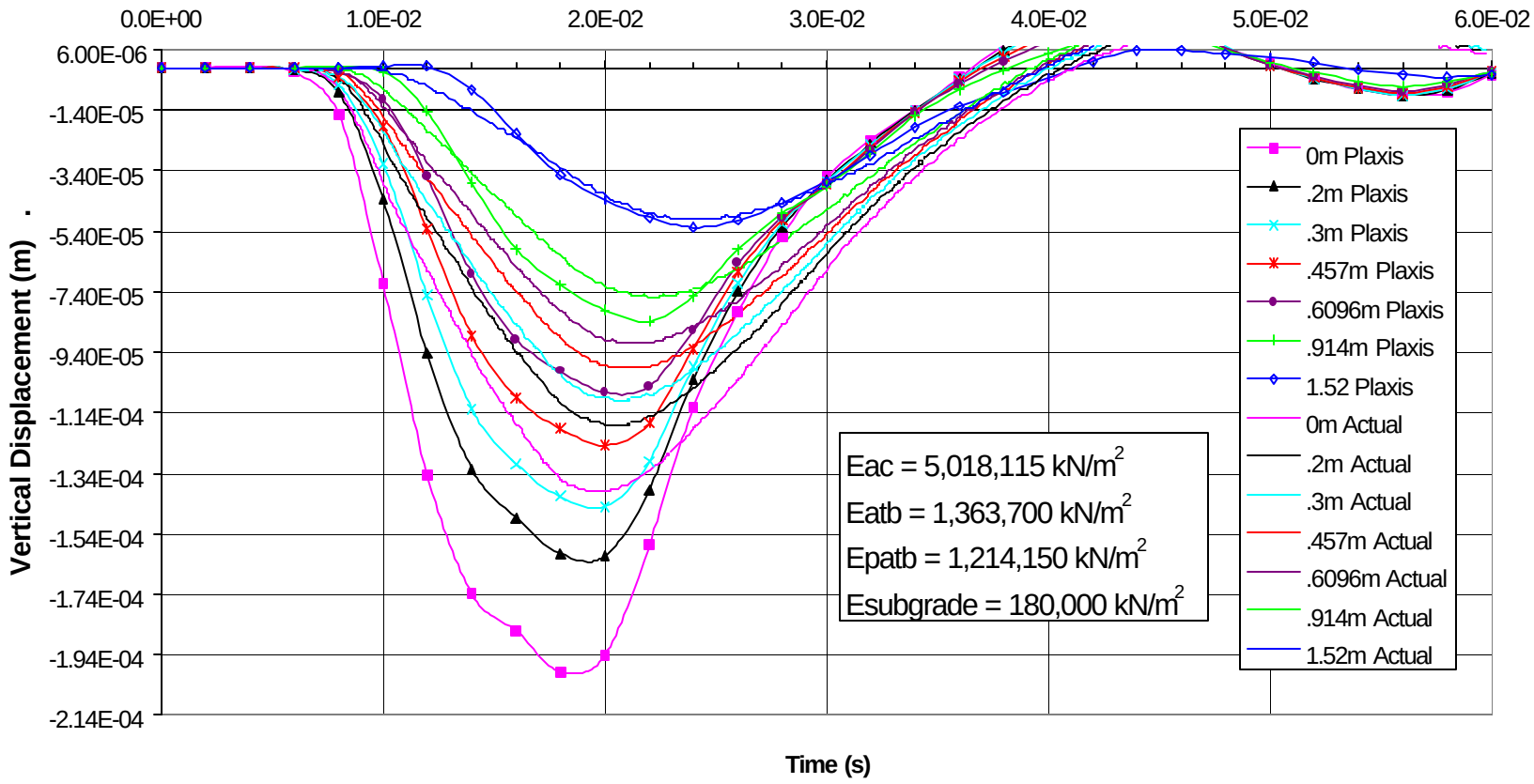

Figure 6.9. Plaxis Results For 390112 Station 500 Lane Center Line 9/15/99

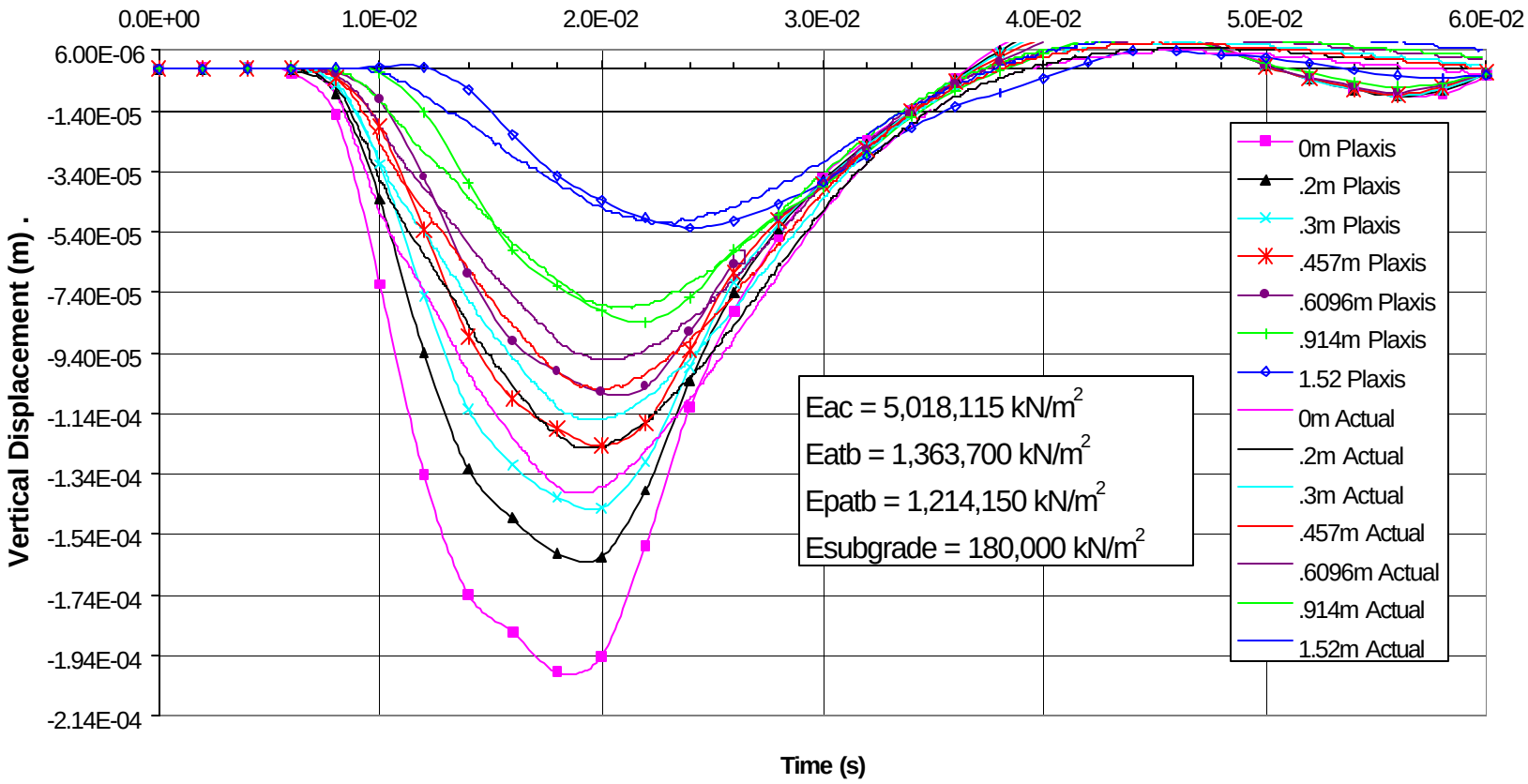

Figure 6.10 Plaxis Results For 390112 Station 0 Right Wheel Path 9/15/99

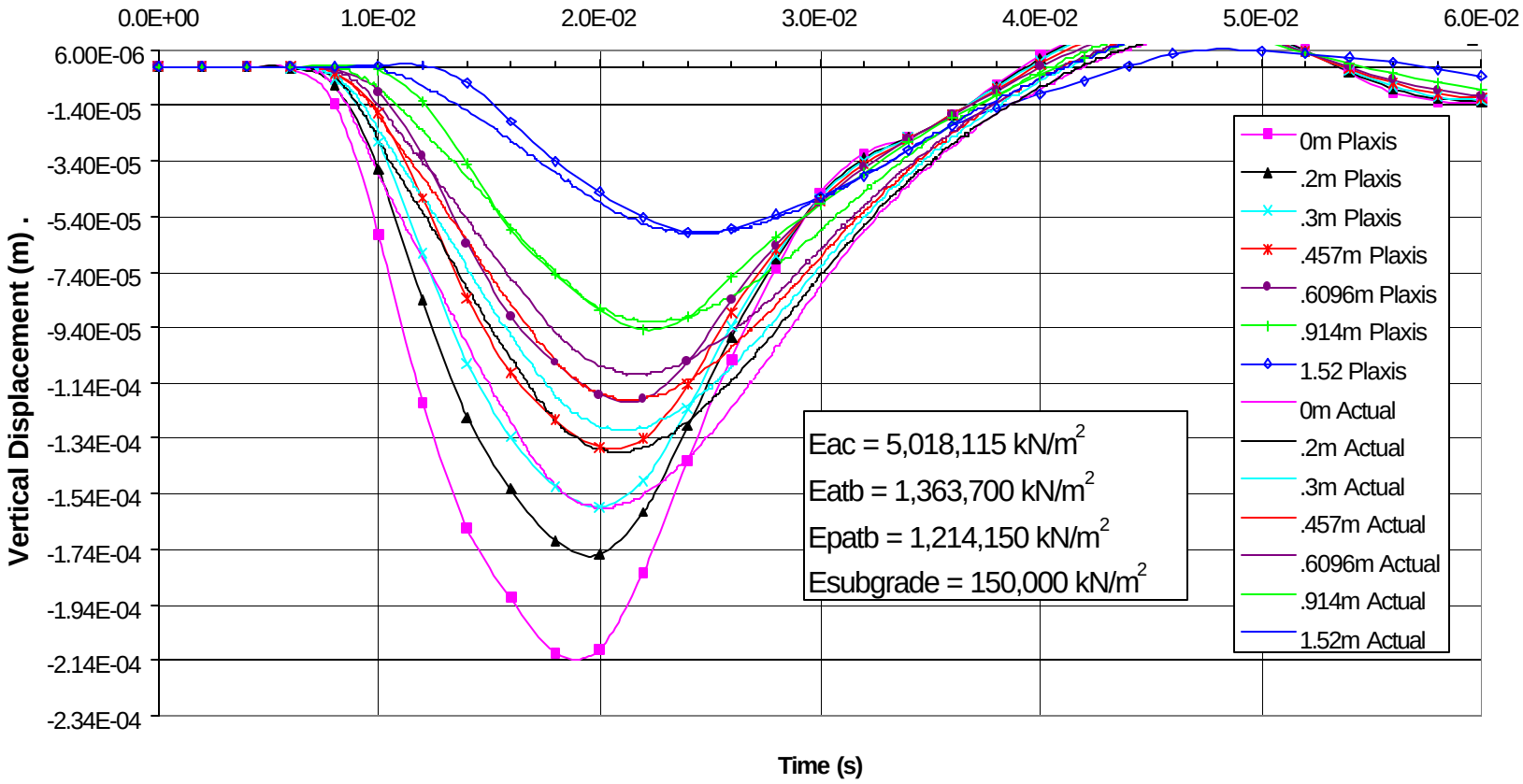

Figure 6.11. Plaxis Results For 390112 Station 250 Right Wheel Path 9/15/99

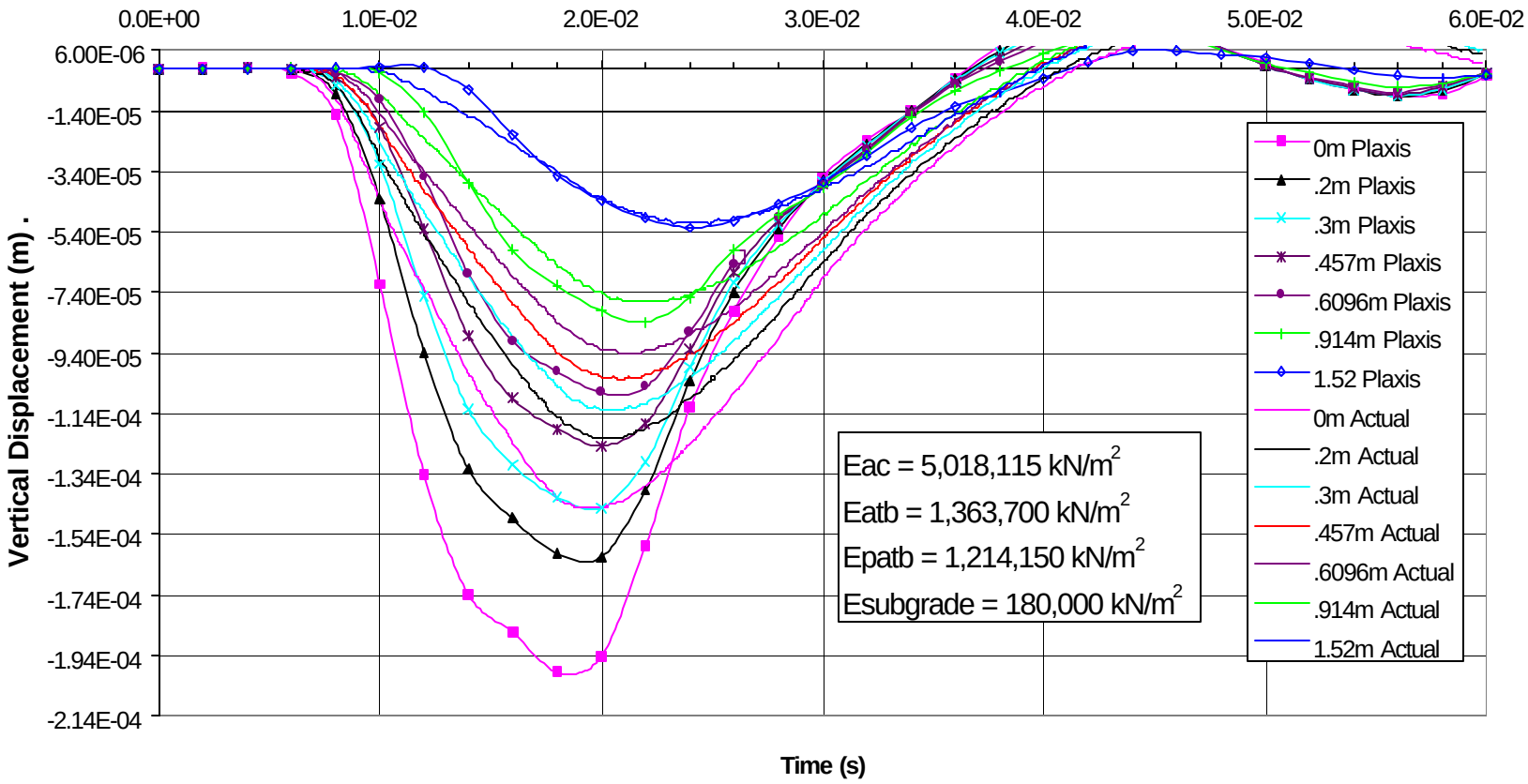

Figure 6.12. Plaxis Results For 390112 Station 500 Right Wheel Path 9/15/99

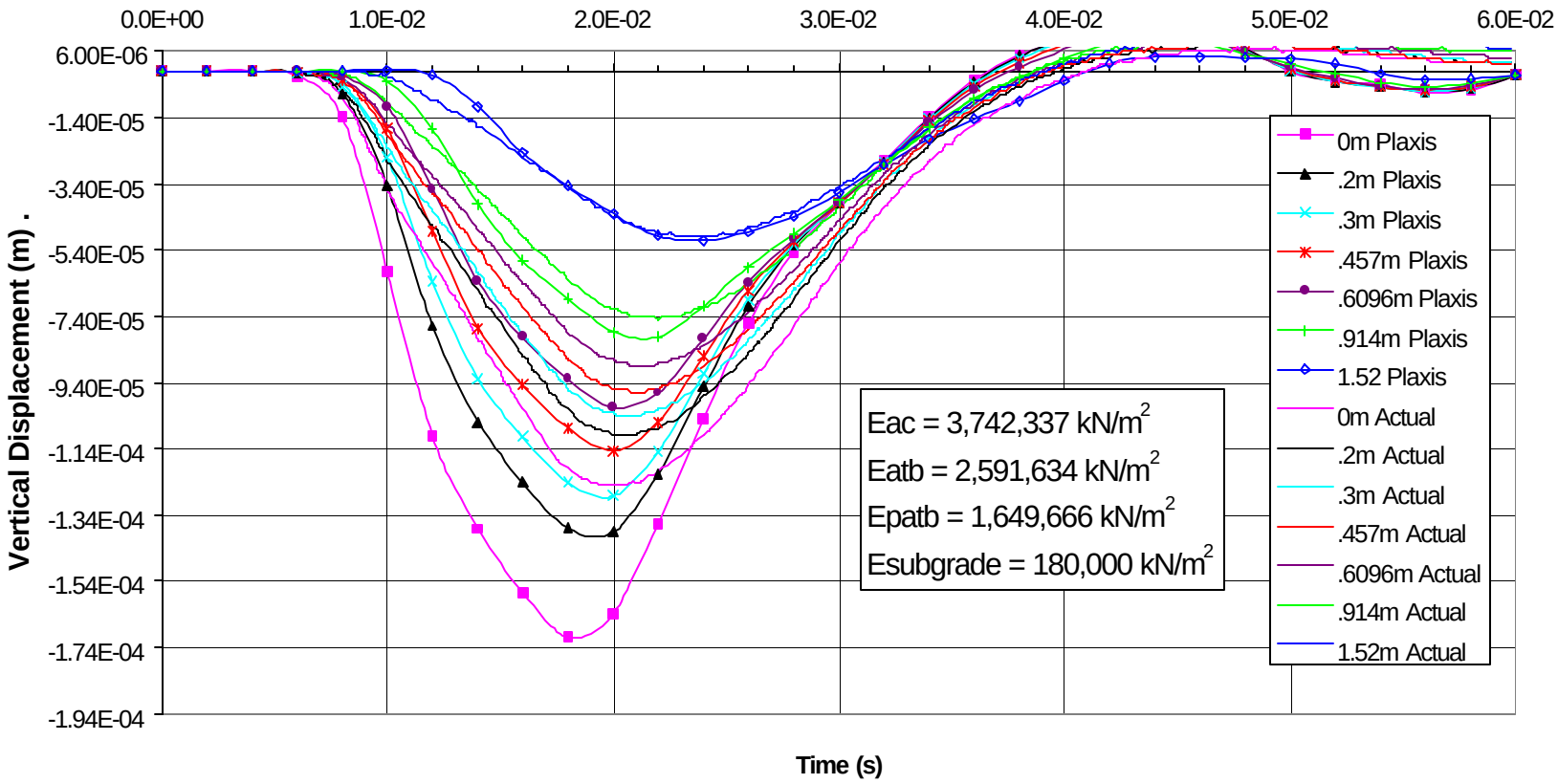

Figure 6.13. Plaxis Results For 390112 Station 0 Lane Center Line 9/26/00

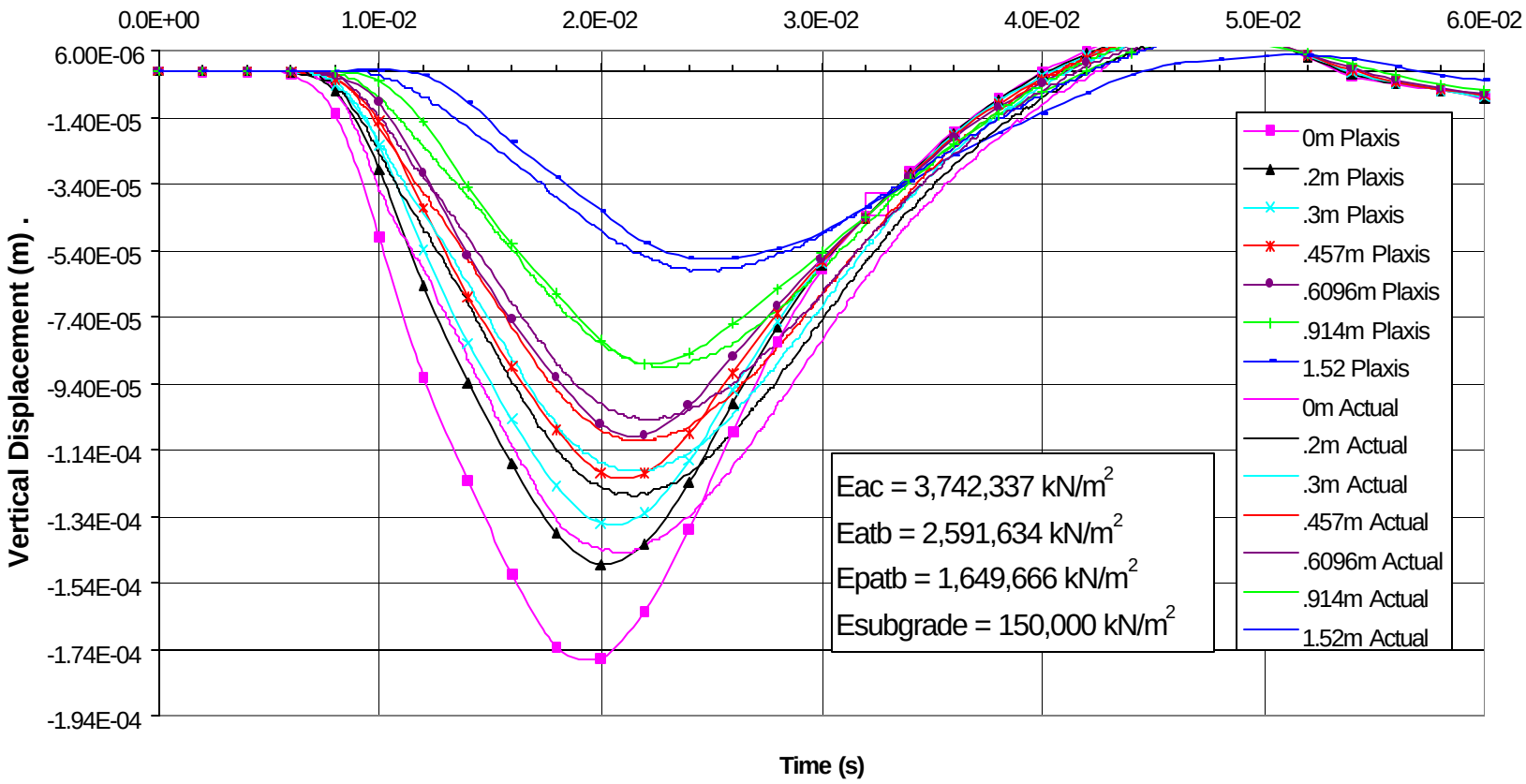

Figure 6.14. Plaxis Results For 390112 Station 250 Lane Center Line 9/26/00

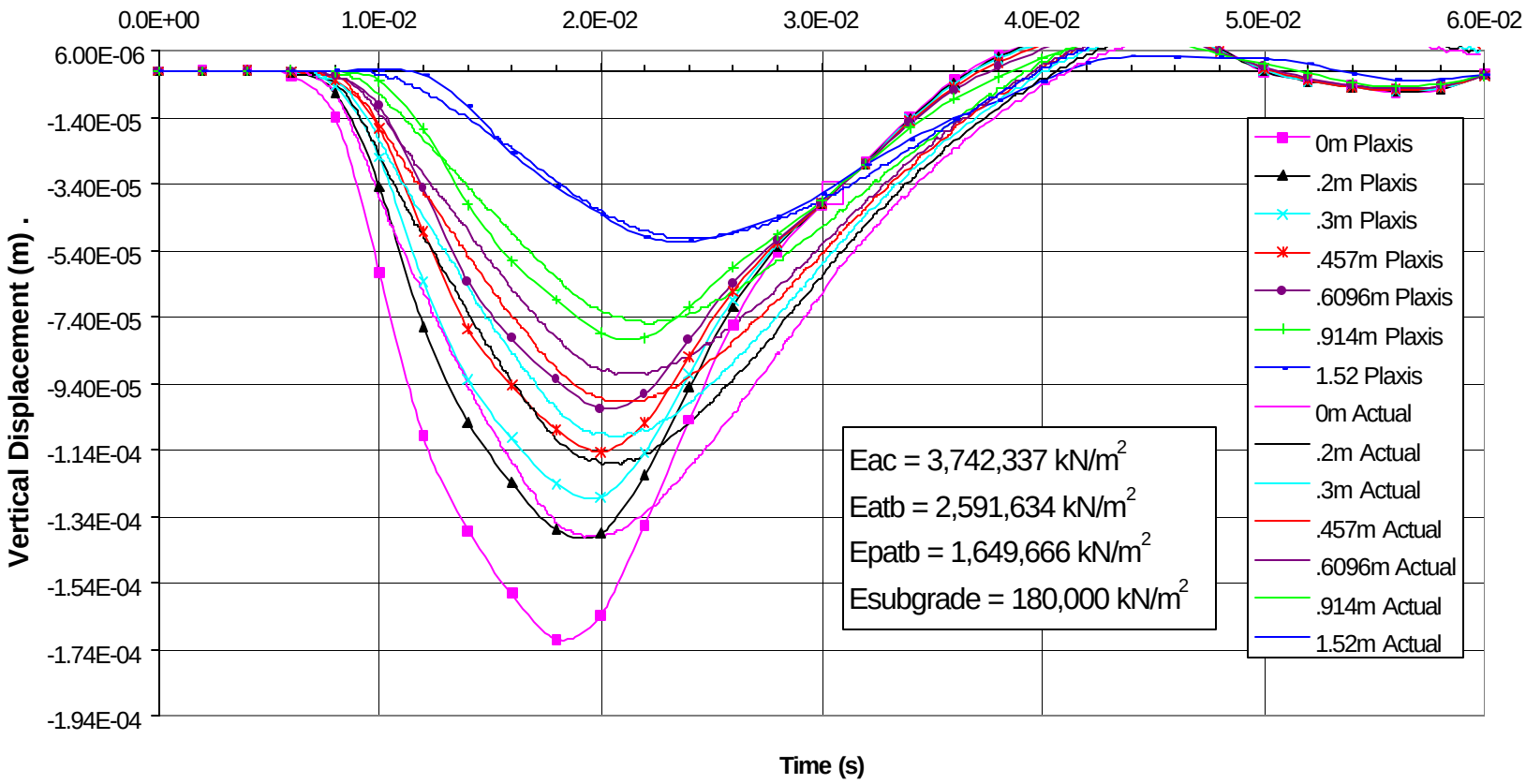

Figure 6.15. Plaxis Results For 390112 Station 500 Lane Center Line 9/26/00

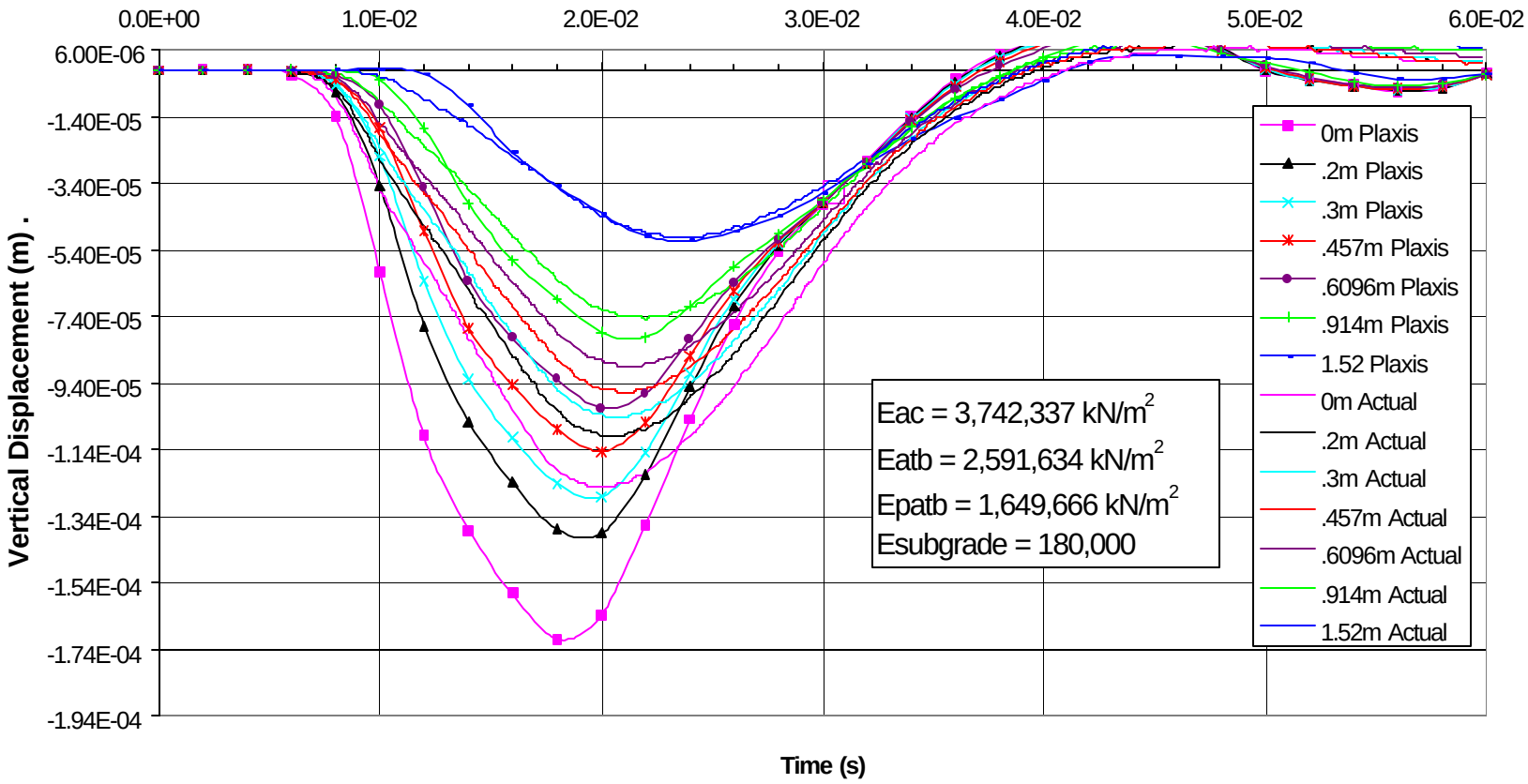

Figure 6.16. Plaxis Results For 390112 Station 0 Right Wheel Path 9/26/00

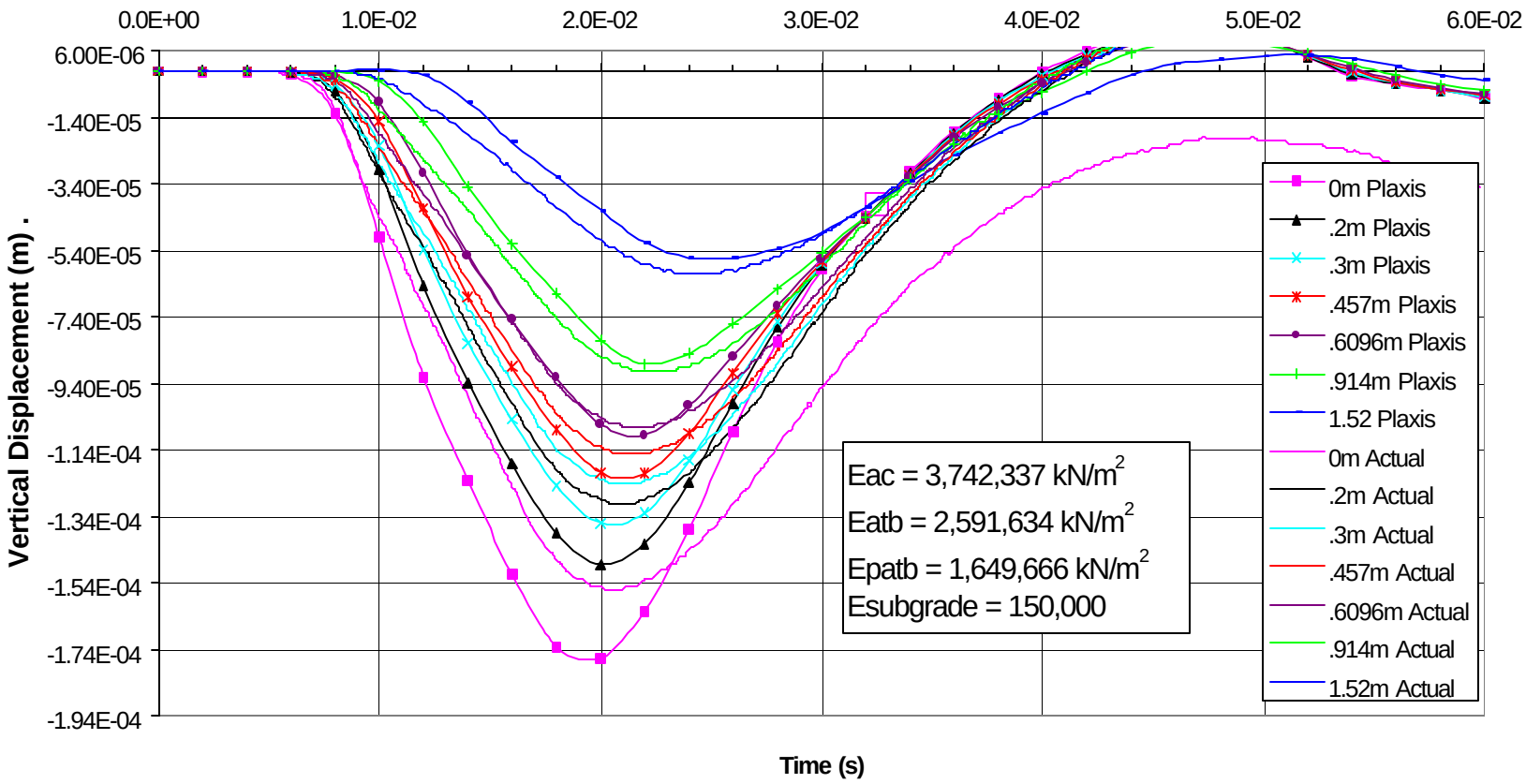

Figure 6.17. Plaxis Results For 390112 Station 250 Right Wheel Path 9/26/00

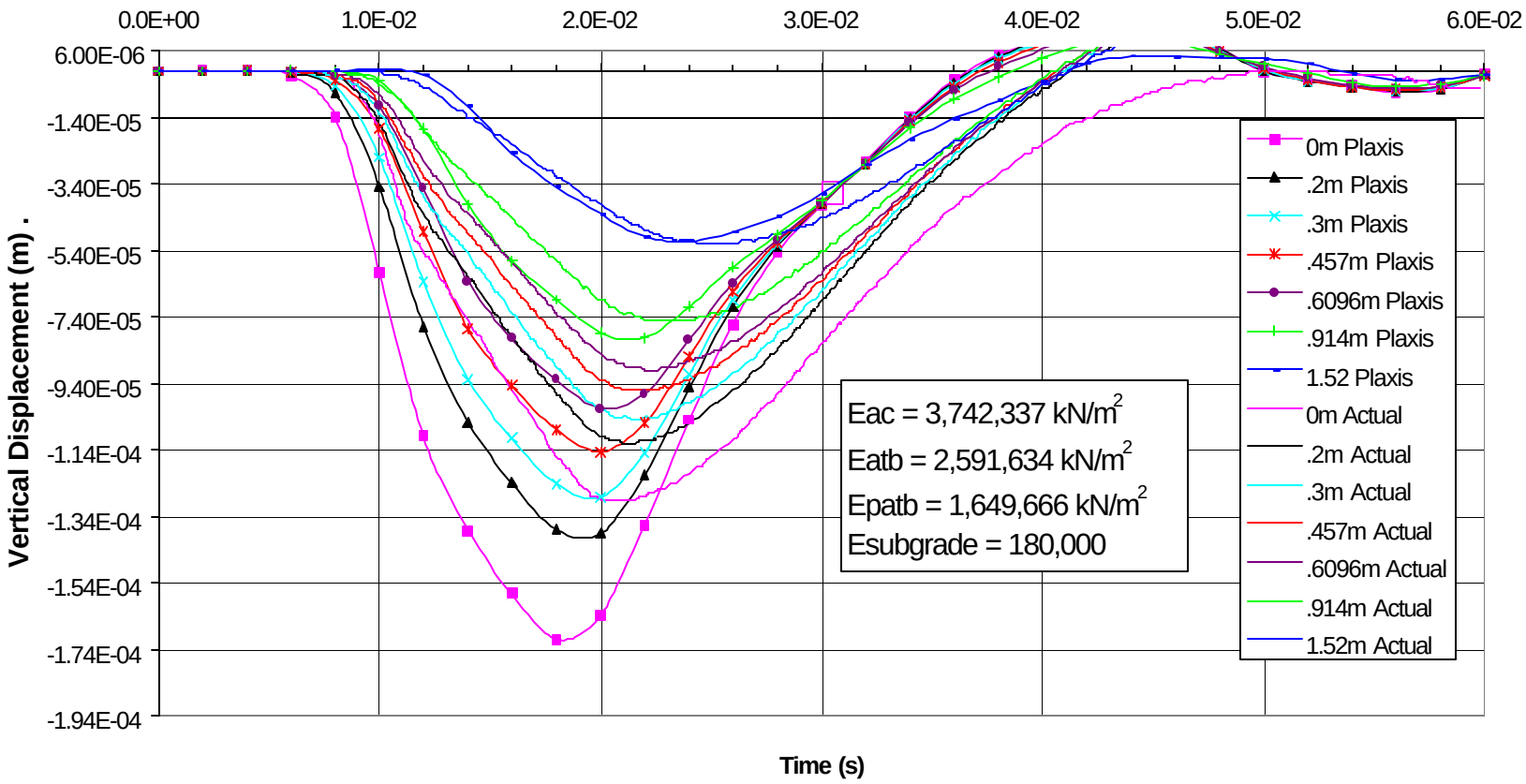

Figure 6.18 Plaxis Results For 390112 Station 500 Right Wheel Path 9/26/00

6.3.3. Displacement Response Conclusions

Despite the match obtained at points far from the load, the points located closest to the load still deviated from actual values. These discrepancies and the obvious need to increase the elastic modulus of the pavement and base layers to achieve a better match for deflections close to the load plate are a consequence of the viscoelastic nature of asphalt concrete. Viscoelastic materials display a change in elastic modulus that is dependant on the rate of loading. Resilient modulus data used for the models was based on a loading pulse with a duration of 0.1 seconds. The FWD load pulse has a duration of around 0.03-0.04 seconds. This increased rate of loading will result in a higher elastic modulus for the materials.

The final elastic modulus used for the analyzed section is summarized in the following table.

Table 6.5. Subgrade Moduli From Plaxis Models (Section 390112)

Date	Station	Subgrade Modulus kPa
9/15/99 (258) and 9/26/00 (270)	0	180,000
	250	150,000
	500	180,000

Comparing the results of the three stations, it was found that as the testing moved toward the center of the section (station 250), the deflections increased, and the modulus of the subgrade decreased. This observation is important since it shows that one cannot expect complete uniformity in pavement response along

an entire section of road. The response will be similar along a section, but will vary slightly. Such variations can stem from construction practices.

A comparison of the shapes of the actual and computed deflection curves shows that both peak at the same time. This similarity helps justify the validity of the model used. The computed deflection curves however tend to return to zero much sooner than the actual deflection curves. This discrepancy may be corrected by increasing the elastic modulus of the pavement and base materials once testing is done to characterize the elastic modulus of the relevant materials at the higher load rate corresponding to that of the FWD test. Another difference between the actual and calculated deflection curves is the oscillatory behavior demonstrated at the tail end of the calculated curves after the load has been applied and removed. This behavior does not have any apparent relevance and can be ignored. Again, this oscillatory behavior may be reduced by an increase in the elastic modulus of the pavement and base materials resulting in a better correlation between the behavior of the calculated and actual deflection curves.

6.3.4 Stress-Strain Response Results

Instrumentation installed at the Ohio Test Road includes structural response sensors, such as LVDTs, strain gauges and pressure cells. Although structural response data is not presently available for comparison, the stress strain responses of the Plaxis model at key positions were calculated for purposes of software evaluation. For each test date, time histories of stress and strain were generated. Stress was calculated at one position: at the top of the

subgrade soil, just below the base, directly under the center of the load Figures 6.19 and 6.22). Strain response was recorded at nine positions throughout the asphalt concrete layer: along the axis of symmetry and along the bottom of the layer. Each curve in the plots of strain time history along the axis of symmetry corresponds to a depth below the asphalt concrete surface (Figures 6.20 and 6.23). On the other hand, each curve in the plots of strain time history along the bottom fiber of the asphalt concrete corresponds to a distance from the axis of symmetry (Figures 6.21 and 6.24). It should be noted that positive values correspond to tension while negative values refer to compression in all curves.

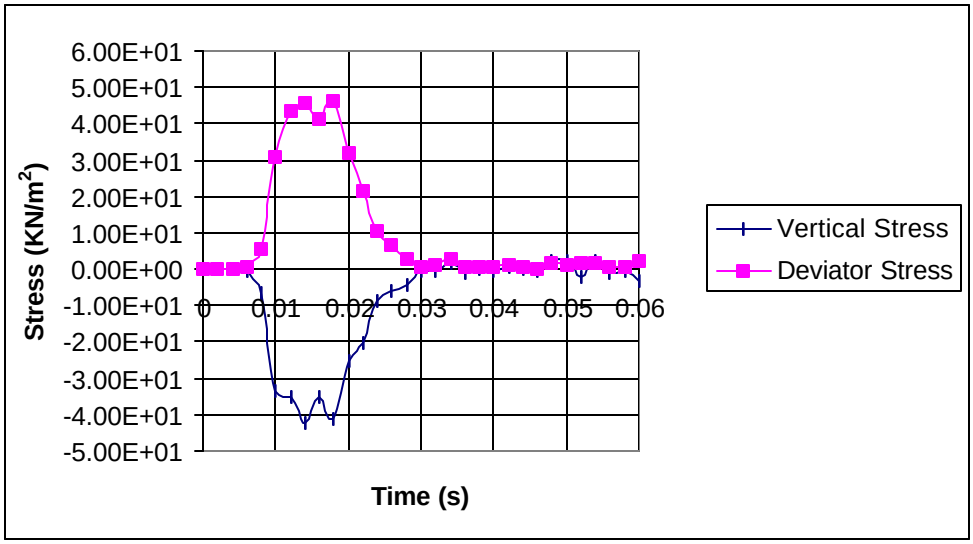

Figure 6.19. Subgrade stress time history under center of loading Section 390112 9/15/99

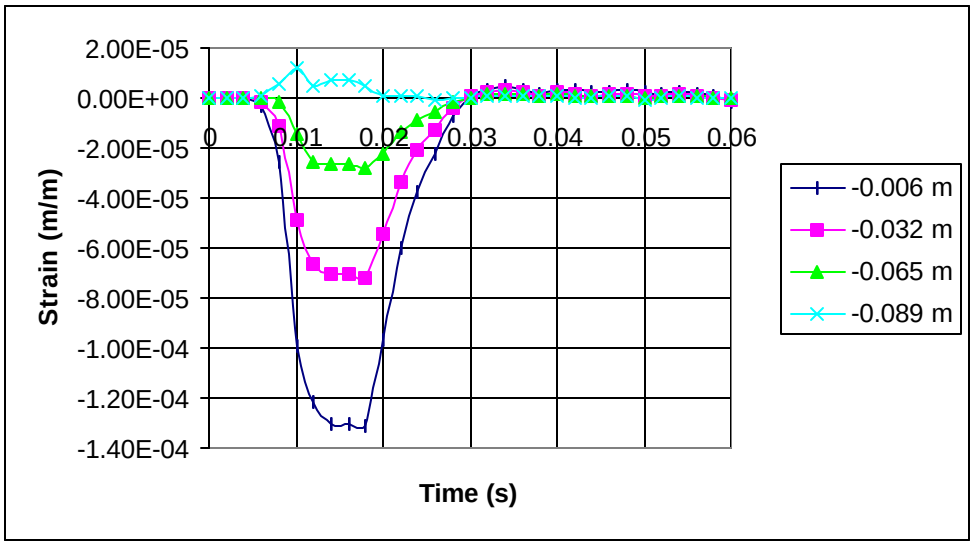

Figure 6.20. Asphalt concrete radial strain time history along axis of symmetry Section 390112 9/15/99 (Curves at depth from AC surface)

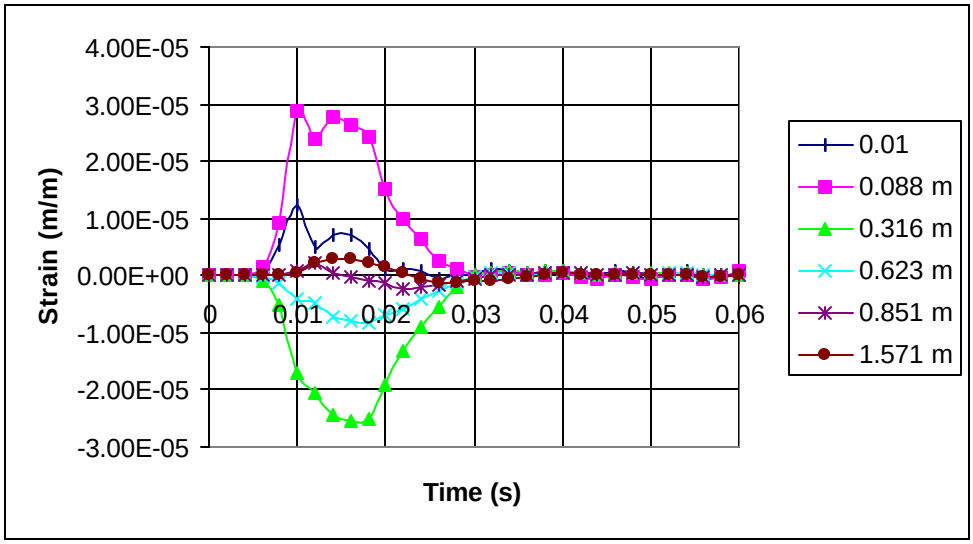

Figure 6.21. Asphalt concrete radial strain time history along bottom fiber Section 390112 9/15/99 (Curves at radial distance from center of load application)

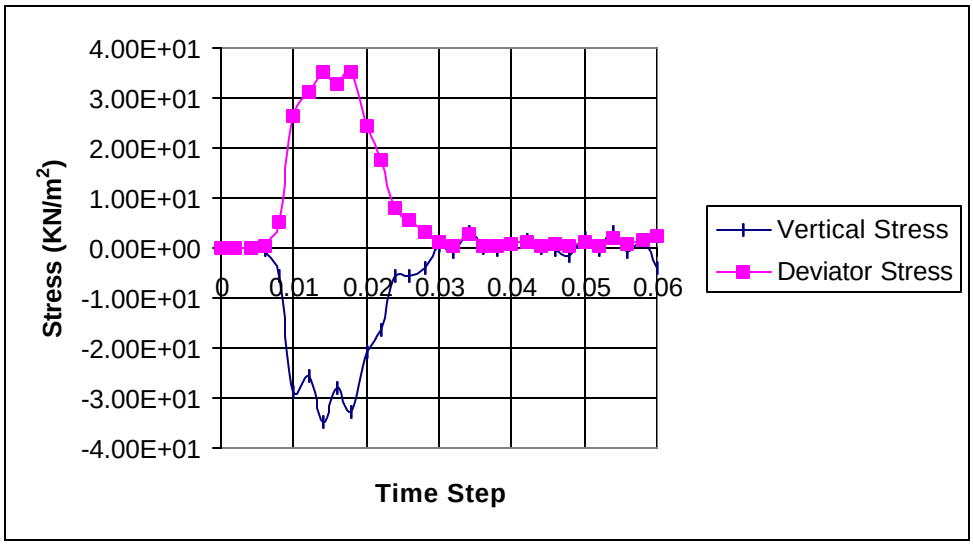

Figure 6.22. Subgrade stress time history under center of loading Section 390112 9/26/00

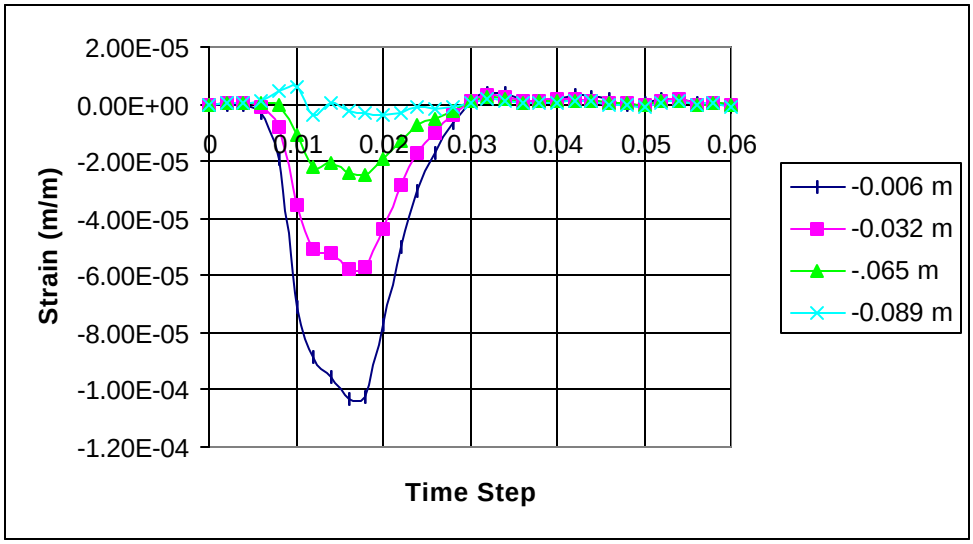

Figure 6.23. Asphalt concrete radial strain time history along axis of symmetry Section 390112 9/26/00 (Curves at depth from AC surface)

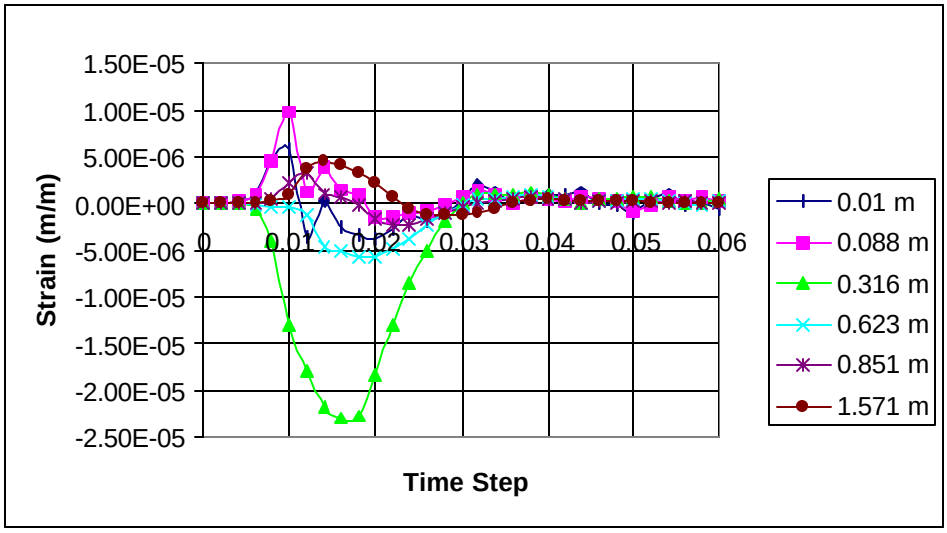

Figure 6.24. Asphalt concrete radial strain time history along bottom fiber Section 390112 9/26/00 (Curves at radial distance from center of load application)

6.3.5 Stress Strain Response Conclusions

The double peaks shown on these stress and strain time history plots are the result of the double peaked load pulse of the Dynatest FWD. Other interesting behavior includes the effect of the layer profile and the modulus of the asphalt layers on the time history responses.

A comparison of the behavior of section 390112 for the 9/15/99 and 9/26/00 test dates shows that, although the AC modulus used for 9/15/99 was significantly higher than that used for 9/26/00, (refer back to Table 6.4) the lower ATB and PATB modulus used for 9/15/99 resulted in slightly higher stress applied to the subgrade, higher compressive strains at the top of the AC layer, and higher tensile strains at the bottom of the AC under the load plate. This result demonstrates the role played by the ATB and PATB in this section, where the 10.16cm (4") AC layer is much smaller than the 40.64cm (16") base (30.48cm or 12" ATB and 10.16cm or 4" PATB).

A comparison between the magnitudes of the deviator stress applied on the subgrade and the elastic modulus used does not reflect the relationship between deviator stress and resilient modulus obtained during laboratory testing. Again, this discrepancy can be explained by the fact that the elastic modulus used was based on resilient modulus testing of pavements at a loading rate that is slower than the rate of loading applied by the FWD (Farzaneh, 2001).

In order to gain more insight into the behavior of the pavement layers, it was found useful to generate two plots for each FWD test simulation:

1. Depth vs. maximum radial strain of the AC along the axis of symmetry. (Figures 6.25 and 6.27) This type of plot is intended to show the strain profile of the AC under the center of the load. The vertical position, or depth where the strain is specified is normalized by the AC layer thickness. The strain is plotted as Microstrain.
2. Maximum strain and deflection of the AC layer vs. distance from the axis of symmetry (Figures 6.26 and 6.28). The horizontal position of the strain and deflection measurements have been normalized by the radius of the FWD load plate, which is .15 m (6”) in radius. Both actual and calculated deflections have been plotted and the maximum radial strain is plotted in Microstrain.

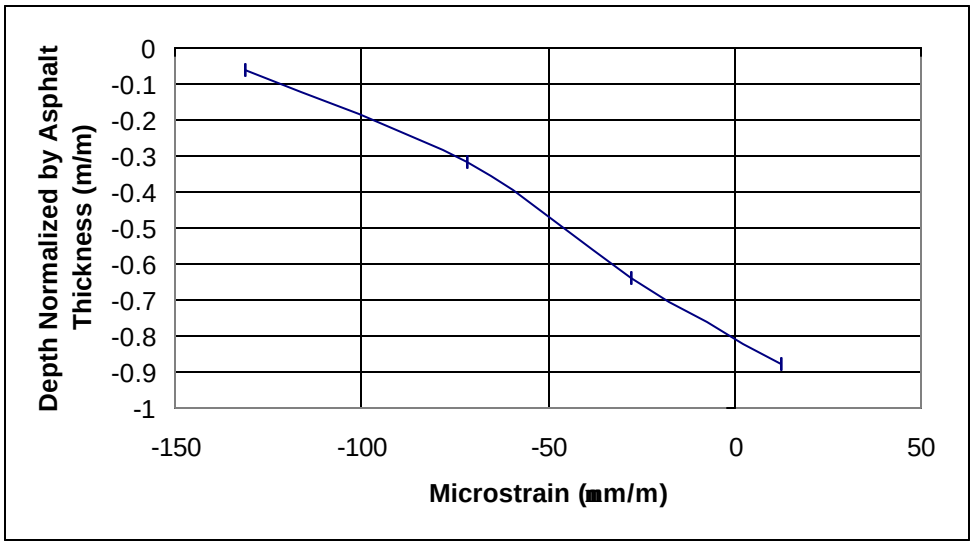

Figure 6.25. Maximum strain vs. depth along axis of symmetry Section 390112 9/15/99

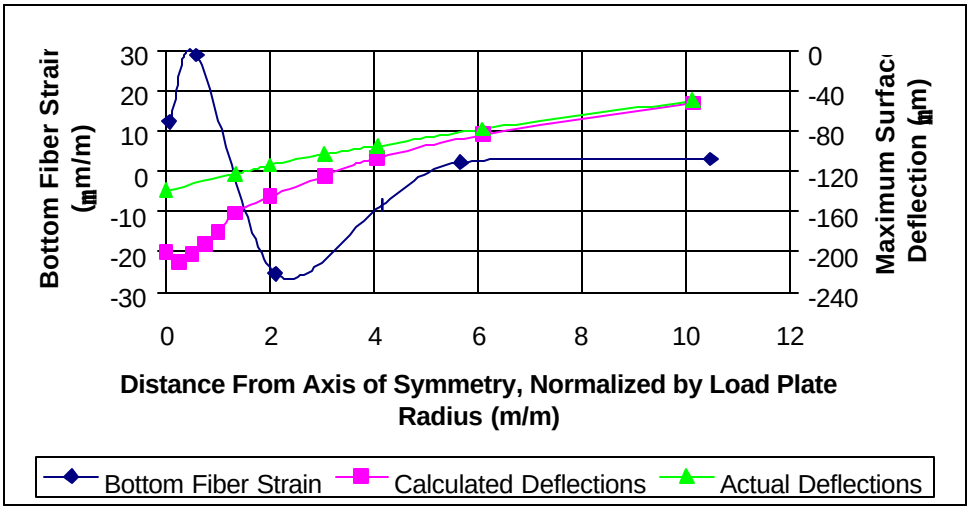

Figure 6.26. Maximum strain and deflection in asphalt layer Section 390112 9/15/99

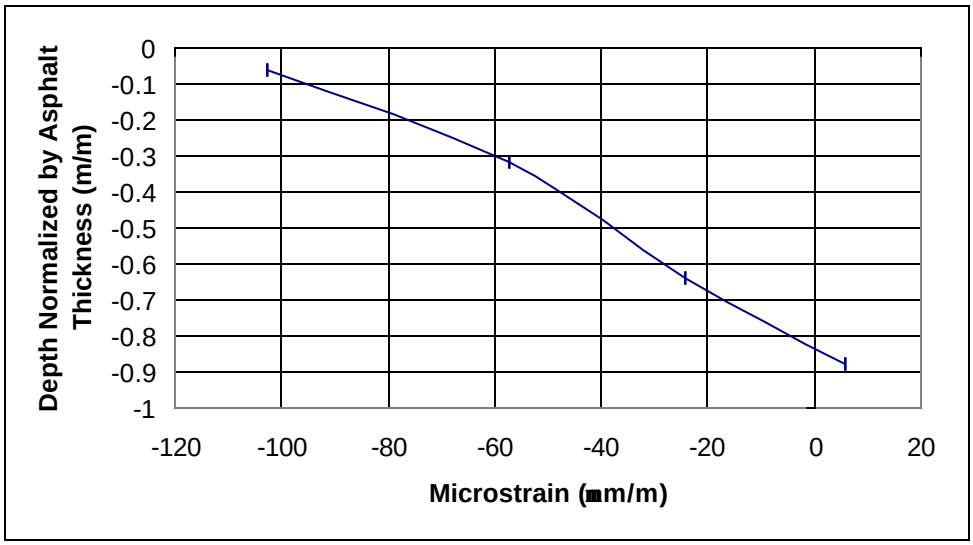

Figure 6.27. Maximum strain vs. depth along axis of symmetry Section 390112 9/26/00

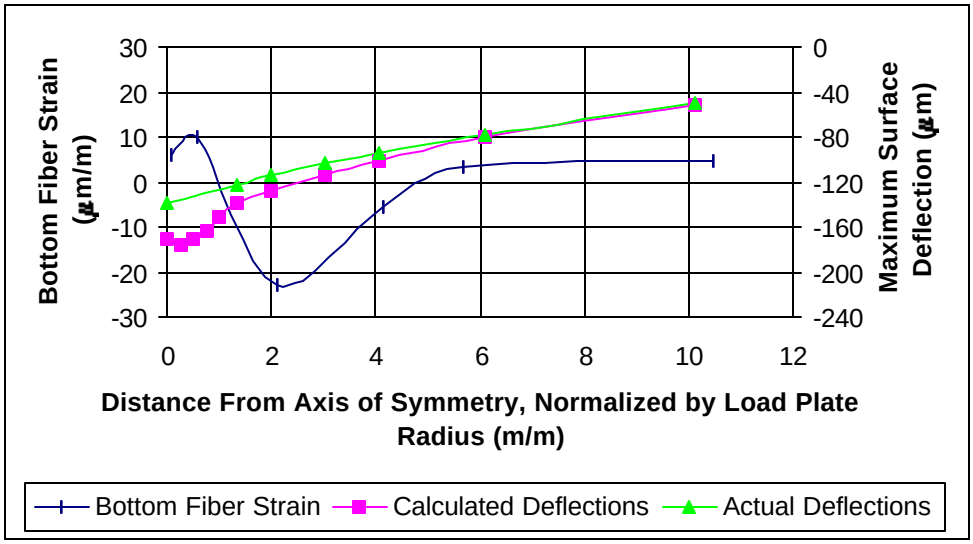

Figure 6.28. Maximum strain and deflection in asphalt layer Section 390112 9/26/00

The obvious difference between the behavior of the pavement section at the different test dates can be seen by comparing the plots of maximum strain along the axis of symmetry. A higher compressive strain is observed during the 9/15/99 test since the AC layer is stiffer than in the 9/26/00 test. Due to the thin configuration of the AC layer (10.16cm or 4") as compared to the thickness of the

ATB and PATB layers (ATB = 30.48cm or 12” and PATB = 10.16cm or 4”), the AC layer takes more compressive strain because the neutral axis of the pavement system has been shifted down towards the base materials. In fact, the neutral axis is very close to the bottom of the AC layer, implying that the base layers experience high tensile strains. The plots of the strain profile can prove very useful in modeling of multi layered pavement systems because they show the strain distribution between the AC and base layers. For the simulations presented here, it was assumed that the interaction between the layers was perfectly bonded. Analysis of actual field data may show less than perfectly bonded behavior that will have to be taken into account.

An interesting observation obtained from the plots of the strain along the length of the AC layer is the change in sign of the strain along this length. This can be attributed to the change of curvature of the AC layer, as demonstrated by the plot of the maximum surface deflection that is displayed along with the strain. Under and near the loading plate the asphalt concrete will have a positive curvature and tensile strains in the bottom fiber. The curvature quickly changes outside of the region of loading to negative curvature and compressive strains in the bottom layer.

6.4. Analysis with FWD-DYN

6.4.1. Overview

FWD-DYN is a linear dynamic analysis program especially written for the analysis and simulation of FWD testing on multi-layered pavement systems. FWD-DYN performs both a forward modeling and inversion of field data. Forward modeling involves inputting the structural profile and material properties of the multi-layered pavement system and calculating the response. Forward modeling is carried out using the transfer matrix and layer stiffness matrix method developed by Kausel (U. of Texas, 1994). Inversion involves predicting the material properties of the multi-layered pavement system based on the known structural profile and response to a FWD test. FWD-DYN accepts data directly from a Dynatest field data file. Inversion is carried out by one of three different methods chosen by the user: static inversion, in which the maximum field deflections are assumed to be from a statically applied load; pseudo-dynamic inversion, in which measured displacements are used to create experimental transfer functions to create a modified static deflection basin, which is then used to perform a static inversion as in the first option; and dynamic inversion, in which a full dynamic, iterative analysis is conducted.

Inversion of actual FWD test data was performed using FWD-DYN. The results were not realistic, especially the modulus of the AC layer which was excessively high. Better results were obtained in the forward modeling option, which will be presented in this chapter. The simulations conducted for the three sections of the Ohio Test Road in Plaxis were performed using FWD-DYN for

comparison purposes. The forward modeling part of FWD-DYN allows for structural and material properties of multi-layered pavements systems to be entered manually through interactive screen commands or through a batch file. Necessary parameters include: radius of load plate, bottom boundary condition (rigid or infinite half space), and number of layers. For each layer, layer thickness, modulus of elasticity, Poisson's ratio, unit weight, and damping are needed. FWD-DYN will compute maximum stresses and strains at four points in the structure, whose coordinates area also entered into the input.

Time histories of displacement are automatically calculated at 7 points along the AC pavement surface. These points are: 0 ft (0 m), 1ft (0.15 m), 2ft (0.31 m), 3 ft (0.61 m), 4 ft (0.91 m), 5 ft (1.22 m), 6 ft (1.52 m), and 7 ft (1.83 m). These distances are the same as those measured by the FWD used on the Ohio Test Road, with the exception that Ohio Test Road FWD tests include a measurement at 1.5 ft (0.2 m) and does not include a measurement at 7 ft (1.83 m). FWD-DYN produces three output files that include: transfer functions, peak displacements, peak stresses and strains (at the predefined points), and time history of displacements at the different receivers. It should be noted that FWD-DYN applies a normalized load pulse with a triangular shape and a maximum value of one. As a consequence of the normalized load pulse, all results produced must be multiplied by the maximum load from the field test (kN or lbs) for comparison with actual data. Figure 6.29 shows an actual FWD load pulse and an FWD-DYN load pulse multiplied by the maximum value of the actual load pulse. The idealized load pulse used by FWD-DYN is similar to actual load

pulses except in the loading portion of the pulse where the double peak characteristic of the Dynatest FWD is not replicated. Also, the FWD-DYN load pulse peaks slightly earlier than the actual load pulse.

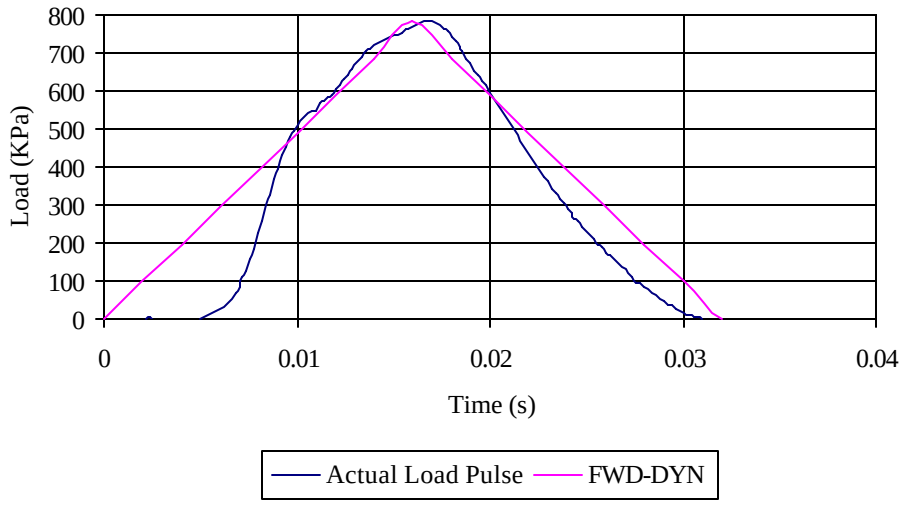

Figure 6.29. Actual load pulse and idealized load pulse used by FWD-DYN

A total of five models were created for analysis in FWD-DYN, each corresponding to the actual field test at station 0 for each year. Material properties were exactly the same as those used in the Plaxis models. Damping was not included since none was used in the Plaxis simulations. For each test simulation, FWD-DYN had to be run three times since the piece of software only allows for the calculation of stress/strain at a maximum of four points for each simulation.

6.4.2 FWD-DYN Results

Time history of displacement plots were created for each simulation to compare the performance of Plaxis with FWD-DYN. Since some of the positions where deflections are calculated by FWD-DYN are not the same as those measured in tests conducted at the Ohio Test Road, only deflections at common positions were compared.

It was clear that both FWD-DYN and Plaxis produced similar results. However, a few obvious differences were apparent in the results. The deflections calculated by FWD-DYN peak earlier and are greater in magnitude than those calculated by Plaxis. The difference in peak time is a result of the load pulse peaking earlier than FWD-DYN. The increased deflections may also stem from the use of the idealized load pulse, which has a slightly longer duration on the loading side of the pulse. It was found that a suitable comparison could only be made if the same load pulse was used for both software packages. When Plaxis was run using the idealized load pulse used in FWD-DYN, it corrected the difference in the peak time, but the magnitude of the maximum deflections only changed negligibly. It can therefore be concluded that analyses with FWD-DYN will result in slightly higher deflections than Plaxis.

Time histories of displacement are not shown for any stations and test dates because they exhibit similar results and have been excluded for brevity. Figures 6.30 and 6.31 given below show a comparison of the strain behavior of the bottom fiber of the AC layer for section 390112.

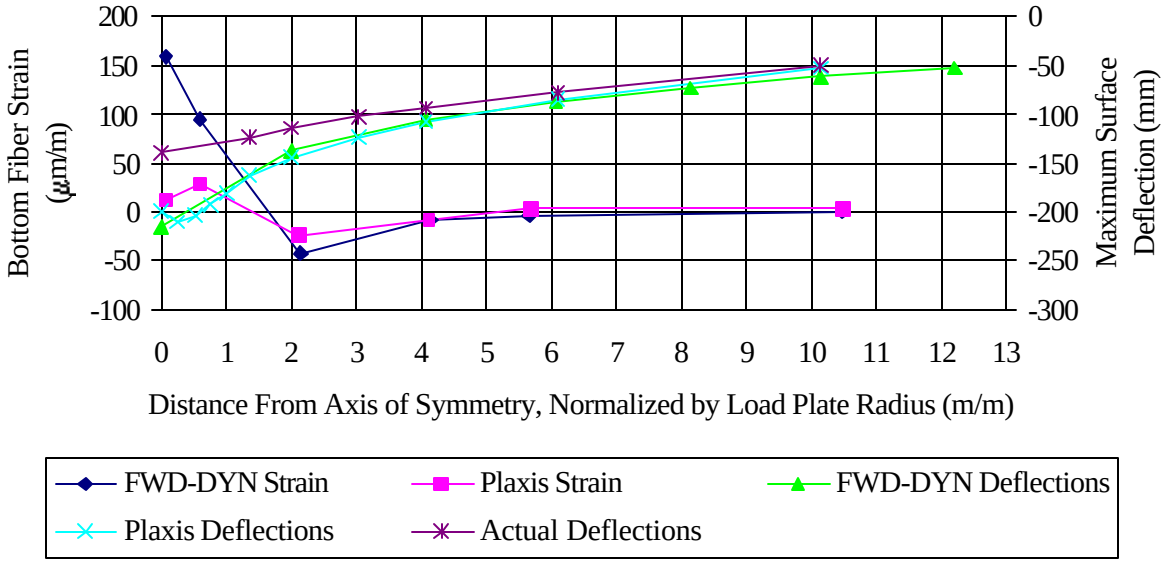

Figure 6.30. Maximum strain and displacements as computed by FWD-DYN and Plaxis Section 390112 9/15/99

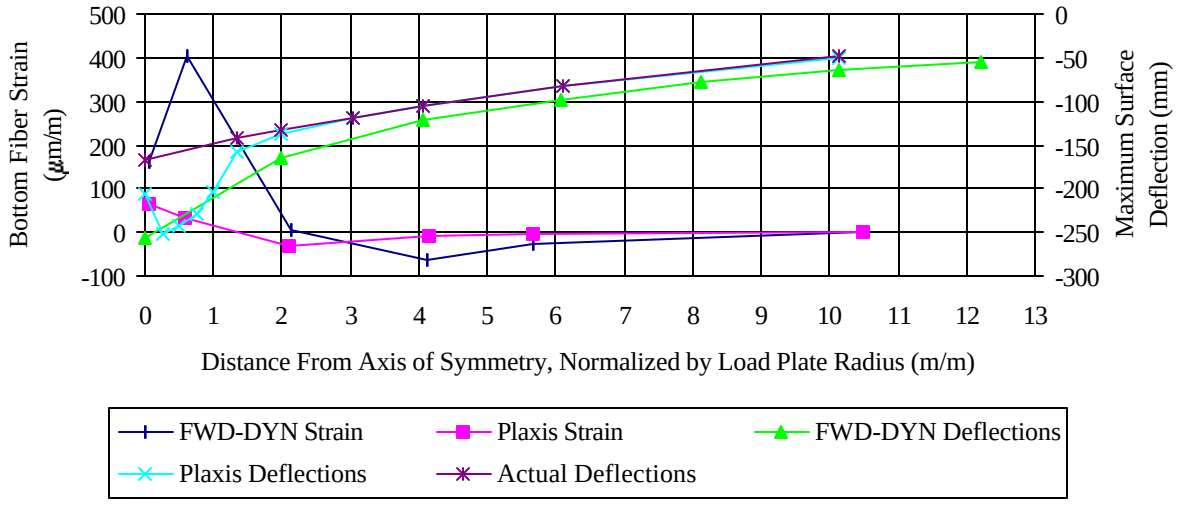

Figure 6.31. Maximum strain and displacement as computed by FWD-DYN and Plaxis Section 390112 9/26/00

6.4.3 Conclusions

The deflection bowls calculated by FWD-DYN are very similar to those calculated by Plaxis. The major difference between the two is that FWD-DYN produces deflections that are slightly higher in magnitude as compared with Plaxis, especially near the axis of symmetry. These larger deflections result in much higher strains near the axis of symmetry. This difference in calculated strain behavior is important in that the magnitudes of the strains are so different, and can lead to different mechanistic designs. Further with actual field data is required for validation of either computer code.

6.5 Comparison with ILLIPAVE Nomographs

6.5.1 Analysis

As previously described, nomographs based on a compilation of results from the static, non-linear finite element program, ILLIPAVE, were generated based on regressions relating deflection, load, AC thickness, base thickness, AC modulus, and subgrade modulus.

The regression equations, as well as the constants are shown in Table 6.6 (reproduced from Tables 5.2 and 5.3 in both the SI and English systems).

Table 6.6. ILLIPAVE regression equations and constants

$\log(d) = a_0 + a_1 \cdot t_{ac} + a_2 \cdot t_{base} + a_3 \cdot E_{ac} + a_4 \cdot E_{ri} + a_5 \cdot P$						
Units	**a_0**	**a_1**	**a_2**	**a_3**	**a_4**	**a_5**
SI	-0.43973	-0.0011948	-0.0011932	-4.6502E-05	-0.0021085	8.4059E-03
English	-1.84457	-0.03035	-0.03031	-3.2059E-04	-0.0145362	3.73961E-05

For the purposes of comparing this method with dynamic analysis, the above equations were solved for the resilient modulus of the subgrade. Table 6.7 shows the subgrade resilient modulus computed using the above equations and Plaxis. It is important to note that ILLIPAVE determines the subgrade modulus by iterating until the stress and modulus correspond to a point on an bilinear curve relating deviator stress and resilient modulus input into the program. The subgrade resilient modulus obtained from Plaxis was computed by running Plaxis and changing the resilient modulus until a match was found between the computed and actual displacement of the furthest sensor.

Table 6.7 Resilient modulus calculated by ILLIPAVE and Plaxis

Section	Year	ILLIPAVE Regress. Equations		Plaxis	
		Resilient Modulus		Resilient Modulus	
		MPa	ksi	MPa	ksi
390112	1999	87.14	12.64	180.0	26.1
390112	2000	133.41	19.36	180.0	26.1

6.5.2. Conclusions

Resilient moduli calculated by ILLIPAVE regression equations are consistently lower than those found using Plaxis. This can be attributed, again, to the difference in loading rates between the repeated load material testing and the computer simulation by Plaxis. The bilinear models used as input in ILLIPAVE

are based on testing with a 0.1 second load duration, while the Plaxis simulation was conducted using a load with of a shorter duration.

THIS PAGE LEFT INTENTIONALLY BLANK

Chapter 7

CONCLUSIONS AND RECOMMENDATIONS

Flexible and rigid pavement sections were monitored at the Ohio Test Road as part of the FHWA Strategic Highway Research Program (SHRP). A general weather station and seasonal instrumentation including Time Domain Reflectometry (TDR) probes, MRC thermistors and resistivity probes are installed at each of the instrumented pavement sections to study the climatic agents affecting pavement life.

Laboratory tests characterized the temperature dependency of the resilient modulus of the ATB and the PATB. Further comparisons between MRC sensors and weather data led to a useful air vs. AC temperature relationship. A methodology introduced in a previous study by Figueroa et al. (1994), was used to develop relationships between the air temperature and the resilient modulus for all three bituminous materials: AC, ATB and PATB.

All test data, including moisture content, pavement and soil temperature and resistivity, as well as weather-related parameters collected at all instrumented sections at the test road was processed and subjected to quality control, to be uploaded into national databases.

Problems with Topp's universal equation for volumetric moisture content determination from TDR readings were found. Laboratory experiments were proposed and performed and a three-dimensional calibration equation was developed. Calibration coefficients for Klemunes' mixing model for volumetric moisture content estimation were also established. Both procedures are

recommended to determine the volumetric moisture content of subgrade soils at the Ohio Test Road.

Resilient modulus tests were performed and a relationship between the degree of saturation (S_r) and the resilient modulus at the break point (E_{ri}) was established for the embankment soil prevalent at the road site. TDR readings were used in combination with the developed TDR calibration procedures to study the monthly and seasonal variation of the degree of saturation at four of the test sections. Generally, ranges of the degree of saturation between 85 and 100 percent were recorded. The highest saturation was found in the summer and the lowest in the winter. Both spring and fall periods showed intermediate saturation values.

A lag of 80 to 85 days between the increase in degree of saturation within the subgrade soil with respect to increased precipitation was identified at the Ohio Test Road site.

Among the analyzed sections, sections 390212 and 390901 were built with lateral drains, while sections 390203 and 390205 were built without drainage. The examination of figures of degree of saturation vs. depth for each section does not show any significant influence in reducing the degree of saturation in sections with drains.

Alternatively, seasonal variations of the resilient modulus at the break point at four of the instrumented sections were determined. These were calculated from the average degree of saturation for each section and the

relationship between the resilient modulus at the break point and the degree of saturation previously developed.

The significant correlation between solar radiation and air temperature was confirmed. Temperature differentials in a PCC slab were established and average values for the positive and negative slab temperature gradients were calculated as 0.543 ^{o}C/cm (1.38 ^{o}C/in), and -0.279 ^{o}C/cm (-0.71 ^{o}C/in) respectively. Typical hours of the day for the positive and negative slab temperature gradients and no temperature differentials were obtained. The positive gradient occurred around 3 p.m., the negative gradient at 7 a.m. and 12 a.m., while the minimum temperature differential during the summer occurred around 11 a.m. and 10 p.m.

A direct procedure to estimate the frost penetration of a soil was developed and evaluated with the results obtained from temperature sensors installed at four of the test sections for three freezing seasons (1996-1999). This method is strongly recommended for frost penetration prediction, given the high degree of accuracy obtained.

With the thorough stiffness characterization of pavement materials used at the Ohio Test Road, easy to apply back calculation procedures based on finite elements analyses were developed for both flexible and rigid pavements. Using the moisture content and the air temperature variation, measured at the test road, finite elements analyses with ILLIPAVE were conducted and followed by statistical analyses to develop back calculation regression equations applicable to flexible pavements. Nomographs for all pavement profiles built at the test road

were configured based on the regression equations to back calculate the resilient modulus at the break point from the maximum FWD deflection. For rigid pavements, the finite elements code: ILLISLAB was used as the basis to develop a back calculation program. Convergence was readily achieved and a similar statistical analysis as in the flexible pavement case was implemented to develop a regression equation and a nomograph. These are applicable to any three-layer rigid pavement system (PCC-Base-Subgrade) with slab dimensions of 3.65x4.57 m (12x15 feet), to back calculate the modulus of subgrade reaction from the maximum FWD deflection measured at mid slab.

Displacement time histories measured by the FWD were evaluated, along with two dynamic pavement analysis programs. The finite elements code, Plaxis, was used to model FWD tests conducted at flexible pavement section 390112 of the test road. Data input consisted of the known pavement profile and asphaltic material stiffness inferred from thermistor readings collected at the time of FWD testing. Subgrade modulus was varied until a close match was obtained between the calculated and actual displacement of the sensor farthest from the point of impact. Simulations were conducted on tests conducted at the beginning, middle, and end of the section in both the center of the lane and the right wheel path. Comparisons of time history of displacement plots of both actual and simulated data showed that Plaxis over estimated deflections at and near the point of loading. It was concluded that resilient modulus testing of asphaltic concrete and base materials needs to be conducted at load rates matching those of the FWD

test, given the fact that the resilient modulus of viscoelastic materials is dependent on the rate of loading.

Time histories of subgrade stress and strain along the axis of symmetry and along the bottom of the asphalt layer were computed. Although some test sections at the Ohio Test Road are equipped with structural instrumentation, and FWD testing is conducted at points of structural instrumentation, data is not yet available for comparison purposes. It is inferred, however, that Plaxis will also over estimate stresses and strains as a result of overestimation of displacements.

A second computer code: FWD-DYN, was also used to simulate FWD test results. For comparison purposes, the same pavement section and properties used in Plaxis as input for FWD-DYN. FWD-DYN calculations resulted in displacements that were slightly higher than Plaxis calculations, and therefore higher strains.

As a final evaluation of dynamic analysis methods, subgrade moduli calculated by Plaxis were compared to those obtained from ILLIPAVE- based back calculation nomographs. The nomographs yielded lower subgrade moduli than Plaxis and they also varied more between stations, due to the bilinear stress-dependent resilient modulus model implicit in these nomographs.

THIS PAGE LEFT INTENTIONALLY BLANK

APPENDIX A

RW. BAS Program

RW.BAS Program

```
10 PRINT:PRINT:INPUT " ONS file to be modified ";ALTT1$
20 PRINT:PRINT:INPUT "ONS file to store modified DATA ";ALTT3$
30 OPEN ALTT1$ FOR INPUT AS #1
40 OPEN ALTT3$ FOR OUTPUT AS #3
42 OPEN "Y1996" FOR INPUT AS #2
45 WOPEN=0
46 MAXTEMP=-50
47 MINTEMP=50
50 INPUT #1,A$
52 NN=VAL(A$)
55 IF NN=1 THEN 100
60 IF NN=2 THEN 200
65 IF NN=3 THEN 300
70 IF NN=4 THEN 400
75 IF NN=5 THEN 500
80 IF NN=6 THEN 600
85 IF NN=7 THEN 700
90 PRINT "CHECK FIRST LINE ON ORIGINAL DATA FILE"
92 PRINT " DAY ",C$," HOUR ",D$
95 GOTO 50
100 INPUT #1,B$,C$,D$,E$,F$,G$,H$,I$,J$,K$,L$,M$,N$,O$,P$
110 GOSUB 1000
120 L$=TIMAX$
125 N$=TIMIN$
185 PRINT #3,A$;",";B$;",";C$;",";D$;",";E$;",";F$;",";G$;",";H$;","
;I$;",";J$;",";K$;",";L$;",";M$;",";N$;",";O$;",";P$
186 MAXTEMP=-50
187 MINTEMP=50
190 GOTO 50
200 INPUT #1,B$,C$,D$,E$,F$,G$,H$,I$,J$,K$,L$,M$,N$,O$,P$,Q$,R$,S$,T$
,U$,V$
210 PRINT #3,A$;",";B$;",";C$;",";D$;",";E$;",";F$;",";G$;",";H$;","
;I$;",";J$;",";K$;",";L$;",";M$;",";N$;",";O$;",";P$;",";Q$;",";R$
;",";S$;",";T$;",";U$;",";V$
290 GOTO 50
300 INPUT #1,B$,C$,D$,E$,F$,G$,H$,I$,J$,K$,L$,M$,N$,O$,P$,Q$,R$,S$
,T$,U$,V$,W$,X$,Y$,Z$,A1$,B1$,C1$,D1$,E1$,F1$,G1$,H1$,I1$,J1$,K1$
,L1$,M1$,N1$
310 PRINT #3,A$;",";B$;",";C$;",";D$;",";E$;",";F$;",";G$;",";H$;","
;I$;",";J$;",";K$;",";L$;",";M$;",";N$;",";O$;",";P$;",";Q$;",";R$
;",";S$;",";T$;",";U$;",";V$;",";W$;",";X$;",";Y$;",";Z$;",";A1$;","
;B1$",";C1$;",";D1$;",";E1$;",";F1$;",";G1$;",";
320 PRINT #3,H1$;",";I1$;",";J1$;",";K1$;",";L1$;",";M1$;",";N1$
390 GOTO 50
400 INPUT #1,B$,C$,D$,E$,F$,G$,H$,I$,J$,K$,L$,M$,N$,O$,P$,Q$,R$,S$
,T$,U$,V$,W$,X$,Y$,Z$,A1$,B1$,C1$,D1$,E1$,F1$,G1$,H1$,I1$,J1$,K1$
,L1$,M1$,N1$
410 PRINT #3,A$;",";B$;",";C$;",";D$;",";E$;",";F$;",";G$;",";H$;","
;I$;",";J$;",";K$;",";L$;",";M$;",";N$;",";O$;",";P$;",";Q$;",";R$
;",";S$;",";T$;",";U$;",";V$;",";W$;",";X$;",";Y$;",";Z$;",";A1$;","
;B1$",";C1$;",";D1$;",";E1$;",";F1$;",";G1$;",";
420 PRINT #3,H1$;",";I1$;",";J1$;",";K1$;",";L1$;",";M1$;",";N1$
490 GOTO 50
500 INPUT #1,B$,C5$,D5$,E5$,F5$,G5$
```

```
510 IF D5$="2400" GOTO 540
520 GOSUB 1000
530 GOTO 580
540 F5$=F524$
550 G5$=G524$
580 PRINT #3,A$;",";B$;",";C5$;",";D5$;",";E5$;",";F5$;",";G5$
590 GOTO 50
600 INPUT #1,B$,C$,D$,E$,F$,G$,H$,I$
610 PRINT #3,A$;",";B$;",";C$;",";D$;",";E$;",";F$;",";G$;",";H$
;",";I$
690 GOTO 50
700 INPUT #1,B$,C$,D$,E$,F$,G$,H$,I$,J$,K$,L$,M$,N$,O$,P$,Q$,R$,S$
,T$,U$,V$,W$,X$,Y$,Z$,A1$,B1$,C1$,D1$,E1$,F1$,G1$,H1$,I1$,J1$,K1$
,L1$,M1$
710 PRINT #3,A$;",";B$;",";C$;",";D$;",";E$;",";F$;",";G$;",";H$;","
;I$;",";J$;",";K$;",";L$;",";M$;",";N$;",";O$;",";P$;",";Q$;",";R$
;",";S$;",";T$;",";U$;",";V$;",";W$;",";X$;",";Y$;",";Z$;",";A1$;","
;B1$",";C1$;",";D1$;",";E1$;",";F1$;",";G1$;",";H1$;
720 PRINT #3,",";I1$;",";J1$;",";K1$;",";L1$;",";M1$
790 GOTO 50
1000 REM SUBROUTINE TO PICK WEATHER DATA
1020 IF B$="1996" GOTO 1120
1025 IF B$="1997" GOTO 1130
1030 IF B$="1998" GOTO 1140
1035 IF B$="1999" GOTO 1150
1040 IF B$="2000" GOTO 1160
1045 IF B$="2001" GOTO 1170
1050 IF B$="2002" GOTO 1180
1055 IF B$="2003" GOTO 1190
1120 IF WOPEN=96 THEN 1200
1121 CLOSE #2
1122 OPEN "Y1996" FOR INPUT AS #2
1124 WOPEN=96
1125 GOTO 1200
1130 IF WOPEN=97 THEN 1200
1131 CLOSE #2
1132 OPEN "Y1997" FOR INPUT AS #2
1134 WOPEN=97
1135 GOTO 1200
1140 IF WOPEN=98 THEN 1200
1141 CLOSE #2
1142 OPEN "Y1998" FOR INPUT AS #2
1144 WOPEN=98
1145 GOTO 1200
1150 IF WOPEN=99 THEN 1200
1151 CLOSE #2
1152 OPEN "Y1999" FOR INPUT AS #2
1154 WOPEN=99
1155 GOTO 1200
1160 IF WOPEN=2000 THEN 1200
1161 CLOSE #2
1162 OPEN "Y2000" FOR INPUT AS #2
1164 WOPEN=2000
1165 GOTO 1200
1170 IF WOPEN=2001 THEN 1200
1171 CLOSE #2
1172 OPEN "Y2001" FOR INPUT AS #2
```

```
1174 WOPEN=2001
1175 GOTO 1200
1180 IF WOPEN=2002 THEN 1200
1181 CLOSE #2
1182 OPEN "Y2002" FOR INPUT AS #2
1184 WOPEN=2002
1185 GOTO 1200
1190 IF WOPEN=2003 THEN 1200
1191 CLOSE #2
1192 OPEN "Y2003" FOR INPUT AS #2
1194 WOPEN=2003
1195 GOTO 1200
1200 INPUT #2,WA$
1210 WN=VAL(WA$)
1220 IF WN=111 THEN 1300
1230 IF WN=222 THEN 1500
1240 IF WN=444 THEN 1700
1250 GOTO 1200
1300 INPUT #2,YR$,DA$,TI$,AVA$,MXA$,MNA$,MXH$,MNH$,SR$,MWS$,MWD$
,MXWS$,TMXWS$,DMXWS$,TPRE$
1310 IF DA$=C5$ GOTO 1340
1320 GOTO 1200
1340 IF TI$="2400" GOTO 1344
1342 GOTO 1349
1344 F524$=AVA$
1345 G524$=TPRE$
1346 IF VAL(MXA$)>MAXTEMP THEN TIMAX$=TI$ : IF VAL(MXA$)>MAXTEMP THEN
MAXTEMP=VAL(MXA$)
1347 IF VAL(MNA$)<MINTEMP THEN TIMIN$=TI$ : IF VAL(MNA$)<MINTEMP THEN
MINTEMP=VAL(MNA$)
1348 GOTO 1200
1349 IF TI$=D5$ GOTO 1360
1350 GOTO 1200
1360 F5$=AVA$
1370 G5$=TPRE$
1372 IF VAL(MXA$)>MAXTEMP THEN TIMAX$=TI$ : IF VAL(MXA$)>MAXTEMP THEN
MAXTEMP=VAL(MXA$)
1374 IF VAL(MNA$)<MINTEMP THEN TIMIN$=TI$ : IF VAL(MNA$)<MINTEMP THEN
MINTEMP=VAL(MNA$)
1380 GOTO 1800
1500 INPUT #2,WWB$,JULIAN$,WWD$,AVAIR$,MAXAIR$,MINAIR$,WWH$,WWI$
,WWJ$,WWK$,WWL$,WWM$,WWN$,WWO$,PRECIP$,WWQ$,WWR$
1520 IF JULIAN$=C$ GOTO 1550
1530 GOTO 1200
1550 J$=AVAIR$
1560 K$=MAXAIR$
1570 M$=MINAIR$
1580 O$=PRECIP$
1690 GOTO 1800
1700 INPUT #2,WWWB$,WWWC$,WWWD$,WWWE$
1790 GOTO 1200
1800 REM  ---------------CLOSE#2
1810 REM   ----------------WOPEN=0
1900 RETURN
1910 CLOSE #1
1920 CLOSE #3
2000 END
```

APPENDIX B
COLLECTED FILES SUMMARY

APPENDIX B1

ONS FILES SUMMARY

TABLE B1. ONS FILES SUMMARY **Section 390204 UT** **Page 1**

NEW FILE	OLD FILE	FROM				TO			
		D.Type	YEAR	DAY	HOUR	D.Type	YEAR	DAY	HOUR
39SB96AB	39SB96AB	7	1996	43	1234	6	1996	44	1100
BH	BH	7	“	193	1622	6	“	214	1100
CJ	CJ	7	“	209	100	6	“	290	1600
Gap DL	DL	5	“	325	1400	6	“	353	1400
Gap 97AB	97BB	7	“	362	100	6	1997	50	1200
BC	CC	5	1997	50	1300	6	“	71	1600
CC	DC	5	“	71	1700	6	“	85	1600
DD	ED	5	“	85	1700	6	“	100	1300
ED	FD	5	“	100	1400	6	“	114	900
FE	GE	5	“	114	1000	6	“	142	1100
GF	HF	5	“	142	1200	6	“	170	1300
HH	JH	5	“	170	1400	6	“	218	1500
Gap IJ	LJ	3	“	241	2400	6	“	296	1000
JK	MK	5	“	296	1100	6	“	324	1000
KL	NL	5	“	324	1100	6	“	351	2400
98AA	98AA	5	“	351	1900	6	1998	20	1100
Not needed	BB	7	1998	41	1200	6	“	45	1100
Gap BC	CC	7	“	42	100	6	“	71	1000
CD	DD	5	“	71	1100	6	“	114	1300
DE	EE	5	“	79	2300	6	“	134	800
Gap EG	EG	2	“	137	2400	6	“	192	1100
Delete	FG	2	“	137	2400	6	“	192	1100
FI	GI	5	“	192	1200	6	“	272	900
Gap GJ	HJ	5	“	273	1700	6	“	288	1100
Gap HK	IK	7	“	325	100	6	“	327	800
Gap IL	KL	7	“	329	100	6	“	349	1200
Gap 99AA	99AA	5	“	356	1000	6	1999	26	1100
BB	BB	5	1999	26	1200	6	“	42	1300
CC	CC	5	“	42	1400	6	“	71	1200

TABLE B1. ONS FILES SUMMARY **Section 390204 UT** **Page 2**

NEW FILE	OLD FILE	FROM				TO			
		D.Type	YEAR	DAY	HOUR	D.Type	YEAR	DAY	HOUR
39SB99DD	39SB99DD	5	1999	71	1300	6	1999	112	1100
EE	EE	5	“	112	1200	6	“	140	1200
FF	FF	5	“	140	1300	6	“	169	1100
GG	GG	5	“	169	1200	6	“	201	1100
HH	HH	5	“	201	1200	6	“	223	1200
II	II	5	“	223	1300	6	“	259	900
JJ	JJ	5	“	259	1000	6	“	287	1100
KK	KK	5	“	287	1200	6	“	316	1200
LL	LL	5	“	316	1300	6	“	356	1200
00AA	00AA	5	“	356	1100	6	2000	17	1000
Little BB	Not usedBB	7	2000	46	1059	6	“	46	1100
Not needed	DC	5	“	67	1100	6	“	83	1100
Not needed	ED	5	“	83	1200	6	“	97	1000
CD	FD	7	“	67	1100	6	“	116	1100
Gap DE	GE	5	“	116	1300	6	“	146	1100
EG	HG	5	“	146	1100	6	“	200	800
Nothing	II								
1 hr FK	Not used JK	7	“	316	1351	6	“	316	1400
GL	KL	5	“	316	1500	6	“	351	1300
01AA	01AA	5	“	351	1300	6	2001	13	1100
BB	BB	5	2001	12	1200	6	“	44	1100
CC	CC	5	“	44	1200	6	“	67	1100
DD	DD	5	“	67	1200	6	“	95	1200
Gap EE	EE	5	“	95	1400	6	“	137	1100
FF	FF	5	“	137	1200	6	“	165	1000
GG	GG	5	“	165	1100	6	“	198	1100
HH	HH	5	“	198	1200	6	“	221	1000
II	II	5	“	221	1100	6	“	254	1400
JJ	LJ	5	“	254	1500	6	“	288	1100

TABLE B1. ONS FILES SUMMARY **Section 390204 UT** **Page 3**

NEW FILE	OLD FILE	FROM				TO			
		D.Type	YEAR	DAY	HOUR	D.Type	YEAR	DAY	HOUR
39SB01KK	39SB01MK	5	2001	288	1200	6	2001	316	1300
NL	LL	5	"	316	1300	6	2002	354	1200
02AA	02AA	5	"	354	1300	6	"	10	1200
BB	BB	5	2002	10	1300	6	"	39	900
CC	CC	5	"	39	1000	6	"	67	1300
DD	DD	5	"	67	1400	6	"	108	800
Gap EE	EE	7	"	108	1004	6	"	135	1000
FF	FF	5	"	135	1100	6	"	168	1300
Gap GL	NL	7	"	338	1013	6	"	351	1300
03AA	03AA	5	"	351	1400	6	2003	18	1100
						6			
						6			
						6			
						6			
						6			
						6			
						6			
						6			
						6			
						6			
						6			
						6			
						6			
						6			
						6			
						6			
						6			
						6			
						6			

TABLE B2. ONS FILES SUMMARY Section 390212 CWRU Page 1

NEW FILE	OLD FILE	FROM				TO			
		D.Type	YEAR	DAY	HOUR	D.Type	YEAR	DAY	HOUR
39SC96AH	39SC96AH	7	1996	164	100	6	1996	228	1300
BI	BI	6	“	208	2400	6	“	263	1600
CJ	CJ	5	“	234	2400	6	“	289	1600
DK	DK	5	“	289	1700	6	“	324	1500
EL	EL	5	“	324	1600	6	“	355	2400
97AA	97AA	5	“	356	100	6	1997	16	1200
Noneed BB	BB	3	“	358	2400	6	“	47	1300
CC	CC	3	1997	16	1300	6	“	70	1300
Noneed DC	DC	5	“	28	100	6	“	70	1200
ED	ED	5	“	70	1300	6	“	99	1300
FD	FD	5	“	82	1600	6	“	115	1500
Noneed GE	GE	5	“	115	1600	6	“	143	900
HF	HF	3	“	112	2400	6	“	167	1200
JH	JH	3	“	162	2400	6	“	217	1300
KI	KI	3	“	197	2400	6	“	252	1300
LJ	LJ	5	“	252	1400	6	“	289	1100
MK	MK	5	“	289	1200	6	“	324	1200
NL	NL	5	“	324	1300	6	“	349	2400
98AA	98AA	5	“	350	100	6	1998	22	1100
BB	BB	5	1998	22	1200	6	“	55	1200
CC	CC	5	“	55	1300	6	“	85	1000
DD	DD	5	“	85	1100	6	“	107	1500
EE	EE	5	“	107	1600	6	“	140	1100
FF	FF	5	“	140	1400	6	“	169	1300
GG	GG	5	“	169	1400	6	“	202	1000
Gap HH	HH	7	“	203	100	6	“	231	1600
II	II	5	“	231	1700	6	“	260	1200
JJ	JJ	5	“	260	1300	6	“	293	1000
KK	KK	3	“	268	2400	6	“	323	1200

TABLE B2. ONS FILES SUMMARY Section 390212 CWRU Page 2

NEW FILE	OLD FILE	FROM				TO			
		D.Type	YEAR	DAY	HOUR	D.Type	YEAR	DAY	HOUR
39SC98LL	39SC98LL	5	1998	323	1300	6	1998	349	2400
99AA	99AA	5	"	350	100	6	1999	21	1400
BB	BB	5	1999	21	1500	6	"	47	1500
CC	CC	4	"	24	2400	6	"	79	1400
DD	DD	5	"	79	1500	6	"	112	1500
EE	EE	5	"	112	1600	6	"	139	1300
FF	FF	5	"	139	1400	6	"	166	1400
GG	GG	5	"	166	1500	6	"	196	1500
HH	HH	5	"	196	1600	6	"	236	1800
Noneed II	II	5	"	236	1900	6	"	259	1300
JJ	JJ	5	"	229	2400	6	"	284	1800
KK	KK	5	"	284	1900	6	"	322	1200
LL	LL	4	"	287	2400	6	"	342	2400
00AA	00AA	5	"	343	100	6	2000	13	1300
BB	BB	5	2000	13	1400	6	"	52	1600
CC	CC	5	"	52	1700	6	"	83	1200
DD	DD	5	"	83	1300	6	"	111	1600
EE	EE	5	"	111	1700	6	"	143	1300
FF	FF	5	"	143	1400	6	"	171	1500
GG	GG	5	"	171	1600	6	"	203	1000
HH	HH	5	"	203	1100	6	"	229	1100
II	II	7	"	229	100	6	"	262	1600
JJ	JJ	5	"	262	1700	6	"	291	1200
KK	KK	5	"	291	1300	6	"	316	1600
LL	LL	5	"	316	1700	6	"	344	2400
01AA	01AA	5	"	345	100	6	2001	11	1200
BB	BB	7	2001	10	100	6	"	44	1300
CC	CC	5	"	44	1400	6	"	79	1100
DD	DD	5	"	79	1200	6	"	109	900

TABLE B2. ONS FILES SUMMARY Section 390212 CWRU Page 3

NEW FILE	OLD FILE	FROM				TO			
		D.Type	YEAR	DAY	HOUR	D.Type	YEAR	DAY	HOUR
39SC01EE	39SC01EE	5	2001	109	1000	6	2001	137	1200
FF	FF	5	“	137	1300	6	“	171	300
Gap GH	GH	7	“	200	1200	6	“	225	1900
Gap HI	HI	7	“	227	1400	6	“	256	1700
IJ	IJ	5	“	256	1800	6	“	284	1100
JK	JK	5	“	284	1200	6	“	319	1200
KL	KL	5	“	319	1300	6	“	353	2400
02AA	02AA	5	“	354	100	6	2002	22	1700
BB	BB	5	2002	22	1800	6	“	53	1800
CC	CC	5	“	53	1900	6	“	81	1600
DD	DD	5	“	81	1700	6	“	115	1400
EE	EE	5	“	115	1500	6	“	136	1100
FF	FF	5	“	136	1200	6	“	162	1100
GG	GG	5	“	162	1200	6	“	187	2400
Gap HH	HH	5	“	198	1130	6	“	217	1100
Gap II	II	5	“	232	1144	6	“	262	1700
JJ	JJ	5	“	262	1800	6	“	297	1800
KK	KK	5	“	297	1900	6	“	324	1900
LL	LL	5	“	324	2000	6	“	351	2400
03AA	03AA	5	“	352	100	6	2003	17	1400
						6			
						6			
						6			
						6			
						6			
						6			
						6			
						6			
						6			

TABLE B3. ONS FILES SUMMARY **Section 390202 UT** **Page 1**

NEW FILE	OLD FILE	FROM				TO			
		D.Type	YEAR	DAY	HOUR	D.Type	YEAR	DAY	HOUR
39SD96AH	39SD96AH	7	1996	193	1655	6	1996	241	1000
BI	BI	7	“	209	1000	6	“	263	1900
CJ	CJ	5	“	263	2000	6	“	290	1500
DK	DK	5	“	290	1600	6	“	325	1500
EL	EL	5	“	325	1600	6	“	353	1500
97CC	97CC	wrong	date						
DC	DC	wrong	date						
Gap AD	ED	7	1997	86	100	6	1997	100	1300
BD	FD	5	“	100	1400	6	”	114	900
CE	GE	5	“	114	1000	6	“	142	1100
DF	HF	5	“	142	1200	6	“	170	1000
EH	JH	5	“	170	1100	6	“	218	1400
Gap FJ	LJ	7	“	254	1234	6	“	296	1000
GK	MK	5	“	296	1100	6	“	324	1100
HL	NL	5	“	324	1200	6	“	351	2400
98AA	98AA	5	”	352	100	6	1998	20	1100
BB	BB	5	1998	20	1200	6	”	45	1200
CC	CC	5	“	45	1300	6	“	71	1300
DD	DD	4	“	59	2400	6	“	114	1500
EE	EE	2	“	79	2400	6	“	134	900
Bad sensors	EH	7	“	192	1333	6	“	224	1200
Bad sensors	FH	7	“	192	1333	6	“	224	1200
Bad sensors	GI	5	“	224	1300	6	“	272	1000
Bad sensors	HJ	5	“	272	1100	6	“	288	1200
Bad sensors	IK	5	”	288	1300	6	“	327	1100
Bad sensors	JL	5	“	327	1200	6	“	349	1100
Bad sensors	99AA	5	”	349	1200	6	1999	26	1200
Bad sensors	BB	5	1999	26	1300	6	“	42	1300
Bad sensors	CC	5	“	42	1400	6	”	71	1300

TABLE B3. ONS FILES SUMMARY **Section 390202 UT** **Page 2**

NEW FILE	OLD FILE	FROM				TO			
		D.Type	YEAR	DAY	HOUR	D.Type	YEAR	DAY	HOUR
Bad sensors	39SD99DD	7	1999	71	1350	6	1999	112	1200
Bad sensors	EE	5	“	112	1400	6	“	140	1300
Bad sensors	GG	3	“	146	2400	6	“	201	1200
Bad sensors	HH	6	“	201	1300	6	“	223	1200
Bad sensors	II	5	“	259	1100	7	“	359	1100
Bad sensors	JJ	5	”	259	1200	6	”	287	1200
Bad sensors	KK	5	“	287	1300	6	“	316	1200
Bad sensors	LL	5	”	316	1200	6	“	356	1100
Bad sensors	00AA	3	“	327	2400	6	2000	17	1100
Bad sensors	BB	5	2000	17	1200	6	“	46	1100
Bad sensors	CC	5	“	46	1200	6	“	67	900
Bad sensors	DC	5	“	67	1100	6	“	83	1100
Bad sensors	FD	5	“	83	1200	6	”	116	1100
Bad sensors	GE	7	”	116	1312	6	“	146	1200
Bad sensors	HF	5	“	146	1200	6	”	168	1100
Bad sensors	IG	5	”	168	1200	6	“	201	1100
Bad sensors	JH	5	“	201	1200	6	“	223	1100
Bad sensors	KI	5	“	223	1200	6	“	266	1200
Bad sensors	LJ	5	“	267	1300	6	“	288	1400
Bad sensors	MK	4	“	260	2400	6	”	316	1400
Bad sensors	NL	5	”	316	1500	6	”	351	1400
Bad sensors	01AA	5		351	1500	6	2001	13	1200
Bad sensors	BB	5	2001	13	-1300	6	“	45	1200
nothing	02BB	-	-	-	-	-	-	-	-

TABLE B4. ONS FILES SUMMARY Section 390205 CWRU Page 1

NEW FILE	OLD FILE	FROM				TO			
		D.Type	YEAR	DAY	HOUR	D.Type	YEAR	DAY	HOUR
39SE96AH	39SE96AH	5	1996	164	100	6	1996	228	1200
BI	BI	5	"	228	1300	6	"	263	1500
CJ	CJ	5	"	234	2400	6	"	289	1600
DK	DK	5	"	289	1700	6	"	324	1600
EL	EL	5	"	324	1700	6	"	356	2400
97AA	97AA	5	"	357	100	6	1997	16	1400
BB	BB	4	"	358	2400	6	"	47	1400
CC	CC	3	1997	15	2400	6	"	70	1200
No need DC	DC	5	"	70	1200	6	"	82	1600
ED	ED	5	"	70	1200	6	"	99	1200
FD	FD	5	"	82	1700	6	"	115	1400
No need GE	GE	6	"	88	2200	6	"	143	900
HF	HF	2	"	113	2400	6	"	168	1100
Gap IH	IH	5	"	205	1100	6	"	217	2400
JI	JI	5	"	217	1500	6	"	252	1500
KJ	KJ	5	"	252	1600	6	"	289	1200
LK	LK	4	"	263	2400	6	"	318	1400
ML	ML	4	"	294	2400	6	"	349	2400
98AA	98AA	5	"	350	100	6	1998	22	1200
BB	BB	5	1998	22	1300	6	"	55	1400
CC	CC	5	"	55	1500	6	"	85	1200
No need DD	DD	5	"	85	1300	6	"	107	1600
EE	EE	3	"	85	2400	6	"	140	1300
Gap FH	FH	5	"	211	1100	6	"	231	1700
GI	GI	5	"	231	1800	6	"	260	1200
HJ	HJ	5	"	260	1300	6	"	293	1000
IK	IK	3	"	268	2400	6	"	323	1300
JL	JL	5	"	323	1400	6	"	349	2400
99AA	99AA	5	"	350	100	6	1999	21	1500

TABLE B4. ONS FILES SUMMARY Section 390205 CWRU Page 2

NEW FILE	OLD FILE	FROM				TO			
		D.Type	YEAR	DAY	HOUR	D.Type	YEAR	DAY	HOUR
39SE99BB	39SE99BB	5	1999	21	1600	6	1999	47	1200
CC	CC	5	“	47	1300	6	“	79	1300
DD	DD	5	“	79	1400	6	“	112	1400
EE	EE	5	“	112	1500	6	“	139	1200
FF	FF	5	“	139	1300	6	“	166	1400
GG	GG	5	“	166	1500	6	“	196	1400
HH	HH	5	“	196	1500	6	“	236	1800
II	II	5	“	236	1900	6	“	259	1400
JJ	JJ	5	“	259	1500	6	“	284	1800
KK	KK	5	“	284	1900	6	“	322	1200
LL	LL	3	“	287	2400	6	“	342	2400
00AA	00AA	5	“	343	100	6	2000	13	1400
BB	BB	5	2000	13	1500	6	“	52	1700
CC	CC	5	“	52	1800	6	“	83	1200
DD	DD	5	“	83	1300	6	“	111	1700
EE	EE	5	“	111	1800	6	“	143	1300
FF	FF	5	“	143	1400	6	“	171	1500
GG	GG	5	“	171	1600	6	“	203	1100
HH	HH	5	“	203	1200	6	“	229	1100
II	II	5	“	229	1200	6	“	262	1500
JJ	JJ	5	“	262	1600	6	“	291	1200
KK	KK	5	“	291	1300	6	“	316	1700
LL	LL	5	“	316	1800	6	“	344	2400
01AA	01AA	5	“	345	100	6	2001	11	1300
BB	BB	5	2001	11	1400	6	“	44	1300
CC	CC	5	“	44	1400	6	“	79	1200
Gap DE	Gap DE	5	“	123	1900	6	“	137	1200
EF	EF	5	“	137	1300	6	“	170	1500
FG	FG	5	“	170	1600	6	“	200	1100

TABLE B4. ONS FILES SUMMARY Section 390205 CWRU Page 3

NEW FILE	OLD FILE	FROM				TO			
		D.Type	YEAR	DAY	HOUR	D.Type	YEAR	DAY	HOUR
39SE01GH	39SE01GH	5	2001	200	1200	6	2001	227	1200
HI	HI	5	“	227	1300	6	“	256	1700
IJ	IJ	5	“	256	1800	6	“	284	1200
JK	JK	5	“	284	1300	6	“	319	1200
KL	KL	5	“	319	1300	6	“	353	2400
02AA	02AA	5	“	354	100	6	2002	22	1700
BB	BB	5	2002	22	1800	6	“	53	1800
CC	CC	5	“	53	1900	6	“	81	1600
DD	DD	5	“	81	1700	6	“	115	1400
EE	EE	5	“	115	1500	6	“	136	1200
FF	FF	5	“	136	1300	6	“	162	1100
GG	GG	5	“	162	1200	6	“	198	1100
HH	HH	5	“	198	1200	6	“	232	1100
II	II	5	“	232	1200	6	“	262	1500
JJ	JJ	5	“	262	1600	6	“	297	1600
KK	KK	5	“	297	1700	6	“	324	1700
LL	LL	5	“	324	1800	6	“	351	2400
03AA	03AA	5	“	352	100	6	2003	17	1200
			“				“		

TABLE B5. ONS FILES SUMMARY Section 390201 OSU Page 1

NEW FILE	OLD FILE	FROM				TO			
		D.Type	YEAR	DAY	HOUR	D.Type	YEAR	DAY	HOUR
39SF96AI	39SF96AI	7	1996	255	1411	6	1996	256	1000
No need BI	BI	5	"	256	1100	6	"	268	1100
CJ	CJ	5	"	256	1100	6	"	288	1400
DK	DK	5	"	288	1500	6	"	323	1400
EL	EL	5	"	323	1500	6	"	366	2400
97AA	97AA	7	1997	1	100	6	1997	23	1200
BB	BB	5	"	23	1300	6	"	49	1100
CC	CC	5	"	49	1200	6	"	69	900
DC	DC	5	"	69	1000	6	"	85	1300
ED	ED	5	"	85	1400	6	"	98	1400
FD	FD	5	"	98	1500	6	"	112	1400
GE	GE	5	"	112	1500	6	"	140	1400
HF	HF	5	"	140	1500	6	"	167	1300
IG	IG	5	"	167	1400	6	"	180	2000
Faulty Data	JH	5	"	190	1400	6	"	218	1400
Faulty Data	KI	5	"	218	1500	6	"	246	1100
Faulty Data	NL	5	"	302	2400	6	"	357	1600
Faulty Data	98AA	5	"	357	1700	6	1998	16	1200
Faulty Data	EH	5	1998	212	1259	6	"	240	1000
Faulty Data	FI	BAD							
Faulty Data	GJ	BAD							
Faulty Data	HK	BAD							
Faulty Data	IL	BAD							
Gap 00AA	00AA	7	"	363	100	6	2000	14	1200
BB	BB	5	2000	14	1300	6	"	47	1400
CC	CC	5	"	47	1500	6	"	82	1200
DD	DD	5	"	82	1300	6	"	111	1500
ED	DE	5	"	111	1600	6	"	119	1300
FE	EE	5	"	119	1400	6	"	136	1300

TABLE B5. ONS FILES SUMMARY Section 390201 OSU Page 2

NEW FILE	OLD FILE	FROM				TO			
		D.Type	YEAR	DAY	HOUR	D.Type	YEAR	DAY	HOUR
39SF00GF	39SF00FF	5	2000	136	1400	6	2000	178	900
HG	GG	5	“	178	1000	6	“	202	900
IH	HH	5	“	202	1000	6	“	228	1000
JI	II	2	“	196	2400	6	“	251	1100
KJ	JJ	5	“	251	1200	6	“	286	1300
LK	KK	5	“	286	1400	6	“	319	1400
MK	KL	5	“	319	1500	6	“	326	1500
NL	LL	5	“	326	1600	6	“	354	2400
01AA	01AA	7	“	355	100	6	2001	18	1300
BB	BB	5	2001	18	1400	6	“	46	1200
CC	CC	5	“	46	1300	6	“	67	1400
deleted	CD	5	“	46	1300	6	“	67	1400
DC	CE	5	“	67	1500	6	“	81	1000
ED	DD	5	“	81	1100	6	“	99	1000
Gap FE	EE	5	“	114	1400	6	“	137	800
GF	FF	5	“	137	900	6	“	171	900
HG	GG	5	“	171	1000	6	“	205	900
IH	HH	5	“	205	1000	6	“	233	1200
Gap JJ	JJ	7	“	263	1340	6	“	282	1200
KK	KK	5	“	282	1300	6	“	310	1200
LL	LL	5	“	310	1300	6	“	343	2400
02AA	02AA	7	“	344	100	6	2002	10	1400
BB	BB	5	2002	10	1500	6	“	45	1400
CC	CC	5	“	45	1500	6	“	73	1300
DD	DD	5	“	73	1400	6	“	100	1300
ED	DE	5	“	100	1400	6	“	119	1200
FE	EE	5	“	119	1300	6	“	142	1200
GF	FF	5	“	142	1300	6	“	167	1900
HG	GG	5	“	194	100	6	“	207	1300

TABLE B5. ONS FILES SUMMARY Section 390201 OSU Page 3

NEW FILE	OLD FILE	FROM				TO			
		D.Type	YEAR	DAY	HOUR	D.Type	YEAR	DAY	HOUR
39SF02IH	39SF02HH	5	2002	207	1400	6	2002	233	1100
JI	II	5	“	233	1200	6	“	266	1100
KJ	JJ	5	“	266	1200	6	“	291	1300
LK	KK	5	“	291	1400	6	“	314	1500
Gap ML	LL	5	“	334	100	6	“	351	1100
03AA	03AA	7	“	326	100	6	2003	15	1300

TABLE B6. ONS FILES SUMMARY Section 390211 OSU Page 1

NEW FILE	OLD FILE	FROM				TO			
		D.Type	YEAR	DAY	HOUR	D.Type	YEAR	DAY	HOUR
39SG96AI	39SG96BI	7	1996	250	1611	6	1996	269	1400
BJ	CJ	5	“	256	1200	6	“	289	1400
CK	DK	5	“	289	1500	6	“	324	1500
97AA	EL	5	“	324	1600	6	1996	346	1900
Faulty BB	97AB	5	1997	4	100	6	“	31	1300
Faulty Data	BB	BAD							
Faulty Data	CC	BAD							
Faulty Data	DC	BAD							
Faulty Data	ED	BAD							
Faulty Data	FD	BAD							
Faulty Data	GE	BAD							
Faulty Data	HF	BAD							
Faulty Data	IG	BAD							
Faulty Data	JH	BAD							
Faulty Data	KI	BAD							
Faulty Data	NL	BAD							
Faulty Data	98AA	BAD							
Faulty Data	EF	BAD							
Faulty Data	FG	BAD							
Faulty Data	GH	BAD							
Faulty Data	HI	BAD							
Faulty Data	IJ	BAD							
Faulty Data	JK	BAD							
Faulty Data	KL	BAD							
Faulty Data	99LA	BAD							
Faulty Data	MB	BAD							
Faulty Data	NC	BAD							
Faulty Data	OC	BAD							
Faulty Data	PD	BAD							

TABLE B6. ONS FILES SUMMARY **Section 390211 OSU** **Page 2**

NEW FILE	OLD FILE	FROM				TO			
		D.Type	YEAR	DAY	HOUR	D.Type	YEAR	DAY	HOUR
Faulty Data	39SG99QD	BAD							
Faulty Data	RE	BAD							
Faulty Data	SH	BAD							
Faulty Data	TI	BAD							
Faulty Data	UJ	BAD							
Faulty Data	00AA	BAD	2000	4	1446	6	2000	14	1300
39SG02AD	02DD	7	2002	100	1417	6	2002	119	1300
Gap BJ	JJ	5	"	266	1200	6	"	291	1400
CK	KK	5	"	291	1500	6	"	319	1300
DL	LL	5	"	319	1400	6	"	351	1200
03AA	03AA	7	"	326	100	6	2003	15	1400

TABLE B7. ONS FILES SUMMARY Section 390203 CWRU Page 1

NEW FILE	OLD FILE	FROM				TO			
		D.Type	YEAR	DAY	HOUR	D.Type	YEAR	DAY	HOUR
39SH96AH	39SH96AH	5	1996	163	2400	6	1996	218	1100
BI	BI	4	“	208	2400	6	“	263	1100
CJ	CJ	5	“	234	2400	6	“	289	1600
DK	DK	5	“	289	1700	6	“	324	1600
EL	EL	5	“	324	1700	6	“	356	2400
97AA	97AA	5	“	357	100	6	1997	16	1500
BB	BB	4	“	358	2400	6	“	47	1500
CC	CC	2	1997	15	2400	6	“	70	1100
DC	DC	5	“	28	100	6	“	82	1600
No need ED	ED	4	“	44	2400	6	“	65	1700
FD	FD	5	“	82	1700	6	“	115	1400
GE	GE	6	“	88	2300	6	“	143	1000
HF	HF	3	“	117	2400	6		168	1200
JH	JH	4	“	162	2400	6	“	217	1400
KI	KI	5	“	217	1500	6	“	252	1400
LJ	LJ	3	“	234	2400	6	“	289	1200
MK	MK	5	“	289	1300	6	“	324	1300
NL	NL	5	“	324	1400	6	“	349	2400
98AA	98AA	5	“	350	100	6	1998	22	1100
BB	BB	5	1998	22	1100	6	“	55	1300
CC	CC	5	“	55	1400	6	“	85	1400
DD	DD	5	“	85	1500	6	“	107	1500
EE	EE	3	“	85	2400	6	“	140	1300
FF	FF	5	“	140	1400	6	“	169	1400
GG	GG	5	“	169	1500	6	“	202	1100
HH	HH	5	“	202	1200	6	“	231	1500
II	II	5	“	231	1600	6	“	260	1200
JJ	JJ	5	“	260	1300	6	“	293	1100
KK	KK	5	“	293	1200	6	“	323	1400

39SH97IG NOT NEEDED

TABLE B7. ONS FILES SUMMARY Section 390203 CWRU Page 2

NEW FILE	OLD FILE	FROM				TO			
		D.Type	YEAR	DAY	HOUR	D.Type	YEAR	DAY	HOUR
39SH98LL	39SH98LL	5	1998	323	1500	6	1998	349	2400
99AA	99AA	5	"	350	100	6	1999	21	1500
BB	BB	5	1999	21	1600	6	"	47	1100
CC	CC	5	"	47	1200	6	"	79	1200
Gap DD	DD	3	"	113	100	6	"	119	1100
EE	EE	4	"	113	100	6	"	139	1200
FF	FF	5	"	139	1300	6	"	166	1300
GG	GG	5	"	166	1400	6	"	196	1400
HH	HH	5	"	196	1500	6	"	236	900
II	II	5	"	236	1000	6	"	259	1400
JJ	JJ	5	"	259	1500	6	"	284	1900
KK	KK	5	"	284	2000	6	"	322	1100
LL	LL	5	"	322	1200	6	"	342	2400
00AA	00AA	5	"	343	100	6	2000	13	1200
BB	BB	5	2000	13	1300	6	"	43	1400
CC	CC	2	"	28	2400	6	"	83	1100
DD	DD	5	"	83	1200	6	"	111	1400
EE	EE	5	"	111	1500	6	"	143	1200
FF	FF	5	"	143	1300	6	"	171	1400
GG	GG	5	"	171	1500	6	"	203	1100
HH	HH	5	"	203	1200	6	"	229	1000
II	II	5	"	229	1100	6	"	262	1500
JJ	JJ	5	"	262	100	6	"	291	1100
KK	KK	5	"	291	1200	6	"	316	1400
LL	LL	5	"	316	1500	6	"	344	2400
01AA	01AA	5	"	345	100	6	2001	11	1100
BB	BB	5	2001	10	100	6	"	44	1200
CC	CC	5	"	44	1300	6	"	79	1100
DD	DD	5	"	79	1200	6	"	109	1100

TABLE B7. ONS FILES SUMMARY Section 390203 CWRU Page 3

NEW FILE	OLD FILE	FROM				TO			
		D.Type	YEAR	DAY	HOUR	D.Type	YEAR	DAY	HOUR
39SH01EE	39SH01EE	5	2001	109	1200	6	2001	137	1200
FF	FF	5	“	137	1300	6	“	170	1400
GG	GG	5	“	170	1500	6	“	200	900
HH	HH	5	“	200	1000	6	“	227	1000
II	II	5	“	227	1100	6	“	256	1600
JJ	JJ	5	“	256	1700	6	“	284	1000
KK	KK	5	“	284	1100	6	“	319	1100
LL	LL	5	“	319	1200	6	“	353	2400
02AA	02AA	5	“	354	100	6	2002	22	1600
BB	BB	5	2002	22	1700	6	“	53	1800
CC	CC	5	“	53	1900	6	“	81	1800
DD	DD	5	“	81	1900	6	“	115	1500
EE	EE	5	“	115	1600	6	“	136	1200
FF	FF	5	“	136	1300	6	“	162	1000
GG	GG	5	“	162	1100	6	“	198	1000
HH	HH	5	“	198	1100	6	“	232	1000
II	II	5	“	232	1100	6	“	262	1400
JJ	JJ	5	“	262	1500	6	“	297	1500
KK	KK	5	“	297	1600	6	“	324	1600
LL	LL	5	“	324	1700	6	“	351	2400
03AA	03AA	5	“	352	100	6	2003	17	1100

TABLE B8. ONS FILES SUMMARY **Section 390208 OU** **Page 1**

NEW FILE	OLD FILE	FROM				TO			
		D.Type	YEAR	DAY	HOUR	D.Type	YEAR	DAY	HOUR
39SI96AH	39SI96AH	7	1996	191	1232	6	1996	228	1300
Gap39SI97AB	39SI97BB	7	1997	23	1507	6	1997	49	1300
Deleted	39SC97HF	PART	OF	390212					
All above	1997 Files								

TABLE B8. ONS FILES SUMMARY Section 390208 OU Page 2

NEW FILE	OLD FILE	FROM				TO			
		D.Type	YEAR	DAY	HOUR	D.Type	YEAR	DAY	HOUR
Gap 39SI98AF	39SI98EF	6	1998	106	2200	6	1998	161	900
Gap SI98BH	SH98HH	7	"	190	1014	6	1998	236	1000
SI98CI	SH98II	5	"	236	1100	6	"	260	1000
SI98DJ	SH98JJ	5	"	260	1100	6	"	287	1600
Deleted	SI98TK	NOT	same	Data	With	next	File		
Gap SI98EL	UL	3	1998	296	2400	6	1998	351	1200
99AA	99VA	5	"	351	1300	6	1999	19	1400
BB	WB	5	1999	19	1500	6	"	48	1000
CC	XC	5	"	48	1100	6	"	67	1500
DC	YC	5	"	67	1600	6	"	83	1300
ED	ZD	5	"	83	1400	6	"	104	900
FD	AD	5	"	104	1000	6	"	116	1400
GE	BE	5	"	116	1500	6	"	134	1000
HF	CF	5	"	134	1100	6	"	162	1000
IG	DG	5	"	162	1000	6	"	197	900
JH	DH	5	"	197	1000	6	"	224	1000
KI	EI	5	"	224	1100	6	"	266	1200
LJ	FJ	5	"	266	1300	6	"	288	1000
MK	GK	5	"	288	1100	6	"	323	1000
00AA	SI100H	5	"	323	1100	6	2000	4	1400
BB	SI100I	5	2000	4	1500	6	"	47	1400
CC	SI100J	5	"	47	1500	6	"	82	1400
DD	SI100K	5	"	82	1500	6	"	109	1300
EE	00LE	5	"	109	1400	6	"	136	1300
FF	MF	4	"	110	2400	6	"	165	1100
GG	NG	5	"	165	1200	6	"	202	1400
HH	OH	5	"	202	1500	6	"	230	1200
II	OI	5	"	230	1300	6	"	265	1200

TABLE B8. ONS FILES SUMMARY **Section 390208 OU** **Page 3**

NEW FILE	OLD FILE	FROM				TO			
		D.Type	YEAR	DAY	HOUR	D.Type	YEAR	DAY	HOUR
39SI00JJ	39SI00PJ	5	2000	265	1300	6	2000	286	900
Not needed	QJ	6	“	231	2300	6	“	286	1000
00KK	RK	2	“	266	2400	6	“	321	1100
LL	SL	5	“	321	1200	6	“	355	1100
01AA	01TA	5	“	355	1200	6	2001	18	1100
BB	UB	5	2001	18	1200	6	“	47	1100
CC	VC	5	“	47	1200	6	“	73	1500
DD	WD	5	“	73	1600	6	“	106	1400
EF	XF	5	“	106	1500	6	“	152	1200
FF	YF	5	“	152	1300	6	“	171	1400
GG	ZG	5	“	171	1500	6	“	204	1400
HH	AH	5	“	204	1500	6	“	228	1400
II	BH	5	“	228	1500	6	“	263	1000
JJ	CJ	5	“	263	1100	6	“	291	1400
KK	DK	5	“	291	1500	6	“	312	1300
LL	EL	5	“	312	1400	6	“	353	1300
02AA	02FA	5	“	353	1400	6	2002	22	1100
BB	GB	5	2002	22	1200	6	“	50	1200
CC	HC	5	“	50	1300	6	“	71	1500
DD	ID	5	“	71	1600	6	“	100	1100
Gap EG	FG	5	“	149	2400	6	“	204	1600
Gap SI02FJ	SH02JJ	5	“	255	1000	6	“	297	900
SI02GK	SH02KL	2	“	283	2400	6	“	307	1400
Gap SI03AA	SH03AA	4	“	318	2400	6	2003	8	1400

TABLE B9. ONS FILES SUMMARY Section 390263 OSU Page 1

NEW FILE	OLD FILE	FROM				TO			
		D.Type	YEAR	DAY	HOUR	D.Type	YEAR	DAY	HOUR
Deleted	39SJ96AI	NO	DATA						
39SJ96AJ	BJ	7	1996	268	1319	6	1996	288	1500
BK	CK	2	“	268	2400	6	“	323	1100
CL	DL	5	“	323	1200	6	“	366	1100
97AB	97AB	5	“	366	1200	6	1997	37	1000
BB	BB	5	1997	37	1100	6	“	49	1200
CC	CC	5	“	49	1300	6	“	85	1200
DD	DD	5	“	85	1300	6	“	98	1300
ED	ED	5	“	98	1400	6	“	112	1500
FE	FE	5	“	112	1600	6	“	140	1500
GF	GF	5	“	140	1600	6	“	167	1000
HG	HG	5	“	167	1100	6	“	190	1000
IH	IH	5	“	190	1100	6	“	218	1300
JI	JI	5	“	218	1400	6	“	246	900
Gap KL	NL	4	“	302	2400	6	“	357	1400
98AA	98AA	5	“	357	1500	6	1998	16	1100
Gap BF	EF	4	1998	104	2400	6	“	159	1400
CG	FG	5	“	159	1500	6	“	212	1000
DH	FH	5	“	212	1100	6	“	240	1000
EI	GI	5	“	240	1100	6	“	272	1300
FJ	HJ	5	“	272	1400	6	“	296	1100
GK	IK	5	“	296	1200	6	“	328	1300
HK	JK	5	“	328	1400	6	“	334	1500
IL	KL	5	“	334	1600	6	“	362	1200
99AA	99LA	5	“	362	1300	6	1999	28	1200
BB	LB	5	1999	28	1300	6	“	49	1200
Gap CC	MC	5	“	74	1300	6	“	89	1600
Gap DD	ND	5	“	109	700	6	“	120	700
EE	OE	5	“	120	800	6	“	140	900

TABLE B9. ONS FILES SUMMARY Section 390263 OSU Page 2

NEW FILE	OLD FILE	FROM				TO			
		D.Type	YEAR	DAY	HOUR	D.Type	YEAR	DAY	HOUR
39SJ99FF	39SJ99PF	5	1999	140	1000	6	1999	176	1400
GG	QG	5	"	176	1500	6	"	197	1100
HH	RH	5	"	197	1200	6	"	232	900
II	SI	2	"	202	2400	6	"	257	1100
00AB	00BB	5	"	362	1200	6	2000	47	1000
BC	CC	5	2000	47	1100	6	"	82	1000
Gap CG	Not usedGG	6	"	147	2200	6	"	202	900
Deleted	HH	Bad	Sensor						
Deleted	II	Bad	Sensor						
Deleted	JJ	Bad	Sensor						
Deleted	KK	Bad	Sensor						
Deleted	KL	Bad	Sensor						
Deleted	LL	Bad	Sensors						
Deleted	01AA	Bad	Sensors						
Deleted	BB	Bad	Sensors						
Deleted	CC	Bad	Sensors						
Deleted	CD	Bad	Sensors						
Deleted	DD	Bad	Sensors						
Deleted	DE	Bad	Sensors						
Deleted	EE	Bad	Sensors						
Deleted	FF	Bad	Sensors						
Deleted	GG	Bad	Sensors						
Deleted	GH	Bad	Sensors						
Deleted	HH	Bad	Sensors						
Deleted	II	Bad	Sensors						
Deleted	IJ	Bad	Sensors						
Gap 02AB	02BB	7	2002	10	1203	6	2002	45	1000
BC	CC	5	"	45	1100	6	"	73	1100
CD	DD	5	"	73	1200	6	"	100	900

TABLE B9. ONS FILES SUMMARY Section 390263 OSU Page 3

NEW FILE	OLD FILE	FROM				TO			
		D.Type	YEAR	DAY	HOUR	D.Type	YEAR	DAY	HOUR
39SJ02DE	39SJ02EE	5	2002	100	1000	6	2002	142	900
EF	FF	5	"	142	1000	6	"	170	800
FG	GG	5	"	170	900	6	"	207	1000
GH	HH	5	"	207	1100	6	"	233	900
HI	II	5	"	233	1000	6	"	266	900
IJ	JJ	5	"	266	1000	6	"	291	1000
JK	KK	5	"	291	1100	6	"	319	1000
KL	LL	5	"	319	1100	6	"	346	1000
03AA	03AA	2	"	325	2400	6	2003	15	1100

TABLE B10. ONS FILES SUMMARY Section 390901 CWRU Page 1

NEW FILE	OLD FILE	FROM				TO			
		D.Type	YEAR	DAY	HOUR	D.Type	YEAR	DAY	HOUR
39SK96AH	39SK96AH	7	1996	165	1200	6	1996	218	1500
BI	BI	4	"	208	2400	6	"	263	1200
CJ	CJ	4	"	234	2400	6	"	289	1500
DK	DK	5	"	289	1600	6	"	324	1500
EL	EL	5	"	324	1600	6	"	355	2400
97AA	97AA	5	"	356	100	6	1997	16	1100
BB	BB	3	"	358	2400	6	"	47	1300
CC	CC	5	1997	16	1200	6	"	70	1400
DC	DC	5	"	47	1400	6	"	82	900
ED	ED	5	"	44	2400	6	"	99	1300
SEN 1 FD	@86 FD	5	"	82	1000	6	"	115	1500
1 GE	GE	5	"	115	1600	6	"	143	800
1 HF	HF	2	"	112	2400	6	"	167	1100
1 GAP JH	JH	5	"	167	1300	6	"	217	1300
1 KI	KI	5	"	217	1400	6	"	252	1400
1 LJ	LJ	2	"	234	2400	6	"	289	1100
1 MK	MK	5	"	289	1200	6	"	324	1200
1 NL	NL	5	"	324	1300	6	"	349	2400
1 98AA	98AA	5	"	350	100	6	1998	22	1100
1 BB	BB	5	1998	22	1200	6	"	55	1300
1 CC	CC	5	"	55	1400	6	"	85	1100
1,2 DD	@86 DD	5	"	52	2400	6	"	107	1700
1,2 EE	EE	5	"	107	1800	6	"	140	1100
1,2 FF	FF	5	"	140	1200	6	"	169	1100
1,2 GG	GG	5	"	169	1200	6	"	202	900
1,2 HH	HH	5	"	202	1000	6	"	231	1600
1,2 II	II	5	"	231	1700	6	"	260	1200
1,2 JJ	JJ	5	"	260	1300	6	"	293	900
1,2 KK	KK	5	"	293	1000	6	"	323	1100

BAD SENSORS INDICATED IN COLUMN 1 – STARTING DAY IN COLUMN 2

TABLE B10. ONS FILES SUMMARY Section 390901 CWRU Page 2

NEW FILE	OLD FILE	FROM				TO			
		D.Type	YEAR	DAY	HOUR	D.Type	YEAR	DAY	HOUR
39SK98LL	39SK98LL	5	1998	323	1200	6	1998	349	2400
1,2 99AA	99AA	5	"	350	100	6	1999	21	1200
1,2 BB	BB	5	1999	21	1300	6	"	47	1100
1,2 CC	CC	5	"	47	1200	6	"	79	1400
1,2 DD	DD	5	"	79	1500	6	"	112	1400
1,2 EE	EE	5	"	112	1500	6	"	139	1200
1,2,3 FF	@150 F	5	"	139	1300	6	"	166	1500
1,2,3 GG	GG	5	"	166	1600	6	"	196	1500
1,2,3 HH	HH	5	"	196	1600	6	"	236	1700
1,2,3 II	II	3	"	204	2400	6	"	259	1300
1,2,3 JJ	JJ	5	"	259	1400	6	"	284	1700
1,2,3 KK	KK	5	"	284	1800	6	"	322	1300
1,2,3 LL	LL	5	"	322	1400	6	"	342	1400
Restart ML	ML	3	"	295	2400	6	"	350	1300
00AA	00AA	5	"	351	1100	6	2000	13	1600
BB	BB	7	2000	11	100	6	"	52	1800
CC	CC	7	"	50	100	6	"	83	1300
DD	DD	7	"	81	100	6	"	111	1600
EE	EE	7	"	110	100	6	"	143	1200
FF	FF	7	"	142	100	6	"	171	1500
GG	GG	7	"	170	100	6	"	203	1000
HH	HH	7	"	200	100	6	"	229	1200
II	II	7	"	229	100	6	"	262	1600
1-5 JJ	JJ	7	"	261	100	6	"	291	1100
1-5 KK	KK	7	"	290	100	6	"	312	1400
1-5 LL	LL	7	"	315	100	6	"	343	2400
1-5 01AA	01AA	7	"	344	100	6	2001	11	1100
1 BB	BB	7	2001	10	100	6	"	44	1100
1 CC	CC	7	"	44	100	6	"	66	1100

BAD SENSORS INDICATED IN COLUMN 1 – STARTING DAY IN COLUMN 2

TABLE B10. ONS FILES SUMMARY Section 390901 CWRU Page 3

NEW FILE	OLD FILE	FROM				TO			
		D.Type	YEAR	DAY	HOUR	D.Type	YEAR	DAY	HOUR
39SK01DE	39SK01DE	7 Gap	2001	101	100	6	2001	137	1300
1,2,3 EF	EF	7	"	137	100	6	"	170	1400
1,2,3 FG	FG	7	"	170	100	6	"	200	1000
1,2,3 GH	GH	7	"	200	100	6	"	227	1100
1,2,3 HI	HI	7	"	227	100	6	"	256	1700
IJ	IJ	7	"	256	100	6	"	284	1100
JK	JK	7	"	284	100	6	"	319	1200
KL	KL	7	"	319	100	6	"	352	2400
02AA	02AA	7	"	353	100	6	2002	22	1600
BB	BB	7	2002	22	100	6	"	53	1700
CC	CC	7	"	53	110	6	"	81	1500
DD	DD	7	"	81	100	6	"	115	1300
EE	EE	7	"	115	100	6	"	136	1000
FF	FF	7	"	136	100	6	"	162	1000
GG	GG	7	"	162	100	6	"	198	1100
HH	HH	7	"	198	100	6	"	232	1100
Gap II	II	5	"	244	2400	6	"	262	1500
JJ	JJ	7	"	262	100	6	"	297	1600
KK	KK	7	"	297	100	6	"	324	1600
LL	LL	7	"	324	100	6	"	350	1200
03AA	03AA	7	"	351	100	6	2003	17	2400

BAD SENSORS INDICATED IN COLUMN 1 – STARTING DAY IN COLUMN 2

TABLE B11. ONS FILES SUMMARY Section 390904 OSU Page 1

NEW FILE	OLD FILE	FROM				TO			
		D.Type	YEAR	DAY	HOUR	D.Type	YEAR	DAY	HOUR
39SL96AI	39SL96BI	7	1996	250	1442	6	1996	269	1000
BJ	CJ	5	“	256	1300	6	“	289	1300
CK	DK	5	“	289	1400	6	“	324	1300
DL	EL	5	“	324	1400	6	“	352	1300
97AB	97AB	5	“	352	1400	6	1997	38	1200
BB	BB	5	1997	38	1300	6	“	50	1100
CC	CC	5	“	50	1200	6	“	70	1000
DC	DC	5	“	70	1100	6	“	86	1300
ED	ED	5	“	86	1400	6	“	99	1500
FD	FD	5	“	99	1600	6	“	113	1400
GE	GE	5	“	113	1500	6	“	141	1400
HF	HF	5	“	141	1500	6	“	168	1100
IG	IG	5	“	168	1200	6	“	192	900
JH	JH	5	“	192	1000	6	“	204	1900
Gap 98AD	98ED	5	1998	104	1340	6	1998	118	1600
BF	FF	5	“	118	1700	6	“	159	1400
CG	GG	5	“	159	1500	6	“	212	1100
DH	HH	5	“	212	1200	6	“	240	1000
EI	II	5	“	240	1100	6	“	272	1400
FJ	JJ	5	“	272	1500	6	“	296	1200
GK	KK	5	“	296	1300	6	“	334	1600
HL	LL	5	“	334	1700	6	“	362	1300
99AA	97MA	5	“	362	1400	6	1999	28	1300
BB	NB	5	1999	28	1400	6	“	49	1300
CC	OC	5	“	74	1400	6	“	89	1700
DD	PD	5	“	89	1800	6	“	109	700
ED	QD	5	“	109	800	6	“	120	800
Gap FL	RL	7	“	323	1154	6	“	362	1000
00AA	00AA	5	“	362	1100	6	2000	14	1200

TABLE B11. ONS FILES SUMMARY Section 390904 OSU Page 2

NEW FILE	OLD FILE	FROM				TO			
		D.Type	YEAR	DAY	HOUR	D.Type	YEAR	DAY	HOUR
39SL00BB	39SL00BB	5	2000	14	1300	6	2000	47	1300
CC	CC	5	“	47	1400	6	“	82	1100
DD	DD	5	“	82	1200	6	“	111	1600
ED	DE	5	“	111	1700	6	“	119	1300
FE	EE	5	“	119	1400	6	“	136	1200
GF	FF	5	“	136	1300	6	“	178	900
HG	GG	6	“	147	2200	6	“	202	900
IH	HH	6	“	202	1000	6	“	228	1000
JI	II	2	“	196	2400	5	“	246	1300
Gap KJ	JJ	5	“	251	1200	6	“	286	1200
LK	KK	5	“	286	1300	6	“	319	1400
MK	KL	5	“	319	1500	6	“	326	1400
NL	LL	5	“	326	1500	6	“	354	1100
01AA	01AA	5	“	354	1200	6	2001	18	1300
BB	BB	5	2001	18	1400	6	“	46	1200
CC	CC	5	“	46	1300	6	“	67	1300
DC	CD	5	“	67	1400	6	“	81	1000
ED	DD	5	“	81	1100	6	“	99	1000
FE	EE	5	“	99	1100	6	“	137	800
GF	FF	5	“	137	900	6	“	171	800
HG	GG	5	“	171	900	6	“	183	800
IG	GH	6	“	150	2100	6	“	205	800
JH	HH	5	“	205	900	6	“	233	1100
KI	II	5	“	233	1200	6	“	254	1100
LJ	JJ	5	“	254	1200	6	“	282	900
Gap ML	LL	7	“	310	1134	6	“	344	1100
02AA	02AA	5	“	344	1200	6	2002	10	1200
BB	BB	5	2002	10	1300	6	“	45	1200
CC	CC	5	“	45	1300	6	“	73	1200

TABLE B11. ONS FILES SUMMARY Section 390904 OSU Page 3

NEW FILE	OLD FILE	FROM				TO			
		D.Type	YEAR	DAY	HOUR	D.Type	YEAR	DAY	HOUR
39SL02DD	39SL02DD	5	2002	73	1300	6	2002	100	1000
ED	DE	5	"	100	1100	6	"	119	1100
FE	EE	5	"	119	1200	6	"	142	1000
GF	FF	5	"	142	1100	6	"	170	900
HG	GG	5	"	152	2400	6	"	207	1100
IH	HH	5	"	207	1200	6	"	233	1000
JI	II	5	"	233	1100	6	"	266	1000
KJ	JJ	5	"	266	1100	6	"	291	1200
LK	KK	5	"	291	1300	6	"	319	1100
ML	LL	5	"	319	1200	6	"	351	1100
03AA	03AA	3	"	325	2400	6	2003	15	1300
			2003				"		

TABLE B12. ONS FILES SUMMARY Section 390112 UT Page 1

NEW FILE	OLD FILE	FROM				TO			
		D.Type	YEAR	DAY	HOUR	D.Type	YEAR	DAY	HOUR
39SM96AH	39SM96AH	7	1996	193	917	6	1996	241	1300
BI	BI	5	“	208	2400	6	“	263	1700
CJ	CJ	5	“	263	1800	6	“	290	1100
DK	DK	5	“	290	1200	6	“	325	1200
EL	EL	5	“	325	1300	6	“	353	1200
DELETE	97AA	7	“	193	1533	6	“	205	1200
DELETE	CC	7	1997	50	1743	6	1997	71	1300
DELETE	DC	7	“	50	1743	6	“	85	1000
Gap AD	ED	7	“	50	1743	6	“	100	1100
BD	FD	5	“	100	1200	6	“	114	1100
CE	GE	5	“	114	1200	6	“	142	1000
DF	HF	5	“	142	1100	6	“	170	900
EH	JH	5	“	170	1000	6	“	218	1300
Gap FK	MK	5	“	296	1000	6	“	324	1000
GL	NL	5	“	324	1100	6	“	351	1300
98AA	98AA	6	“	330	2300	6	1998	20	1000
BB	BB	5	1998	20	1100	6	“	45	1100
CC	CC	5	“	45	1200	6	“	71	1400
DD	DD	5	“	71	1500	6	“	114	1300
EE	EE	4	“	79	2400	6	“	134	1300
BAD SENS	FG	2	“	137	2400	6	“	192	1100
BAD SENS	GH	7	“	192	1113	6	“	224	1000
BAD SENS	HI	5	“	224	1100	6	“	272	1100
BAD SENS	IJ	5	“	272	1200	6	“	288	1000
BAD SENS	IK	5	“	288	1100	6	“	327	1100
BAD SENS	KL	5	“	327	1200	6	“	349	1100
BAD SENS	99AA	5	“	349	1200	6	“	26	1100
BAD SENS	BB	5	“	26	1200	6	“	42	1300
BAD SENS	CC	5	“	42	1400	6		71	1200

TABLE B12. ONS FILES SUMMARY Section 390112 UT Page 2

NEW FILE	OLD FILE	FROM				TO			
		D.Type	YEAR	DAY	HOUR	D.Type	YEAR	DAY	HOUR
BAD SENS	39SM99DD	7	1999	71	1222	6	1999	112	1000
BAD SENS	EE	5	“	112	1100	6	“	140	1000
BAD SENS	FF	5	“	140	1200	6	“	169	1100
BAD SENS	GG	7	“	201	1045	6	“	201	1100
BAD SENS	HH	BAD	FILE						
BAD SENS	II	7	“	224	1419	6	“	259	1200
BAD SENS	JJ	5	“	259	1300	6	“	287	1000
BAD SENS	KK	5	“	287	1100	6	“	316	1100
BAD SENS	LL	2	“	301	2400	6	“	356	1000
BAD SENS	00AA	5	“	356	1000	6	2000	17	1000
BAD SENS	BB	6	“	356	2200	6	“	46	900
BAD SENS	CC	5	2000	46	1000	6	“	67	800
BAD SENS	DC	5	“	67	1000	6	“	83	1000
BAD SENS	FD	5	“	83	1100	6	“	116	900
BAD SENS	GE	5	“	116	1200	6	“	146	1000
BAD SENS	HF	5	“	146	1100	6	“	168	1100
BAD SENS	IG	5	“	168	1100	6	“	201	1000
BAD SENS	JH	5	“	201	1100	6	“	223	1000
BAD SENS	KI	5	“	223	1100	6	“	266	1000
BAD SENS	LJ	5	“	266	1100	6	“	288	1300
BAD SENS	MK	5	“	288	1400	6	“	316	1300
BAD SENS	NL	5	“	316	1400	6	“	351	1200
DELETE	02BB	4	LINES	OF	DATA	ONLY			
	NOTHING								
	BEYOND								
	02BB								

TABLE B13. ONS FILES SUMMARY Section 390104 UT Page 1

NEW FILE	OLD FILE	FROM				TO			
		D.Type	YEAR	DAY	HOUR	D.Type	YEAR	DAY	HOUR
Not needed	39SN96AH	7	1996	193	1731	6	1996	228	1700
39SN96AH	BH	7	“	193	1731	6	“	241	1600
BI	CI	5	“	215	1300	6	“	263	1700
CJ	DJ	5	“	263	1800	6	“	290	1000
Not needed	EK	2	“	235	2400	6	“	290	1100
Gap DL	FL	7	“	325	1024	6	“	353	1000
97AA	97AA	5	“	353	1100	6	1997	24	900
BB	BB	5	“	361	2400	6	“	50	1600
Not needed	CC	5	1997	50	1700	6	“	71	1200
Not needed	DC	5	“	71	1300	6	“	85	1300
CD	ED	6	“	45	2300	6	“	100	1000
DD	FD	5	“	100	1100	6	“	114	1100
EE	GE	5	“	114	1200	6	“	142	900
FF	HF	5	“	142	1000	6	“	170	800
GH	JH	5	“	170	900	6	“	218	100
HI	KI	7	“	200	100	6	“	254	800
IJ	LJ	6	“	241	2100	6	“	296	800
JK	MK	6	“	269	2200	6	“	324	900
KL	NL	3	“	296	2400	6	“	351	1200
98AA	98AA	5	“	351	1300	6	1998	20	900
BB	BB	6	“	355	2300	6	“	45	1000
CC	CC	5	1998	45	1100	6	“	71	1300
DD	DD	5	“	71	1400	6	“	114	1200
Gap EG	FG	6	“	137	2300	6	“	192	1000
Gap FH	GH	7	“	192	1049	6	“	224	900
GI	HI	5	“	224	1000	6	“	272	1200
HJ	IJ	5	“	272	1300	6	“	288	900
IK	JK	5	“	288	1000	6	“	327	1000
JL	KL	5	“	327	1000	6	“	349	900

TABLE B13. ONS FILES SUMMARY Section 390104 UT Page 2

NEW FILE	OLD FILE	FROM				TO			
		D.Type	YEAR	DAY	HOUR	D.Type	YEAR	DAY	HOUR
39SN99AA	39SN99AA	6	1998	336	2200	6	1999	26	900
BB	BB	5	1999	26	1000	6	"	42	1100
CC	CC	5	"	42	1200	6	"	71	1000
DD	DD	5	"	71	1100	6	"	112	1000
EE	EE	5	"	112	1200	6	"	140	1000
New FF	FF	5	"	140	1100	6	"	169	900
GG	GG	5	"	169	1000	6	"	201	900
HH	HH	5	"	201	1000	6	"	223	1000
II	II	5	"	223	1100	6	"	259	1200
JJ	JJ	5	"	259	1300	6	"	287	1000
KK	KK	5	"	287	1100	6	"	316	1000
LL	LL	5	"	316	1100	6	"	356	900
00AA	00AA	5	"	356	1000	6	2000	17	1000
BB	BB	6	"	356	2200	6	"	46	800
CC	CC	5	2000	46	900	6	"	67	700
Nothing	DC								
Gap DD	ED	5	2000	83	1100	6	"	97	900
Gap ED	FD	5	"	97	1100	6	"	116	900
FE	GE	5	"	116	1000	6	"	146	1000
GF	HF	5	"	146	1000	6	"	168	1000
HG	IG	5	"	168	1000	6	"	201	900
IH	JH	5	"	201	1000	6	"	223	1000
JI	KI	5	"	223	1100	6	"	266	1000
KJ	LJ	5	"	266	1100	6	"	287	1200
01AA	01AA	5	"	351	1300	6	2001	13	1100
BB	BB	5	2001	12	1100	6	"	44	1000
CC	CC	5	"	44	1100	6	"	67	1000
DD	DD	5	"	67	1100	6	"	95	900
Bad Data	GG	7	"	165	1152	6	"	198	1000

TABLE B13. ONS FILES SUMMARY Section 390104 UT Page 3

NEW FILE	OLD FILE	FROM				TO			
		D.Type	YEAR	DAY	HOUR	D.Type	YEAR	DAY	HOUR
Bad Data	39SN01HH	5	2001	198	1100	6	2001	221	900
Bad Data	II	5	“	221	1000	6	“	254	1300
Nothing	02AA								
Nothing	BB								
39SN02AC	CC	7	2002	39	1045	6	2002	67	1200
BD	DD	5	“	67	1300	6	“	108	800
Gap CE	EE	5	“	108	1000	6	“	135	900
DF	FF	5	“	135	1000	6	“	168	1200
2 sets EG	GG	5	“	168	1300	6	“	211	900
Restart FH	HH	7	“	211	952	6	“	220	1000
Gap LJ	LJ	5	“	257	1000	6	“	294	1400
Restart HK	MK	7	“	294	1426	6	“	327	900
IL	NL	5	“	327	900	6	“	351	1400
03AA	03AA	5	“	351	1500	6	2003	18	900

TABLE B14. ONS FILES SUMMARY Section 390101 UT Page 1

NEW FILE	OLD FILE	FROM				TO			
		D.Type	YEAR	DAY	HOUR	D.Type	YEAR	DAY	HOUR
Not needed	39SO96BH	7	1996	193	1533	6	1996	228	1500
39SO96AI	CI	7	“	193	1533	6	“	257	700
BI	DI	7	“	209	100	6	“	263	1600
Gap CJ	Not used EJ	7	“	290	848	6	“	290	1000
Gap DL	FL	7	“	326	100	6	“	353	900
97AA	97AA	5	“	353	1000	6	“	24	800
BB	BB	4	“	361	2400	6	1997	50	1500
CC	CC	5	1997	50	1600	6	“	71	1100
DC	DC	5	“	71	1200	6	“	85	1200
Gap ED	FD	7	“	100	928	6	“	114	1000
FE	GE	5	“	114	1100	6	“	142	800
GF	HF	5	“	142	900	6	“	170	700

TABLE B15. ONS FILES SUMMARY Section 390102 CWRU Page 1

NEW	OLD	FROM				TO			
FILE	FILE	D.Type	YEAR	DAY	HOUR	D.Type	YEAR	DAY	HOUR
39SP96AH	39SP96AH	7	1996	161	100	6	1996	228	1500
BI	BI	5	“	228	1600	6	“	263	1200
PAV.	FAILED								

TABLE B16. ONS FILES SUMMARY Section 390108 OSU Page 1

NEW FILE	OLD FILE	FROM				TO			
		D.Type	YEAR	DAY	HOUR	D.Type	YEAR	DAY	HOUR
39SQ96AH	39SQ96AH	5 Bad	1996	212	1100	6	1996	215	1100
BH	BH	5	"	212	1100	6	"	215	1100
Gap CI	CI	5	"	250	1300	6	"	256	1200
DI	DI	5	"	256	1300	6	"	269	1500
EJ	EJ	5	"	256	1300	6	"	289	1500
FK	FK	5	"	289	1600	6	"	324	1200
GL	GL	5	"	324	1300	6	"	352	1200
97AB	97AB	5	"	352	1300	6	1997	38	1100
BB	BB	5	1997	38	1200	6	"	50	1000
CC	CC	5	"	50	1100	6	"	70	900
DC	DC	5	"	70	1000	6	"	86	1200
ED	ED	5	"	86	1300	6	"	113	1300
FE	FE	5	"	113	1400	6	"	141	1500
GF	GF	5	"	141	1600	6	"	168	1100
HG	HG	5	"	168	1200	6	"	192	1200
IH	IH	5	"	192	1300	6	"	219	1300
JI	JI	5	"	219	1400	6	"	247	900
Gap KL	NL	4	"	303	2400	6	"	358	1500
98AA	98AA	5	"	358	1600	6	1998	17	1100
Gap BF	EF	7	1998	107	1215	6	"	159	1400
CG	FG	5	"	159	1500	6	"	212	1000
DH	GH	5	"	212	1100	6	"	240	1000
EI	HI	5	"	240	1100	6	"	272	1300
FJ	IJ	5	"	272	1400	6	"	296	1200
GK	JK	5	"	296	1300	6	"	334	1600
HL	KL	5	"	334	1700	6	"	362	1300
99AA	99LA	5	"	362	1400	6	1999	28	1300
BB	MB	5	1999	28	1400	6	"	49	1300
Gap CE	PE	5	"	120	900	6	"	140	900

TABLE B16. ONS FILES SUMMARY Section 390108 OSU Page 2

NEW FILE	OLD FILE	FROM				TO			
		D.Type	YEAR	DAY	HOUR	D.Type	YEAR	DAY	HOUR
39SQ99DF	39SQ99QF	5	1999	140	1000	6	1999	176	1500
EG	RG	5	“	176	1600	6	“	197	1200
FH	SH	5	“	197	1300	6	“	232	1000
GI	TI	5	“	232	1100	6	“	257	1400
HJ	UJ	5	“	257	1500	6	“	288	1500
Gap 00AA	00AA	5	“	362	1200	6	2000	14	1300
BB	BB	5	2000	14	1400	6	“	47	1500
Gap CD	DD	5	“	82	1500	6	“	111	1600
DD	DE	5	“	111	1700	6	“	119	1400
EE	EE	5	“	119	1500	6	“	136	1400
FF	FF	5	“	136	1500	6	“	178	1000
GG	GG	5	“	178	1100	6	“	202	1000
HH	HH	5	“	202	1100	6	“	228	1100
II	II	5	“	196	2400	6	“	251	1200
JJ	JJ	5	“	251	1300	6	“	286	1300
KK	KK	5	“	286	1400	6	“	319	1500
LK	KL	5	“	319	1600	6	“	326	1500
ML	LL	5	“	326	1600	6	“	354	1200
01AA	01AA	5	“	354	1300	6	2001	18	1400
BB	BB	5	2001	18	1500	6	“	46	1300
CC	CC	5	“	46	1400	6	“	67	1400
DC	CD	5	“	67	1500	6	“	81	1100
ED	DD	5	“	81	1200	6	“	99	1100
FD	DE	5	“	99	1200	6	“	114	1300
GE	EE	5	“	114	1400	6	“	137	900
HF	FF	5	“	137	1000	6	“	171	900
IG	GG	5	“	171	1000	6	“	183	1000
JG	GH	5	“	183	1100	6	“	187	2400
Gap KJ	JJ	5	“	263	1228	6	“	282	1000

TABLE B16. ONS FILES SUMMARY Section 390108 OSU Page 3

NEW FILE	OLD FILE	FROM				TO			
		D.Type	YEAR	DAY	HOUR	D.Type	YEAR	DAY	HOUR
39SQ01LK	39SQ01KK	5	2001	282	1100	6	2001	310	1200
ML	LL	5	“	310	1300	6	“	344	1200
02AA	02AA	5	“	344	1300	6	2002	10	1300
BB	BB	5	2002	10	1400	6	“	45	1300
CC	CC	5	“	45	1400	6	“	73	1200
DD	DD	5	“	73	1300	6	“	100	1100
ED	DE	2	“	64	2400	6	“	119	1100
FE	EE	5	“	100	1200	6	“	142	1000
GF	FF	5	“	142	1100	6	“	170	900
HH	HH	5	“	170	1000	6	“	233	1000
II	II	5	“	233	1100	6	“	266	1000
JJ	JJ	5	“	266	1100	6	“	291	1100
KK	KK	3	“	264	2400	6	“	319	1200
LL	LL	5	“	319	1300	6	“	346	1100
03AA	03AA	3	“	325	2400	6	2003	15	1200
			“						
			“						
			“						
			“						
			“						
			“						
			“						

TABLE B17. ONS FILES SUMMARY Section 390110 OU Page 1

NEW FILE	OLD FILE	FROM				TO			
		D.Type	YEAR	DAY	HOUR	D.Type	YEAR	DAY	HOUR
39SR96AG	39SR96AH	7	1996	191	1141	6	1996	228	1300
BI	BI	5	“	215	1200	6	“	267	1300
CJ	CJ	7	“	267	1355	6	“	289	1300
DK	DK	7	“	289	1313	6	“	324	1400
EL	EL	3	“	297	2400	6	“	352	1200
Gap 97AB	97BB	5	“	361	1200	6	1997	49	1400
BC	CC	7	1997	49	1416	6	“	70	1300
CC	DC	5	“	70	1400	6	“	84	1100
DD	FD	5	“	84	1200	6	“	111	1000
EE	GE	5	“	89	100	6	“	143	1100
FF	HF	5	“	139	1100	6	“	167	800
GG	IG	5	“	167	900	6	“	191	1500
HH	JH	5	“	191	1600	6	“	217	1700
II	KI	5	“	199	100	6	“	253	1100
JJ	LJ	5	“	242	100	6	“	296	1000
KK	MK	5	“	296	1100	6	“	318	1100
LL	NL	5	“	318	1200	6	“	346	1100
98AA	98AA	5	“	346	1200	6	1998	20	1000
BB	BB	4	“	365	2400	6	“	55	1400
CC	CC	3	1998	22	2400	6	“	77	1300
DD	DD	2	“	49	2400	6	“	104	1100
Gap EF	EF	6	“	106	2300	6	“	161	1000
FG	GG	5	“	161	1100	6	“	190	1100
GH	HH	5	“	190	1200	6	“	236	1100
HI	RI	5	“	236	1200	6	“	260	1000
IJ	SJ	5	“	260	1100	6	“	287	1600
JK	TK	2	“	269	2400	6	“	324	1100
KL	UL	3	“	296	2400	6	“	351	1300
99AA	99VA	5	“	351	1400	6	1999	19	1500

TABLE B17. ONS FILES SUMMARY Section 390110 OU Page 2

NEW FILE	OLD FILE	FROM				TO			
		D.Type	YEAR	DAY	HOUR	D.Type	YEAR	DAY	HOUR
39SR99BB	39SR99WB	5	1999	19	1600	6	1999	48	1100
CC	XC	5	“	48	1200	6	“	67	1600
DC	YC	5	“	67	1700	6	“	83	1300
ED	ZD	5	“	83	1400	6	“	104	1000
FD	AD	5	“	104	1100	6	“	116	1400
GE	BE	5	“	116	1500	6	“	134	1100
HF	CF	5	“	134	1200	6	“	162	1100
IG	EG	6	“	147	2300	6	“	202	1000
JH	FH	5	“	202	1100	6	“	224	1100
KI	GI	7	“	224	1119	6	“	265	1200
LJ	HJ	5	“	265	1300	6	“	288	1000
Gap MK	IK	5	“	288	1200	6	“	323	1100
00AA	100J	5	“	323	1200	6	2000	4	1500
BB	100K	5	2000	4	1600	6	“	47	1500
CC	100L	5	“	47	1600	6	“	82	1400
DD	100M	5	“	82	1500	6	“	109	1300
EE	NE	5	“	109	1400	6	“	136	1300
FF	OF	4	“	110	2400	6	“	165	1100
Gap GG	PG	7	“	165	1213	6	“	202	1400
HH	QH	6	“	202	1500	6	“	230	1300
II	QI	5	“	230	1400	6	“	265	1600
Gap JK	RK	3	“	266	2400	6	“	321	1200
KL	SL	5	“	321	1300	6	“	355	1200
01AA	01TA	5	“	355	1300	6	2001	18	1200
BB	UB	5	2001	18	1300	6	“	47	1200
CC	VC	5	“	47	1300	6	“	73	1500
DD	WD	5	“	73	1600	6	“	97	1700
Bad ED	XF	5	“	97	1800	6	“	113	2000
Gap FF	YF	7	“	152	1319	6	“	171	1400

TABLE B17. ONS FILES SUMMARY Section 390110 OU Page 3

NEW FILE	OLD FILE	FROM				TO			
		D.Type	YEAR	DAY	HOUR	D.Type	YEAR	DAY	HOUR
39SR01GF	39SR01ZG	5	2001	171	1500	6	2001	173	1000
Gap HI	AJ	7	“	235	1604	6	“	263	1800
IJ	BK	5	“	263	1900	6	“	284	1800
JK	CL	5	“	284	1900	6	“	325	1800
KL	02DA	5	“	325	1900	6	“	359	1600
02AA	02EB	5	“	359	1700	6	2002	22	1700
BB	FC	5	2002	22	1800	6	“	43	2000
CC	GD	5	“	17	2400	6	“	72	1600
Gap DF	FG	5	“	122	100	6	“	176	2100

TABLE B18. ONS FILES SUMMARY Section 390162 OU Page 1

NEW FILE	OLD FILE	FROM				TO			
		D.Type	YEAR	DAY	HOUR	D.Type	YEAR	DAY	HOUR
39SZ98AA	S390162A	7	1997	346	1237	6	1998	20	1100
BB	S390162B	4	“	365	2400	6	“	55	1400
CC	S390162C	3	1998	22	2400	6	“	77	1300
DD	S390162D	5	“	77	1400	6	“	107	1000
Gap EH	98HH	4	“	181	2400	6	“	236	1100
FI	ZI	5	“	236	1200	6	“	260	1100
GJ	AJ	5	“	260	1200	6	“	287	1700
HK	TK	5	“	287	1800	6	“	324	1200
IL	UL	5	“	324	1300	6	“	351	1400
99AA	99VA	5	“	351	1500	6	1999	19	1500
BB	WB	5	1999	19	1600	6	“	48	1100
CC	WC	5	“	48	1200	6	“	67	1600
DC	XC	5	“	67	1700	6	“	83	1300
ED	YD	5	“	83	1400	6	“	104	1000
FD	ZD	7	“	104	1100	6	“	116	1300
GE	AE	5	“	116	1400	6	“	134	1100
Gap HG	BG	2	“	147	2400	6	“	202	1100
IH	CH	5	“	202	1200	6	“	224	1100
JI	DI	5	“	224	1200	6	“	265	1100
KJ	EJ	5	“	265	1200	6	“	288	1200
LK	FK	5	“	288	1300	6	“	323	1100
00AA	100G	5	“	323	1200	6	2000	4	1500
BB	100H	5	2000	4	1600	6	“	47	1500
CC	100I	5	“	47	1600	6	“	82	1500
DD	100J	5	“	82	1600	6	“	109	1400
EE	00KE	5	“	109	1500	6	“	136	1400
FF	LF	4	“	110	2400	6	“	165	1200
GG	MG	5	“	165	1300	6	“	202	1400
HH	NH	5	“	202	1500	6	“	230	1300

TABLE B18. ONS FILES SUMMARY Section 390162 OU Page 2

NEW FILE	OLD FILE	FROM				TO			
		D.Type	YEAR	DAY	HOUR	D.Type	YEAR	DAY	HOUR
39SZ00II	39SZ00OI	5	2000	230	1400	6	2000	265	1700
JJ	PJ	5	“	265	1800	6	“	286	1000
Gap 01AA	01QA	7	“	355	1216	6	2001	18	1100
BB	RB	5	2001	18	1200	6	“	47	1100
CD	SD	7	“	73	1531	6	“	106	1600
DF	TF	7	“	152	1332	6	“	171	1500
EG	UG	5	“	171	1600	6	“	204	1500
FH	VH	5	“	204	1600	6	“	228	1400
GI	WI	5	“	228	1500	6	“	263	1400
HJ	XJ	5	“	263	1500	6	“	291	1500
IK	YK	5	“	291	1600	6	“	312	1400
JL	YL	4	“	298	2400	6	“	353	1500
02AA	02ZA	5	“	353	1600	6	2002	22	1200
BB	AB	5	2002	22	1300	6	“	50	1300
CC	BC	5	“	50	1400	6	“	71	1600
Gap DG	FG	6	“	150	2300	6	“	205	1000
Gap EJ	JJ	3	“	242	2400	6	“	297	1200
FL	KL	3	“	283	2400	6	“	338	1200
03AA	03AA	4	“	318	2400	6	2003	8	1500

PAGE LEFT INTENTIONALLY BLANK

APPENDIX B2

MOB FILES SUMMARY

TABLE B19. MOB FILES SUMMARY Section 390204 UT Page 1

NEW FILE	OLD FILE	DATE COLLECTED	NEW FILE	OLD FILE	DATE COLLECTED
Bad Date	39SB96AI	2/13/96	39SB99CC	39SB99CC	3/12/99
39SB96AJ	39SB96BJ	10/16/96	DC	DC	3/25/99
BL	DL	12/18/96	ED	ED	4/8/99
97AB	BB	2/19/97	FD	FD	4/22/99
BC	CC	3/12/97	GE	GE	5/20/99
CC	DC	3/26/97	HF	HF	6/18/99
DD	ED	4/10/97	IG	IG	7/20/99
ED	FD	4/24/97	JH	JH	8/11/99
FE	GE	5/22/97	KI	KI	9/16/99
GF	HF	6/19/97	LJ	LJ	10/14/99
HH	JH	8/6/97	MK	MK	11/12/99
IJ	LJ	10/23/97	NL	NL	12/22/99
JK	MK	11/20/97	00AA	00AA	1/17/00
KL	NL	12/17/97	Bad File	BB	2/15/00
98AA	98AA	1/20/98	BC	CC	3/7/00
Bad File	BB	2/14/98	CD	ED	4/6/00
BC	CC	3/12/98	DD	FD	4/25/00
CD	DD	4/24/98	EE	GE	5/25/00
DE	EE	5/14/98	FF	HF	6/16/00
Duplicate	FG	7/11/98	GG	IG	7/19/00
EG	GG	7/11/98	HH	JH	8/10/00
Bad File	GH	8/12/98	II	KI	9/23/00
Bad File	HH	8/12/98	JJ	LJ	10/14/00
FI	HI	9/29/98	KK	MK	11/11/00
GJ	IJ	10/15/98	LL	NL	12/15/00
HK	JK	11/23/98	01AA	01AA	1/12/01
IL	KL	12/15/98	BB	BB	2/13/01
99AA	99AA	1/26/99	CC	CC	3/8/01
BB	BB	2/11/99	DC	DC	3/22/01

TABLE B19. MOB FILES SUMMARY **Section 390204 UT Page 2**

NEW FILE	OLD FILE	DATE COLLECTED	NEW FILE	OLD FILE	DATE COLLECTED
39SB01ED	39SB01ED	4/5/01			
FD	FD	4/19/01			
GE	GE	5/17/01			
HF	HF	6/14/01			
IG	IG	7/17/01			
JH	JH	8/9/01			
KI	KI	9/11/01			
LJ	LJ	10/15/01			
MK	MK	11/12/01			
NL	NL	12/20/01			
02AA	02AA	1/10/02			
BB	BB	2/8/02			
CC	CC	3/8/02			
DC	DC	3/22/02			
ED	ED	4/5/02			
FD	FD	4/18/02			
GE	GE	5/15/02			
HF	HF	6/17/02			
IG	IG	7/30/02			
JH	JH	8/8/02			
KI	KI	9/14/02			
LJ	LJ	10/21/02			
MK	MK	11/23/02			
NL	NL	12/17/02			
03AA	03AA	1/18/03			

TABLE B20. MOB FILES SUMMARY Section 390212 CWRU Page 1

NEW FILE	OLD FILE	DATE COLLECTED	NEW FILE	OLD FILE	DATE COLLECTED
39SC96AH	39SC96AH	8/5/96	39SC98JJ	39SC98JJ	10/20/98
BH	BH	8/15/96	KK	KK	11/19/98
CI	CI	9/19/96	LL	LL	12/15/98
DJ	DJ	10/15/96	99AA	99AA	1/21/99
EK	EK	11/19/96	BB	BB	2/16/99
FL	FL	12/21/96	CC	CC	3/4/99
97AA	97AA	1/16/97	DC	DC	3/20/99
BB	BB	2/16/97	ED	ED	4/8/99
CC	CC	3/11/97	FD	FD	4/22/99
DC	DC	3/23/97	GE	GE	5/19/99
Nothing	ED	4/9/97	HF	HF	6/15/99
ED	FD	4/25/97	IG	IG	7/15/99
FE	GE	5/23/97	JH	JH	8/24/99
GF	HF	6/16/97	KI	KI	9/16/99
HG	IG	7/10/97	LJ	LJ	10/11/99
IH	JH	8/5/97	MK	MK	11/18/99
JI	KI	9/9/27	NL	NL	12/8/99
KJ	LJ	10/16/97	00AA	00AA	1/13/00
LK	MK	11/20/97	BB	BB	2/12/00
ML	NL	12/15/97	CC	CC	3/7/00
98AA	98AA	1/22/98	DC	DC	3/23/00
BB	BB	2/24/98	ED	ED	4/4/00
CC	CC	3/26/98	FD	FD	4/20/00
DD	DD	4/17/98	GE	GE	5/22/00
EE	EE	5/20/98	HF	HF	6/19/00
FF	FF	6/18/98	IG	IG	7/21/00
GG	GG	7/21/98	JH	JH	8/16/00
HH	HH	8/19/98	KI	KI	9/18/00
II	II	9/17/98	LJ	LJ	10/17/00

TABLE B20. MOB FILES SUMMARY Section 390212 CWRU Page 2

NEW FILE	OLD FILE	DATE COLLECTED	NEW FILE	OLD FILE	DATE COLLECTED
39SC00MK	39SC00MK	11/11/00	39SC02NL	39SC02NL	12/17/02
NL	NL	12/9/00	03AA	03AA	1/17/03
01AA	01AA	1/11/01	BB	BB	2/28/03
BB	BB	2/13/01	CC	CC	3/7/03
CC	CC	3/7/01	DC	DC	3/21/03
DC	DC	3/20/01			
ED	ED	4/5/01			
FD	FD	4/19/01			
GE	GE	5/17/01			
HF	HF	6/19/01			
IG	IG	7/19/01			
JH	JH	8/15/01			
KI	KI	9/13/01			
LJ	LJ	10/11/01			
MK	MK	11/15/01			
NL	NL	12/19/01			
02AA	02AA	1/22/02			
BB	BB	2/22/02			
CC	CC	3/7/02			
DC	DC	3/22/02			
ED	ED	4/5/02			
FD	FD	4/25/02			
GE	GE	5/16/02			
HF	HF	6/11/02			
IG	IG	7/17/02			
JH	JH	8/20/02			
KI	KI	9/19/02			
LJ	LJ	10/24/02			
MK	MK	11/20/02			

TABLE B21. MOB FILES SUMMARY Section 390202 UT Page 1

NEW FILE	OLD FILE	DATE COLLECTED	NEW FILE	OLD FILE	DATE COLLECTED
39SD96AH	39SD96AI	8/1/96	39SD99ED	39SD99ED	4/8/99
BI	BI	9/16/96	FD	FD	4/22/99
No Date	CJ	No Date	GE	GE	5/20/99
CK	DK	11/20/96	Bad data HF	HF	6/18/99
DL	EL	12/18/96	Bad data IG	IG	7/20/99
97AB	97BB	2/19/97	JH	JH	8/11/99
BC	CC	3/12/97	KI	KI	9/16/99
CC	DC	3/26/97	LJ	LJ	10/14/99
DD	ED	4/10/97	MK	MK	11/12/99
ED	FD	4/24/97	NL	NL	12/22/99
FE	GE	5/22/97	00AA	00AA	1/17/00
GH	JH	8/6/97	BB	BB	2/15/00
HJ	LJ	10/23/97	CC	CC	3/7/00
IK	MK	11/20/97	DC	DC	3/23/00
JL	NL	12/17/97	ED	ED	4/6/00
98AA	98AA	1/20/98	FE	GE	5/25/00
BC	CC	3/12/98	GF	HF	6/16/00
CD	DD	4/24/98	HG	IG	7/19/00
DE	EE	5/14/98	IH	JH	8/10/00
EG	FF	7/11/98	JI	KI	9/23/00
FH	GH	8/12/98	KJ	LJ	10/14/00
GI	HI	9/29/98	LK	MK	11/11/00
HJ	IJ	10/15/98	ML	NL	12/15/00
IK	JK	11/23/98	01AA	01AA	1/12/01
JL	KL	12/15/98	BB	BB	2/13/01
99AA	99AA	1/26/99	CC	CC	3/8/01
BB	BB	2/11/99	DC	DC	3/22/01
CC	CC	3/12/99	ED	ED	4/5/01
DC	DC	3/25/99	FD	FD	4/19/01

TABLE B21. MOB FILES SUMMARY **Section 390202 UT Page 2**

NEW FILE	OLD FILE	DATE COLLECTED	NEW FILE	OLD FILE	DATE COLLECTED
39SD01GE	39SD01GE	5/17/01			
HF	HF	6/14/01			
IG	IG	7/17/01			
JH	JH	8/9/01			
KI	KI	9/11/01			
LJ	LJ	10/15/01			
MK	MK	11/12/01			
Bad Data	NL	12/20/01			
02AA	02AA	1/10/02			
BB	BB	2/8/02			
CC	CC	3/8/02			
DD	ED	4/5/02			
ED	FD	4/18/02			
FE	GE	5/15/02			
HF	HF	6/17/02			
IG	IG	7/30/02			
JH	JH	8/8/02			
KI	KI	9/14/02			
LJ	LJ	10/21/02			
MK	MK	11/23/02			
NL	NL	12/17/02			
03AA	03AA	1/18/03			

TABLE B22. MOB FILES SUMMARY Section 390205 CWRU Page 1

NEW FILE	OLD FILE	DATE COLLECTED	NEW FILE	OLD FILE	DATE COLLECTED
39SE96AH	39SE96AH	8/5/96	39SE98JJ	39SE98JJ	10/20/98
BH	BH	8/15/96	KK	KK	11/19/98
CI	CI	9/19/96	LL	LL	12/15/98
DJ	DJ	10/15/96	99AA	99AA	1/21/99
EK	EK	11/19/96	BB	BB	2/16/99
FL	FL	12/21/96	CC	CC	3/4/99
97AA	97AA	1/16/97	DC	DC	3/20/99
BB	BB	2/16/97	ED	ED	4/8/99
CC	CC	3/11/97	FD	FD	4/22/99
DC	DC	3/23/97	GE	GE	5/19/99
Nothing	ED	4/9/97	HF	HF	6/15/99
ED	FD	4/25/97	IG	IG	7/15/99
FE	GE	5/23/97	JH	JH	8/24/99
GF	HF	6/16/97	KI	KI	9/16/99
HG	IG	7/10/97	LJ	LJ	10/11/99
IH	JH	8/15/97	MK	MK	11/18/99
JI	KI	9/9/27	NL	NL	12/8/99
KJ	LJ	10/16/97	00AA	00AA	1/13/00
LK	MK	11/20/97	BB	BB	2/12/00
ML	NL	12/15/97	CC	CC	3/7/00
98AA	98AA	1/22/98	DC	DC	3/23/00
BB	BB	2/24/98	ED	ED	4/4/00
CC	CC	3/26/98	FD	FD	4/20/00
DD	DD	4/17/98	GE	GE	5/22/00
EE	EE	5/20/98	HF	HF	6/19/00
FF	FF	6/18/98	IG	IG	7/21/00
GG	GG	7/21/98	JH	JH	8/16/00
HH	HH	8/19/98	KI	KI	9/18/00
II	II	9/17/98	LJ	LJ	10/17/00

TABLE B22. MOB FILES SUMMARY Section 390205 CWRU Page 2

NEW FILE	OLD FILE	DATE COLLECTED	NEW FILE	OLD FILE	DATE COLLECTED
39SE00MK	39SE00MK	11/11/00	39SE02NL	39SE02NL	12/17/02
NL	NL	12/9/00	03AA	03AA	1/17/03
01AA	01AA	1/11/01	BB	BB	2/28/03
BB	BB	2/13/01	CC	CC	3/7/03
CC	CC	3/7/01	DC	DC	3/21/03
DC	DC	3/20/01			
ED	ED	4/5/01			
FD	FD	4/19/01			
GE	GE	5/17/01			
HF	HF	6/19/01			
IG	IG	7/19/01			
JH	JH	8/15/01			
KI	KI	9/13/01			
LJ	LJ	10/11/01			
MK	MK	11/15/01			
NL	NL	12/19/01			
02AA	02AA	1/22/02			
BB	BB	2/22/02			
CC	CC	3/7/02			
DC	DC	3/22/02			
ED	ED	4/5/02			
FD	FD	4/25/02			
GE	GE	5/16/02			
HF	HF	6/11/02			
IG	IG	7/17/02			
JH	JH	8/20/02			
KI	KI	9/19/02			
LJ	LJ	10/24/02			
MK	MK	11/20/02			

TABLE B23. MOB FILES SUMMARY **Section 390201 OSU** **Page 1**

NEW FILE	OLD FILE	DATE COLLECTED	NEW FILE	OLD FILE	DATE COLLECTED
39SF96AH	39SF96AH	8/15/96	39SF99HH	39SF99JH	8/20/99
BI	BI	9/11/96	II	JI	9/14/99
CI	CI	9/24/96	JK	JK	11/12/99
DJ	DJ	10/22/96	KL	JJ	12/28/99
EK	EK	11/18/96	00AA	00AA	1/14/00
FL	FL	12/31/96	BB	BB	2/16/00
97AA	97AA	1/23/97	CC	CC	3/22/00
BB	BB	2/20/97	DD	DD	4/20/00
CC	CC	3/26/97	ED	DE	4/28/00
DD	DD	4/8/97	FE	EE	5/15/00
ED	ED	4/22/97	GF	FF	6/26/00
FE	FE	5/20/97	HG	GG	7/20/00
GF	GF	6/16/97	Nothing	HH	
HG	HG	7/9/97	IH	II	8/15/00
IH	IH	8/6/97	JI	II	9/7/00
JI	JI	9/3/97	KJ	JJ	10/12/00
KL	NL	12/23/97	LK	KK	11/14/00
98AA	98AA	1/16/98	MK	KL	11/21/00
BI	GI	9/29/98	NL	LL	12/19/00
CJ	HJ	10/23/98	01AA	01AA	1/18/01
DL	JL	12/28/98	BC	CC	3/9/01
99AA	99JA	1/28/99	CC	CD	3/22/01
BB	JB	2/18/99	DD	DD	4/9/01
CC	JC_1	3/15/99	EE	EE	5/17/01
DC	JC	3/30/99	FF	FF	6/20/01
Deleted	JD	3/30/99	GG	GG	7/24/01
EE	JE	5/20/99	HH	HH	8/21/01
FF	JF	6/25/99	II	II	9/11/01
GG	JG	7/16/99	JJ	JJ	10/9/01

TABLE B23. MOB FILES SUMMARY Section 390201 OSU Page 2

NEW FILE	OLD FILE	DATE COLLECTED	NEW FILE	OLD FILE	DATE COLLECTED
39SF01KK	39SF01KK	11/6/01			
LL	LL	12/10/01			
02AA	02AA	1/10/02			
BB	BB	2/14/02			
CC	CC	3/14/02			
DD	DD	4/10/02			
ED	DE	4/29/02			
FE	EE	5/22/02			
GF	FF	6/19/02			
HG	GG	7/26/02			
IH	HH	8/21/02			
JI	II	9/23/02			
KJ	JJ	10/18/02			
LK	KK	11/15/02			
ML	LL	12/18/02			
03AA	03AA	1/15/03			
BB	BB	2/20/03			

TABLE B24. MOB FILES SUMMARY Section 390211 OSU Page 1

NEW FILE	OLD FILE	DATE COLLECTED	NEW FILE	OLD FILE	DATE COLLECTED
39SG96AI	39SG96BI	9/4/96	39SG99FD	39SG99RD	4/30/99
BI	BI	9/11/96	GE	SE	5/20/99
CI	BI	9/24/96	HG	SG	7/16/99
DJ	CJ	10/22/96	IH	TH	8/20/99
EK	DK	11/18/96	JI	UI	9/14/99
FL	EL	12/31/96	KJ	VJ	10/15/99
97AA	97AB	1/23/97	LK	UK	11/12/99
BB	AB	2/6/97	00AA	00AA	1/14/00
CB	BB	2/20/97	BB	BB	2/16/00
DC	CC	3/26/97	CD	DD	4/28/00
ED	DD	4/8/97	DF	FF	6/26/00
FD	DD	4/22/97	EG	GG	7/20/00
GE	EE	5/20/97	FH	HH	8/15/00
HF	FF	6/16/97	GI	II	9/7/00
IG	GG	7/9/97	HJ	JJ	10/12/00
JH	HH	8/6/97	IK	KK	11/14/00
KI	II	9/3/97	JK	KL	11/21/00
LL	NL	12/23/97	KL	LL	12/19/00
98AA	98AA	1/16/98	Delete Same	01AA	1/18/01
BF	EF	6/8/98	01AA	01AB	1/18/01
CG	GG	7/31/98	BB	BB	2/15/01
DI	II	9/29/98	CC	CC	3/9/01
EJ	JJ	10/23/98	DC	CD	3/22/01
FL	LL	12/28/98	ED	DD	4/9/01
99AA	MA	1/28/99	FF	FF	6/20/01
BB	NB	2/18/99	GG	GG	7/24/01
CC	OC	3/15/99	HH	HH	8/21/01
DC	PC	3/30/99	II	II	9/11/01
ED	QD	4/19/99	JJ	JJ	10/9/01

TABLE B24. MOB FILES SUMMARY **Section 390211 OSU** **Page 2**

NEW FILE	OLD FILE	DATE COLLECTED	NEW FILE	OLD FILE	DATE COLLECTED
39SG01KK	39SG01KK	11/6/01			
LL	LL	12/10/01			
02AA	02AA	1/10/02			
BB	BB	2/14/02			
CC	CC	3/14/02			
DD	DD	4/10/02			
ED	DE	4/29/02			
FE	EE	5/22/02			
GF	FF	6/19/02			
HG	GG	7/26/02			
IH	HH	8/21/02			
JI	II	9/23/02			
KJ	JJ	10/18/02			
LK	KK	11/15/02			
ML	LL	12/18/02			
03AA	03AA	1/15/02			
BB	BB	2/20/02			

TABLE B25. MOB FILES SUMMARY Section 390203 CWRU Page 1

NEW FILE	OLD FILE	DATE COLLECTED	NEW FILE	OLD FILE	DATE COLLECTED
39SH96AG	39SH96AG	7/22/96	39SH98JJ	39SH98JJ	10/20/98
BH	BH	8/5/96	KK	KK	11/19/98
CI	CI	9/19/96	LL	LL	12/15/98
DJ	DJ	10/15/96	99AA	99AA	1/21/99
EK	EK	11/19/96	BB	BB	2/16/99
FL	FL	12/21/96	CC	CC	3/4/99
97AA	97AA	1/16/97	DC	DC	3/20/99
BB	BB	2/16/97	ED	ED	4/8/99
CC	CC	3/11/97	FD	FD	4/22/99
DC	DC	3/23/97	GE	GE	5/19/99
ED	ED	4/9/97	HF	HF	6/15/99
FD	FD	4/25/97	IG	IG	7/15/99
GE	GE	5/23/97	JH	JH	8/24/99
HF	HF	6/16/97	KI	KI	9/16/99
IG	IG	7/10/97	LJ	LJ	10/11/99
JH	JH	8/5/97	MK	MK	11/18/99
KI	KI	9/9/27	NL	NL	12/8/99
LJ	LJ	10/16/97	00AA	00AA	1/13/00
MK	MK	11/20/97	BB	BB	2/12/00
NL	NL	12/15/97	CC	CC	3/7/00
98AA	98AA	1/22/98	DC	DC	3/23/00
BB	BB	2/24/98	ED	ED	4/4/00
CC	CC	3/26/98	FD	FD	4/20/00
DD	DD	4/17/98	GE	GE	5/22/00
EE	EE	5/20/98	HF	HF	6/19/00
FF	FF	6/18/98	IG	IG	7/21/00
GG	GG	7/21/98	JH	JH	8/16/00
HH	HH	8/19/98	KI	KI	9/18/00
II	II	9/17/98	LJ	LJ	10/17/00

TABLE B25. MOB FILES SUMMARY **Section 390203 CWRU Page 2**

NEW FILE	OLD FILE	DATE COLLECTED	NEW FILE	OLD FILE	DATE COLLECTED
39SH00MK	39SH00MK	11/11/00	39SH02NL	39SH02NL	12/17/02
NL	NL	12/9/00	03AA	03AA	1/17/03
01AA	01AA	1/11/01	BB	BB	2/28/03
BB	BB	2/13/01	CC	CC	3/7/03
CC	CC	3/7/01	DC	DC	3/21/03
DC	DC	3/20/01			
ED	ED	4/5/01			
FD	FD	4/19/01			
GE	GE	5/17/01			
HF	HF	6/19/01			
IG	IG	7/19/01			
JH	JH	8/15/01			
KI	KI	9/13/01			
LJ	LJ	10/11/01			
MK	MK	11/15/01			
NL	NL	12/19/01			
02AA	02AA	1/22/02			
BB	BB	2/22/02			
CC	CC	3/7/02			
DC	DC	3/22/02			
ED	ED	4/5/02			
FD	FD	4/25/02			
GE	GE	5/16/02			
HF	HF	6/11/02			
IG	IG	7/17/02			
JH	JH	8/20/02			
KI	KI	9/19/02			
LJ	LJ	10/24/02			
MK	MK	11/20/02			

TABLE B26. MOB FILES SUMMARY Section 390208 OU Page 1

NEW FILE	OLD FILE	DATE COLLECTED	NEW FILE	OLD FILE	DATE COLLECTED
39SI96AH	39SI96AH	8/15/96	39SI00EE	39SI00ME	5/15/00
97AA	97AA	1/21/97	FF	NF	6/13/00
BB	BB	2/18/97	GG	OG	7/20/00
DELETED	HF	6/16/97	HI	PI	9/19/00
98AD	98DD	4/14/98	IJ	QJ	10/7/00
BF	EF(1)	6/10/98	JJ	RJ	10/11/00
CG	EF(2)	7/9/98	KK	SK	11/16/00
DH	HH	8/24/98	LL	TL	12/20/00
EI	SH98II	9/17/98	01AA	01UA	1/18/01
FJ	SI98JJ	10/14/98	BB	VB	2/16/01
GK	TK	11/20/98	CC	WC	3/14/01
HL	UL	12/17/98	DD	XD	4/16/01
99AA	99VM	1/19/99	EF	YF	6/1/01
BB	WB	2/17/99	FF	ZF	6/20/01
CC	XC	3/8/99	GG	AG	7/23/01
DC	YC	3/24/99	HH	CH	8/23/01
ED	ZD	4/14/99	IJ	DJ	10/18/01
FD	AD	4/26/99	JK	EK	11/8/01
GE	BE	5/14/99	KL	FL	12/19/01
HF	CF	6/11/99	02AA	02GA	1/22/02
IG	DG	7/21/99	BB	HB	2/19/02
JH	EH	8/12/99	CC	IC	3/3/02
KI	FI	9/23/99	DD	JD	4/10/02
LJ	GJ	10/15/99	DELETE	SH02JJ	10/24/02
MK	HK	11/19/99	39SI02EJ	SH02KJ	10/24/02
00AA	100I	1/4/00	FK	SH02LL	11/4/02
BB	100J	2/16/00	03AA	SH03AA	1/8/02
CC	100K	3/22/00			
DD	100L	4/18/00			

TABLE B27. MOB FILES SUMMARY **Section 390263 OSU** **Page 1**

NEW FILE	OLD FILE	DATE COLLECTED	NEW FILE	OLD FILE	DATE COLLECTED
39SJ96AI	39SJ96BI	9/24/96	39SJ99GH	39SJ99SH	8/20/99
BK	CK	11/1/96	ONS FILE	39SJ99SI	--
CK	DK	11/18/96	39SJ99HI	TI	9/14/99
DL	EL	12/31/96	IJ	TJ	10/28/99
NOTHING	97AB	-	JK	TK	11/12/99
97AB	BB	2/20/97	00AB	00BB	2/16/00
BC	CC	3/26/97	BD	DD	4/28/00
CD	DD	4/8/97	CF	FF	6/26/00
DD	ED	4/22/97	DG	GG	7/20/00
EE	FE	5/20/97	EH	HH	8/15/00
FF	GF	6/16/97	FI	II	9/7/00
GG	HG	7/9/97	GJ	JJ	10/12/00
HH	IH	8/6/97	HK	KK	11/14/00
II	JI	9/3/97	IK	KL	11/21/00
JL	NL	12/23/97	JL	LL	12/19/00
98AA	98AA	1/16/98	01AA	01AA	1/18/01
BF	FF	6/8/98	BB	BB	2/15/01
CG	GG	7/31/98	CC	CC	3/8/01
DI	IJ	9/29/98	DC	CD	3/22/01
EJ	IJ	10/23/98	ED	DD	4/9/01
FK	JK	11/24/98	FD	DE	4/24/01
GL	LL	12/28/98	GE	EE	5/15/01
99AA	99MA	1/28/99	HF	FF	6/20/01
BB	MB	2/8/99	IG	GG	7/2/01
DELETE	NC	3/30/99	JG	GH	7/24/01
CC	OD	3/30/99	KH	HH	8/21/01
DE	OE	5/20/99	LI	II	9/11/01
EF	GF	6/25/99	MJ	JJ	10/19/01
FG	RG	7/16/99	NK	KK	11/6/01

TABLE B27. MOB FILES SUMMARY Section 390263 OSU Page 2

NEW FILE	OLD FILE	DATE COLLECTED	NEW FILE	OLD FILE	DATE COLLECTED
39SJ01OL	39SJ01LL	12/10/01			
02AA	02AA	1/10/02			
BB	BB	2/14/02			
CC	CC	3/14/02			
DD	DD	4/10/02			
ED	DE	4/29/02			
FE	EE	5/22/02			
GF	FF	6/19/02			
HG	GG	7/26/02			
IH	HH	8/21/02			
JI	II	9/23/02			
KJ	JJ	10/18/02			
LK	KK	11/15/02			
ML	LL	12/18/02			
03AA	03AA	1/15/02			
BB	BB	2/20/02			

TABLE B28. MOB FILES SUMMARY **Section 390901 CWRU Page 1**

NEW FILE	OLD FILE	DATE COLLECTED	NEW FILE	OLD FILE	DATE COLLECTED
39SK96AH	39SK96AH	8/5/96	39SK98KK	39SK98KK	11/19/98
BI	BI	9/19/96	LL	LL	12/15/98
CJ	CJ	10/15/96	99AA	99AA	1/21/99
DK	DK	11/19/96	BB	BB	2/16/99
EL	EL	12/21/96	CC	CC	3/4/99
97AA	97AA	1/16/97	DC	DC	3/20/99
BB	BB	2/16/97	ED	ED	4/8/99
CC	CC	3/11/97	FD	FD	4/22/99
DC	DC	3/23/97	GE	GE	5/19/99
NOTHING	ED	4/9/97	HF	HF	6/15/99
ED	FD	4/25/97	IG	IG	7/15/99
FE	GE	5/23/97	JH	JH	8/24/99
GF	HF	6/16/97	KI	KI	9/16/99
HG	IG	7/10/97	LJ	LJ	10/11/99
IH	JH	8/5/97	MK	MK	11/18/99
JI	KI	9/9/27	NL	NL	12/8/99
KJ	LJ	10/16/97	00AA	00AA	1/13/00
LK	MK	11/20/97	BB	BB	2/12/00
NL	NL	12/15/97	CC	CC	3/7/00
98AA	98AA	1/22/98	DC	DC	3/23/00
BB	BB	2/24/98	ED	ED	4/4/00
CC	CC	3/26/98	FD	FD	4/20/00
DD	DD	4/17/98	GE	GE	5/22/00
EE	EE	5/20/98	HF	HF	6/19/00
FF	FF	6/18/98	IG	IG	7/21/00
GG	GG	7/21/98	JH	JH	8/16/00
HH	HH	8/19/98	KI	KI	9/18/00
II	II	9/17/98	LJ	LJ	10/17/00
JJ	JJ	10/20/98	MK	MK	11/11/00

TABLE B28. MOB FILES SUMMARY Section 390901 CWRU Page 2

NEW FILE	OLD FILE	DATE COLLECTED	NEW FILE	OLD FILE	DATE COLLECTED
39SK00NL	39SK00NL	12/9/00	39SK03AA	39SK03AA	1/17/03
01AA	01AA	1/11/01	BB	BB	2/28/03
BB	BB	2/13/01	CC	CC	3/7/03
CC	CC	3/7/01	DC	DC	3/21/03
DC	DC	3/20/01			
ED	ED	4/5/01			
FD	FD	4/19/01			
GE	GE	5/17/01			
HF	HF	6/19/01			
IG	IG	7/19/01			
JH	JH	8/15/01			
KI	KI	9/13/01			
LJ	LJ	10/11/01			
MK	MK	11/15/01			
NL	NL	12/19/01			
02AA	02AA	1/22/02			
BB	BB	2/22/02			
CC	CC	3/7/02			
DC	DC	3/22/02			
ED	ED	4/5/02			
FD	FD	4/25/02			
GE	GE	5/16/02			
HF	HF	6/11/02			
IG	IG	7/17/02			
JH	JH	8/20/02			
KI	KI	9/19/02			
LJ	LJ	10/24/02			
MK	MK	11/20/02			
NL	NL	12/17/02			

TABLE B29. MOB FILES SUMMARY Section 390904 OSU Page 1

NEW FILE	OLD FILE	DATE COLLECTED	NEW FILE	OLD FILE	DATE COLLECTED
39SL96AI	39SL96BI(1)	9/11/96	39SL99FF	39SL99RF	6/25/99
BI	BI(2)	9/24/96	GG	RG	7/16/99
CJ	CJ	10/1/96	HH	RH	8/20/99
DJ	DJ	10/22/96	II	RI	9/14/99
EK	EK	11/18/96	JJ	RJ	10/15/99
FL	FL	12/16/96	KK	RK	11/12/99
97AB	97AB	2/6/97	LL	SL	12/28/99
BB	BB	2/20/97	00AA	00AA	1/14/00
CC	CC	3/26/97	BB	BB	2/16/00
DD	DD	4/8/97	CC	CC	3/22/00
ED	ED	4/22/97	DD	DD	4/20/00
FE	FE	5/20/97	ED	DE	4/28/00
GF	GF	6/16/97	FE	EE	5/15/00
HG	HG	7/11/97	GF	FF	6/26/00
IH	IH	8/6/97	HG	GG	7/20/00
JI	JI	9/3/97	IH	HH	8/15/00
KL	NL	12/23/97	JI	II	9/7/00
98AD	98FD	4/28/98	KJ	JJ	10/12/00
BF	GF	6/8/98	LK	KK	11/14/00
DELETE	HG	7/31/98	MK	KL	11/21/00
CI	JI	9/29/98	NL	LL	12/19/00
DJ	KJ	10/23/98	01AA	01AA	1/18/01
EL	ML	12/28/98	BB	BB	2/15/01
DELETE	99NA	--	CC	CC	3/9/01
99AB	99OB	2/18/99	DC	CD	3/22/01
BC	PC	3/30/99	ED	DD	4/9/01
CD	QD	4/19/99	FD	DE	4/24/01
DD	RD	4/30/99	GE	EE	5/15/01
EE	RE	5/20/99	HF	FF	6/20/01

TABLE B29. MOB FILES SUMMARY **Section 390904 OSU Page 2**

NEW FILE	OLD FILE	DATE COLLECTED	NEW FILE	OLD FILE	DATE COLLECTED
39SL01IG	39SL01GG	7/2/01			
JG	GH	7/24/01			
KH	HH	8/21/01			
LI	II	9/11/01			
MJ	JJ	10/9/01			
DELETE	KK				
NL	LL	12/10/01			
02AA	02AA	1/10/02			
BB	BB	2/14/02			
CC	CC	3/14/02			
DD	DD	4/10/02			
ED	DE	4/29/02			
FE	EE	5/22/02			
GF	FF	6/19/02			
HG	GG	7/26/02			
IH	HH	8/21/02			
JI	II	9/23/02			
KJ	JJ	10/18/02			
LK	KK	11/15/02			
ML	LL	12/18/02			
03AA	03AA	1/15/02			
BB	BB	2/20/02			

TABLE B30. MOB FILES SUMMARY Section 390112 UT Page 1

NEW FILE	OLD FILE	DATE COLLECTED	NEW FILE	OLD FILE	DATE COLLECTED
39SM96AH	39SM96AI	8/01/96	39SM99ED	39SM99ED	4/8/99
DELETED	BI	BAD DATE	FD	FD	4/22/99
BJ	CJ	10/16/96	GE	GE	5/20/99
CK	DK	11/20/96	HF	HF	6/18/99
DL	EL	12/18/96	IG	IG	7/20/99
97AC	97CC	3/12/97	JH	JH	8/11/99
BC	DC	3/26/97	KI	KI	9/16/99
DELETED	ED	BAD DATE	LJ	LJ	10/14/99
CD	FD	4/24/97	MK	MK	11/12/99
DE	GE	5/22/97	NL	NL	12/22/99
DELETED	HF	BAD DATE	00AA	00AA	1/17/00
EH	JH	8/6/97	BB	BB	2/15/00
FK	MK	11/20/97	CC	CC	3/7/00
GL	NL	12/17/97	DELETED	DC	3/23/00
98AA	98AA	1/20/98	DC	DD	3/23/00
BB	BB	2/14/98	DELETED	ED	BAD DATE
CC	CC	3/12/98	ED	FD	4/25/00
DD	DD	4/24/98	FE	GE	5/25/00
EE	EE	5/14/98	GF	HF	6/16/00
FG	FG	7/11/98	HG	IG	7/19/00
GH	GH	8/12/98	IH	JH	8/10/00
HI	HI	9/29/98	JI	KI	9/23/00
IJ	IJ	10/15/98	KJ	LJ	10/14/00
JK	JK	11/23/98	LK	MK	11/11/00
KL	KL	12/15/98	ML	NL	12/15/00
99AA	99AA	1/26/99	01AA	01AA	1/12/01
BB	BB	2/11/99	BB	BB	2/13/01
CC	CC	3/12/99	CC	CC	3/8/01
DC	DC	3/25/99	DC	DC	3/22/01

TABLE B30. MOB FILES SUMMARY Section 390112 UT Page 2

NEW FILE	OLD FILE	DATE COLLECTED	NEW FILE	OLD FILE	DATE COLLECTED
39SM01ED	39SM01ED	4/5/01			
FD	FD	4/19/01			
GE	GE	5/17/01			
HF	HF	6/14/01			
IG	IG	7/17/01			
JH	JH	8/9/01			
KI	KI	9/11/01			
LJ	LJ	10/15/01			
MK	MK	11/12/01			
NL	NL	12/20/01			
02AA	02AA	1/10/02			
BB	BB	2/8/02			
CC	CC	3/8/02			
DC	DC	3/22/02			
ED	ED	4/5/02			
FD	FD	4/18/02			
GE	GE	5/15/02			
HF	HF	6/17/02			
IG	IG	7/30/02			
JH	JH	8/8/02			
KI	KI	9/14/02			
LJ	LJ	10/21/02			
MK	MK(1)	11/23/02			
NL	NL	12/17/02			
03AA	03AA	1/18/03			

TABLE B31. MOB FILES SUMMARY Section 390104 UT Page 1

NEW FILE	OLD FILE	DATE COLLECTED	NEW FILE	OLD FILE	DATE COLLECTED
39SN96AG	39SN96AH(5)	7/31/96	39SN98KL	39SN98KL	12/15/98
BH	AH	8/15/96	99AA	99AA	1/26/99
CI	BI	9/19/96	BB	BB	2/11/99
DJ	CJ	10/16/96	CC	CC	3/12/99
EK	DK	11/20/96	DC	DC	3/25/99
FL	EL	12/18/96	ED	ED	4/8/99
97AA	97AA	1/24/97	FD	FD	4/22/99
BB	BB	2/19/97	GE	GE	5/20/99
CC	CC	3/12/97	HF	HF	6/18/99
DC	DC	3/26/97	IG	IG	7/20/99
ED	ED	4/10/97	JH	JH	8/11/99
FD	FD	4/24/97	KI	KI	9/16/99
GE	GE	5/22/97	LJ	LJ	10/14/99
HF	HF	6/19/97	MK	MK	11/12/99
IH	JH(2)	8/6/97	NL	NL	12/22/99
JI	KI(1)	9/11/97	00AA	00AA	1/17/00
KJ	LJ	10/23/97	BB	BB	2/15/00
LK	MK	11/20/97	CC	CC	3/7/00
ML	NL	12/17/97	DC	DC	3/23/00
98AA	98AA	1/20/98	ED	ED	4/6/00
BB	BB	2/14/98	FD	FD	4/25/00
CC	CC	3/12/98	GE	GE	5/25/00
DD	DD	4/24/98	HF	HF	6/16/00
EE	EE	5/14/98	IG	IG	7/19/00
FG	FG	7/11/98	JH	JH	8/10/00
Bad read. GH	GH	8/12/98	KI	KI	9/22/00
HI	HI	9/29/98	LJ	LJ	10/14/00
IJ	IJ	10/15/98	MK	MK	11/11/00
JK	JK	11/23/98	NL	NL	12/15/00

TABLE B31. MOB FILES SUMMARY Section 390104 UT Page 2

NEW FILE	OLD FILE	DATE COLLECTED	NEW FILE	OLD FILE	DATE COLLECTED
39SN01AA	39SN 01AA	1/12/01			
BB	BB	2/13/01			
CC	CC	3/8/01			
DC	DC	3/22/01			
ED	ED	4/5/01			
FD	FD	4/19/01			
GE	GE	5/17/01			
HF	HF	6/14/01			
IG	IG	7/17/01			
JH	JH	8/9/01			
KI	KI	9/11/01			
LJ	LJ	10/15/01			
MK	MK	11/12/01			
NL	NL	12/20/01			
02AA	02AA	1/10/02			
BB	BB	2/8/02			
CC	CC	3/8/02			
DC	DC	3/22/02			
ED	ED	4/5/02			
FD	FD	4/18/02			
GE	GE	5/15/02			
HF	HF	6/17/02			
IG	IG	7/30/02			
JH	JH	8/8/02			
KI	KI	9/14/02			
LJ	LJ	10/21/02			
MK	MK	11/23/02			
NL	NL	12/17/02			
03AA	03AA	1/18/03			

TABLE B32. MOB FILES SUMMARY Section 390101 UT Page 1

NEW FILE	OLD FILE	DATE COLLECTED	NEW FILE	OLD FILE	DATE COLLECTED
DELETE	M390101	7/26/96			
39SO96AG	39SO96AI(2)	7/26/96			
BH	AI(3)	8/2/96			
CH	AI(4)	8/15/96			
DI	AI(5)	9/19/96			
EJ	BJ	10/16/96			
FK	CK	11/20/96			
GL	DL	12/18/96			
DELETE	97AA	NO DATE			
97AB	97BB(2)	2/19/97			
BC	CC	3/12/97			
CC	DC	3/26/97			
DD	ED	4/10/97			
ED	FD	4/24/97			
FE	GE	5/22/97			
GF	HF	6/19/97			

TABLE B33. MOB FILES SUMMARY **Section 390102 CWRU Page 1**

NEW FILE	OLD FILE	DATE COLLECTED	NEW FILE	OLD FILE	DATE COLLECTED
39SP96AG	39SP96AG	7/25/96			
BH	BH	8/2/96			
CH	CH	8/15/96			
PAVEMENT	FAILED				

TABLE B34. MOB FILES SUMMARY Section 390108 OSU Page 1

NEW FILE	OLD FILE	DATE COLLECTED	NEW FILE	OLD FILE	DATE COLLECTED
39SQ96AG	39SQ96BH	7/25/96	39SQ99DE	39SQ99QE	5/20/99
BH	BH	8/2/96	EF	RF	6/25/99
CH	CH	8/15/96	FG	SG	7/16/99
DI	DI	9/11/96	DELETE	TH	BAD
EI	EI	9/24/96	GI	UI	9/14/99
FJ	FJ	10/1/96	HJ	VJ	10/15/99
GJ	FJ	10/22/96	IK	VK	11/12/99
HK	GK	11/18/96	JK	WK	11/19/99
IL	HL	12/16/96	00AA	00AA	1/14/00
97AB	97AB	2/6/97	BB	BB	2/16/00
BB	BB	2/20/97	CC	CC	3/22/00
CC	CC	3/26/97	DD	DD	4/20/00
DD	DD	4/8/97	ED	DE	4/28/00
ED	DD	4/22/97	FE	EE	5/15/00
FE	EE	5/20/97	GF	FF	6/26/00
GF	FF	6/16/97	HG	GG	7/20/00
HG	GG	7/11/97	IH	HH	8/15/00
DELETED	HH	NO DATE	JI	II	9/7/00
II	II	9/3/97	KJ	JJ	10/12/00
JL	NL	12/13/97	LK	KK	11/14/00
98AA	98AA	1/16/98	MK	KL	11/21/00
BF	FF	6/8/98	NL	LL	12/19/00
DELETED	GG	BAD FILE	01AA	01AA	1/18/01
CI	II	9/29/98	BB	BB	2/15/01
DJ	JJ	10/23/98	CC	CC	3/8/01
EL	LL	12/28/98	DC	CD	3/22/01
99AA	99MA	1/28/99	ED	DD	4/9/01
BB	NB	2/18/99	FD	DE	4/24/01
CC	OC_1	3/15/99	GE	EE	5/17/01

TABLE B34. MOB FILES SUMMARY **Section 390108 OSU Page 2**

NEW FILE	OLD FILE	DATE COLLECTED	NEW FILE	OLD FILE	DATE COLLECTED
39SQ01HF	39SQ01FF	6/20/01			
IG	GG	7/2/01			
JG	GH	7/24/01			
KH	HH	8/21/01			
LI	II	9/11/01			
MJ	JJ	10/9/01			
NK	KL	11/6/01			
OL	LL	12/10/01			
02AA	02AA	1/10/02			
BB	BB	2/14/02			
CC	CC	3/14/02			
DD	DD	4/10/02			
ED	DE	4/29/02			
FE	EE	5/22/02			
GF	FF	6/19/02			
HG	GG	7/26/02			
IH	HH	8/21/02			
JI	II	9/23/02			
KJ	JJ	10/18/02			
LK	KK	11/15/02			
ML	LL	12/18/02			
03AA	03AA	1/15/02			
BB	BB	2/20/02			

TABLE B35. MOB FILES SUMMARY Section 390110 OU Page 1

NEW FILE	OLD FILE	DATE COLLECTED	NEW FILE	OLD FILE	DATE COLLECTED
39SR96AH	39SR96AH	8/2/96	39SR98JK	39SR98TK	11/20/98
BH	AH	8/15/96	KL	UL	12/17/98
CI	BI	9/23/96	99AA	99VM	1/19/99
DJ	CJ	10/15/96	DELETE	WB	NOTHING
EK	DK	11/26/96	BC	XC	3/8/99
FL	EL	12/17/96	CC	YC	3/24/99
97AB	97BB	2/18/97	DD	ZD	4/4/99
BC	CC	3/11/97	ED	AD	4/26/99
CC	DC	3/25/97	FE	BE	5/14/99
DELETE	ED	NOTHING	GF	DF	6/11/99
DD	FD	4/21/97	HG	FG	7/21/99
EE	GE	5/23/97	IH	GH	8/12/99
FF	HF	6/16/97	JI	HI	9/22/99
GG	IG	7/10/97	KJ	IJ	10/15/99
HH	JH	8/5/97	LK	JK	11/19/99
II	KI	9/11/97	00AA	100K	1/4/00
JJ	LJ	10/23/97	BB	100L	2/16/00
KK	MK	11/14/97	CC	100M	3/22/00
LL	NL	12/12/97	DD	100N	4/18/00
98AA	98AA	1/20/98	EE	OE	5/15/00
BB	BB	2/24/98	FF	PF	6/13/00
CC	CC	3/18/98	GG	QG	7/20/00
DD	DD	4/14/98	HI	RI	9/21/00
DELETE	GF	NOTHING	IK	SK	11/16/00
EF	IH	6/18/98	DELETE	TL	Bad 12/20/00
FG	IH	7/9/98	01AA	01UA	1/18/01
GH	IH	8/24/98	BB	VB	2/16/01
HI	SI	9/17/98	CC	WC	3/14/01
IJ	SJ	10/14/98	DD	XD	4/16/01

TABLE B35. MOB FILES SUMMARY Section 390110 OU Page 2

NEW FILE	OLD FILE	DATE COLLECTED	NEW FILE	OLD FILE	DATE COLLECTED
39SR01EF	39SR01YF	6/1/01			
FF	ZF	6/20/01			
GG	AG	7/23/01			
HH	AH	8/23/01			
IJ	BJ	10/18/01			
JK	CK	11/8/01			
KL	DL	12/19/01			
02AA	02EA	1/22/02			
BB	FB	2/19/02			
CC	GC	3/3/02			

TABLE B36. MOB FILES SUMMARY Section 390162 OU Page 1

NEW FILE	OLD FILE	DATE COLLECTED	NEW FILE	OLD FILE	DATE COLLECTED
39SZ97AL	M390162	12/12/97	39SZ00GG	39SZ00NG	7/20/00
98AA	M390162A	1/20/98	HI	PI	9/21/00
BB	M390162B	2/24/98	IJ	QJ	10/11/00
CC	M390162C	3/18/98	JK	QK	11/16/00
DELETE	39SZ98DD	NOTHING	KL	QL	12/20/00
DD	HH	4/17/98	01AA	01RA	1/18/01
EH	HH	8/24/98	BB	SB	2/16/01
FI	AI	9/17/98	CC	SC	3/14/01
GJ	AJ	10/14/98	DD	TD	4/16/01
HK	TK	11/20/98	EF	TF	6/1/01
IL	UL	12/17/98	FF	UF	6/20/01
99AA	VM	1/19/99	GG	VG	7/23/01
BB	WB	2/17/99	HI	XI	9/20/01
CC	WC	3/8/99	IJ	YJ	10/18/01
DC	XC	3/24/99	JK	YK	11/8/01
ED	ZD	4/14/99	KL	ZL	12/19/01
FD	ZD	4/26/99	02AA	02AA	1/22/02
GE	AE	5/14//99	BB	BB	2/19/02
HG	CG	7/21/99	CG	FG	7/24/02
IH	DH	8/12/99	DJ	JJ	10/24/02
JI	EI	9/19/99	EL	KL	12/4/02
KJ	FJ	10/15/99	03AA	03AA	1/8/03
LK	GK	11/19/99			
00AA	100H	1/4/00			
BB	100I	2/16/00			
CC	100J	3/22/00			
DD	100K	4/18/00			
EE	00LE	5/15/00			
FF	MF	6/13/00			

THIS PAGE LEFT INTENTIONALLY BLANK

APPENDIX B3

WEATHER STATION FILES SUMMARY

TABLE B37. AWS FILES SUMMARY 39A Section 0203 Page 1

FILE	FROM			TO		
	YEAR	DAY	HOUR	YEAR	DAY	HOUR
3902W201.294	1994	251	1500	1994	354	1400
310.395	“	251	1500	1995	90	1700
200.795	“	251	1500	“	113	1300
Gap 030.895	1995	183	1100	“	215	1800
140.895	“	215	1900	“	226	1500
121.095	“	215	1900	“	285	1200
220.196	“	285	1300	1996	22	1300
050.496	1996	22	1400	“	96	1500
050.696	“	22	1400	“	157	1100
200.796	“	22	1400	“	202	1400
150.896	“	22	1400	“	228	1700
190.996	“	35	400	“	263	1000
201.296	“	127	1800	“	355	1600
230.597	“	281	1700	1997	143	1200
090.997	1997	143	1300	“	252	1600
220.198	“	154	1515	1998	22	1200
180.698	“	306	500	“	169	1400
300.798	“	347	500	“	211	1000
191.198	1998	101	100	“	323	1400
040.399	“	196	600	1999	63	1200
280.599	“	282	1400	“	148	800
260.899	1999	75	2100	“	238	1100
031.199	“	238	1200	“	307	1700
130.100	“	238	1200	2000	13	1500
070.300	2000	13	1600	“	67	1500
160.800	“	13	1600	“	229	1400
110.101	“	147	2400	2001	11	1100
190.601	“	309	1400	“	170	1600
151.101	2001	92	100	“	319	1300

TABLE B37. AWS FILES SUMMARY 39A Section 0203 Page 2

FILE	FROM			TO		
	YEAR	DAY	HOUR	YEAR	DAY	HOUR
3902W220.202	2001	188	1800	2002	53	1900

THIS PAGE LEFT INTENTIONALLY BLANK

APPENDIX C

DEPTH OF FROST PENETRATION ESTIMATIONS

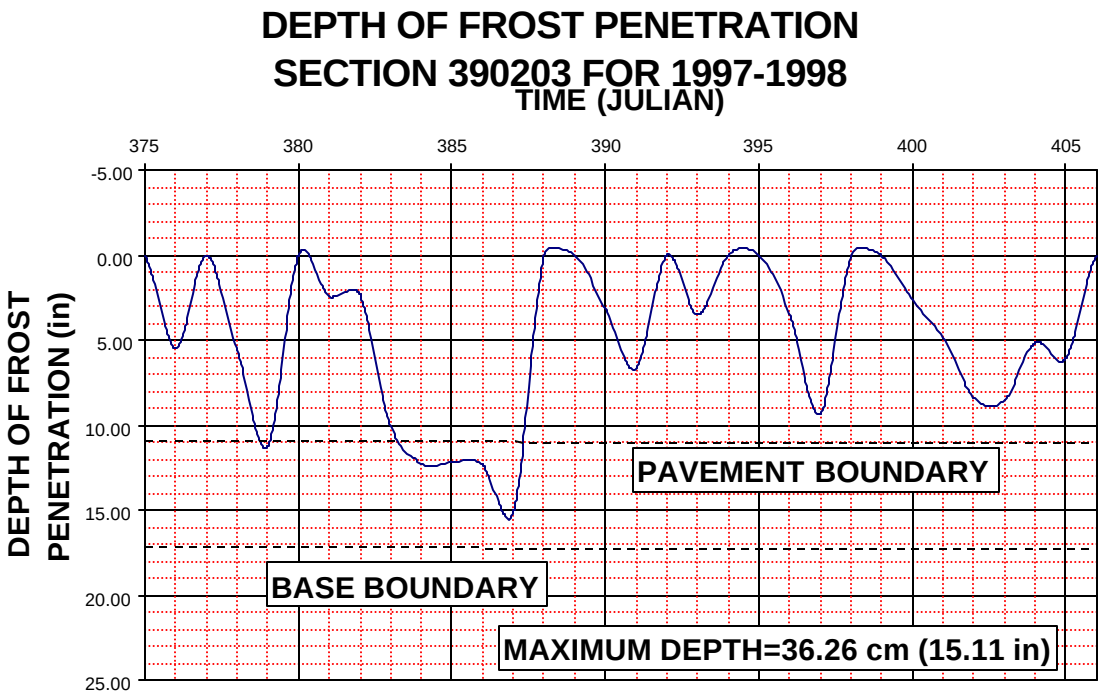

Figure C.1. Depth of Frost Penetration vs. Time [1997-1998]

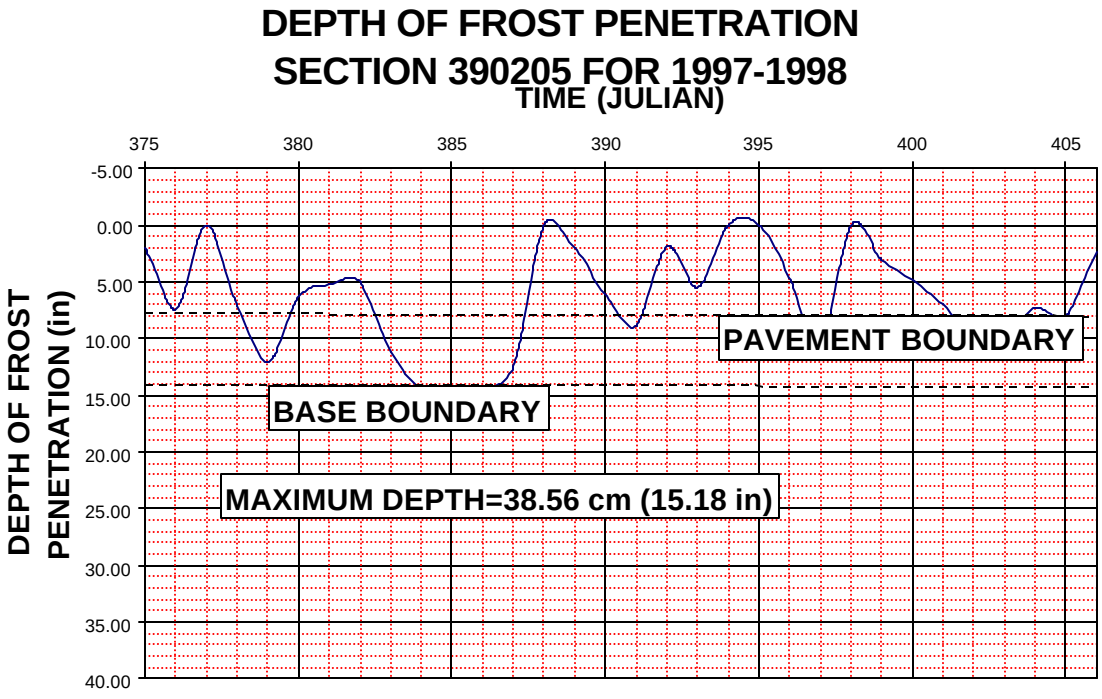

Figure C.1. Depth of Frost Penetration vs. Time [1997-1998] (cont.)

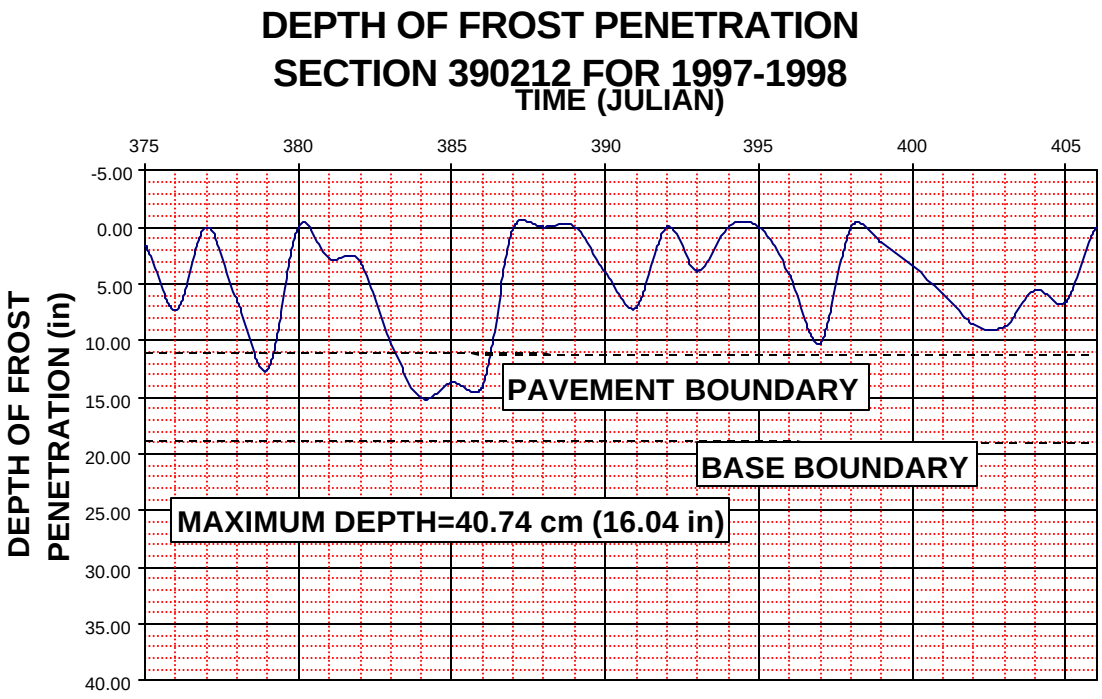

Figure C.1. Depth of Frost Penetration vs. Time [1997-1998] (cont.)

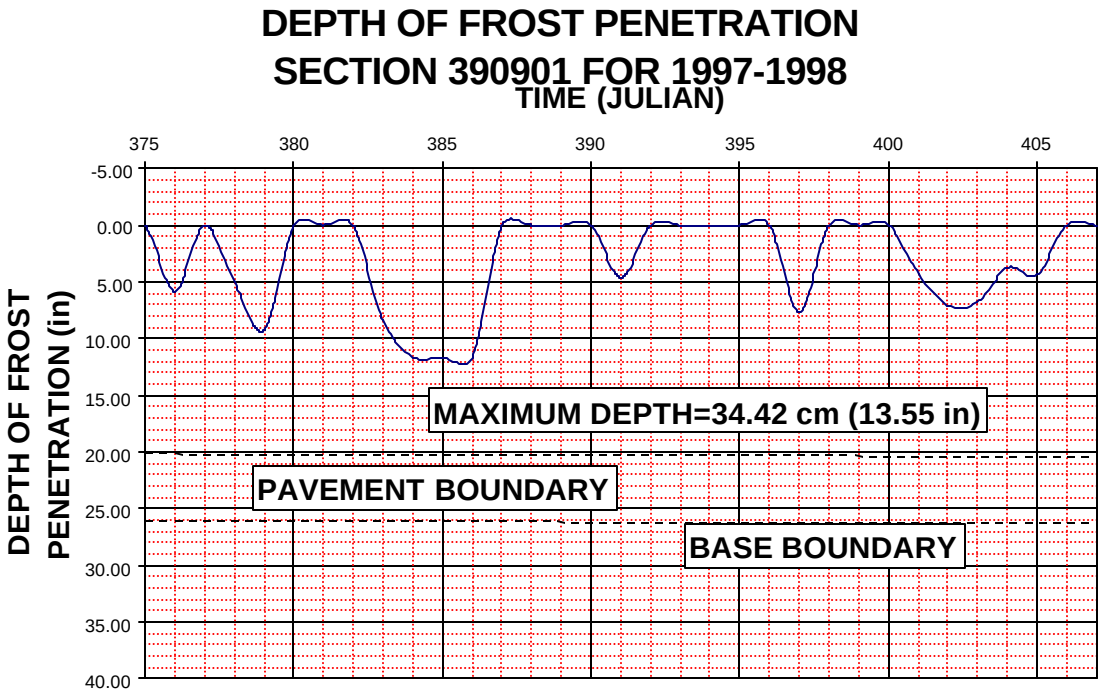

Figure C.1. Depth of Frost Penetration vs. Time [1997-1998] (cont.)

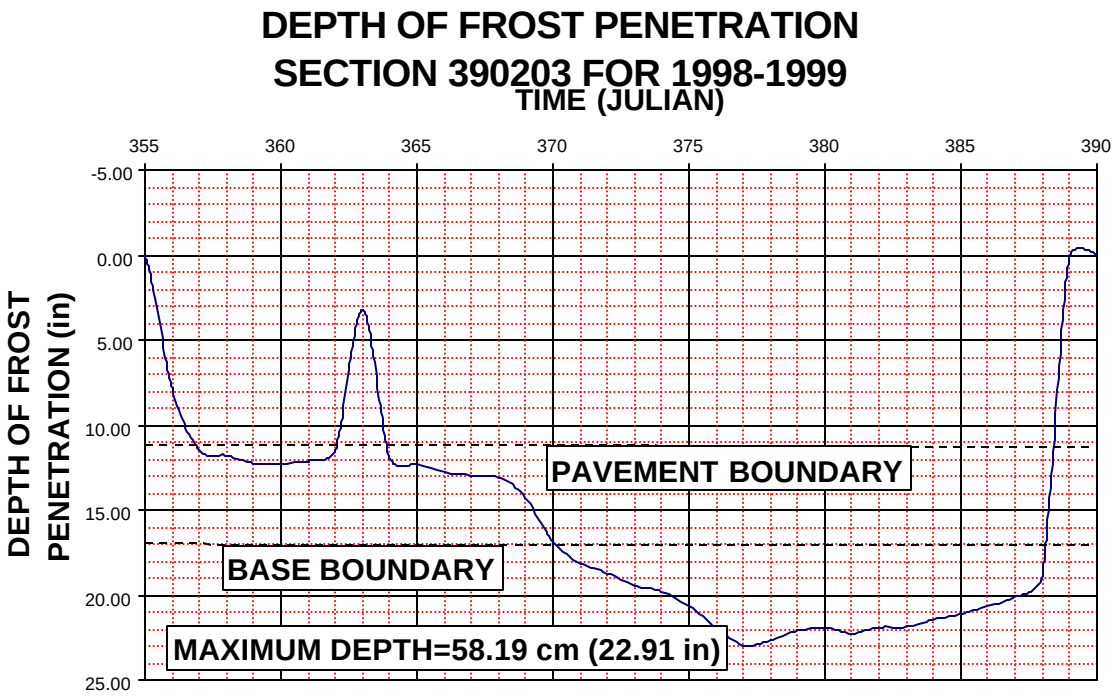

Figure C.2. Depth of Frost Penetration vs. Time [1998-1999]

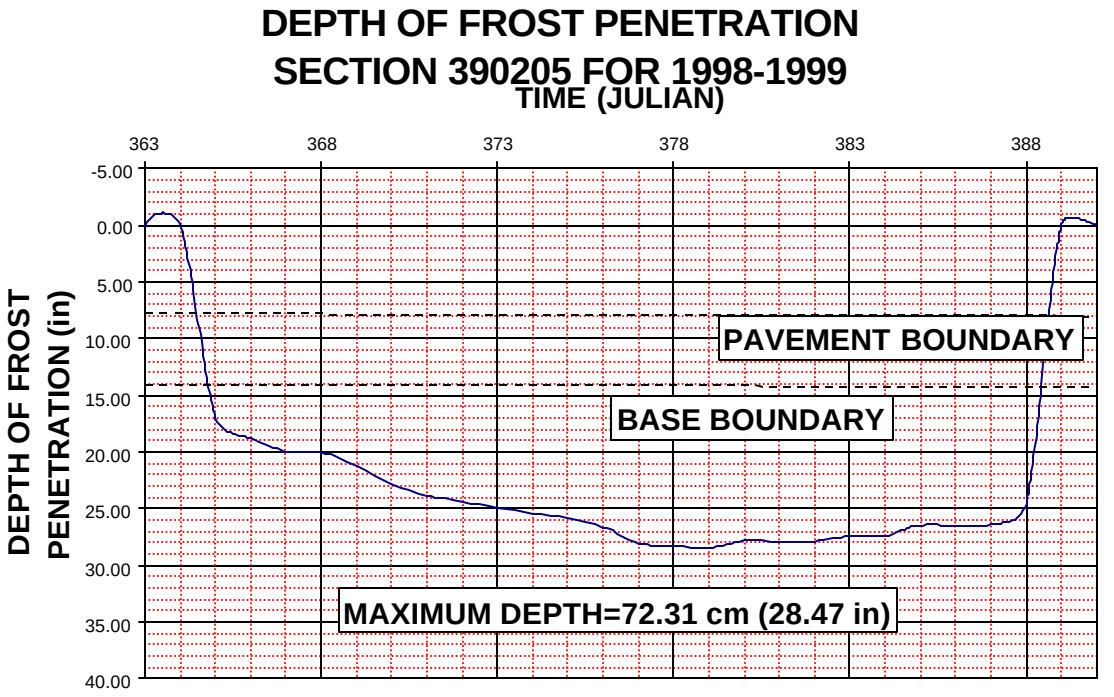

Figure C.2. Depth of Frost Penetration vs. Time [1998-1999] (cont.)

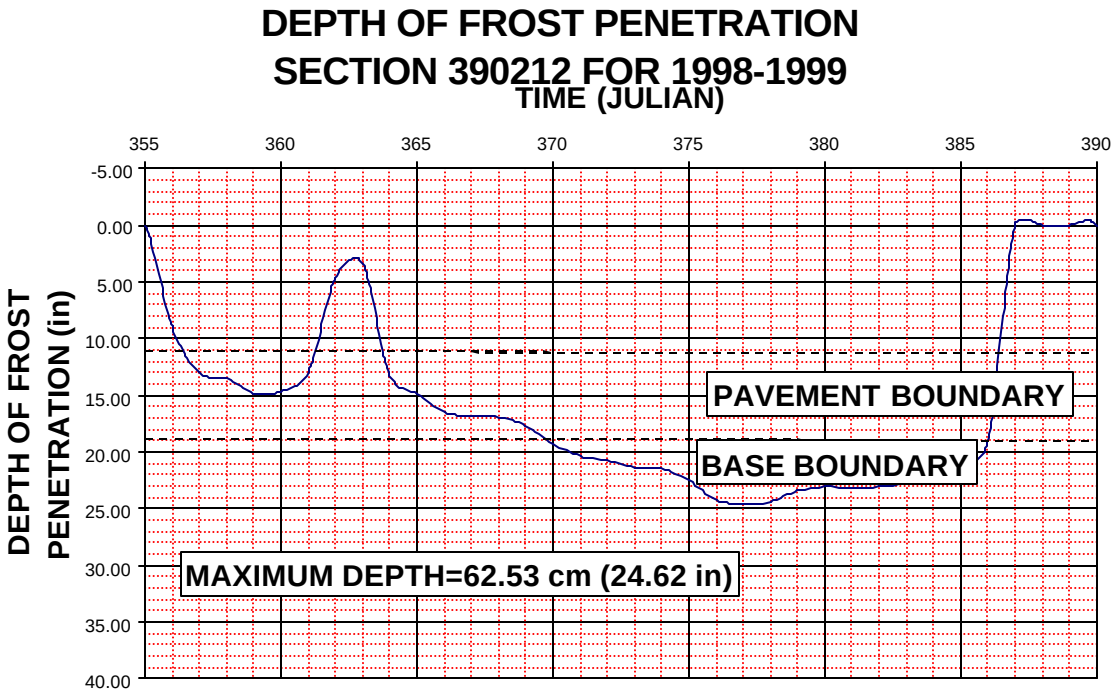

Figure C.2. Depth of Frost Penetration vs. Time [1998-1999] (cont.)

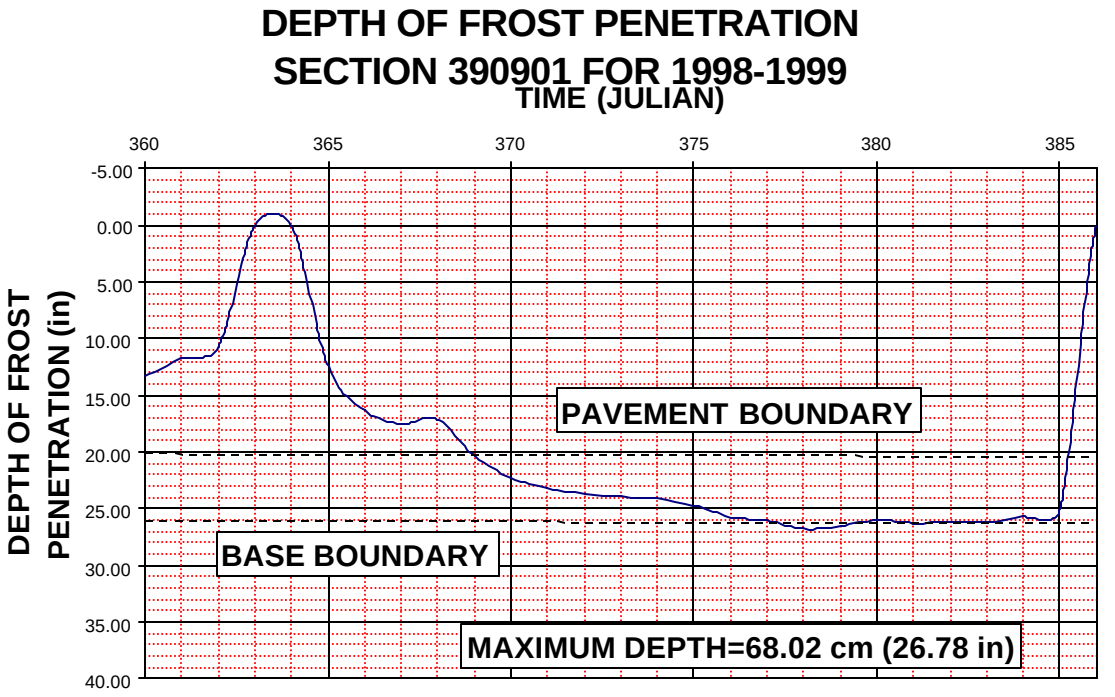

Figure C.2. Depth of Frost Penetration vs. Time [1998-1999] (cont.)

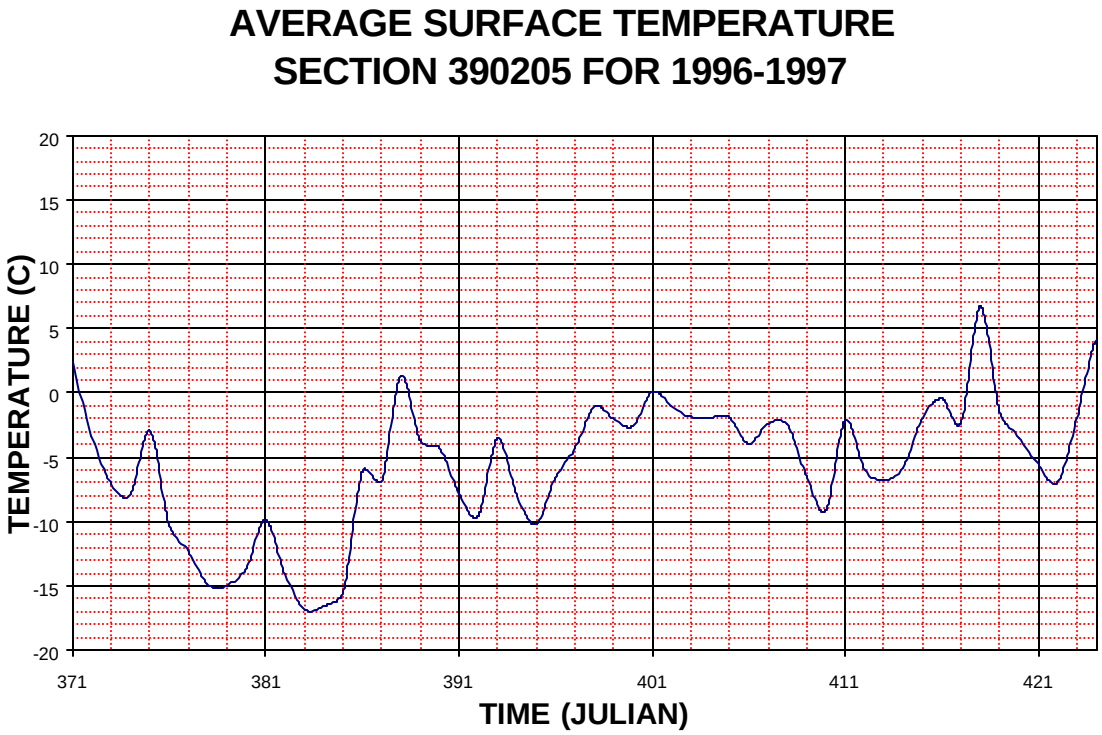

Figure C.3. Surface Temperature vs. Time [1996-1997]

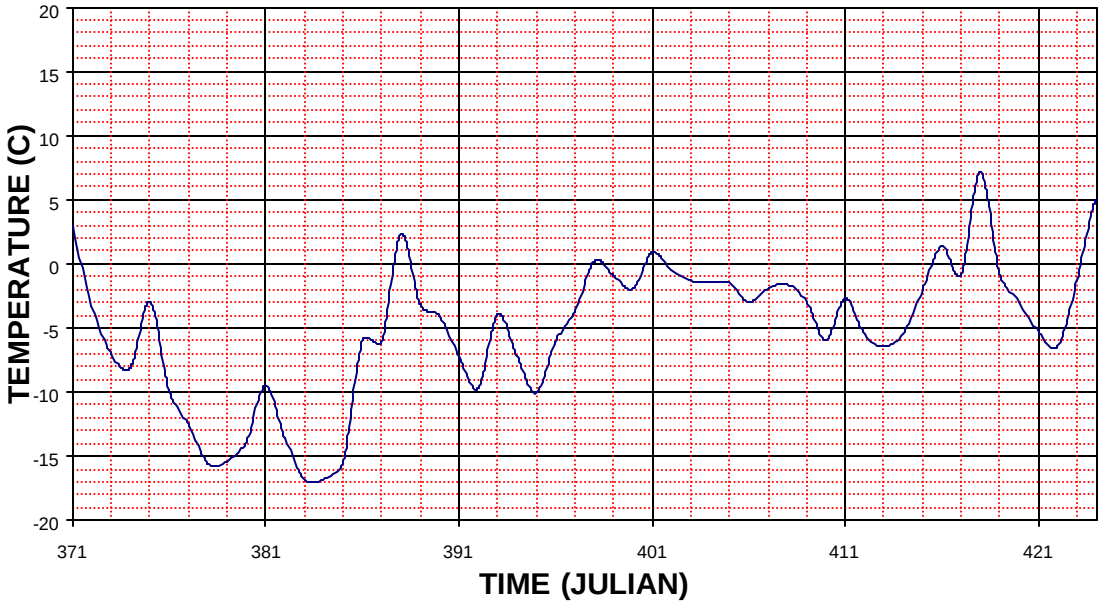

Figure C.3. Surface Temperature vs. Time [1996-1997] (cont.)

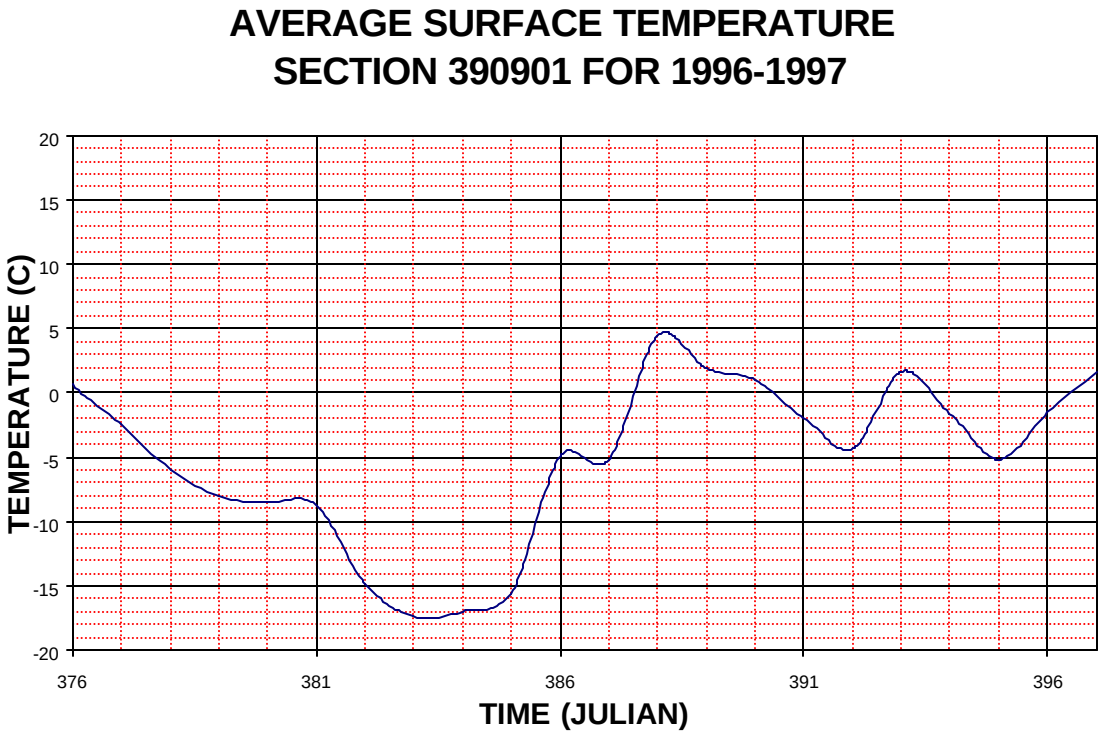

Figure C.3. Surface Temperature vs. Time [1996-1997] (cont.)

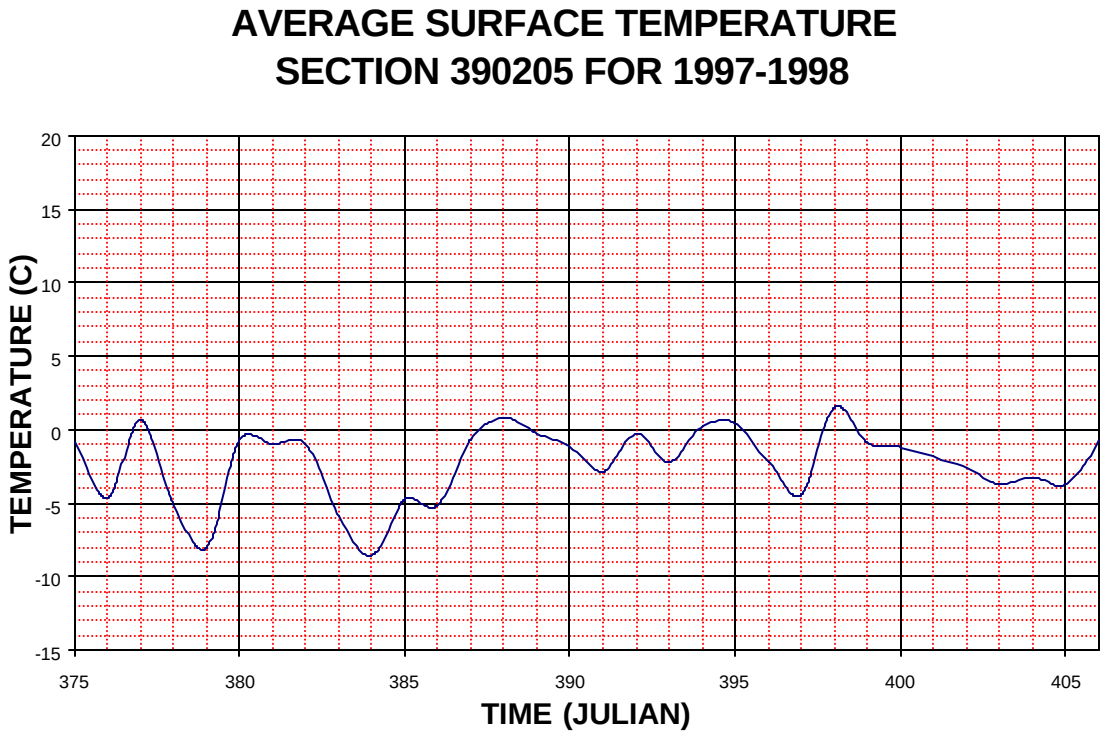

Figure C.4. Surface Temperature vs. Time [1997-1998]

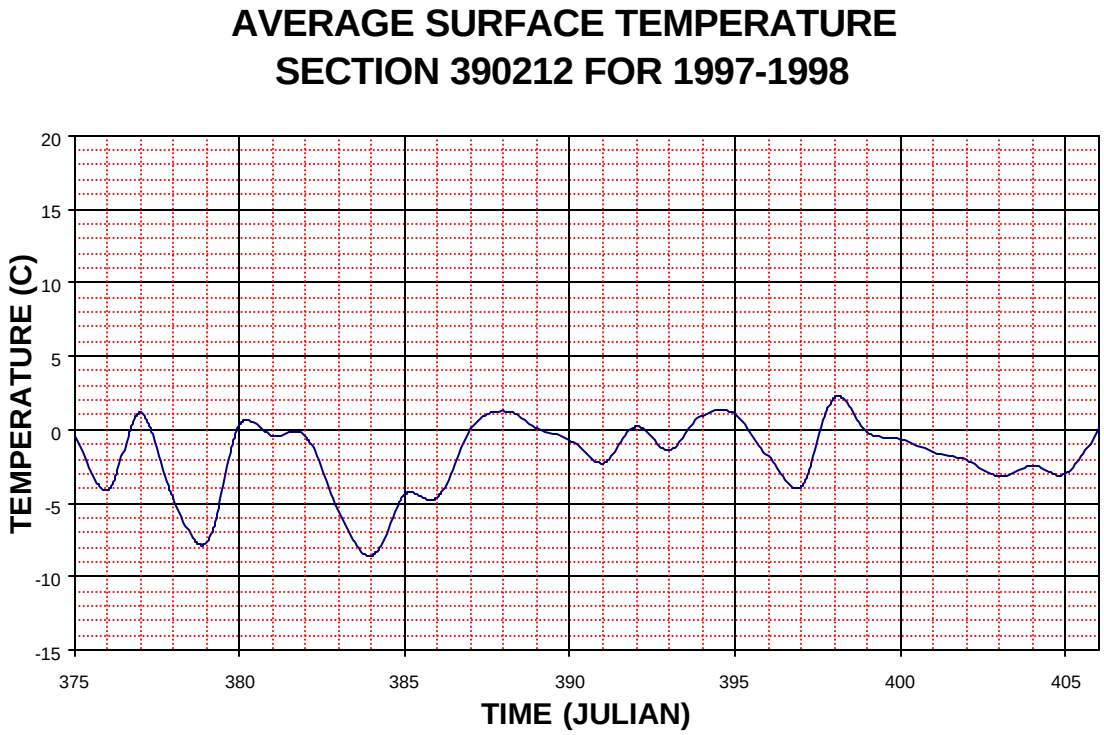

Figure C.4. Surface Temperature vs. Time [1997-1998] (cont.)

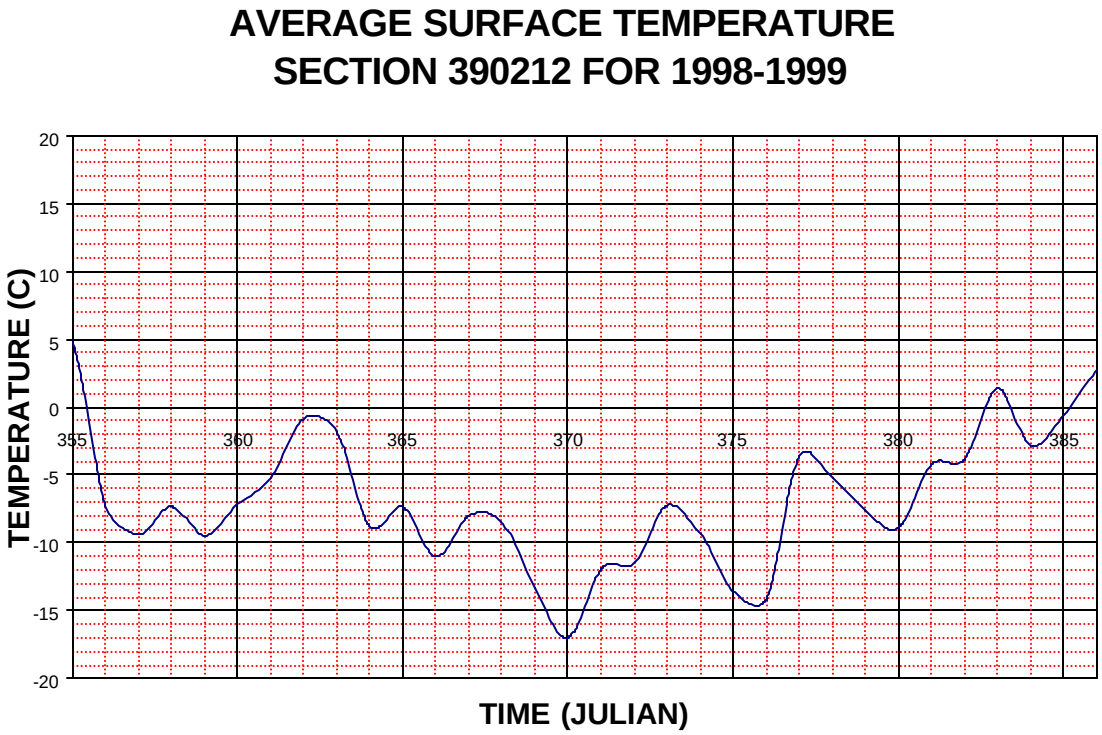

Figure C.5. Surface Temperature vs. Time [1998-1999]

THIS PAGE LEFT INTENTIONALLY BLANK

APPENDIX D

SOIL SATURATION READINGS

AND RAINFALL DATA

Table D.1. Sensor Saturation Values for Section 390203

YEAR	MONTH	DAY	JULIAN	S1	S2	S3	S4	S5	S6	S7	S8	S9	S10
1996	JULY	22	204	69.9	95.1	94.8	100.0	100.0	99.7	99.7	98.5	97.7	100.0
1996	AUG.	5	218	56.3	95.1	96.0	100.0	99.9	99.7	100.0	98.5	99.1	100.0
1996	SEPT.	19	263	75.9	93.8	92.3	96.6	97.2	98.2	99.7	98.5	97.7	98.8
1996	OCT.	15	288	56.3	87.2	91.0	96.6	97.2	98.2	98.2	96.9	97.7	100.0
1996	NOV.	19	324	77.4	85.9	91.0	94.0	94.4	92.1	92.1	95.4	96.3	100.0
1996	DEC.	21	356	39.2	84.5	91.0	92.7	90.2	87.4	89.0	95.4	97.7	97.4
1997	JAN.	16	16	2.7	56.6	68.1	81.7	88.8	87.4	90.6	95.4	97.7	98.8
1997	FEB.	16	47	47.6	81.8	88.5	91.4	90.2	89.0	90.6	92.2	100.0	100.0
1997	MAR.	11	70	69.9	84.5	89.8	90.0	88.8	90.6	90.6	95.4	100.0	
1997	MAR.	23	113	59.3	84.5	88.5	88.7	85.9	89.0	90.6	93.8	100.0	98.8
1997	APR.	9	99	56.3	85.9	89.8	90.0	91.6	92.1	92.1	96.9	100.0	
1997	APR.	25	115	71.4	84.5	88.5	90.0	90.2	93.7	90.6	96.9	100.0	98.8
1997	MAY	23	143	66.8	87.2	91.0	92.7	94.4	95.2	95.2	95.4	100.0	100.0
1997	JUNE	17	168	75.9	92.5	94.8	95.3	95.8	98.2	96.7	98.5	100.0	100.0
1997	AUG.	5	217	77.4	95.1	96.0	97.9	98.5	98.2	100.0	100.0	100.0	100.0
1997	SEPT.	9	252	49.0	93.8	96.0	100.0	98.5	100.0	100.0	98.5	100.0	100.0
1997	OCT.	16	289	46.2	88.6	96.0	97.9	95.8	99.7	100.0	98.5	100.0	100.0
1997	NOV.	20	324	49.0	85.9	92.3	92.7	91.6	92.1	93.7	96.9	100.0	100.0
1997	DEC.	15	349	57.8	85.9	93.6	92.7	90.2	93.7	93.7	93.8	100.0	100.0
1998	JAN.	22	22	56.3	88.6	93.6	91.4	91.6	92.1	93.7	93.8	99.1	100.0
1998	FEB.	24	55	71.4	87.2	91.0	91.4	90.2	92.1	93.7	93.8	100.0	100.0
1998	MAR.	31	90	89.4	89.9	93.6	94.0	93.0	95.2	95.2	96.9	100.0	100.0
1998	APR.	17	107	92.3	89.9	94.8	94.0	94.4	92.1	95.2	98.5	100.0	100.0
1998	MAY	20	140	63.8	98.8	96.0	100.0	100.0	95.2	96.7	98.5	100.0	100.0
1998	JUNE	18	169	74.4	98.8	97.2	97.9	98.5	96.7	95.2	96.9	100.0	100.0
1998	JULY	21	202	65.3	100.0	100.0	99.1	100.0	100.0	100.0	100.0	100.0	100.0
1998	AUG.	19	231	53.4	100.0	100.0	100.0	100.0	100.0	100.0			
1998	SEPT.	17	260	46.2	100.0	100.0	100.0	99.9	100.0	100.0	100.0	100.0	100.0
1998	OCT.	20	293	66.8	92.5	100.0	96.6	97.2	100.0	99.7	100.0	100.0	100.0
1998	NOV.	19	323	40.6	89.9	96.0	96.6	97.2	96.7	98.2	100.0	100.0	100.0
1998	DEC.	15	349	37.8	88.6	98.4	97.9	94.4	96.7	98.2	100.0	99.1	100.0
1999	JAN.	21	21	89.4	100.0	98.4	90.0	85.9	92.1	96.7	98.5		100.0
1999	FEB.	16	47	75.9	92.5	91.0	95.3	90.2	96.7	96.7	100.0		100.0
1999	MAR.	4	63	86.4	93.8	92.3	96.6	91.6	96.7	95.2	96.9		100.0
1999	MAR.	20	79	71.4	95.1	93.6	96.6	91.6	96.7	96.7	95.4		100.0
1999	APR.	8	98	80.5	98.8	98.4	100.0	99.9	99.7	95.2	96.9		100.0
1999	APR.	22	112	98.0	100.0	99.6	100.0	93.0	100.0	99.7	98.5		100.0
1999	MAY	19	139	65.3	100.0	100.0	94.0	100.0	100.0	100.0	100.0	100.0	
1999	JUNE	15	166	90.9	100.0	100.0	100.0	100.0	100.0	100.0	100.0	100.0	100.0
1999	JULY	15	196	59.3	100.0	100.0	100.0	100.0	100.0	100.0	100.0	100.0	100.0
1999	AUG.	24	236	56.3	100.0	100.0	100.0	100.0	100.0	100.0	100.0	100.0	100.0
1999	SEPT.	16	259	53.4	100.0	100.0	100.0	100.0	100.0	100.0	100.0	100.0	100.0
1999	OCT.	11	284	78.9	100.0	100.0	100.0	100.0	100.0	100.0	100.0	100.0	100.0

1999	NOV.	18	322	39.2	92.5	99.6	96.6	98.5	100.0	100.0	100.0	100.0	100.0
1999	DEC.	8	342	80.5	91.2	98.4	95.3	93.0	98.2	100.0	100.0	100.0	100.0
2000	JAN.	13	13	68.3	85.9	89.8	87.3	91.6	89.0	98.2	96.9		
2000	FEB.	12	43	100.0	100.0	93.6	88.7	85.9	89.0	96.7	93.8		
2000	MAR.	7	67	66.8	100.0	98.4	92.7	90.2	89.0	100.0	96.9		
2000	MAR.	23	83	90.9	100.0	94.8	94.0	90.2	95.2	96.7	100.0		
2000	APR.	4	95	86.4	100.0	100.0	92.7	95.8	95.2	96.7	96.9		
2000	APR.	20	111	85.0	100.0	100.0	95.3	98.5	96.7	100.0	100.0		
2000	MAY	22	143	90.9	100.0	100.0	96.6	100.0	100.0	100.0	100.0		
2000	JUNE	19	171	87.9	100.0	100.0	100.0	100.0	99.7	100.0	100.0		
2000	JULY	21	203	63.8	100.0	100.0	100.0	100.0	100.0	100.0	100.0		100.0
2000	AUG.	16	229	63.8	100.0	100.0	100.0	100.0	100.0	100.0	100.0		100.0
2000	SEPT.	18	262	66.8	100.0	100.0	100.0	100.0	100.0	100.0	100.0		100.0
2000	OCT.	17	291	66.8	100.0	100.0	100.0	100.0	100.0	100.0	100.0		100.0
2000	NOV.	11	316	66.8	100.0	100.0	100.0	100.0	100.0	100.0	100.0		100.0
2000	DEC.	9	344	57.8	89.9	97.2	92.7	91.6	98.2	100.0	100.0		100.0
2001	JAN.	11	11		31.5	61.2	71.8	78.6	89.0	93.7	100.0		64.9
2001	FEB.	13	44	78.9	100.0	84.5	88.7	91.6	90.6	98.2	100.0		
2001	MAR.	7	66	66.8	100.0	89.8	90.0	87.4	90.6	96.7	95.4		
2001	MAR.	20	79	87.9	100.0	94.8	85.9	87.4	90.6	96.7	95.4		
2001	APR.	5	95	83.5	97.6	96.0	91.4	91.6	95.2	98.2	96.9		
2001	APR.	19	109	87.9	96.3	100.0	92.7	91.6	96.7	98.2	100.0		
2001	MAY	17	137	83.5	100.0	100.0	100.0	99.9	100.0	100.0	100.0		
2001	JUNE	19	170	82.0	100.0	100.0	100.0	100.0	100.0	100.0	100.0		
2001	JULY	19	200	80.5	100.0	100.0	100.0	100.0	100.0	100.0	100.0		100.0
2001	AUG.	15	227		100.0	100.0	100.0	100.0	100.0	100.0	100.0	100.0	100.0
2001	SEPT.	13	256	72.9	100.0	100.0	100.0	100.0	100.0	100.0	100.0	100.0	100.0
2001	OCT.	11	284	65.3	96.3	100.0	100.0	99.9	100.0	100.0	100.0	100.0	100.0
2001	NOV.	15	319	47.6	88.6	100.0	100.0	99.9	100.0	100.0	100.0	100.0	100.0
2001	DEC.	19	353	80.5	85.9	98.4	94.0	98.5	100.0	100.0	100.0	100.0	100.0
2002	JAN.	22	22	68.3	81.8	91.0	83.1	88.8	93.7	100.0	98.5		
2002	FEB.	22	53	75.9	81.8	87.2	85.9	88.8	96.7	100.0	92.2		
2002	MAR.	7	66	82.0	84.5	88.5	88.7	97.2	98.2	100.0	100.0		
2002	MAR.	22	81	78.9	87.2	93.6	94.0	94.4	98.2	100.0	100.0		
2002	APR.	5	95	82.0	87.2	91.0	91.4	88.8	96.7	99.7	96.9		
2002	APR.	25	115	87.9	87.2	96.0	94.0	97.2	100.0	100.0	100.0		
2002	MAY	16	136	82.0	95.1	98.4	99.1	99.9	100.0	100.0	100.0		100.0
2002	JUNE	11	162	78.9	100.0	100.0	97.9	99.9	100.0	100.0	100.0	100.0	100.0
2002	JULY	17	198	49.0	100.0	100.0	100.0	100.0	100.0	100.0	100.0	100.0	100.0
2002	AUG.	20	232	69.9	100.0	100.0	100.0	100.0	100.0	100.0	100.0	100.0	100.0
2002	SEPT.	19	262	75.9	100.0	100.0	100.0	100.0	100.0	100.0	100.0	100.0	100.0
2002	OCT.	24	297	54.9	92.5	100.0	100.0	98.5	100.0	100.0	100.0	100.0	100.0
2002	NOV.	20	324	74.4	88.6	99.6	99.1	95.8	100.0	100.0	100.0	100.0	100.0
2002	DEC.	17	351	74.4	83.2	88.5	91.4	90.2	98.2	100.0	100.0	100.0	100.0

Table D.2. Sensor Saturation Values for Section 390205

YEAR	MONTH	DAY	JULIAN	S1	S2	S3	S4	S5	S6	S7	S8	S9	S10
1996	AUG.	5	218	90.5	93.6	93.6	93.5	99.9		99.8	100.0	100.0	100.0
1996	AUG.	15	229	93.5	96.6	96.6	94.9	99.9		100.0	100.0	100.0	100.0
1996	SEPT.	19	263	89.1	90.6	92.1	96.3	100.0		100.0	100.0	100.0	100.0
1996	OCT.	15	289	89.1	89.1	93.6	96.3	99.9		100.0	99.9	100.0	100.0
1996	NOV.	19	324	86.1	86.1	90.6	93.5	99.9		96.8	97.3	100.0	100.0
1996	DEC.	21	356	83.1	84.6	87.6	90.5	97.3		93.7	89.0	100.0	100.0
1997	JAN.	16	16	44.8	80.0	84.6	87.6	94.5		93.7	94.5	100.0	100.0
1997	FEB.	16	47	84.6	87.6	87.6	92.0	90.4		92.2	90.4	100.0	100.0
1997	MAR.	11	70	86.1	86.1	86.1	96.3	90.4		92.2	95.9	100.0	
1997	MAR.	23	113	84.6	86.1	87.6	94.9	93.2		93.7	90.4	100.0	100.0
1997	APR.	25	115	86.1	86.1	86.1	94.9	93.2		93.7	93.2	100.0	
1997	MAY	23	143	89.1	87.6	93.6	99.2	94.5		95.3	95.9	100.0	100.0
1997	JUNE	17	168	92.0	92.1	92.1	99.2	95.9		98.3	100.0	100.0	100.0
1997	AUG.	5	217	93.5	95.1	99.5	100.0	100.0		100.0	100.0	100.0	100.0
1997	SEPT.	9	252	94.9	92.1	96.6	100.0	100.0		100.0	100.0	100.0	100.0
1997	OCT.	16	289	93.5	96.6	96.6	100.0	100.0		100.0	100.0	100.0	100.0
1997	NOV.	14	324		90.6	90.6	97.8	98.6		98.3	98.6		100.0
1997	DEC.	15	349	89.1	86.1	90.6	96.3	98.6		99.8	95.9	100.0	100.0
1998	JAN.	22	22	89.1	87.6	95.1	96.3	98.6		96.8	95.9	100.0	100.0
1998	FEB.	24	55	93.5	90.6	93.6	94.9	97.3		93.7	98.6	100.0	100.0
1998	MAR.	31	90	99.2	92.1	98.0	96.3	99.9		96.8	98.6	100.0	100.0
1998	APR.	17	107	100.0	98.0	98.0	97.8	98.6		98.3	97.3	100.0	100.0
1998	MAY	20	140	100.0	100.0	100.0	100.0	100.0		100.0	100.0	100.0	100.0
1998	JUNE	18	169	100.0	100.0	100.0	100.0	100.0		100.0	100.0	100.0	100.0
1998	JULY	21	202	100.0	100.0	100.0	100.0	100.0		100.0	100.0	100.0	100.0
1998	AUG.	19	231	100.0	100.0	100.0	100.0	100.0		100.0			
1998	SEPT.	17	260	100.0	100.0	100.0	100.0	100.0		100.0			
1998	OCT.	20	293	99.2	99.5	100.0	100.0	100.0		100.0	100.0	100.0	100.0
1998	NOV.	19	323	93.5	89.1	99.5	99.2	95.9		99.8	100.0	100.0	100.0
1998	DEC.	15	349	94.9	87.6	100.0	99.2	98.6		100.0	100.0	100.0	100.0
1999	JAN.	21	21	51.9	73.9	89.1	89.1	87.5		99.8	98.6	100.0	100.0
1999	FEB.	16	47	89.1	89.1	98.0	96.3	91.8		95.3	97.3	100.0	100.0
1999	MAR.	4	63	90.5	90.6	96.6	96.3	91.8		98.3	94.5	100.0	100.0
1999	MAR.	20	79	93.5	93.6	98.0	97.8	93.2		98.3	95.9	100.0	
1999	APR.	8	98	93.5	92.1	100.0	97.8	95.9		96.8	97.3	100.0	98.9
1999	APR.	22	112	94.9	95.1	100.0	97.8	94.5		98.3	98.6	100.0	100.0
1999	MAY	19	139	99.2	100.0	100.0	100.0	97.3		100.0	100.0	100.0	100.0
1999	JUNE	15	166	100.0	100.0	100.0	100.0	100.0		100.0	100.0	100.0	
1999	JULY	15	196	100.0	100.0	100.0	100.0	100.0		100.0	100.0	100.0	
1999	AUG.	24	236	100.0	100.0	100.0	100.0	100.0		100.0	100.0	100.0	
1999	SEPT.	16	259	100.0	100.0	100.0	100.0	100.0		100.0	100.0	100.0	
1999	OCT.	11	284	77.1	89.1	100.0	92.0	87.5		100.0	100.0	96.5	
1999	NOV.	18	322	90.5	96.6	100.0	100.0	99.9		100.0	100.0	100.0	

1999	DEC.	8	342	90.5	93.6	100.0	99.2	97.3		98.3	100.0	100.0	
2000	JAN.	13	13	89.1	93.6	98.0	99.2	97.3		100.0	98.6	100.0	
2000	FEB.	21	52	89.1	93.6	92.1	92.0	89.0		93.7	93.2	100.0	
2000	MAR.	7	67	92.0	95.1	100.0	94.9	90.4		95.3	98.6	100.0	
2000	MAR.	23	83	94.9	93.6	100.0	93.5	94.5		95.3	95.9	100.0	
2000	APR.	4	95	90.5	95.1	99.5	100.0	91.8		95.3	97.3	100.0	
2000	APR.	20	111	93.5	93.6	100.0	97.8	94.5		96.8	97.3	100.0	
2000	MAY	22	143	100.0	100.0	100.0	99.2	98.6		100.0	100.0	100.0	
2000	JUNE	19	171	100.0	100.0	100.0	100.0	100.0		100.0	100.0	100.0	
2000	JULY	21	203	100.0	100.0	100.0	100.0	100.0		100.0	100.0	100.0	
2000	AUG.	16	229	100.0	100.0	100.0	100.0	100.0		100.0	100.0	100.0	
2000	SEPT.	18	262	100.0	100.0	100.0	100.0	100.0		100.0	100.0	100.0	
2000	OCT.	17	291	100.0	100.0	100.0	100.0	100.0		100.0	100.0	100.0	
2000	NOV.	11	316	100.0	100.0	100.0	100.0	98.6		100.0	100.0	100.0	
2000	DEC.	9	344	87.6	93.6	100.0	100.0	98.6		100.0	100.0	100.0	
2001	JAN.	11	11	30.5	61.7	86.1	87.6	81.8		93.7	97.3	100.0	
2001	FEB.	13	44	87.6	95.1	98.0	97.8	93.2		93.7	100.0	100.0	
2001	MAR.	7	66	86.1	93.6	98.0	97.8	94.5		96.8	97.3	97.7	
2001	MAR.	20	79	94.9	95.1	99.5	97.8	97.3		93.7	99.9	96.5	
2001	APR.	5	95	97.8	99.5	100.0	96.3	97.3		93.7	100.0	100.0	
2001	APR.	19	109	94.9	100.0	100.0	99.2	98.6		96.8	100.0	100.0	
2001	MAY	17	137		100.0	100.0	100.0	100.0		100.0	100.0	100.0	
2001	JUNE	19	170	100.0	100.0	100.0	100.0	100.0		100.0	100.0	100.0	
2001	JULY	19	200		100.0	100.0	100.0	100.0		100.0	100.0	100.0	
2001	AUG.	15	227		100.0	100.0	100.0	100.0		100.0	100.0	100.0	
2001	SEPT.	13	256	100.0	100.0	100.0	100.0	100.0		100.0	100.0	100.0	
2001	OCT.	11	284	100.0	100.0	100.0	100.0	100.0		100.0	100.0	100.0	
2001	NOV.	15	319		100.0	100.0	100.0	100.0		100.0	100.0	100.0	
2001	DEC.	19	353	90.5	100.0	100.0	100.0	100.0		100.0	100.0	100.0	
2002	JAN.	22	22	83.1	90.6	100.0	100.0	99.9		99.8	99.9	100.0	
2002	FEB.	22	53	89.1	90.6	98.0	100.0	99.9		93.7	99.9	98.9	
2002	MAR.	7	66	96.3	100.0	100.0	100.0	98.6		99.8	100.0	100.0	
2002	MAR.	22	81	99.2	98.0	100.0	100.0	98.6		96.8	100.0	96.5	
2002	APR.	5	95	87.6	93.6	100.0	100.0	100.0		93.7	100.0	100.0	
2002	APR.	25	115	99.2	100.0	100.0	100.0	100.0		100.0	100.0	98.9	
2002	MAY	16	136	100.0	100.0	100.0	100.0	100.0		100.0	100.0	100.0	
2002	JUNE	11	162	100.0	100.0	100.0	100.0	100.0		100.0	100.0	100.0	
2002	JULY	17	198	100.0	100.0	100.0	100.0	100.0		100.0	100.0	100.0	
2002	AUG.	20	232	100.0	100.0	100.0	100.0	100.0		100.0	100.0	100.0	
2002	SEPT.	19	262	100.0	100.0	100.0	100.0	100.0		100.0	100.0	100.0	
2002	OCT.	24	297	99.2	99.5	100.0	100.0	100.0		100.0	100.0	100.0	
2002	NOV.	20	324	93.5	98.0	100.0	100.0	100.0		100.0	100.0	100.0	
2002	DEC.	17	351	84.6	92.1	100.0	100.0	100.0		96.8	100.0	98.9	

Table D.3. Sensor Saturation Values for Section 390212

YEAR	MONTH	DAY	JULIAN	S1	S2	S3	S4	S5	S6	S7	S8	S9	S10
1996	AUG.	5	218	72.6	100.0	98.5	98.5	98.8	100.0	100.0	100.0	100.0	100.0
1996	AUG.	15	229	74.3	100.0	100.0	100.0	100.0	100.0	98.8	100.0	100.0	100.0
1996	SEPT.	19	263	74.3	94.1	96.9	96.9	100.0	100.0	100.0	100.0	100.0	100.0
1996	OCT.	15	289	74.3	90.8	96.9	95.4	100.0	100.0	100.0	100.0	100.0	100.0
1996	NOV.	19	324	74.3	89.1	95.4	92.2	97.2	100.0	98.8	100.0	100.0	100.0
1996	DEC.	21	356	75.9	87.5	89.1	93.8	98.8	100.0	95.6	100.0	100.0	100.0
1997	JAN.	16	16	48.6	74.0	82.6	87.5	95.6	100.0	94.0	99.5	100.0	100.0
1997	FEB.	16	47	75.9	82.4	87.5	87.5	87.5	89.2	95.6	99.5	100.0	100.0
1997	MAR.	11	70	77.6	87.5	85.8	87.5	90.7	91.0	94.0	98.2	100.0	
1997	MAR.	23	113	75.9	85.8	87.5	87.5	90.7	92.9	95.6	99.5	100.0	100.0
1997	APR.	25	115	77.6	87.5	89.1	89.1	90.7	94.7	95.6	100.0	99.4	
1997	MAY	23	143	77.6	90.8	89.1	90.6	95.6	98.3	95.6	100.0	100.0	100.0
1997	JUNE	16	167	79.2	95.7	93.8	100.0	94.0	100.0	97.2	100.0	100.0	100.0
1997	AUG.	5	217	75.9	97.4	98.5	100.0	100.0	100.0	100.0	100.0	100.0	100.0
1997	OCT.	16	289	75.9	90.8	96.9	95.4	100.0	96.5	100.0	100.0	100.0	100.0
1997	NOV.	20	318	77.6	87.5	93.8	93.8	94.0	94.7	97.2	100.0	100.0	100.0
1997	DEC.	15	349	75.9	89.1	90.6	93.8	95.6	94.7	97.2	100.0	98.0	100.0
1998	JAN.	22	22	77.6	89.1	93.8	93.8	95.6	96.5	97.2	100.0	100.0	100.0
1998	FEB.	24	55	79.2	87.5	92.2	90.6	94.0	94.7	97.2	100.0	100.0	100.0
1998	MAR.	26	85	89.1	89.1	92.2	90.6	97.2	98.3	98.8	100.0	100.0	100.0
1998	APR.	17	107	85.8	95.7	92.2	95.4	95.6	94.7	97.2	100.0	100.0	100.0
1998	MAY	20	140	82.5	100.0	98.5	98.5	100.0	94.7	100.0	100.0	100.0	100.0
1998	JUNE	18	169	75.9	100.0	100.0	96.9	97.2	96.5	100.0		100.0	100.0
1998	JULY	21	202	82.5	100.0	100.0	100.0	100.0	100.0	100.0		100.0	100.0
1998	AUG.	19	231	79.2	100.0	100.0	100.0	100.0	100.0	100.0			
1998	SEPT.	17	260	74.3	100.0	100.0	96.9	100.0	100.0	100.0			
1998	OCT.	20	293	75.9	94.1	93.8	93.8	98.8	98.3	100.0			
1998	NOV.	19	323	79.2	92.4	92.2	93.8	92.3	98.3	100.0	100.0	100.0	100.0
1998	DEC.	15	349	75.9	92.4	96.9	95.4	94.0	96.5	98.8		100.0	100.0
1999	JAN.	21	21	80.9	77.4	82.6	85.8	90.7	87.4	95.6		98.0	100.0
1999	FEB.	16	47	82.5	82.4	89.1	90.6	89.1	85.6	95.6		100.0	100.0
1999	MAR.	4	63	82.5	82.4	89.1	87.5	89.1	85.6	95.6		99.4	100.0
1999	MAR.	20	79	85.8	85.8	90.6	89.1	89.1	85.6	97.2		100.0	100.0
1999	APR.	8	98	89.1	90.8	92.2	90.6	90.7	87.4	95.6		100.0	
1999	APR.	22	112	90.7	87.5	89.1	90.6	94.0	85.6	97.2		100.0	100.0
1999	MAY	19	139	90.7	97.4	96.9	98.5	97.2	98.3	98.8		100.0	100.0
1999	JUNE	15	166	90.7	100.0	100.0	100.0	97.2	100.0	100.0		100.0	100.0
1999	JULY	15	196	85.8	99.0	100.0	100.0	98.8	100.0	100.0	0.0	100.0	100.0
1999	AUG.	24	236	87.5	95.7	100.0	100.0	100.0	100.0	100.0	100.0	100.0	100.0
1999	SEPT.	16	259	79.2	90.8	100.0	95.4	97.2	100.0	100.0	100.0	100.0	100.0
1999	OCT.	11	284	80.9	94.1	100.0	95.4	95.6	96.5	100.0	100.0	100.0	100.0
1999	NOV.	18	322	75.9	90.8	95.4	92.2	94.0	91.0	100.0	100.0	99.4	100.0
1999	DEC.	8	342	80.9	89.1	98.5	90.6	94.0	89.2	100.0	100.0	98.0	100.0

2000	JAN.	13	13	79.2	89.1	93.8	93.8	92.3	92.9	100.0	100.0	95.0	100.0
2000	FEB.	21	52	84.2	79.1	90.6	81.0	87.5	81.9	100.0	100.0	89.0	100.0
2000	MAR.	7	67	80.9	84.1	85.8	87.5	85.8	91.0	98.8	98.2	96.5	100.0
2000	MAR.	23	83	89.1	90.8	90.6	85.8	84.2	81.9	100.0	100.0	92.0	100.0
2000	APR.	4	95	94.0	85.8	89.1	87.5	85.8	85.6	100.0	100.0	95.0	100.0
2000	APR.	20	111	90.7	85.8	90.6	87.5	94.0	83.8	98.8	100.0	96.5	100.0
2000	MAY	22	143	89.1	89.1	93.8	92.2	94.0	92.9	97.2	100.0	100.0	100.0
2000	JUNE	19	171	87.5	97.4	98.5	100.0	95.6	94.7	100.0	100.0	98.0	100.0
2000	JULY	21	203	79.2	100.0	100.0	98.5	95.6	98.3	100.0	100.0	100.0	100.0
2000	AUG.	16	229	85.8	80.7	100.0	100.0	100.0	92.9	100.0	100.0	100.0	100.0
2000	SEPT.	18	262	72.6	89.1	98.5	100.0	100.0	94.7	100.0	100.0	100.0	100.0
2000	OCT.	17	291	80.9	90.8	100.0	93.8	90.7	98.3	100.0	100.0	100.0	100.0
2000	NOV.	11	316	69.4	92.4	95.4	93.8	95.6	87.4	98.8	100.0	100.0	100.0
2000	DEC.	9	344	74.3	89.1	92.2	92.2	94.0	91.0	95.6	100.0	90.5	100.0
2001	JAN.	11	11	23.6	51.1	77.8	77.8	80.9	76.5	89.1	94.2	90.5	96.3
2001	FEB.	13	44	89.1	82.4	90.6	85.8	84.2	81.9	87.5	88.7	92.0	100.0
2001	MAR.	7	66	84.2	75.7	87.5	85.8	85.8	81.9	95.6	95.6	95.0	100.0
2001	MAR.	20	79	75.9	80.7	93.8	82.6	84.2	76.5	90.7	92.9	92.0	100.0
2001	APR.	5	95	80.9	89.1	90.6	84.2	85.8	80.1	89.1	96.9	95.0	100.0
2001	APR.	19	109	89.1	92.4	90.6	89.1	92.3	81.9	94.0	100.0	95.0	100.0
2001	MAY	17	137	94.0	94.1	98.5	93.8	95.6	94.7	100.0	100.0	98.0	100.0
2001	JUNE	19	170	89.1	100.0	100.0	96.9	100.0	98.3	100.0	100.0	99.4	100.0
2001	JULY	19	200	85.8	99.0	100.0	100.0	100.0	98.3	100.0	100.0	100.0	100.0
2001	AUG.	15	227	82.5	100.0	100.0	100.0	100.0	100.0	100.0	100.0	100.0	100.0
2001	SEPT.	13	256	82.5	97.4	100.0	98.5	97.2	100.0	100.0	100.0	100.0	100.0
2001	OCT.	11	284	77.6	97.4	100.0	95.4	94.0	96.5	97.2	100.0	100.0	100.0
2001	NOV.	15	319	72.6	94.1	100.0	90.6	97.2	91.0	100.0	100.0	99.4	100.0
2001	DEC.	19	353	77.6	95.7	96.9	95.4	97.2	92.9	95.6	100.0	98.0	100.0
2002	JAN.	22	22	77.6	87.5	98.5	90.6	94.0	94.7	97.2	100.0	96.5	100.0
2002	FEB.	22	53	77.6	85.8	96.9	89.1	97.2	85.6	92.3	100.0	100.0	100.0
2002	MAR.	7	66	85.8	100.0	100.0	93.8	100.0	98.3	98.8	100.0	96.5	100.0
2002	MAR.	22	81	85.8	100.0	100.0	96.9	98.8	94.7	98.8	100.0	99.4	100.0
2002	APR.	5	95	89.1	90.8	98.5	92.2	97.2	89.2	100.0	100.0	99.4	100.0
2002	APR.	25	115	92.3	100.0	100.0	96.9	100.0	98.3	100.0	100.0	98.0	100.0
2002	MAY	16	136	89.1	100.0	100.0	100.0	100.0	100.0	100.0	100.0	99.4	100.0
2002	JUNE	11	162	84.2	100.0	100.0	96.9	100.0	96.5	100.0	100.0	100.0	100.0
2002	JULY	17	198	84.2	100.0	100.0	100.0	100.0	100.0	100.0	100.0	100.0	100.0
2002	AUG.	20	232	82.5	100.0	100.0	100.0	100.0	100.0	100.0	100.0	100.0	100.0
2002	SEPT.	19	262	87.5	99.0	100.0	100.0	100.0	98.3	100.0	100.0	100.0	100.0
2002	OCT.	24	297	80.9	94.1	98.5	98.5	97.2	100.0	100.0	100.0	100.0	100.0
2002	NOV.	20	324	80.9	87.5	96.9	90.6	98.8	96.5	98.8	100.0	100.0	100.0
2002	DEC.	17	351	77.6	84.1	100.0	90.6	97.2	96.5	94.0	100.0	100.0	100.0

Table D.4. Sensor Saturation Values for Section 390901

YEAR	MONTH	DAY	JULIAN	S1	S2	S3	S4	S5	S6	S7	S8	S9
1996	AUG.	5	218	31.3	89.1	100.0	100.0	100.0	98.3	100.0	100.0	95.6
1996	SEPT.	19	263	27.3	92.4	100.0	100.0	100.0	96.5	100.0	100.0	97.7
1996	OCT.	15	289	27.3	94.1	99.0	96.5	100.0	92.9	97.7	100.0	95.6
1996	NOV.	19	324	26.0	94.1	92.4	96.5	100.0	94.7	99.7	100.0	97.7
1996	DEC.	21	356	24.8	97.4	92.4	89.2	93.1	89.2	95.6	100.0	99.7
1997	JAN.	16	16	22.3	72.4	90.8	89.2	91.2	89.2	95.6	99.2	99.7
1997	FEB.	16	47	34.0	85.8	87.5	89.2	93.1	91.0	93.5	97.2	100.0
1997	MAR.	11	70	34.0	84.1	89.1	89.2	91.2	89.2	93.5	99.2	99.7
1997	MAR.	23	113	71.0	77.4	89.1	87.4	89.3	91.0	95.6	100.0	97.7
1997	APR.	25	115	31.3	89.1	92.4	91.0	95.0	92.9	100.0	97.2	95.6
1997	JUNE	16	167	29.9	90.8	92.4	100.0	100.0	94.7	100.0	99.2	95.6
1997	AUG.	5	217	24.8	92.4	100.0	100.0	100.0	100.0	100.0	100.0	97.7
1997	SEPT.	9	252	27.3	89.1	99.0	100.0	100.0	98.3	100.0	100.0	100.0
1997	OCT.	16	289	20.0	70.7	95.7	100.0	98.7	94.7	100.0	100.0	100.0
1997	NOV.	20	318	31.3	90.8	92.4	96.5	93.1	89.2	97.7	99.2	93.5
1997	DEC.	15	349	31.3	90.8	92.4	96.5	93.1	89.2	97.7	97.2	91.5
1998	JAN.	22	22	31.3	92.4	90.8	94.7	96.8	89.2	97.7	99.2	97.7
1998	FEB.	24	55	28.6	94.1	92.4	92.9	91.2	89.2	91.5	97.2	95.6
1998	MAR.	26	85	28.6	100.0	94.1	92.9	91.2	87.4	95.6	99.2	95.6
1998	APR.	17	107	23.6	97.4	97.4	100.0	98.7	91.0	97.7	97.2	95.6
1998	MAY	20	140	18.8	100.0	100.0	96.5	100.0	92.9	97.7	100.0	95.6
1998	JUNE	18	169	22.3	100.0	100.0	100.0	100.0	98.3	97.7	100.0	97.7
1998	JULY	21	202	21.1	95.7	100.0	100.0	100.0	98.3	100.0	100.0	97.7
1998	AUG.	19	231	21.1	94.1	100.0	100.0	100.0	98.3	100.0		
1998	SEPT.	17	260	27.3	97.4	100.0	100.0	100.0	94.7	100.0	100.0	100.0
1998	OCT.	20	293	24.8	100.0	95.7	98.3	98.7	91.0	99.7		
1998	NOV.	19	323	29.9	94.1	94.1	98.3	98.7	92.9	99.7	99.2	99.7
1998	DEC.	15	349	20.0	90.8	94.1	96.5	98.7	96.5	100.0	100.0	97.7
1999	JAN.	21	21	42.6	100.0	84.1	92.9	93.1	91.0	95.6	99.2	97.7
1999	FEB.	16	47	27.3	100.0	90.8	91.0	93.1	91.0	93.5	97.2	100.0
1999	MAR.	4	63	28.6	97.4	92.4	94.7	95.0	91.0	95.6	93.3	100.0
1999	MAR.	20	79	34.0	99.0	92.4	94.7	95.0	94.7	97.7	100.0	100.0
1999	APR.	8	98	32.6	100.0	94.1	94.7	95.0	94.7	99.7	99.2	97.7
1999	APR.	22	112	22.3	97.4	95.7	92.9	100.0	92.9	99.7	100.0	100.0
1999	MAY	19	139	23.6	99.0	99.0	98.3	100.0	96.5	100.0	100.0	100.0
1999	JUNE	15	166	21.1	95.7	100.0	100.0	100.0	94.7	100.0	100.0	100.0
1999	JULY	15	196	22.3	100.0	100.0	100.0	100.0	98.3	100.0	100.0	99.7
1999	AUG.	24	236	24.8	95.7	99.0	100.0	100.0	100.0	100.0	100.0	97.7
1999	SEPT.	16	259	27.3	97.4	100.0	100.0	98.7	100.0	100.0	100.0	100.0
1999	OCT.	11	284	22.3	92.4	97.4	100.0	96.8	96.5	99.7	100.0	99.7
1999	NOV.	18	322	17.7	89.1	94.1	96.5	95.0	98.3	100.0	100.0	87.3
1999	DEC.	8	342	18.8	90.8	92.4	96.5	98.7	94.7	99.7	100.0	93.5
2000	JAN.	13	13	22.3	94.1	90.8	96.5	93.1	92.9	97.7	97.2	99.7

2000	FEB.	12	43	32.6	94.1	84.1	85.6	81.7	92.9	97.7	93.3	99.7
2000	MAR.	7	67	28.6	92.4	87.5	89.2	87.4	91.0	99.7	95.3	100.0
2000	MAR.	23	83	21.1	99.0	89.1	91.0	87.4	98.3	99.7	100.0	100.0
2000	APR.	4	95	21.1	95.7	89.1	96.5	89.3	96.5	99.7	100.0	100.0
2000	APR.	20	111	18.8	94.1	90.8	92.9	95.0	87.4	95.6	91.3	93.5
2000	MAY	22	143	22.3	87.5	99.0	98.3	96.8	98.3	100.0	100.0	100.0
2000	JUNE	19	171	21.1	95.7	100.0	98.3	100.0	94.7	100.0	100.0	100.0
2000	JULY	21	203	22.3	95.7	100.0	100.0	100.0	100.0	100.0	100.0	100.0
2000	AUG.	16	229	17.7	92.4	99.0	100.0	100.0	100.0	100.0	100.0	100.0
2000	SEPT.	18	262	9.5	94.1	100.0	100.0	98.7	100.0	97.7	100.0	100.0
2000	OCT.	17	291	11.4	92.4	95.7	98.3	100.0	96.5	100.0	100.0	100.0
2000	NOV.	11	316	12.4	90.8	94.1	100.0	95.0	98.3	99.7	100.0	100.0
2000	DEC.	9	344	22.3	95.7	90.8	98.3	89.3	96.5	93.5	100.0	100.0
2001	JAN.	11	11	10.4	44.9	85.8	81.9	87.4	92.9	97.7	100.0	100.0
2001	FEB.	13	44	29.9	100.0	87.5	87.4	83.6	91.0	95.6	100.0	100.0
2001	MAR.	7	66	26.0	100.0	92.4	91.0	89.3	92.9	97.7	100.0	95.6
2001	MAR.	20	79	23.6	100.0	87.5	89.2	87.4	98.3	93.5	97.2	99.7
2001	APR.	5	95	20.0	100.0	92.4	89.2	89.3	94.7	99.7	95.3	95.6
2001	APR.	19	109	14.4	100.0	94.1	92.9	96.8	96.5	83.2	91.3	87.3
2001	MAY	17	137	38.2	97.4	95.7	100.0	98.7	98.3	100.0	100.0	97.7
2001	JUNE	19	170	17.7	94.1	100.0	100.0	100.0	100.0	100.0	100.0	99.7
2001	JULY	19	200	13.4	90.8	100.0	100.0	100.0	100.0	100.0	100.0	100.0
2001	AUG.	15	227		99.0	100.0	100.0	100.0	100.0	100.0	100.0	100.0
2001	SEPT.	13	256	17.7	94.1	100.0	100.0	98.7	98.3	100.0	100.0	100.0
2001	OCT.	11	284	10.4	95.7	97.4	98.3	96.8	94.7	99.7	100.0	100.0
2001	NOV.	15	319	10.4	97.4	97.4	98.3	95.0	94.7	100.0	100.0	100.0
2001	DEC.	19	353	9.5	95.7	97.4	94.7	91.2	94.7	97.7	100.0	100.0
2002	JAN.	22	22	22.3	89.1	92.4	92.9	93.1	91.0	100.0	100.0	100.0
2002	FEB.	22	53	26.0	99.0	95.7	91.0	91.2	96.5	99.7	93.3	91.5
2002	MAR.	7	66	29.9	100.0	97.4	100.0	98.7	98.3	100.0	100.0	100.0
2002	MAR.	22	81	32.6	100.0	97.4	100.0	100.0	98.3	100.0	100.0	100.0
2002	APR.	5	95	20.0	100.0	92.4	98.3	95.0	94.7	89.4	97.2	91.5
2002	APR.	25	115	27.3	100.0	100.0	100.0	100.0	98.3	100.0	100.0	100.0
2002	MAY	16	136	27.3	100.0	100.0	100.0	100.0	100.0	100.0	100.0	100.0
2002	JUNE	11	162	16.6	100.0	100.0	100.0	100.0	98.3	100.0	100.0	100.0
2002	JULY	17	198	15.5	100.0	100.0	100.0	100.0	100.0	100.0	100.0	100.0
2002	AUG.	20	232	16.6	100.0	100.0	100.0	100.0	100.0	100.0	100.0	100.0
2002	SEPT.	19	262	17.7	100.0	100.0	100.0	100.0	100.0	100.0	100.0	95.6
2002	OCT.	24	297	15.5	90.8	100.0	100.0	98.7	98.3	100.0	100.0	95.6
2002	NOV.	20	324	12.4	89.1	94.1	100.0	100.0	94.7	100.0	95.3	87.3
2002	DEC.	17	351	14.4	89.1	87.5	92.9	98.7	89.2	93.5	85.4	85.3

Table D.5. Average Seasonal Saturation Values vs. Subgrade Depth (Section 390203)

		cm (in)	cm (in)	cm (in)	cm (in)	cm (in)	cm (in)	cm (in)	cm (in)	cm (in)
	DEPTH	**7.6 (3)**	**22.9 (9)**	**38.1 (15)**	**53.3 (21)**	**68.6 (27)**	**83.8 (33)**	**99.1 (39)**	**129.5 (51)**	**160.0 (63)**
	SPRING									
1996	**SUMMER**	94.6	94.4	98.9	99.0	99.2	99.8	98.5	98.2	99.6
	FALL	85.9	91.0	94.4	93.9	92.6	93.1	95.9	97.2	99.1
	WINTER	83.2	89.1	90.7	89.3	89.0	90.6	94.3	99.2	99.4
	SPRING	86.9	90.5	91.3	91.6	93.6	93.0	96.3	100.0	99.4
1997	**SUMMER**	94.4	96.0	98.9	98.5	99.1	100.0	99.3	100.0	100.0
	FALL	86.8	94.0	94.4	92.6	95.2	95.8	96.4	100.0	100.0
	WINTER	71.4	87.2	91.0	91.4	90.9	92.1	93.7	93.8	99.6
	SPRING	94.3	95.4	96.5	96.5	94.8	95.6	97.7	100.0	100.0
1998	**SUMMER**	100.0	100.0	99.7	100.0	100.0	100.0	100.0	100.0	100.0
	FALL	90.3	98.1	97.0	96.3	97.8	98.7	100.0	99.7	100.0
	WINTER	95.3	93.8	94.6	89.9	95.6	96.3	97.7		100.0
	SPRING	99.7	99.5	98.5	98.2	99.9	98.7	98.9	100.0	100.0
1999	**SUMMER**	100.0	100.0	100.0	100.0	100.0	100.0	100.0	100.0	100.0
	FALL	94.6	99.3	97.3	97.2	99.4	100.0	100.0	100.0	100.0
	WINTER	95.3	93.9	89.5	89.3	89.0	98.3	95.9		
	SPRING	100.0	99.0	95.7	96.9	97.4	98.7	99.4		
2000	**SUMMER**	100.0	100.0	100.0	100.0	100.0	100.0	100.0		100.0
	FALL	96.6	99.1	97.6	97.2	99.4	100.0	100.0		100.0
	WINTER	100.0	87.2	89.3	89.5	90.6	97.5	97.7		
	SPRING	98.8	98.2	94.0	94.1	96.5	98.6	98.5		
2001	**SUMMER**	100.0	100.0	100.0	100.0	100.0	100.0	100.0	100.0	100.0
	FALL	90.3	99.5	98.0	99.4	100.0	100.0	100.0	100.0	100.0
	WINTER	82.7	88.9	85.9	91.6	96.2	100.0	96.9		
	SPRING	91.3	95.8	95.3	96.0	99.0	99.9	99.4	100.0	100.0
2002	**SUMMER**	100.0	100.0	100.0	100.0	100.0	100.0	100.0	100.0	100.0
	FALL	88.1	96.0	96.8	94.8	99.4	100.0	100.0	100.0	100.0
	WINTER									

Table D.6. Average Seasonal Saturation Values vs. Subgrade Depth (Section 390205)

		cm (in)	cm (in)	cm (in)	cm (in)	cm (in)	cm (in)	cm (in)	cm (in)	cm (in)
	DEPTH	**15.2 (6)**	**30.5 (12)**	**45.7 (18)**	**60.9 (24)**	**76.2 (30)**	**91.4 (36)**	**106.7 (42)**	**121.9 (48)**	**152.4 (60)**
	SPRING									
1996	**SUMMER**	91.0	93.6	94.1	94.9	100.0		99.9	100.0	100.0
	FALL	86.1	86.6	90.6	93.5	99.0		96.8	95.4	100.0
	WINTER	85.4	86.8	86.8	92.0	91.8		92.7	93.6	100.0
	SPRING	88.0	88.0	89.9	97.0	94.2		95.3	94.9	100.0
1997	**SUMMER**	94.2	93.6	98.0	100.0	100.0		100.0	100.0	100.0
	FALL	91.3	91.1	92.6	98.0	99.1		99.3	98.2	100.0
	WINTER	91.3	89.1	94.3	95.6	97.9		95.3	97.3	100.0
	SPRING	99.8	97.5	99.0	98.5	99.6		98.8	99.0	100.0
1998	**SUMMER**	100.0	100.0	100.0	100.0	100.0		100.0	100.0	100.0
	FALL	95.9	92.1	99.8	99.5	98.2		99.9	100.0	100.0
	WINTER	91.0	91.1	97.5	94.9	91.1		97.9	96.6	100.0
	SPRING	96.9	96.8	100.0	98.9	96.9		98.8	99.0	100.0
1999	**SUMMER**	100.0	100.0	100.0	100.0	100.0		100.0	100.0	100.0
	FALL	86.1	93.1	100.0	97.1	94.9		99.4	100.0	98.8
	WINTER	90.1	94.1	96.7	95.4	92.2		96.3	96.8	100.0
	SPRING	95.8	96.5	99.9	98.1	95.9		97.5	98.1	100.0
2000	**SUMMER**	100.0	100.0	100.0	100.0	100.0		100.0	100.0	100.0
	FALL	95.9	97.9	100.0	100.0	99.1		100.0	100.0	100.0
	WINTER	74.8	86.4	95.4	95.2	91.7		94.5	98.6	98.5
	SPRING	97.6	99.9	100.0	98.9	99.0		97.6	100.0	100.0
2001	**SUMMER**	100.0	100.0	100.0	100.0	100.0		100.0	100.0	100.0
	FALL	95.3	100.0	100.0	100.0	100.0		100.0	100.0	100.0
	WINTER	89.5	93.7	99.3	100.0	99.5		97.8	100.0	99.6
	SPRING	97.2	98.3	100.0	100.0	99.7		98.1	100.0	99.1
2002	**SUMMER**	100.0	100.0	100.0	100.0	100.0		100.0	100.0	100.0
	FALL	92.4	96.5	100.0	100.0	100.0		98.9	100.0	99.6
	WINTER									

Table D.7. Average Seasonal Saturation Values vs. Subgrade Depth (Section 390212)

		cm (in)	cm (in)	cm (in)	cm (in)	cm (in)	cm (in)	cm (in)	cm (in)	cm (in)
	DEPTH	**10.2 (4)**	**25.4 (10)**	**40.6 (16)**	**55.9 (22)**	**71.1 (28)**	**86.36 (34)**	**101.6 (40)**	**132.1 (52)**	**162.6 (64)**
	SPRING									
1996	**SUMMER**	98.0	98.5	98.5	99.6	100.0	99.6	100.0	100.0	100.0
	FALL	89.1	93.8	93.8	98.6	100.0	98.1	100.0	100.0	100.0
	WINTER	84.9	86.7	87.5	89.1	90.1	94.8	98.9	100.0	100.0
	SPRING	89.9	89.8	91.8	92.7	96.4	96.0	99.9	99.9	100.0
1997	**SUMMER**	97.4	98.5	100.0	100.0	100.0	100.0	100.0	100.0	100.0
	FALL	89.1	93.8	94.3	96.5	95.3	98.1	100.0	99.3	100.0
	WINTER	88.3	93.0	92.2	94.8	95.6	97.2	100.0	100.0	100.0
	SPRING	96.2	95.7	95.4	97.5	96.0	99.0	100.0	100.0	100.0
1998	**SUMMER**	100.0	100.0	99.0	100.0	100.0	100.0		100.0	100.0
	FALL	93.0	94.3	94.3	95.0	97.7	99.6	100.0	100.0	100.0
	WINTER	82.0	87.8	88.3	89.5	86.0	96.0		99.4	100.0
	SPRING	93.9	94.6	94.9	94.8	92.8	97.9		100.0	100.0
1999	**SUMMER**	95.2	100.0	98.5	98.6	100.0	100.0	100.0	100.0	100.0
	FALL	91.3	98.0	92.8	94.5	92.2	100.0	100.0	99.1	100.0
	WINTER	84.1	90.1	87.4	88.5	88.6	99.6	99.4	93.5	100.0
	SPRING	89.8	92.5	90.6	90.7	87.8	99.2	100.0	96.3	100.0
2000	**SUMMER**	90.0	99.5	99.5	98.5	95.3	100.0	100.0	100.0	100.0
	FALL	90.8	95.9	93.3	93.4	92.2	98.1	100.0	96.8	100.0
	WINTER	72.5	87.4	83.0	83.8	79.2	90.7	92.8	92.4	99.1
	SPRING	93.9	94.9	91.0	93.4	88.8	95.8	99.2	96.9	100.0
2001	**SUMMER**	98.8	100.0	99.5	99.1	99.4	100.0	100.0	100.0	100.0
	FALL	95.7	99.0	93.8	96.1	93.5	97.6	100.0	99.1	100.0
	WINTER	91.1	98.5	91.2	97.0	92.8	96.1	100.0	97.7	100.0
	SPRING	98.2	99.7	96.6	99.2	95.7	99.8	100.0	99.3	100.0
2002	**SUMMER**	99.7	100.0	100.0	100.0	99.4	100.0	100.0	100.0	100.0
	FALL	88.6	98.5	93.3	97.7	97.6	97.6	100.0	100.0	100.0
	WINTER									

Table D.8. Average Seasonal Saturation Values vs. Subgrade Depth (Section 390901)

		cm (in)	cm (in)	cm (in)	cm (in)	cm (in)	cm (in)	cm (in)	cm (in)
	DEPTH	**7.6 (3)**	**22.9 (9)**	**38.1 (15)**	**53.3 (21)**	**68.6 (27)**	**83.8 (33)**	**99.1 (39)**	**129.5 (51)**
	SPRING								
1996	**SUMMER**	90.8	100.0	100.0	100.0	97.4	100.0	100.0	96.6
	FALL	95.2	94.6	94.1	97.7	92.2	97.7	100.0	97.7
	WINTER	84.9	88.3	89.2	92.1	90.1	93.5	98.2	99.9
	SPRING	85.8	91.3	92.8	94.7	92.9	98.5	98.8	96.3
1997	**SUMMER**	90.8	99.5	100.0	100.0	99.1	100.0	100.0	98.8
	FALL	84.1	93.5	97.6	95.0	91.0	98.4	98.8	95.0
	WINTER	93.3	91.6	93.8	94.0	89.2	94.6	98.2	96.6
	SPRING	99.1	99.1	98.8	99.6	94.1	97.7	99.1	96.3
1998	**SUMMER**	95.7	100.0	100.0	100.0	97.1	100.0	100.0	98.8
	FALL	95.0	94.7	97.7	98.7	93.5	99.8	99.6	98.7
	WINTER	99.1	89.9	93.3	94.0	91.9	95.6	97.4	99.4
	SPRING	98.0	97.2	96.4	98.7	94.7	99.9	99.8	99.4
1999	**SUMMER**	97.7	99.7	100.0	99.6	99.4	100.0	100.0	99.1
	FALL	90.8	94.6	97.6	96.8	96.5	99.8	100.0	93.5
	WINTER	93.6	87.4	90.4	87.4	92.2	98.4	95.3	99.8
	SPRING	94.4	93.6	95.4	93.7	95.0	99.0	98.3	98.7
2000	**SUMMER**	94.1	99.7	100.0	99.6	100.0	99.2	100.0	100.0
	FALL	93.0	93.5	98.9	94.7	97.1	97.8	100.0	100.0
	WINTER	86.2	88.3	87.4	86.9	93.8	96.1	99.3	98.8
	SPRING	97.9	95.6	95.5	96.2	97.4	95.7	96.6	95.1
2001	**SUMMER**	94.6	100.0	100.0	99.6	99.4	100.0	100.0	100.0
	FALL	96.3	97.4	97.1	94.3	94.7	99.1	100.0	100.0
	WINTER	96.0	95.2	94.6	94.3	95.3	99.9	97.8	97.2
	SPRING	100.0	98.0	99.7	99.0	97.9	97.9	99.4	98.3
2002	**SUMMER**	100.0	100.0	100.0	100.0	100.0	100.0	100.0	98.5
	FALL	89.7	93.9	97.6	99.2	94.1	97.8	93.5	89.4
	WINTER								

Table D.9. Monthly Rainfall (mm) from Weather Station

YEAR	JAN.	FEB.	MAR.	APR.	MAY	JUNE	JULY	AUG.	SEPT.	OCT.	NOV.	DEC.
1996	57.396	42.93	50.802	171.706	202.428	80.77	99.062	62.734	161.534	45.214	72.646	115.318
1997	44.188	33.782	83.3	32.514	84.066	21.336	6.35	6.096	15.24	28.45	58.676	46.994
1998	60.964	53.596	57.406	117.092	51.814	105.146	46.734	51.818	18.288	75.178	44.446	48.254
1999	76.446	63.492	31.498	126.752	42.172	76.448	56.392	56.386	70.358	37.588	52.062	71.124
2000	52.326	56.64	60.962	128.524	109.724	123.188	41.912	93.98	78.996	57.40	49.276	49.282
2001	19.052	35.56	18.54	80.52	117.85	87.88	72.902	115.56	48.264	133.096	73.656	70.364
2002	34.288	36.578	82.80	128.266	89.154	62.992	30.48	76.198	98.548	50.55	65.784	63.248
2003	17.018											

REFERENCES

AASHTO T 265-91, “Laboratory Estimation of Moisture Content of Soils,” 1991.

Al-Khoury, Rafid, et al. “Dynamic Interpretation of Falling Weight Deflectometer Test Results – Spectral Element Method.” Transportation Research Record 1716 Paper No. 00-1330 (2000), 49-54.

Alvarez, C. A. “Study of Environmental Factors and Load Response in Flexible and Rigid Pavements at the Ohio Test Road.” M.S. Thesis. Case Western Reserve University, 2000.

ASTM Standard D 2216-90, “Standard Test Method for Laboratory Determination of Water (Moisture) Content of Soil and Rock by Mass,” 1998.

ASTM Standard D 4123-82, “Standard Test Method for Indirect Tension Test for Resilient Modulus of Bituminous Mixtures,” pp. 421-423, 1995.

Aldrich, H. P., Jr., “Frost Penetration Below Highway and Airfield Pavements,” Bulletin 135, Highway Research Board, National Academy of Sciences – National Research Council, Washington D. C., 1956.

Bliskie, J., Letter to Campbell Scientific, January 4, 1995.

Brinkgreve, R.B.J. ed. “Plaxis Finite Element Code for Soil and Rock Analysis Version 7”. Rotterdam: A.A. Balkema, 1998.

DeButy, P. W. “Ohio Test Road Seasonal Instrumentation and Material Characterization”. M.S. Thesis. Case Western Reserve University 1997.

Dempsey, B., “Climatic Effects on Airport Pavement Systems State of the Art,” Department of Defense Office, Chief of Engineers, U. S. Army, and U. S. Department of Transportation Federal Aviation Administration, Washington, D. C., June 1976.

Farzaneh, V. L. “Dynamic Analysis of Flexible Pavement Systems and Comparative Study of Seasonal and Weather Data Obtained at the Ohio Test Road and at the Moisture-Temperature Monitoring Stations,” M.S. Thesis. Case Western Reserve University 2001.

Figueroa, J. L. “Monitoring and Analysis of Data Obtained From Moisture Temperature Recording Stations, ODOT 8019” Case Western Reserve University, 2001.

Figueroa, J. L., Angyal, E., and Su, X. “Characterization of Ohio Subgrade Types,” Case Western Reserve University, Cleveland, Ohio 1994.

Figueroa, J. L. and Debuty, P. “Resilient Modulus and Fatigue Life Characterization of Asphalt Concrete Mixtures Used in the Ohio Test Road,” Case Western Reserve University, Cleveland, Ohio 1998.

Helkelrath, W., Hamburg, S., and Murphy, F., “Automatic, Real-time Monitoring of Soil Moisture in a Remote Field Area with Time Domain Reflectometry,” Water Resources Research, Vol. 27, pp. 857-864, 1991.

Klemunes, J., “Determining Soil Volumetric Moisture Content Using Time Domain Reflectometry”, FHWA-RD-97-139, February 1998.

Knight, J. H., White, I., and Zegelin, J., “Sampling Volume of TDR Probes Used for Water Content Monitoring,” Symposium and Workshop on Time Domain Reflectometry in Environmental, Infrastructure, and Mining Applications, Special Publication, SP-19-94, U. S. Department of Interior Bureau of Mines, pp. 93-104, 1994.

Majidzadeh, K. “Dynamic Deflection Study for Pavement Condition Investigation”, Final Report. Ohio Department of Transportation, 1974.

McCuen, R., “Hydrologic Analysis and Design”, Prentice-Hall, New Jersey, 1998.

Raab, R., Esch, E., and Andrei, R., “Evaluation of a Time Domain Reflectometry Technique for Seasonal Monitoring of Soil Moisture Content Under Road Pavement Test Sections”, SHRP-P689, June 1994.

Roth, C., Malicki, M., and Plagge, R., “Empirical Evaluation of the Relationship Between Soil Dielectric Constant and Volumetric Water Content as a Basis for Calibrating Soil Moisture Content,” Journal of Soil Science, Vol. 32, pp. 1-13, 1992.

Roth, K., Schulin, R., Fluhler, H., and Attinger, W., “Calibration of Time Domain Reflectometry for Water Content Measurement Using a Composite Dielectric Approach,” Water Resources Research, Vol. 26, No. 10, pp.2267-2273, October 1990.

Sargand, S. “Development of an instrumentation plan for the Ohio SPS Test Pavement (DEL-23-17.48),” Ohio University, Athens, Ohio 1994. [1]

Suwansawat, S., “Using Time Domain Reflectometry for Measuring Water Content in Compacted Clays,” M.S. thesis, University of Wisconsin-Madison, 1997.

Suwansawat, S. and Benson, C. H., "Cell Size for Water Content-Dielectric Constant Calibrations for Time Domain Reflectometry," Geotechnical Testing Journal, GTJODJ, Vol.22, March 1999, pp. 3-12.

Thompson, M. R. and Robnett, Q. L., "Final Report, Resilient Properties of Subgrade Soils," Civil Engineering Studies Transportation Engineering Series No. 14, Illinois Cooperative Highway and Transportation Series No. 160, 1976.

Topp, G. C., and Davis, A. L., "Time Domain Reflectometry (TDR) and its Application to Irrigation Scheduling," Advances in Irrigation, Vol. 3, pp. 107-127, 1985.

Topp, G. C., Davis, J. L., and Annan, A. P., "Electromagnetic Determination of Soil Water Content: Measurements in Coaxial Transmission Lines," Water Resources Research, Vol. 16, No. 3, pp. 574-582, June 1980.

University of Illinois, Department of Civil Engineering, "The ILLIPAVE Program for Pavement Analysis Users Manual". 1979.

University of Illinois, Department of Civil Engineering, "The ILLISLAB Program for Pavement Analysis Users Manual." 1984.

University of Texas at Austin, Department of Civil Engineering, "The FWD-DYN Users Manual" 1994.

U. S. Department of Transportation, Federal Highway Administration, "LTPP Seasonal Monitoring Program: AWSCheck Users Guide", November 1996.]

U. S. Department of Transportation, Federal Highway Administration "LTPP Seasonal Monitoring Program: SMPCheck Users Guide", October 1996.